



HAL
open science

Identification of a novel role of the E3-ubiquitin ligase Mindbomb1 in the non-canonical WNT/Planar Cell Polarity pathway

Vishnu Saraswathy

► **To cite this version:**

Vishnu Saraswathy. Identification of a novel role of the E3-ubiquitin ligase Mindbomb1 in the non-canonical WNT/Planar Cell Polarity pathway. Molecular biology. COMUE Université Côte d'Azur (2015 - 2019), 2019. English. NNT : 2019AZUR6000 . tel-04685212

HAL Id: tel-04685212

<https://theses.hal.science/tel-04685212v1>

Submitted on 3 Sep 2024

HAL is a multi-disciplinary open access archive for the deposit and dissemination of scientific research documents, whether they are published or not. The documents may come from teaching and research institutions in France or abroad, or from public or private research centers.

L'archive ouverte pluridisciplinaire **HAL**, est destinée au dépôt et à la diffusion de documents scientifiques de niveau recherche, publiés ou non, émanant des établissements d'enseignement et de recherche français ou étrangers, des laboratoires publics ou privés.

THÈSE DE DOCTORAT

Identification d'un nouveau rôle de la E3-ubiquitin ligase Mindbomb1 dans la voie Polarité Cellulaire Planaire

Vishnu M Saraswathy

Institut de Biologie Valrose (iBV)

Présentée en vue de l'obtention

du grade de docteur en Sciences de la Vie et de la Santé- Mention : Interactions moléculaires et cellulaires d'Université Côte d'Azur

Dirigée par : Dr. Maximilian FÜRTHAUER

Soutenu le : 9 Septembre 2019

Devant le jury, composé de :

Mme Daniela PANÁKOVÁ, Dr., Max Delbrück Center for Molecular Medicine.

Mr Maximilian FÜRTHAUER, Dr., Université Côte d'Azur.

Mr Pascal THEROND, Dr., Université Côte d'Azur.

Mr Steffen SCHOLPP, Prof., University of Exeter.



Titre et Identification du jury

Identification d'un nouveau rôle de la E3-ubiquitin ligase Mindbomb1 dans la voie Polarité Cellulaire Planaire

Jury

Président du jury:

Mr Pascal THEROND, Dr.,
Institute de Biologie Valrose,
Université Côte d'Azur, Nice, France

Rapporteurs:

Mme Daniela PANÁKOVÁ, Dr.,
Max Delbrück Center for Molecular Medicine (MDC),
Berlin, Deutschland

Mr Steffen SCHOLPP, Prof.,
Living Systems Institute,
University of Exeter, Exeter, United Kingdom

Directeur de these:

Mr Maximilian FÜRTHAUER, Dr.,
Institute de Biologie Valrose,
Université Côte d'Azur, Nice, France

Résumé

Identification d'un nouveau rôle de la E3-ubiquitin ligase Mindbomb1 dans la voie Polarité Cellulaire Planaire

La morphogenèse est le processus qui définit la forme d'un organisme (ou d'une partie d'un organisme) nécessaire à son bon fonctionnement. Au cours de l'embryogenèse, la morphogenèse d'un organe nécessite des processus incluant la division cellulaire, les mouvements cellulaires et la différenciation cellulaire. Cependant, on sait peu de choses sur la façon dont ces différents processus sont coordonnés au cours de la morphogenèse d'un organe. Au cours de ma thèse, j'ai étudié deux voies de signalisation cellulaire différentes qui régulent la morphogenèse au cours de l'embryogenèse du poisson zèbre. Mon étude a révélé que la voie de signalisation Notch et la voie PCP (Polarité Cellulaire Planaire) contrôlée par Mib1 régulent respectivement la morphogenèse du tube neural et l'extension de l'axe embryonnaire.

Au cours de la première partie de ma thèse, j'ai étudié le rôle de la signalisation de Notch dans la morphogenèse du tube neural du poisson zèbre. La signalisation Notch a déjà été bien étudiée pour son rôle dans la régulation de la neurogenèse lors du développement du poisson zèbre. Cependant, on ne sait pas si et comment la signalisation Notch régule la morphogenèse du tube neural du poisson zèbre. L'épithélialisation et la c-division sont des événements importants au cours de la morphogenèse du tube neural du poisson zèbre. Nos résultats montrent que, en plus de synchroniser la spécification des cellules neuronales, la suppression de la neurogenèse induite par Notch est essentielle pour l'acquisition de l'architecture neuroépithéliale et pour la réalisation de c-division. Ainsi, la signalisation Notch permet de former la moelle épinière de poisson zèbre.

Les observations de la première partie de ma thèse ont conduit à l'identification du rôle de Mindbomb1 (Mib1) dans la signalisation PCP. Mib1, une ligase ubiquitine-E3 nécessaire à l'activation de Notch, régule les mouvements d'extension convergence (CE) nécessaires à l'élongation de l'axe de l'embryon au cours de la gastrulation du poisson zèbre. De manière intéressante, nous avons montré que Mib1, indépendamment de sa fonction dans la signalisation Notch, agit dans la voie PCP pour réguler l'extension de l'axe de l'embryon. Dans la voie de la PCP, Mib1 agit comme une ligase ubiquitine-E3 et régule l'endocytose du composant de la PCP Ryk afin d'assurer la médiation de la CE lors de la gastrulation. Ainsi, notre étude a révélé que,

indépendamment de son rôle dans la signalisation Delta / Notch, Mib1 est important pour la voie PCP lors de la gastrulation du poisson zèbre.

Mots clés : La morphogenèse, le tube neural, la moelle épinière, la signalisation de Notch, Polarité Cellulaire Planaire, Mindbomb1, Ryk, La ligase ubiquitine-E3, L'épithélialisation, la neurogenèse, la c-division, les mouvements d'extension convergence, le poisson zèbre.

Abstract

Identification of a novel role of the E3-ubiquitin ligase Mindbomb1 in the non-canonical WNT/Planar Cell Polarity pathway

During my PhD, I studied two different cell signaling pathways that regulate morphogenesis during zebrafish development. I found that the Notch signaling pathway and Mib1 mediated Planar Cell Polarity (PCP) pathway regulate neural tube morphogenesis and embryonic axis extension respectively.

During the first part of my PhD, I addressed the role of Notch signaling in zebrafish neural tube morphogenesis. Notch signaling has been well studied for its role in regulating neurogenesis during zebrafish development. However, whether and how it regulates morphogenesis of the zebrafish neural tube is unknown. Epithelialization and c-division are important events during zebrafish neural tube morphogenesis. Our findings show that, in addition to regulating the timing and identity of neuronal cell fate specification, Notch mediated suppression of neurogenesis is essential for the acquisition of polarized neuroepithelial tissue architecture and the execution specific morphogenetic movements called c-divisions, in order to properly shape the zebrafish spinal cord.

Observations from the first part of my PhD led to the identification of the role of Mindbomb1(Mib1) in PCP signaling. Mib1, an E3-ubiquitin ligase required for Notch activation, regulates convergent extension (CE) movements during zebrafish gastrulation, that are required for the axis elongation of the embryo. Interestingly, I found that Mib1, independent of its function in Notch signaling, act in the PCP pathway to regulate axis extension. In the PCP pathway, Mib1 acts as an E3-ubiquitin ligase and regulates endocytosis of the PCP component Ryk to mediate CE during gastrulation. Thus, my study discovered that independent of its role in Delta/Notch signaling, Mib1 is important for the PCP pathway during zebrafish gastrulation.

Keywords : Morphogenesis, Neural tube, Spinal cord, Notch signalling, Planar Cell Polarity, Mindbomb1, E3-Ubiquitin ligase, Epithelialization, Neurogenesis, C-division, Convergent Extension, Ryk, Zebrafish

“And, when you want something, all the universe conspires in helping you to achieve it.”

- Paulo Coelho, The Alchemist

Preamble

Morphogenesis is the process of defining the shape of an organism (or a part of an organism) by which ultimately it can perform its proper function. During embryogenesis, morphogenesis of an organ requires cell divisions, cell movements and cell differentiation. However, little is known about how these different processes are coordinated during organ morphogenesis. During my PhD, I studied two different cell signaling pathways that regulate morphogenesis during zebrafish development. And my study found that the Notch signaling pathway and Mib1 mediated Planar Cell Polarity (PCP) pathway regulate neural tube morphogenesis and embryonic axis extension respectively.

During the first part of my PhD, I addressed the role of Notch signaling in zebrafish neural tube morphogenesis. Notch signaling has been well studied for its role in regulating neurogenesis during zebrafish development. However, whether and how it regulates morphogenesis of the zebrafish neural tube is unknown. Establishment of a polarized epithelium and neural tube midline crossing cell divisions (c-division) are important events during zebrafish neural tube morphogenesis. Our findings show that, in addition to regulating the timing and identity of neuronal cell fate specification, Notch mediated suppression of neurogenesis is essential for the acquisition of polarized neuroepithelial tissue architecture and the execution specific morphogenetic movements called c-divisions, in order to properly shape the zebrafish spinal cord.

Observations from the first part led to the main discovery of my PhD, identification of the novel role of Mindbomb1 (Mib1) in PCP signaling. PCP is the collective alignment of cell polarity across the plane the tissue, by which it performs functions including orientation of cilia, cell migration and oriented cell divisions. In vertebrates, the PCP pathway controls axis elongation of embryos during gastrulation, via directed cell movements called convergent extension (CE). I found that Mib1, an E3-ubiquitin ligase required for Notch activation, regulates CE movements during zebrafish gastrulation. Interestingly, I found that Mib1, independent of its function in Notch signaling, act in the PCP pathway to regulate axis extension. In the PCP pathway, Mib1 acts as an E3-ubiquitin ligase and regulates endocytosis of the PCP component Ryk to mediate CE during gastrulation. Thus, my study discovered that independent of its role in Delta/Notch signaling, Mib1 is important for the PCP pathway during zebrafish gastrulation.

This thesis is organized into four main chapters. The first chapter consists of the introduction and results of the project analyzing the role of Notch signaling in zebrafish neural tube morphogenesis. Then, the introduction and results for the project analyzing the role of Mindbomb1 in the PCP pathway are included in the second chapter. Discussion for both the projects is combined in the third chapter and the general conclusion of my thesis and references can be found in the final chapter.

Acknowledgements

First of all, I would like to extend my sincere gratitude towards my PhD mentor Dr. Maximilian Fürthauer (Max) for allowing me to pursue my passion for science in his lab. I always admire the scientific attitude of Max. I can confidently say that I became a better scientist now than four years before under his rigorous training. Max raised my quality of research into international standards and he inculcated in me the qualities of rational thinking, logical reasoning and critical analysis of scientific data. I am trying to acquire his perfectionist approach and foresightedness in science to become an even better scientist than what I am now.

I would like to thank all my jury members, Dr. Pascal Therond, Dr. Daniela Panáková and Dr. Steffen Scholpp, for accepting my invitation to be part of my thesis defense jury and evaluate my thesis.

I am deeply grateful to all my current and past lab members including Thomas Juan, Sophie Poles and Renaud Rebillard, without them this PhD journey would have been extremely difficult and depressing. Intellectual discussions/debates on scientific and non-scientific aspects with Thomas have made me think out of the box and gave me new perspectives to everything. I have learned a lot from his competitive attitude and love for sports. I am extremely thankful to him for introducing me to many new adventures during my PhD. Sophie, my favorite/most talented French teacher, is one of the kindest persons that I know in my life. Her motivation and support made my life easier in the lab. I owe a very important debt to Sophie for having the patience to teach me French, help me with experiments and listen to my complaints. I have no words to convey my thanks to Renaud for creating a cheerful ambience during my PhD, and for making me laugh even during the toughest times. It is an absolute pleasure for me to have long conversations with this most handsome man in our team. You people are amazing, and I owe big time for you guys.

I would like to specially thank Labex Signallife PhD program for funding my PhD for last four years. In addition, I would like to express my gratitude to Dr. Konstanze Beck for being there as a local guardian. Her constant support and advice to deal with all administrative stuffs in France earned a lot of time for me to concentrate on my PhD.

Finally, I would like to thank all my friends and family for their continuous support and encouragement.

Table of Contents

List of Abbreviation -----	19
List of Figure and Tables -----	23

Chapter -I

Analyzing the role of Notch signaling in zebrafish neural tube morphogenesis

Introduction

I.1 Tubular organ morphogenesis -----	28
I.2 Neural tube morphogenesis -----	30
I.2.a Neurulation in amniotes and amphibians-----	30
I.2.b Neurulation in zebrafish-----	32
I.2.c Midline crossing c-divisions are important for zebrafish neurulation-----	33
I.2.d Epithelialization of neural progenitor cells is important for zebrafish neurulation-----	35
I.2.e Notch signaling regulates radial glial formation during spinal cord morphogenesis-----	36
I.3 The Notch signaling pathway -----	39
I.4 Developmental function of the Notch signaling pathway -----	40
I.4.a Lateral inhibition-----	40
I.4.b Binary cell fate decision-----	42
I.4.c Boundary formation-----	42
I.5 Molecular mechanism of the Notch signaling -----	44
I.5.a Ligand-receptor interaction during Notch signaling-----	44
I.5.b Activation of the Notch signaling pathway-----	47
I.5.c cis-inhibition of Notch signaling-----	49
I.5.d Transcriptional activities of Notch signaling-----	50
I.6 The role of Mindbomb1 in regulating the Notch signaling pathway -----	51
I.6.a Ubiquitination-----	51
I.6.b Mindbomb1 is an E3-ubiquitin ligase-----	52
I.6.c Mindbomb1 is important for the regulation of Notch signaling-----	54
I.7 Non-canonical Notch signaling -----	55

I.8 The importance of Notch signaling in epithelialization of neural progenitors. -----	56
Results	
I.1 Studying the role of Notch signaling during zebrafish spinal cord morphogenesis -----	57
I.2 Article published in the journal Scientific Reports -----	58
I.3 Author contributions -----	59
Conclusion -----	61

Chapter-II

Analyzing the role of Mindbomb1 in the Planar Cell Polarity pathway

Introduction

II.1 Functions regulated by the PCP pathway -----	63
II.1.a PCP and orientation of hairs and cilia-----	63
II.1.b PCP and oriented cell divisions-----	65
II.1.c PCP and cell migration-----	66
II.1.d Convergent Extension-----	69
II.2 The molecular basis of PCP signaling -----	72
II.2.a Classification of Wnt signaling pathways-----	72
II.2.b The core PCP/non-canonical Wnt signaling pathway-----	74
II.2.c The Fat, Dachous and Four-jointed (Ft-Ds-Fj) pathway-----	78
II.3 Mechanism of establishing PCP -----	79
II.3.a Inhibitory and stabilizing interactions-----	79
II.3.b Polarized microtubule trafficking of PCP components-----	81
II.3.c Endocytosis and endosomal trafficking facilitates asymmetric sorting-----	81
II.3.d Post-translational modifications fine-tune PCP protein function-----	83
II.4 Additional regulators of the core PCP pathway -----	84
II.4.a Ryk is an important regulator of the core PCP pathway-----	84
II.5 Mindbomb1 functions independent of Notch signaling -----	88
II.5.a Mib1 regulates Ryk mediated Wnt/ β -catenin signaling-----	88
II.5.b Mib1 regulates directional cell migration-----	88

II.5.c Mib1 regulates apoptosis via extrinsic cell death pathway-----	89
II.5.d Mib1 regulates NF-κB signaling-----	89
II.5.e Mib1 is important for the regulation of ciliogenesis-----	90
II.5.e Role of Mib1 in regulating PCP-----	90

Results

II.1 Analyzing the role of Mib1 in the planar cell polarity pathway-----	92
II.2 Article under review in the journal PNAS Brief Reports-----	93
II.3 Supplementary Information-----	104
II.4 Author contributions-----	108
Conclusion-----	109

Chapter-III

Discussion and Perspectives

III.1 Analyzing the role of Notch signaling in zebrafish neural tube morphogenesis-----	111
III.1.a Notch signaling and apico-basal polarity-----	111
III.1.b Notch signaling and c-divisions-----	113
III.1.c Notch signaling and neural tube morphogenesis-----	113
III.2 Analyzing the role of Mindbomb1 in the planar cell polarity-----	115
III.2.a Mib1 regulates axis extension during gastrulation-----	115
III.2.b Mib1 controls axis extension independently of Notch signaling-----	116
III.2.c Mib1 acts as an E3-ubiquitin ligase in axis extension-----	117
III.2.d Differences between Mib1 morphants and Mib1 mutants in axis extension-----	118
III.2.e Mib1 mediated Ryk endocytosis is necessary for axis extension-----	120
III.2.f Significance of Mib1 mediated Ryk endocytosis-----	120

Chapter IV

General Conclusion

General Conclusion-----	126
References-----	128

List of Abbreviations

- ADAM:** A disintegrin and metalloproteinase
- ANK:** Ankyrin repeats
- A-P axis:** Anterior-Posterior axis
- aPKC:** atypical Protein Kinase C
- Arp2/3:** Actin related protein 2/3
- bHLH:** basic Helix-Loop-Helix protein
- CDC42:** Cell Division Cycle 42
- C-division:** Crossing-division
- CE Angle:** Angle between head and bud of a bud stage zebrafish embryo
- CE:** Convergent Extension
- CELSR1:** Cadherin EGF LAG Seven-Pass G-Type Receptor 1
- CNS:** Central Nervous System
- Crb1:** Crumbs1
- CRD:** Cysteine- Rich-Domain
- CSF:** Cerebro Spinal Fluid
- CSL:** C-promoter Binding Factor 1/Suppressor of hair-less/Lag-1
- CTNNB1:** Catenin Beta 1
- DAAM1:** Disheveled-associated activator of morphogenesis 1
- DAPI:** 4',6-Diamidino-2-Phenylindole, Dihydrochloride
- Dgo:** Diego
- Dlg:** Disc Large
- Dll:** Delta-like
- Ds:** Dachshaus
- Dsh/Dvl:** Dishevelled
- DSL:** Delta, Serrate and Lag2

ECD: Extra Cellular Domain
ECM: Extra Cellular Matrix
EGF: Epidermal Growth Factor
elavl3: ELAV Like RNA Binding Protein 3
EOGT1: O-linked N-Acetylglucosamine Transferase
FBMN: Facial Branchio Motor Neurons
Fj: Four-jointed
Fmi: Flamingo
Ft: Fat
Fz: Frizzled
GAP43: Growth Associated Protein 43
GFAP: Glial Fibrillary Acidic Protein
HECT: Homologous to the E6-AP Carboxyl Terminus
Her4: Hairy enhancer of split-related 4
Hes1: Hairy/enhancer of split
IL-6: Inter Leukin-6
JNK: Jun N-terminal Kinase
LEF: lymphocyte enhancer factor
Lgl: Lethal giant larvae
MAGUK: Members associated Guanylate kinase homologues
MAML: Master mind like
MDCK: Madin-Darby Canine Kidney cells
MHB: Midbrain Hindbrain Boundary
Mib1: Mindbomb1
M-L axis: Medio-Lateral axis
MZ: Maternal-Zygotic
NECD: Notch Extra Cellular Domain

Neur: Neuralized

NFAT: Nuclear Factor of Activated T-Cells

NICD: Notch Intra Cellular Domain

NSCs: Neural Stem Cells

Pals1: Protein associated with Lin7

Par/Pard: Partition defective protein

PCM: Pericentriolar Material

PCP: Planar Cell Polarity

P-D axis: Proximal-Distal axis

PDZ: PSD95-Dlg1-ZO1

Pk: Prickle

pN: pico Newton

POFUT1: Protein O-Fucosyltransferase 1

POGLUT1: Protein O-Glucosyltransferase-1

PTK7: Protein Tyrosine Kinase 7

Rac1: Ras-Related C3 Botulinum Toxin Substrate 1

RBPJ: Recombination Signal Binding Protein For Immunoglobulin Kappa J

RF: RING Finger

RhoA: Ras Homolog Family Member A

RING: Really Interesting New Gene

ROR: Receptor Tyrosine Kinase like orphan receptor

RYK: Receptor related to Tyrosine Kinase

SOP: Sensory Organ Precursor

TCF: T-cell factor

Vangl: VanGogh-like

WNT: merge of homologous protein names Wg (Wingless in *Drosophila*) + Int-1 (mice)

ZO1: Zonula occludend-1

List of Figures and Tables

Chapter I

Analyzing the role of Notch signaling in zebrafish neural tube morphogenesis

Introduction

Figures

Figure 1. Different mechanisms of lumen formation-----	29
Figure 2. Different methods of neurulation in vertebrates-----	32
Figure 3. Midline crossing c-divisions during zebrafish neurulation-----	34
Figure 4. Apico-basal polarity of a tubular epithelium-----	36
Figure 5. The Delta/Notch signaling pathway-----	39
Figure 6. Developmental function of Notch signaling-----	41
Figure 7. Structure of Notch ligands and Notch receptor-----	45
Figure 8. Mechanotransduction of Notch activation-----	45
Figure 9. Ubiquitination by a RING-type E3-ubiquitin ligase-----	53
Figure 10. Structure of Mindbomb1-----	53

Results- Article published in the journal Scientific Reports

Figures

Figure 1. Mindbomb1 is required for zebrafish spinal cord morphogenesis.-----	58.3
Figure 2. Notch pathway activity is required for spinal cord morphogenesis-----	58.4
Figure 3. Notch signaling is dispensable for floor plate apico-basal polarity-----	58.5
Figure 4. Notch signaling is required for the establishment of apico-basal polarity in the dorso-medial spinal cord.-----	58.6
Figure 5. Notch signaling is required to allow the emergence of neuroepithelial identity-----	58.7
Figure 6. Notch loss of function differentially affects neuroepithelial polarity in the brain and spinal cord-----	58.9

Figure 7. Dissection of the spatial requirement for Notch signaling in neural tube morphogenesis-----58.11

Figure 8. Notch loss of function impairs morphogenetic cell movements in the zebrafish spinal cord-----58.12

Supplementary Information-----58.19

Figure S1. Mindbomb1 is important for zebrafish spinal cord morphogenesis

Figure S2. Notch pathway components are required for the apico-basal polarity of the zebrafish spinal cord

Figure S3. Early floor plate morphogenesis occurs in the absence of detectable Notch reporter activity

Figure S4. Excessive neuronal differentiation causes neural tube morphogenesis defects in mindbomb1 mutants

Figure S5. Mindbomb1 double mutants retain neuroepithelial polarity in the midbrain-hindbrain boundary region

Figure S6. Mib1 loss of function impairs the midline-crossing of neural tube cells

Figure S7. Notch-mediated suppression of neurogenesis is required for midline-crossing cell divisions in the zebrafish neural tube

Figure S8. Loss of Notch signaling affects the cell number and proportions of the neural tube

Supplementary Tables

Table S1. Percentage of the neural tube area occupied by elavl3-positive neurons

Table S2. Midline crossing index of zebrafish neural tube cell at the 16 somites stage

Table S3. Midline crossing index of zebrafish neural tube cells at the 18 somites stages

Table S4. Neural tube Width-to-Height ratio at the 30 somites stage

Table S5. Neural tube cell number at the 30 somites stage

Chapter II

Analyzing the role of Mindbomb1 in the Planar Cell Polarity pathway.

Introduction

Figures

Figure 11. Orientation function regulated by Planar Cell polarity-----	64
Figure 12. Directional migration regulated by Planar Cell Polarity-----	67
Figure 13. Convergent Extension (CE) is regulated by Planar Cell Polarity-----	70
Figure 14. Classification of Wnt signaling pathways-----	73
Figure 15. Mechanism of Fat, Dachous and Four-jointed pathway-----	77
Figure 16. PCP core component interactions across a cell border-----	80
Figure 17. Endocytosis, trafficking and degradation events during PCP patterning-----	81
Figure 18. Structure of PCP related Receptor Tyrosine Kinases (RTKs)-----	85

Tables

Table 1. PCP signaling components in both vertebrates and invertebrates-----	75
---	----

Results- Article under review in PNAS Brief Reports

Figures

Figure 1. Mib1 regulates PCP-dependent convergent extension movements-----	98
Figure 2. Mib1 controls PCP by Ryk endocytosis.-----	100

Supplementary Results

Figure S1. Localization of Fz2, Fz7 and Wnt11 under Mib1 overexpression-----	104
Figure S2. Ryk protein level is not affected in Mib1 morphants-----	105

Chapter - I

**Analyzing the role of Notch signaling in zebrafish neural
tube morphogenesis**

Introduction

The primary goal during the first part of my PhD was to understand the role of Notch signaling in regulating neural tube morphogenesis during zebrafish embryogenesis. Therefore, in the introduction of this first chapter, I will highlight the process of neural tube morphogenesis in zebrafish in comparison with other vertebrates and then, describe the role of Delta/Notch signaling and its pathway components in regulating different functions during invertebrate and vertebrate development.

I.1 Tubular organ morphogenesis.

Morphogenesis is the process of establishing the shape and the structure of an organism (or a part of an organism) that is essential for its proper functioning. One of the key events during morphogenesis of organs like the central nervous system, heart, lungs etc. is formation of a lumen/tube that can transport and distribute metabolites that are essential for functioning of the respective organs. For example, morphogenesis of the nervous system involves formation of the neural tube lumen that will later develop as the brain ventricular system that carries cerebrospinal fluid (CSF). And this CSF acts as a circulatory system for the brain and spinal cord that performs functions including the transport of nutrients and wastes(1).

Tubular organs are mainly formed by five mechanisms: wrapping, budding, cord or cell hollowing and cavitation(2-6) (Fig.1). Wrapping and budding occur in a sheet of epithelial cells that are already polarized. During wrapping, an entire row of epithelial cells invaginates to finally pinch off from the sheet that give rise to a long tube running parallel to the plane of the epithelium (Fig.1A). The neural tube of mammalian and avian embryos are formed via wrapping(7). During budding, one or more cells invaginate from an existing tube or sheet of cells to create a new shorter tube orthogonal to the plane of the epithelium (Fig.1B) (e.g. angiogenic sprouting where new blood capillary buds or sprout from an existing blood vessel(8)). In the case of cord hollowing, cell hollowing and cavitation, lumen formation arises from a group of loosely adherent mesenchymal cells that undergo polarization and thus, acquire epithelial identity during the process of lumen formation. In cord hollowing, a group of mesenchymal cells undergo condensation that results in formation of a cylindrical cord. Then the cord undergoes epithelialization and small lumens are created between the cells which all fuse together to form a single central lumen (Fig.1C)

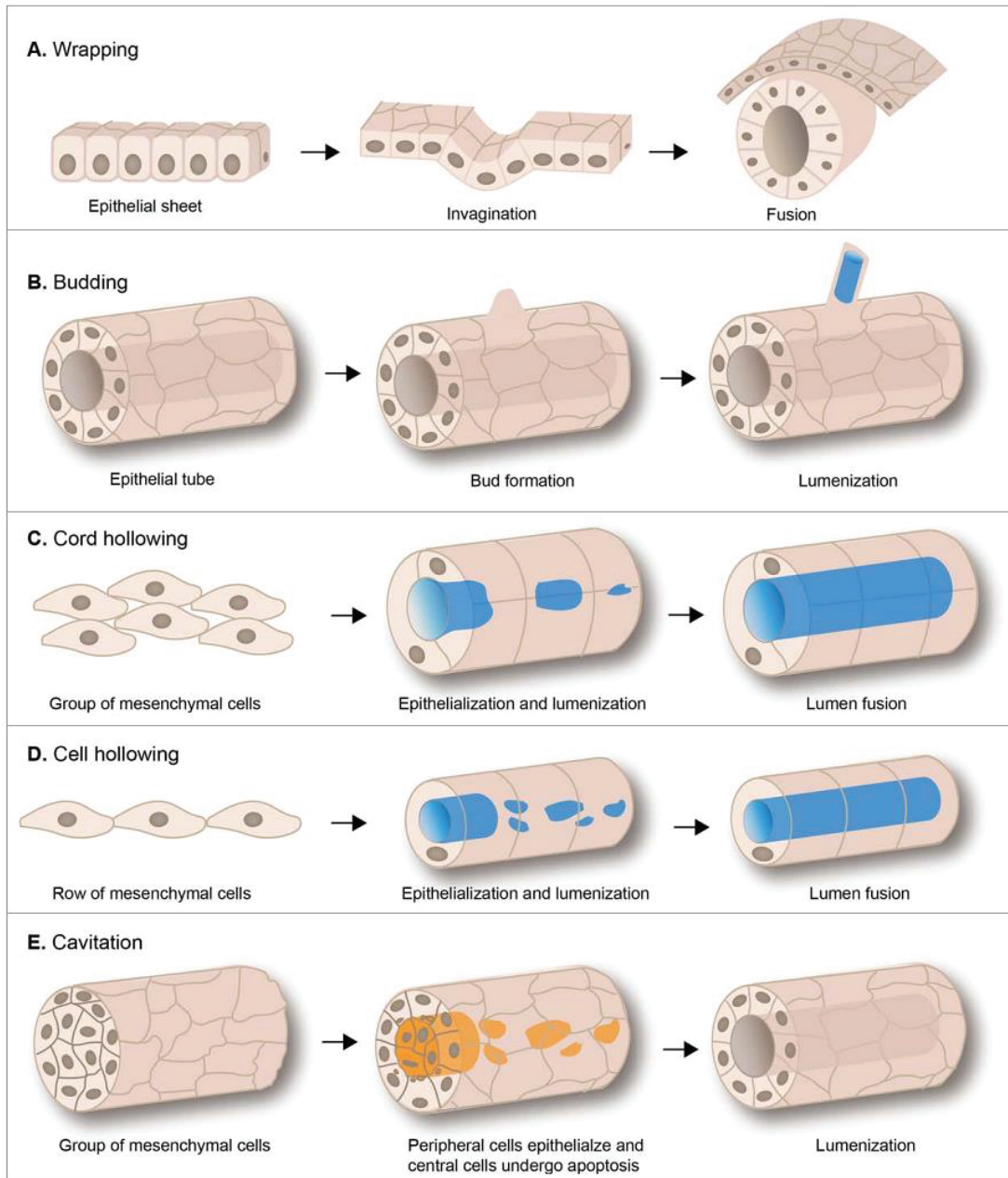


Figure 1. Different mechanisms of lumen formation. A) Wrapping involves the invagination of a sheet of epithelial cells that results in pinching off from the sheet as a tube. B) Budding- invagination of a group cells from a sheet or tube of cells that finally results in a smaller tube orthogonal to the initial plane of epithelium. C, D, E) Cord hollowing, Cell hollowing and Cavitation involve condensation and epithelialization of a group of mesenchymal cells. In Cord hollowing, lumens created between the cells get finally merged to form a single central lumen. Lumen formation in cell hollowing happens intracellularly to get merged as a single lumen. Cavitation involves apoptosis of central cells of the cord that results in the lumen formation. (*Baumholtz et.al. 2017*)

(e.g. the formation of zebrafish gut (9) and *Drosophila* heart (10)). Cell hollowing involves formation of a lumen within the cell. A group of mesenchymal cells condense to form a cord of single cells and after epithelization small lumens are formed intracellularly that fuse together to form a continuous lumen (Fig.1D) (e.g. zebrafish blood vessel formation(11)). During cavitation, mesenchymal cells condense to form a cord and undergo epithelial cell polarization, but the lumen is created by apoptosis of cells in the center of the cord (Fig.1D).

In all these different mechanisms of lumen formation, establishment of apico-basal polarity in epithelial cells is a crucial prerequisite. Lumen growth is initiated by the polarized trafficking of vesicles towards the apical side of the cell facing the lumen and their fusion with the plasma membrane. Lumen formation requires asymmetric distribution of transmembrane proteins such as E-cadherin and integrins. Once they become activated, intracellular signaling leads to cytoskeletal rearrangements, which facilitate recruitment of apical determinants and vesicles necessary for lumen initiation. For example, It has been shown that MDCK cells that lacks β 1-integrin are incapable of initiating polarization and therefore, lumen formation is absent in 3D cell cultures(12). Similarly, in cultured mammalian salivary gland explants, antibody blocking and siRNA knockdown of E-cadherin delay or block polarization and result in the formation of aberrantly dilated lumens filled with apoptotic cells(13). After lumen formation, different steps including tube elongation, lumen expansion and tube maturation will be followed to create a functional tubular organ(4, 6).

I.2. Neural tube morphogenesis

The Central Nervous System (CNS) is one of the several tubular organs that develops a lumen during morphogenesis. The morphogenetic events that result in formation of the neural tube, future brain and spinal cord, are called neurulation. Abnormalities in neurulation will lead to severe neural tube defects that will compromise the functionality of the nervous system.

I.2.a Neurulation in amniotes and amphibians.

Neurulation in amniotes occurs through primary and secondary neurulation, where two different mechanisms are used at each steps(14). The anterior neural tube that extends from the brain to the future trunk (cervicothoracic) region undergoes primary neurulation and the posterior neural tube

from the tail bud region undergoes secondary neurulation. During primary neurulation, neural tube is created by the process of ‘wrapping’, whereas ‘cord hollowing is involved during secondary neurulation(2, 4).

Primary neurulation begins with a neural plate structure that has a layer of pseudo-stratified epithelial cells with a clear apical and basal polarity(15-17). Apico-basal polarity of these epithelial cells is not generated during the neural plate stage, but they were already polarized when they constituted the epiblast of the embryo(18). At first, epithelial cells of the neural plate undergo an elongation along their apico-basal axis to increase their height and as a result, reduce their width to form columnar epithelial cells(19). This elongation step is driven by microtubule assembly controlled by γ -tubulin with the help of Shroom family actin binding proteins(20-22). Shroom proteins are not only required for apico-basal elongation but also for apical constriction that leads to bending or invagination of the neural plate along the midline(23, 24). Through several morphogenetic processes such as cell intercalation, convergent extension, apical neighbor exchange and apical constriction, cells in the neural plate undergo wrapping, and wedge-shaped cells are formed that create lateral hinge points(25, 26). And finally, the neural tube is pinched off by fusion of cells at the hinge points (Fig. 2A).(14, 27). Secondary neurulation in amniotes happens in the posterior neural tube from a group of undifferentiated mesenchymal cells(28, 29). These mesenchymal cells condense to form a rod like structure which will undergo epithelialization. Afterwards, small lumens are created through cavitation and they are fused together to form a single central lumen (Fig. 2D)(30).

In amphibians, the mechanism of neurulation varies from species to species. The Mexican salamander *Ambystoma mexicanum* has a single layer of columnar epithelial cells at the neural plate(31). However, in *Xenopus laevis*, the neural plate at the spinal cord level is a bi-layered tissue composed of a polarized superficial cell layer and a non-polarized underlying cell layer(32, 33). During neurulation, the bi-layered neural plate starts invagination and creates shallow a neural fold around the edge of the neural plate. Cell rearrangements, such as convergent-extension and radial intercalations, happen between the polarized superficial layer and the underlying non-polarized cells. Finally, the neural fold come into close apposition and fusion of cells happen at the hinge points creating a ventral lumen (Fig. 2B).(32, 33)

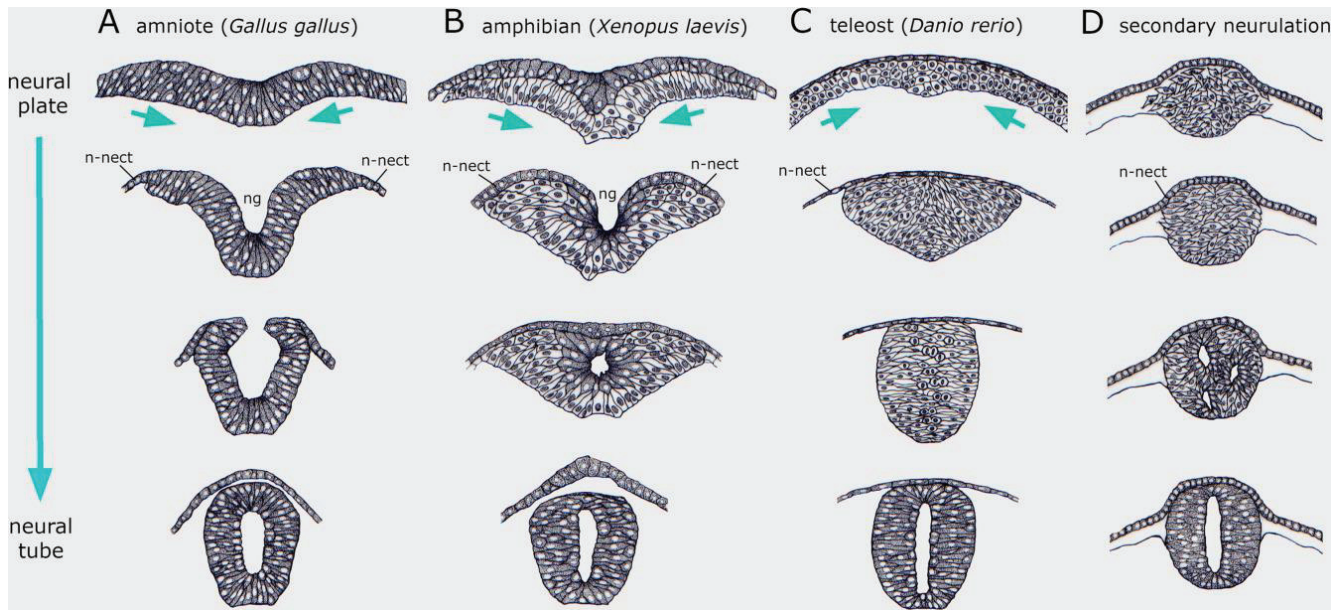


Figure 2. Different methods of neurulation in vertebrates. Only neural ectoderm and non-neural ectoderm (n-nect) are considered for representation. In all pictures, grey cells with white nuclei represent polarized epithelium and white cells with grey nuclei represent non-polarized tissue. Arrows indicate tissue movement; the neural groove is marked as ng. A) Primary neurulation in chick embryos where the neural plate consists of polarized epithelial cells undergo wrapping to create a neural tube. B) Neurulation in frog starts with a bi-layer consisting of a polarized apical layer and a non-polarized basal layer and the neural tube lumen is created by tissue invagination. C) Neurulation in zebrafish begins with non-polarized neural progenitors that undergo cavitation to generate the neural tube lumen. D) Secondary neurulation happens in both chick and mouse where the neural tube lumen is created by cord hollowing. (Araya et. al 2016)

I.2.b Neurulation in zebrafish.

Zebrafish neurulation begins with non-polarized neural progenitor cells that form a multilayered structure at the anterior regions (forebrain, midbrain and hindbrain) of the neural plate, which gradually thins down to become a single layer in the posterior region (spinal cord)(34, 35). Even though the early teleost neural plate does not appear to be organized like a conventional epithelium in other vertebrates, it shows a coherent epithelial-like tissue behavior where cells maintain their relative position among neighbors while undergoing morphogenetic movements(36). These epithelial-like cells clearly lack expression of apical markers of a mature epithelium at the neural plate stage and they are largely cuboidal in shape(37, 38). Therefore, one can consider that these

progenitor cells in the zebrafish neural plate have both epithelial and mesenchymal characteristics(14).

In zebrafish, neurulation starts around 10-11 hours post fertilization (hpf), when cells from both sides of the neural plate start to converge towards the dorsal embryonic midline. Next, around 12 hpf, cells in the neural plate start to internalize at the midline to generate a solid keel-like structure. By 15-17hpf, neuroectodermal cells in the neural keel undergo extensive cell elongation and intercalation that results in formation of a solid cylindrical structure called the neural rod. Finally, at 18hpf, cells on both sides of the neural rod midline establish apico-basal polarity and apical surfaces of these cells start the lumen development to form a neural tube (Fig. 2C).(14, 27, 36, 39-41)

I.2.c Midline crossing cell divisions are important for zebrafish neurulation.

During zebrafish neurulation, progression from the neural keel to the neural rod is characterized by a unique process called midline crossing cell divisions (c-divisions)(36, 42). Neural progenitor cells from one half of the developing neural tube come to the midline and undergo mirror symmetric cell divisions to deposit one of the daughter cells in the contralateral side of the developing neural tube (Fig.3A-D)(36, 42, 43). C-divisions are crucial for morphogenesis of the zebrafish neural tube because apical ends of c-dividing cells have the potential to demarcate the midline of the neural rod which will develop into the future lumen. In a wildtype condition, apical ends of c-dividing cells coincide with the geometric midline of the neural tube. Therefore, only a single neural tube is formed in the developing embryo. If the timing and location of c-divisions are disrupted using a Planar Cell Polarity pathway mutant *vangl2*, which delays the convergence of the neural tissue, c-divisions occur at ectopic locations in the neural tube, and creates a neural tube with two lumens (34, 44). However, c-divisions are not absolutely necessary for developing a single neural tube lumen because studies have shown that inhibition of cell divisions rescue the formation of a single lumen in PCP mutants(44, 45). Nonetheless, such a lumen created in the absence of c-divisions will be malformed. Therefore, c-divisions provide a morphogenetic advantage for the embryo to form a continuous functional lumen(46).

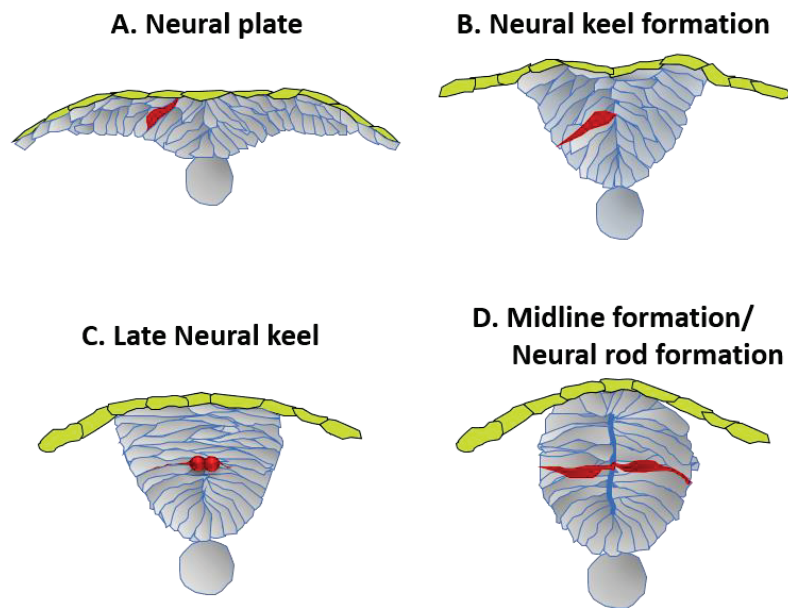


Figure 3. Midline crossing c-divisions during zebrafish neurulation. C-divisions happen between the Neural keel and Neural rod stage of zebrafish neurulation. Neural progenitor cells from one side of the developing neural tube come to the midline, and then undergo cell division to deposit one of the daughter cells on the other side of the developing neural tube. (Picture credits: Priyanka Sharma)

C-divisions are regulated via intrinsic mechanisms of neural progenitor cells. Studies have shown that maternal zygotic (MZ) *vangl2* mutant cells transplanted into wildtype hosts failed to undergo c-divisions whereas wildtype cells transplanted into MZ-*vangl2* mutant hosts undergoes c-divisions(44). Apart from *vangl2*, the PCP pathway component *frizzled 7 (fz7)* is important for c-divisions. In MZ-*fz7a/b* mutant embryos, c-divisions were severely compromised and no coherent midline structure was visible at 16hpf(45). Appearance of apical polarity features in neural progenitor cells seems to be coinciding with the occurrence of c-divisions. During c-divisions, the apical polarity protein Pard3 re-localizes to the cleavage plane and remains at the apical ends even after division. This apical accumulation of Pard3 is essential for cells undergoing c-divisions(34). Another important factor that regulates c-divisions is mitotic spindle orientation. When the polarity protein Scribble and the cell adhesion protein N-cadherin are mutated, spindle orientation is severely affected and perturbs midline crossing c-divisions(47).

I.2.d Epithelialization of neural progenitor cells is important for zebrafish neurulation.

Establishment of apico-basal polarity that leads to epithelialization of neural progenitor cells is a crucial step in neural tube lumen formation(1, 48). A typical epithelial cell has an apical surface, often distinguished by the presence of villi-like structures, that faces either a lumen or an external environment and a basal surface that interacts with an extra-cellular matrix or other cells. Apico-basal polarity of an epithelial cell is the asymmetric distribution of proteins, structures and functions from basal surface to the apical surface. The apico-basal polarity of epithelial cells is mainly governed by three well conserved polarity complexes namely, Par complex (consists of Cdc42, Par3, Par6 and aPKC), Crumbs complex (Crumbs, Pals1 and Patj) and Lethal giant larvae (Lgl) and Scribble complex (Scribble (Scrib), Disc large (Dlg) (Fig.4) (49, 50). Both the Par and Crumbs complexes promote apical membrane identity, whereas Scribble complex promotes basolateral membrane identity by antagonizing the other two. To restrict Par complex to the apical domain, Lgl competes with Par3 for Par6-aPKC(51, 52). Moreover, phosphorylation and inactivation of Lgl at the apical domain by aPKC restricts the Par and Scribble complex in the apical domain and baso-lateral domain respectively(53). Interestingly, aPKC is also able to phosphorylate Crumbs to promote apical localization of the Crumbs complex(54). Therefore, key phosphorylation events and protein-protein interactions make sure that these three polarity complexes are restricted to their respective domains. Cell-cell adhesion molecules including cadherins, nectins and junctional adhesion molecules play a crucial role in triggering the development of apico-basal polarity(55). They interact with conserved cell polarity proteins to regulate the recruitment of polarity complexes to specific sites of cell-cell adhesion and further signaling cascades at those sites will resolve the polarity complexes into different domains(55).

At the beginning of neurulation in zebrafish, neural progenitor cells lack apico-basal polarity (37, 38). The first appearance of apical polarity markers such as Par3, aPKC and tight junction components like ZO1, N-Cad occurs only around mid-segmentation stages when c-divisions start to occur(37, 38, 46, 47). Embryos that are lacking apical polarity proteins such as aPKC(56), Pard6(57) and the MAGUK protein *nagie oko*(58) show discontinuous lumen phenotypes, similar to lumen formation defects of embryos that are blocked for cell division(46). Epithelial polarization during zebrafish neurulation is dependent on microtubule mediated transport. Disruption of microtubular components by nocodazole treatment inhibits the apical accumulation

Pard3 during c-divisions(46). Additional cues are required from the extracellular matrix (ECM) for apico-basal polarization of neural progenitors. For example, knockdown of the ECM protein Laminin1 resulted in ectopic basal accumulation of normally apically localized ZO1(46), and this is thought to be regulated via the $\beta 1$ integrin (59).

Even though c-divisions and epithelialization of neural progenitor cells act in tandem to regulate zebrafish neural tube morphogenesis, we still don't know the connection between these two morphogenetic processes and what is regulating them.

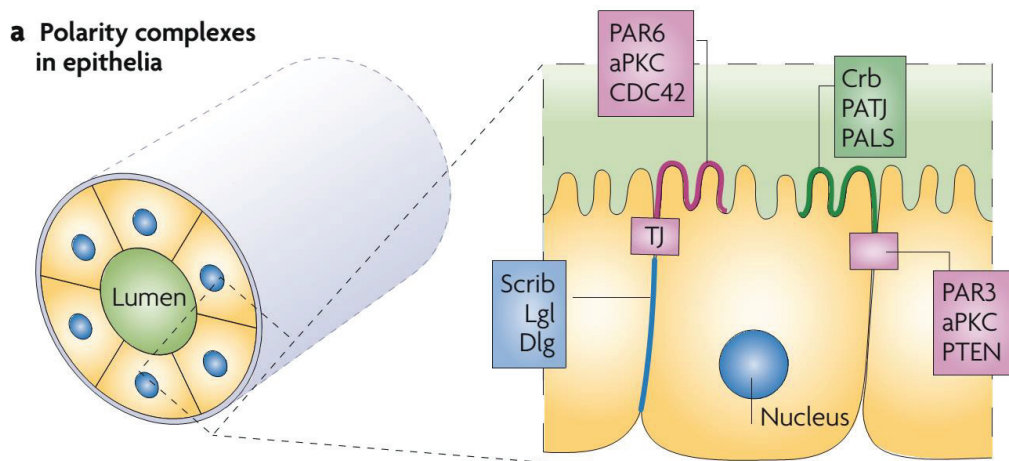


Figure 4. Apico-basal polarity of a tubular epithelium. In a polarized epithelium, there are three polarity complexes: the PAR complex (CDC42-PAR3-PAR6-aPKC), the Crumbs complex (Crb-PALS-PATJ) and the Scribble complex (Scrib-Dlg-Lgl). The PAR complex and Crumbs complex maintains apical polarity, whereas the Scribble complex operates at the basolateral surface. The PAR complex can be divided into two subcomplexes: apical CDC42-PAR6-aPKC and the Tight Junction (TJ) associated PAR3-aPKC. PAR3-aPKC recruits the lipid phosphatase PTEN to the TJ. (Bryant and Mostov, 2008)

I.2.e Notch signaling regulates radial glial formation during spinal cord morphogenesis.

Before neurogenesis, the neural plate of tetrapod embryos is composed of a pseudostratified single layer of neuroepithelial cells that have a well-defined apico-basal polarity(60). During development, neuroepithelial cells, which can be considered as stem cells, initially undergo

symmetric proliferative divisions to generate two daughter stem cells(61). These divisions are followed by many asymmetric self-renewing divisions to generate a daughter stem cell and a more differentiated non-stem cell or a neuron. Neural non-stem cell progenitors typically undergo symmetric differentiating divisions that give rise to terminally differentiated post mitotic cells(61). Notch signaling has been well studied for its role in maintaining the balance between self-renewing neural stem cells and differentiating neurons(62, 63).

Radial glial cells are apico-basally polarized cells that are derived from neuroepithelial cells(61). They exhibit residual properties of both neuroepithelial and astroglial cells, but radial glial cells represent more fate-restricted progenitors compared to neuroepithelial cells(61). Apico-basally polarized neuroepithelial cells along with radial glial cells provide a structural scaffold for the developing Central Nervous System. In the mouse forebrain, ectopic activation of Notch signaling has been shown to promote radial glial identity(64). Disruption of *hes1* and *hes5*, known Notch effector genes, causes rapid depletion of radial glial cells by premature differentiation into neurons(65). Moreover, premature loss of radial glia abolished the inner and outer barriers of mouse spinal cord leading to the escape of neurons into the lumen and surrounding regions. Thus, loss of radial glial cells affected mouse neural tube morphology(65). In zebrafish, Notch signaling is continuously required for maintenance of radial glial cells during embryogenesis(66). Asymmetric cell divisions of radial glial cells generate a self-renewing daughter cell that migrates to a basal position and a differentiating sibling that remains at the apical position of the zebrafish brain(67). Directional Notch signaling from the apical differentiating daughter towards the basal self-renewing daughter is necessary for this binary cell fate decision. Directional segregation of Notch signaling is achieved via unequal segregation of Mindbomb1, an E3-ubiquitin ligase important for Notch signal activation, in a Par3 dependent fashion(67). Tight regulation of adherens junctions, which attach the apical end feets of both neuroepithelial and glial cells, is also required for maintenance of neural stem cells and thus, maintains the epithelial architecture of the developing neural tube(68). These experiments indicate a complex relationship between Notch signaling and embryonic neurogenesis during nervous system morphogenesis.

In contrast to tetrapods, the zebrafish neural primordium lacks a polarized epithelial architecture in the initial stages of zebrafish spinal cord morphogenesis(27, 34, 38). Major hallmarks of apico-basal polarity such as apical Pard3 protein localization, adherens junction and tight junction

components appear only after the beginning of neuronal differentiation(27, 34, 38, 69). And Notch signaling regulates early neuronal differentiation in zebrafish(70). This raises the question whether and how Notch signaling and neuroepithelial morphogenesis are linked during zebrafish neural tube development?

I.3 The Notch signaling pathway.

Notch signaling is a well conserved signaling pathway in multicellular organisms that governs functions such as cell fate specification, proliferation, differentiation, apoptosis etc(62, 71, 72). In brief, the Notch signaling pathway happens over the communication between a signal sending cell and a signal receiving cell. The signal sending cell expresses Notch ligands such as Delta, Serrate and Lag2 (DSL) whereas the signal receiving cell expresses Notch receptors. Upon binding of ligands with Notch receptors, a series of cleavage reactions occur to release the intra-cellular domain of Notch (NICD) into the cytoplasm. Then, the NICD is translocated into the cell nucleus to form a DNA-binding transcription factor complex with CSL (CBF1, RBP-jk/ Su(H)/Lag1) and Mastermind that regulates target gene expression. Studies have shown that endocytosis of Notch ligands in the signal sending cell is necessary for the activation of Notch receptors in the signal receiving cell(73). And this endocytosis is preceded by ubiquitination, a post-translational modification that adds ubiquitin moiety to the target substrate, of Notch ligands. In vertebrates, the E3-ubiquitin ligase Mindbomb1(Mib1) plays a central role in ubiquitinating Notch ligands (Fig.5)(74-78).

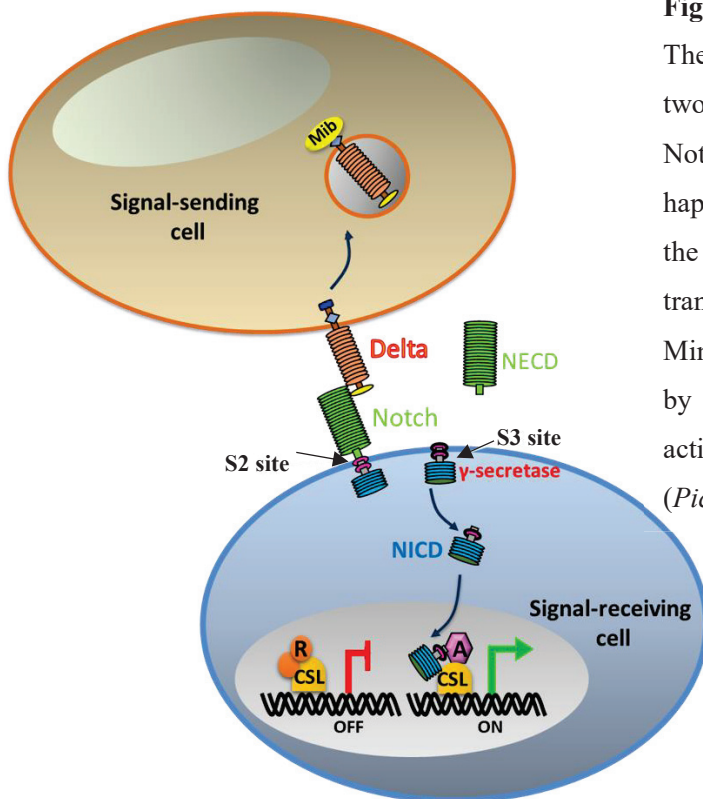


Figure 5. The Delta/Notch signaling pathway.

The Delta/Notch signaling pathway happens between two neighboring cells. Upon binding of Delta with Notch receptor, a series of cleavage reactions happen to the receptor via γ -secretase. Afterwards, the NICD translocates into the nucleus to bind to transcription factors that target gene expression. Mindbomb1 mediates Delta ubiquitination followed by its endocytosis in the signal sending cell to activate Notch signaling in the signal receiving cell.

(Picture credits: Priyanka Sharma)

I.4 Developmental functions of the Notch signaling pathway.

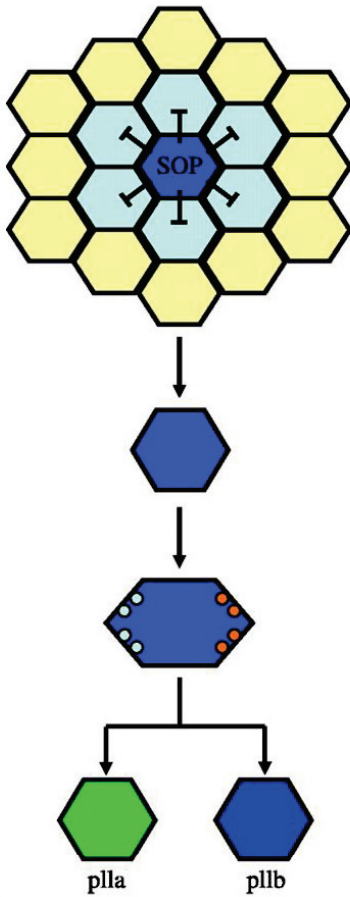
Notch signaling is used repeatedly during development to perform different functions. The modes of action of Notch signaling can be generally divided into three categories: lateral inhibition, binary cell fate decisions and boundary formation(74, 79).

I.4.a Lateral inhibition

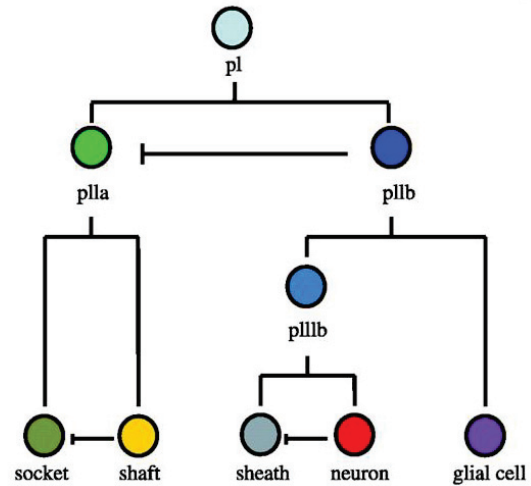
Lateral inhibition happens among a group of progenitor cells that have equal potential to take a particular cell fate. However, only one cell adopts the cell fate and inhibits its surrounding cells from adopting the same cell fate. A classic example for lateral inhibition activity of Notch signaling is the specification of sensory organ precursor (SOP) cells in *Drosophila* neurogenesis. SOP development originates from groups of precursor cells with a similar potential to adopt SOP fate, called proneural clusters. Subtle differences in Delta/Notch signaling among these proneural cells, which are amplified by feedback loops, will create a higher level of Delta in one of them and it will act as the signal sending source cell. This source cell will activate Notch signaling in surrounding cells to inhibit their prospective neural fate(80, 81) (Fig.6A).

Similarly, Notch regulated lateral inhibition can be found in the vertebrate nervous system. For example, in zebrafish, Notch signaling mediates the selection of neural progenitors that become neurons from early proneural cells. The source cell that is singled out via lateral inhibition will express pro-neural genes belonging to the bHLH family of transcription factors, such as Neurogenin1 and Achaete-scute1(82). Pro-neural genes will promote the expression of zebrafish Delta homologs, DeltaA and DeltaD (83, 84), which lead to the activation of Notch signaling in surrounding signal receiving cells. As a result, at least one gene in the Hairy Enhancer-of-split-related family, such as her4, will be activated in signal receiving cells that in turn suppresses the function of proneural genes and thus, prevent them from differentiating into neurons(70, 84, 85). Zebrafish mutants that fail to activate Notch signaling show precocious neurogenesis due to the lack of lateral inhibition whereas ectopic activation of Notch signaling will result in a reduction of neurogenesis(75, 85).

A. Lateral Inhibition



B. Binary cell fate decision



C. Boundary formation

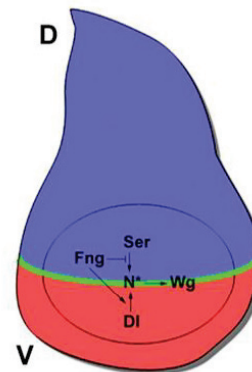


Figure 6. Developmental function of Notch signaling. A) During *Drosophila* neurogenesis, the selection of sensory organ precursor (SOP) cell fate from a proneural cluster is done by lateral inhibition activity of Notch signaling. Asymmetric segregation of polarity components and Notch regulators to opposite poles of the pI/SOP cell will give rise to asymmetric cell division. B) The pI cell undergoes several rounds of asymmetric cell divisions to generate binary cell fates which will ultimately create five different cell types: socket, shaft, sheath, neuron and glia. C) Boundary formation occurs in the *Drosophila* wing imaginal disc by differential expression of Notch regulators in the dorsal (D) and the ventral (V) compartment. (Picture adapted from *Fiuza and Arias, 2007; Tossell et.al. 2011*)

I.4.b Binary cell fate decision.

Binary cell fate decisions occur when Notch signaling is activated in only one of the two daughter cells due to asymmetric distribution of Notch signaling regulators during cell division. For example, in *Drosophila*, a single SOP cell can give rise to five different cell types: shaft, socket, glia, sheath and neuron. This is achieved by four rounds of asymmetric cell divisions. The SOP/pI cell will undergo a first round of division that asymmetrically distributes Notch signaling regulators, such as Numb and Neuralised, to only one of the two daughter cells. The cell that inherits Numb and Neuralised will act as the signal sending cell (pIIb) because these two factors enhance Delta endocytosis and also Numb is shown to negatively regulate Notch receptors. The signal sending cell will inhibit its pIIa sister cell from adopting the same cell fate by activating Notch signaling. This process of asymmetric distribution of Notch regulators is repeated three more times to generate five required cell types (86-88)(Fig.6B).

Similarly, in vertebrates, asymmetric segregation of Notch regulators is required to maintain the balance between self-renewing stem cells and differentiating neurons. Radial glial cells in the developing vertebrate nervous system have stem-cell like properties. Asymmetric division of a radial glial cell will generate one self-renewing daughter and another differentiating sibling. This is achieved by asymmetric distribution of the Notch signaling regulator Mib1 in one the daughter cells in a Par-3 dependent manner(67). Mib1 promotes endocytosis of Delta ligands via ubiquitination. Therefore, the daughter cell that inherits Mib1 will differentiate into a neuron and at the same time inhibits its sibling from acquiring the same fate(67).

I.4.c Boundary formation

Boundary specification in a tissue is achieved by differential gene expression of Notch regulators between two compartments. For example, during dorso-ventral boundary formation of the *Drosophila* wing imaginal disc, the Notch ligand Serrate, and the Notch receptor-modifier Fringe are expressed only in the dorsal compartment whereas the second Notch ligand Delta is expressed only in the ventral compartment and the Notch receptor is expressed in both compartments. Fringe modifies the Notch receptor such that the binding affinity for Serrate ligands is reduced and the Delta ligand binding is increased. The Delta ligand in the ventral compartment preferentially binds to Notch receptors that are modified by Fringe. Therefore, Notch signaling is only possible at the boundary between dorsal and ventral compartment where Serrate from the dorsal compartment

activates non-modified Notch receptor in the ventral compartment and Delta from the ventral compartment activates Fringe modified Notch receptor in the dorsal compartment. This boundary formation is further made robust by feedback loops created by Notch target genes (89, 90)(Fig.6C).

In vertebrates, somite formation is a good example for boundary formation regulated via Notch signaling. There is a continuous cycle of activation and inactivation of Notch transcriptional activity that leads to the pattern of somite formation and segmental boundary in the presomitic mesoderm(91). Oscillations can be achieved through direct autorepression of a gene by its own product within the timeframe necessary for the next round of transcriptional and translational activities(92). In zebrafish, overexpression of Delta ligands will accelerate embryonic segmentation whereas inhibition of Notch signaling disrupts oscillations and results in a perturbed segmentation pattern(93, 94).

I.5 Molecular mechanism of Notch signaling.

The functions of Notch signaling vary depending on the spatial and temporal context. This ability of Notch signaling is attributed to its different molecular components. Therefore, in this section, I will outline important aspects of different components of the Notch signaling pathway and mechanisms by which these components act together to activate Notch signaling.

I.5.a Ligand-receptor interaction during Notch signaling.

Notch signaling occurs via communication between a signal sending cell and a signal receiving cell. Since both the receptor and the ligand of Notch signaling are transmembrane proteins, the extra cellular domains of these proteins have to come together to bind and initiate Notch signaling. All canonical Notch ligands are evolutionarily conserved type I transmembrane proteins belonging to the Delta-Serrate-LAG2 (DSL) family of proteins. *Drosophila* has only two DSL ligands, Delta and Serrate, compared to five mammalian ligands. Out of those five mammalian ligands, three of them belong to the Delta-like family (DLL1, DLL2 and DLL4) and two belong to Jagged family of Serrate homologues (JAG1 and JAG2). In zebrafish, there are four Delta ligands (deltaA, deltaB, deltaC and deltaD) and five Jagged ligands (jag1a, jag1b, jag2a, jag2b and jag3). The extracellular domain of all these Notch ligands have multiple EGF repeats (from 6 to 16), a DSL domain and an amino terminal (NT) domain. Jagged/Serrate ligands contain a cysteine-rich domain (CRD) in addition (Fig.7). The DSL domain and the NT domain contribute to the ligand-receptor interaction by binding the EGF repeats 11-12 in the extracellular domain of Notch(95, 96). Additionally, the NT domains have phospholipid binding properties, therefore binding with the adjacent cell membrane is also possible(97). The intra-cellular region of DSL ligands doesn't show any obvious sequence homology. However, most of them tend to have multiple lysine residues and a C-terminal PDZ ligand motif, which are required for ubiquitination and interaction with the cytoskeleton respectively(74) (Fig.7).

Notch receptors are multidomain transmembrane proteins that are well conserved from invertebrates to vertebrates. There is only one Notch receptor in *Drosophila* but there are four different Notch receptors in mammals (NOTCH 1,2,3 and 4) (98, 99). In Zebrafish, Notch receptors are called Notch1, Notch 2a, Notch2b and Notch3. Like Notch ligands, the extracellular domains of Notch receptors have several EGF repeats (from 29 to 36). These EGF repeats

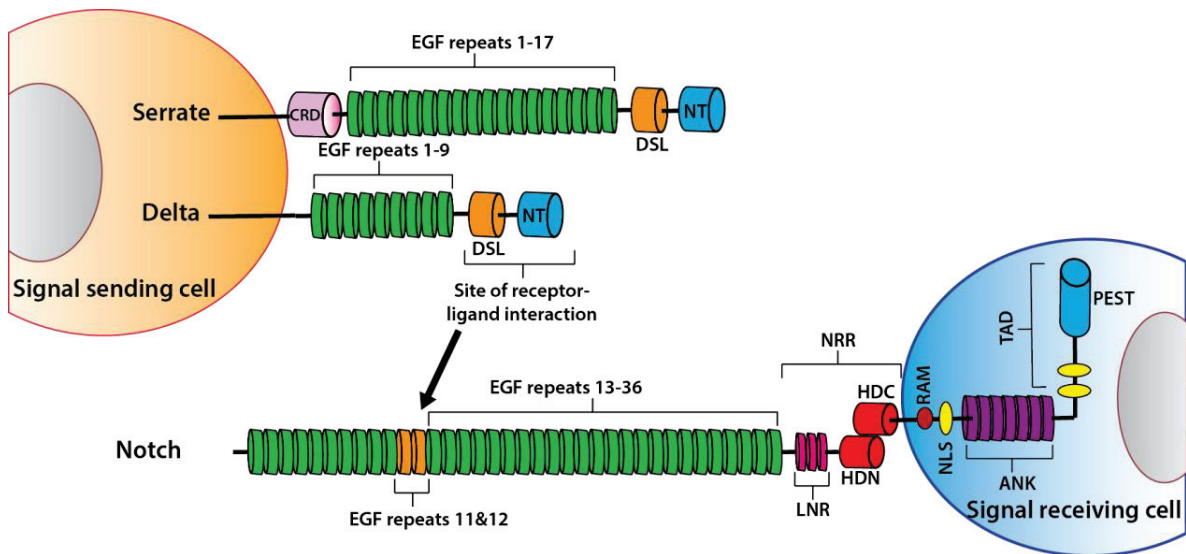


Figure 7. Structure of Notch ligands and Notch receptor. All the canonical Notch ligands belong to the Delta-Serrate-LAG2 (DSL) family of proteins. *Drosophila* has only two DSL ligands, Delta and Serrate, compared to the five mammalian ligands. The extra cellular domain (ECD) of Notch ligands have several EGF repeats, one DSL domain and a NT domain in common whereas Serrate ligands contain a cysteine-rich domain (CRD) in addition. Apart from the several EGF repeats on the ECD of Notch receptors, there is a negative regulatory region (NRR) consisting the cysteine-rich Lin12/Notch repeats (LNR) and two heterodimeric portions (HDN & HDC). The NICD is characterized by a RBPJ-associated module (RAM) domain and ankyrin (ANK) repeats and a PEST domain at the c-terminus. The region from ANK repeats to PEST domain has three nuclear localization sequences, which all together act as trans activation domain (TAD).

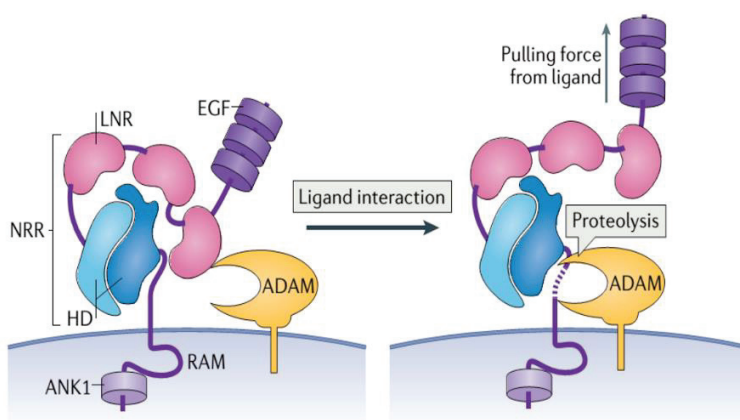


Figure 8. Mechanotransduction of Notch activation. Notch activation is conformationally controlled by the NRR of Notch. Notch activation occurs when a pulling force exerted on the receptor via the ligand that facilitates ADAM access to the cleavage site. (Bray, 2016)

undergo O-linked glycosylation, a post translational modification that adducts different glycan residues to the protein, which are essential for Notch receptor cleavage and ligand sensing(100, 101). Notch receptors are found as heterodimers of its own extracellular portion (HDN) and intracellular portion (HDC) on the cell surface since these receptors are proteolytically cleaved by a furin-like convertase in the Golgi compartment (S1 cleavage) before getting transported to the membrane(102). The two heterodimeric portions along with the cysteine-rich Lin12/Notch repeats (LNR) form the negative regulatory region (NRR) (Fig. 7) and the NRR site guards the cleavage site (S2) from ADAM proteases(103). Upon binding of Notch ligands with the receptor, the S2 cleavage site at the NRR will be exposed to protease activity (Fig. 8) and thus, the Notch extracellular domain (NECD) will be separated from the remaining receptor(104). Afterwards, the remaining transmembrane-intracellular fragment acts as a substrate for the γ -secretase complex, which cleaves the intramembrane S3 site to release the Notch intracellular domain (NICD) (S3-cleavage)(105). After the S3 cleavage, the NICD is translocated into the nucleus to interact with the DNA binding transcription factor CSL, and along with other co-factors they regulate target gene expression(106) (Fig.5). The NICD contains a RBPJ-associated module (RAM) domain and ankyrin (ANK) repeats that are essential for interactions with nuclear transcription factors (Fig. 7)(106, 107). At the c-terminus, NICD has a PEST (means rich in proline, glutamate, serine and threonine) domain that has several motifs recognized by E3-ubiquitinating ligases when phosphorylated (phosphodegrons) and therefore, plays an important role in modulating NICD stability(108). The ANK repeats are flanked by nuclear localization sequences (NLS) and, together with the PEST domain act as a region that can confer transactivation (TAD).

Recent studies have solved the x-ray structures of the Notch1-Dll4 and Notch1-Jag1 complexes (95, 109). Comparison between both receptor-ligand complexes revealed that the interface between Notch1 and Dll4 is larger than the interface between Notch1 and Jag1. This is in accordance with an earlier study showing that Dll4 is having a higher *in vitro* affinity for Notch1 than Jag1(110). An interesting observation is that Notch1-Dll4 interactions involve only EGF11-12 whereas the Notch1-Jag1 complex structure shows that EGF1-3 in Jag1 make additional interactions with EGF8-10 in Notch. This particular type of interaction is indicative of 'catch bonds' in which the strength of interaction increases when greater force is applied or when sheer stress is present(109). A force-clamp spectroscopy study confirmed that indeed Notch1-Jag1 interaction involves catch bonds unlike in Notch1-Dll4 complex(109). These findings suggests

that Jag1 mediated Notch1 activation will be inefficient when a low force is applied (i.e., won't expose the S2 cleavage site in NRR region), whereas Dll4/Notch1 interaction under similar force will result in receptor activation(111).

The EGF repeats of the Notch receptor can undergo modifications such as O-fucosylation, O-glucosylation and O-GlcNAcylation by the enzymes POFUT1, POGLUT1 and EOGT1 respectively(111). Fucosylations can be further extended with N-acetylglucosamine by Fringe proteins to modify the ligand sensing capability of the receptor. For example, in the *Drosophila* wing imaginal disc, modifications by Fringe proteins make Notch insensitive to Serrate ligands(112). Moreover, structural studies have also shown that elongation of an O-fucose on EGF repeat 12 of Notch receptors can add specificities to the receptor-ligand interface(95). This interaction increased affinity of the Notch receptor to Dll1 and Jag1 to a greater extent compared to Dll4(95).

I.5.b Activation of the Notch signaling pathway.

A critical step in Notch signal activation is the extracellular S2 cleavage of the Notch receptor after interacting with ligands. Endocytosis has been shown to be an important factor determining Notch signaling activation(113). Studies have shown that dynamin mediated endocytosis is required in both signal sending and signal receiving cells for efficient Notch signaling. *Shibire/dynamin* mutants in *Drosophila* have excessive neural cells in the absence of Notch signaling mediated lateral inhibition(113). Moreover, studies have shown that Delta and Notch accumulate in endocytic vesicles and endocytosis of Delta or Serrate in the ligand expressing cell is accompanied by “trans-endocytosis” of the Notch extracellular fragment (NECD) from the signal receiving cell(114, 115). Endocytosis of NECD-bound Delta in the signal sending cell is required to activate Notch signaling in the signal receiving cell(73, 116). These experiments have reinforced the fact that endocytosis is crucial for Notch activation.

Based on these observations, two different models have been proposed for endocytosis mediated Notch activation(73, 117, 118). The first “ligand activation model” suggests that DSL ligand endocytosis is required for generating an ‘active ligand’ by preferentially trafficking them into special lipid microdomains where it gets modified to efficiently bind to the Notch receptor. Different experiments conducted using chimeric DSL ligands have provided clues in favor of this model. Deletion of the entire intracellular domain of Delta or specific removal of intracellular

lysines that serve as the target for ubiquitination prevents Delta from Notch activation(75, 119), showing the importance of ubiquitination in Notch signaling. Dll1 ligand that has its intracellular domain replaced with a ubiquitination-defective intracellular domain devoid of lysine residues undergoes endocytosis but, in contrast to the wildtype Dll1, it is unable to be recycled back into the cell surface and bind Notch1 efficiently(120). Dll3 is a Delta homologue naturally devoid of lysines in its intracellular domain. When the Dll1 intracellular domain is replaced with the intracellular domain of Dll3, the chimeric ligand undergoes endocytosis and gets recycled back to the cell surface to interact with Notch1 but is unable to perform Notch activation(120). Interestingly, wildtype Dll1 gets preferentially localized to lipid microdomains (where it is believed to get modified to increase Notch binding affinity), whereas both chimeric Dll1 ligands excluded such domains. These experiments conclude that Dll1 ubiquitination is not required for its initial endocytosis but is rather essential for its preferential trafficking into ‘activating’ lipid microdomains (120).

Another study(119) has provided more evidences showing Delta endocytosis and recycling are necessary for Notch activation. They created a chimeric Delta ligand by replacing its intracellular domain with the intracellular domain of Low-Density Lipoprotein receptor (LDLR), which is shown to undergo rapid recycling. Interestingly, LDLR substituted Delta ligand was successful in activating Notch signaling, but in a ubiquitination independent manner(119). In this case, intracellular trafficking normally mediated by ubiquitination is probably substituted by trafficking directed by motifs in the LDLR intracellular domain. Therefore, this experiment suggests that Delta-LDLR chimera allow Delta to be presented in a more effective manner to Notch because of its endocytosis and recycling(119).

The second “pulling force model” proposes that endocytosis of DSL ligands will generate a pulling force on the Notch receptor to facilitate the S2 cleavage reaction and thus, activate the Notch signaling pathway(121). This model predicts that the NRR of the Notch receptor acts as a mechanosensor which sterically occludes the S2 protease site until ligand binding. In this scenario, ligand binding alone would not be enough to activate Notch. The force generated by endocytosis would induce a conformational exposure of the protease site and thus, activate Notch signaling(121) (Fig.8). This model has gained much popularity recently because of several single molecule force spectroscopic studies(111, 121). Those studies show that a force as small as 4-5pN

is enough to enable cleavage of the NRR by ADAM proteases and thereby, induce activation of Notch receptors(122, 123). A force of 1pN could cluster Notch receptors but could not initiate cleavage reaction even in the presence of Dll1 ligands, confirming the prediction that mere binding of ligands with the receptor is not enough for Notch activation(124). The endocytic pulling force exerted by Dll1 expressing cells averaged around ~3pN but reached up to 10 pN in accordance with the pulling force required for Notch activation(125, 126). These studies provide strong evidences that the NRR of Notch receptor acts as a mechanosensor and the pulling force generated by endocytosis of Notch ligands is sufficient to activate Notch signaling and thus, provide support to the “pulling force model” (Fig.8).

However, there is a possibility that both the ‘ligand activation model’ and the ‘pulling force model’ are not mutually exclusive but act in tandem to activate the Notch signaling pathway.

I.5.c *cis*-inhibition of Notch signaling.

Notch signaling occurs via cell-cell communication of transmembrane proteins where Notch ligands in the signal sending cell *trans*-activate Notch receptor in the signal receiving cell. However, this *trans*-activation of Notch signaling is highly sensitive to the relative number of ligands and receptors present in the signal sending cell owing to a *cis*-inhibition activity, which is an inhibitory interaction that happens between ligands and receptors in the same cell. Studies have shown that high levels of ligand induce a ligand inhibitory effect, whereas lower levels allow ligands to activate Notch in *trans*(90, 127). *cis*-inhibition is necessary for fine-tuning functions regulated by the Notch signaling pathway. For example, during *Drosophila* photoreceptor specification, lack of Delta-mediated *cis*-inhibition reversed the direction of lateral signaling resulting in the formation of a wrong complement of photoreceptors(128). In the chick spinal cord, the Notch ligand Dll1 controls differentiation of neurons by *cis*-inhibition of Notch activity in the signal sending cell(129). Mib1 on the other hand can block Dll1 mediated *cis*-inhibition in the signal sending cell to tightly regulate the delamination of neurons from the apical surface of the spinal cord(129). Similarly, *cis*-inhibition helps to stabilize tip and stalk cell fates during angiogenesis and thus, prevents formation of hybrid tip-stalk cells(130). Interestingly, the mammalian ligand Dll3 has been shown to play only in *cis*-inhibitory mode(131). In an *in vitro* study, Dll3 was unable to *trans*-activate Notch signaling in the neighboring cell. However, when the Dll3 is co-expressed with Notch1, it could inhibit Notch1 from interacting with ligands on the

neighboring cells(131). In accordance with these observations, *in vivo* studies have shown that the loss of Dll3 increased Notch signaling during T cell development (132).

A recent study has demonstrated that *cis*-inhibition is highly dependent on the concentration of ligand versus receptor(133). In an *in vitro* assay to analyze Notch signaling in single cells, *cis*-activation of Notch1 happens with an intermediate concentration of Dll1, whereas at high ligand concentration *cis*-activation is completely replaced by *cis*-inhibition. *Cis*-activation is not a special feature of the Dll1-Notch1 pair but also occurs with other ligands (such as Dll4 and Jag1) and the Notch2 receptor(133).

I.5.d Transcriptional activities of Notch signaling.

Once Notch receptors are cleaved by γ -secretase, NICD peptides are released from the membrane and translocated into the nucleus. Inside the nucleus, the NICD interacts with a DNA binding transcription factor CSL(134, 135). CSL-NICD interaction leads to the recruitment of another co-activator MAML (Master-mind-like) and then NICD, CSL and MAML form a ternary Notch complex that further recruits several chromatin modifiers including the histone acetyltransferase CBP/p300 to regulate target gene expression(106-108, 136, 137).

In the absence of NICD, CSL will be associated with co-repressors such as MINT (MSX2-interacting protein), KyoT2 and Hairless (138-140). Co-repressors, such as class 1 histone deacetylases (HDACs) and the histone demethylases Kdm5 and LSD1, recruit enzyme complexes that can modify the chromatin (141-143). Therefore, CSL remains in a “switched-off” state in the absence of NICD to prevent ligand independent gene regulation. Currently, there are different models that explain how NICD binding could “switch-on” the CSL complex. Initially, a model proposed that upon binding of NICD with the CSL complex, there is a replacement of co-repressors with co-activators (144). However, the binding affinity of CSL for NICD is similar compared to its binding affinity for co-repressors, which argues against the preferential replacement of co-repressors after NICD binding(138, 139, 145, 146). Therefore, a revised model proposes that CSL-activator complexes and CSL-repressor complexes are pre-formed in the nucleus before even binding to the DNA. Upon Notch signaling activation, NICD bound CSL co-activator complexes dynamically competes with CSL co-repressor complexes to bind to the target DNA sequence(136, 147-149).

I.6 The role of Mindbomb1 in regulating the Notch signaling pathway.

Endocytosis of DSL ligands in the signal sending cell is necessary for the activation of Notch signaling in the signal receiving cell(73). It has been shown that ubiquitination of the intracellular domain of DSL ligands is an important prerequisite for their endocytosis(75, 120). In *Drosophila*, there are Neuralized (Neur) and Mindbomb (Mib) playing redundant roles in ubiquitinating DSL ligands(76). However, in vertebrates, only Mindbomb1 (Mib1) is shown to play an important role in ubiquitinating DSL ligands(75, 77). Since there are several paralogues for DSL ligands and Notch receptors, which could function redundantly in vertebrates, Mib1 is chosen more often as a target for inhibiting Notch signaling. Therefore, in this section, I will outline important features of Mib1 and its functional role in ubiquitinating DSL ligands and thereby, regulating Notch signaling.

I.6.a Ubiquitination.

Ubiquitination is a post-translational modification where one or several ubiquitin moieties are covalently added to the target protein. The process of ubiquitination, especially poly-ubiquitination, is usually associated with degradation of the target protein(150, 151). However, mono-ubiquitination or multi-ubiquitination of the target protein will serve alternate functions like endocytic trafficking, kinase activation and transcriptional regulation(150, 151). Ubiquitination happens in three steps: First, an ATP dependent ubiquitin enzyme E1 activates an ubiquitin moiety by adding an ATP molecule (Fig. 9). Then, the activated ubiquitin molecule is transferred to a catalytic cysteine site of the E2-ubiquitin enzyme. This creates a thioester-linked conjugate between the E2 enzyme and the ubiquitin molecule. Finally, the E2-ubiquitin enzyme interacts with the E3-ubiquitin enzyme to transfer the ubiquitin from E2 to a lysine residue in the target protein. The last step can happen in two different ways depending on the type of E3 ubiquitin ligase. In the human genome, two E1 proteins, a family of around 40 E2 enzymes with a conserved catalytic domain and more than 500 E3 ligases have been identified so far(152, 153). E3 ligases have been classified into two categories: HECT domain containing and RING domain containing. Humans have only around 20 HECT domain containing E3 ligases(152). These kind of E3 ligases are directly involved in the catalytic process. At first, ubiquitin is transferred from the E2 enzyme to a catalytic cysteine residue of the HECT domain and then transferred to a lysine residue in the target protein. The second category of E3 ligases are more abundant, known as RING containing E3 ligases. They act like a platform where both the E2-enzyme and the target protein come to

exchange the ubiquitin molecule directly from E2 to a lysine residue of the target protein. Therefore, E3 ubiquitin ligases have a substrate binding N-terminus and an E2-enzyme binding RING domain containing C-terminus (Fig.9 and Fig.10) (152, 154).

I.6.b Mindbomb1 is an E3-ubiquitin ligase.

Mib1 belongs to the most abundant second category of E3-ubiquitin ligases. The N-terminus of Mib1 serves as a substrate recognition region. Unlike most substrate recognition regions of other proteins, the N-terminus of Mib1 has two separate elements that recognize discrete and independent epitopes on the ligand tail, known as MZM and REP (Fig. 10)(155). The MZM element has two Mib-Herc2 subdomains sandwiching the ZZ Zinc finger domain. The second REP domain has two tandem Mib repeats domain that are found only in the Mindbomb family of proteins. Even though Mib-Herc2 and Mib repeats share no sequence identity among them, they have a topological similarity to src homology-3 (SH3) domains (Fig.10) (155, 156). SH3 domains are involved in the regulation of important signaling pathways that control cell proliferation, migration and cytoskeletal modifications(157). Structural and biochemical studies have shown that the MZM and REP domains of Mib1 function synergistically to recognize the Notch ligand Jag1. But they recognize two independent epitopes on the intracellular domain of Jag1: MZM recognizes the N-box sequence (IKNPIEK) and REP recognizes C-box sequence (KQDNRD). The N-box epitope is conserved in both the Delta and Serrate/Jagged ligand families. However, C-box epitopes are not apparent in Delta family of ligands(155).

The C-terminus of Mib1 contains three RING finger (RF) domains, that are essential for binding ubiquitin loaded E2 proteins. But whether all these three RF domains are necessary for E2 binding is still not clear. All Mib1 homologues have three RF domains at their C-terminus and it has been shown that the last RF domain, RF3, is essential for many Mib1 functions such as neurogenesis, apoptosis and ubiquitination of RYK(75, 158, 159) . However, Mindbomb2 (Mib2), the paralogue of Mib1, has only two RF domains. Studies show that functionally Mib1 and Mib2 can act as mutual E3-ubiquitin ligases(160) and in Notch signaling, they have common and specific Delta substrates(160). Nonetheless, Mib2 is dispensable for embryonic development and Notch signaling in zebrafish(77).

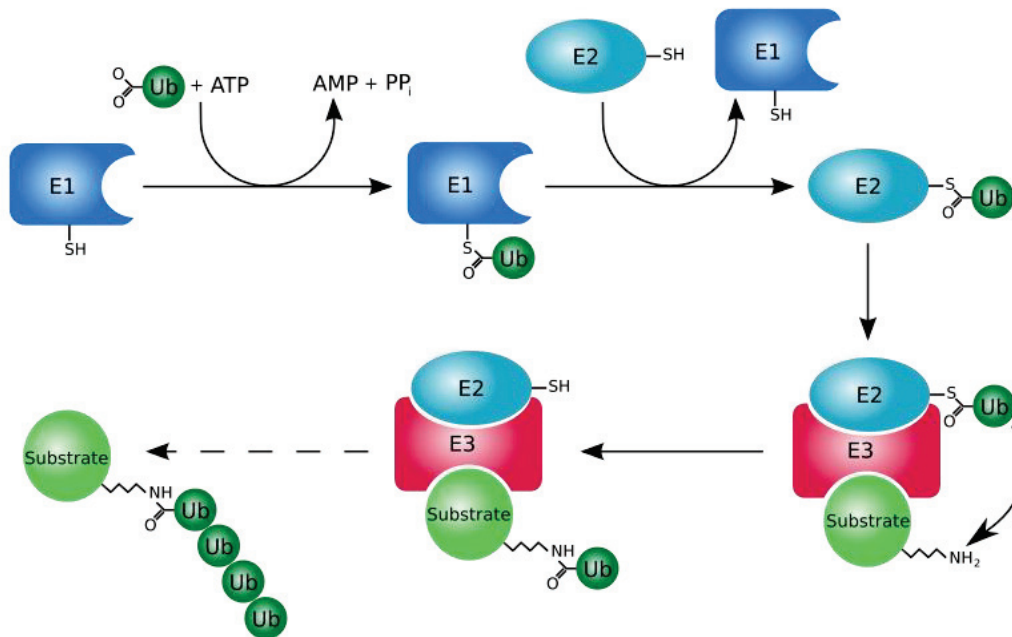


Figure 9. Ubiquitination by a RING-type E3-ubiquitin ligase. Ubiquitination happens in three steps involving an E1 ubiquitin enzyme that activates ubiquitin with the expense of an ATP molecule. Then, activated ubiquitin is transferred to an E2 enzyme, and finally E3 ubiquitin ligase transfer ubiquitin to the target substrate. RING-type E3 ubiquitin ligase acts as a platform where both the E2 enzyme and the target substrate can bind, after with ubiquitin is transferred from E2 to a lysine residue in the target protein. Ubiquitination of a protein can happen once, twice or several times depending on the context. (Picture credits: Roger B. Dodd)

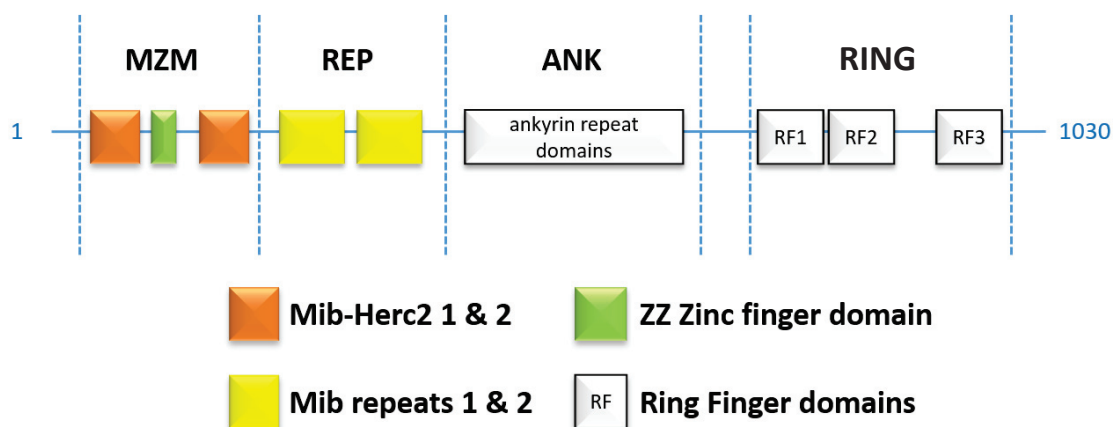


Figure 10. Structure of Mindbomb1. Mib1 is an E3-ubiquitin ligase. The MZM and REP domains of Mib1 recognize two discrete and independent epitopes on the substrate. RING domain contains three ring finger domains which bind to the E2 ubiquitin enzyme loaded with ubiquitin. Finally, the ubiquitin is transferred from the E2 enzyme to the target substrate.

I.6.c Mindbomb1 is important for the regulation of Notch signaling.

Earlier studies have shown that *mib1* mutations in zebrafish are associated with a wide range of phenotypes including precocious neurogenesis, defects in the development of somites, neural crest, ear and vasculature(161-165). These phenotypes have been interpreted as consequences of deficient Notch signaling. Therefore, it was proposed that *mib1* encodes an important component in the Notch signaling pathway. Accordingly, *Itoh et al. 2003* identified Mib1 as an E3-ubiquitin ligase for Delta (75). In both *Drosophila* and *Xenopus*, studies have already shown that Neuralized (Neur), another E3-ubiquitin ligase, monoubiquitinates Delta and promotes its endocytosis to activate Notch signaling(166-168). Interestingly, *Itoh et al. 2003* found that the function of Mib1 in zebrafish is similar to the one of Neur in *Drosophila*. Mib1 promotes internalization of Delta in the signal sending cell to promote Notch signal activation in the signal receiving cell. In the absence of Mib1, lateral inhibition is perturbed in the neurectoderm of zebrafish resulting in precocious neurogenesis(85, 169). As a result, *mib1* mutants show significant reduction in alternative cell fates such as secondary neurons, glial cells and neural crest derived cell types, that are normally supposed to arise from these proliferative precursor cells later in the development(64, 66, 161, 170, 171). Therefore, Mib1 regulated Notch signaling maintains the balance between proliferating precursor cells and differentiating cell types in different tissues throughout the development.

Even though Mib1 has been evolutionarily conserved in diverse metazoan, its function in other model organisms hadn't been yet identified until two groups independently, *Le Borgne et al., 2005*; *Lai et al, 2005* studied the *Drosophila* orthologue of Mindbomb (D-Mib)(172, 173). D-Mib regulates a large number of Notch regulated functions independently of Neur. Moreover, D-Mib can associate with both Delta and Serrate ligands for endocytosis and thereby, regulates Notch signaling in a similar fashion to that of the zebrafish Mib1. In addition, D-Mib is able to functionally replace Neur at several occasions by rescuing Neur mutant phenotype via ectopic expression of D-Mib. Later in the same year, *Koo et al. 2005* found that in mice also Mib1 is essential to regulate Notch signaling(78). *mib1* homozygous mutant mice die before E11.5 showing phenotypes indicative of defective Notch signaling in somitogenesis, neurogenesis, vasculogenesis and cardiogenesis. Expression of Notch target genes such as *hes5*, *hey1*, *hey2* and *heyL* is reduced in *mib1* mutant mice, confirming defective Notch signaling. Moreover, *mib1*

mutants show an accumulation of Dll1 in the plasma membrane, otherwise localized in endosomes in wildtypes, indicating a role of mMib1 in endocytosis of Notch ligands. Interestingly, mMib1 physically interacts with all Notch ligands in mice, which shows its importance in regulating Notch signaling in mice.

I.7 Non-canonical Notch signaling

The Notch signaling that I have described so far is called canonical Notch signaling, where a series of cleavage reactions occur to the Notch receptor due to the binding of Jagged/Delta ligands with Notch receptors. As a result, NICD is translocated into the nucleus to make CSL-MAML-NICD ternary complex and regulates target gene expression. However, variations of this conventional pathway are observed where certain steps are omitted to perform certain functions depending on the cellular context. These altered pathways are called non-canonical Notch signaling.

Non-canonical Notch signaling can be categorized into different subclasses depending on the nature of omitted steps in the conventional pathway. First, there are several reports indicating that Notch signaling can be activated by ligands other than the Jagged/Delta type. For example, the microfibrillar proteins MAGP-1 and MAGP-2 are shown to induce Notch1 extracellular domain dissociation and further receptor activation(174). Similarly, Y-box protein-1, a protein secreted by mesangial and immune cells after cytokine challenge, is shown to bind to the Notch-3 receptor and initiate downstream signaling (175). A second type of non-canonical Notch signaling involves the skipping of the nuclear transcription factor CSL for its target function. For example, Notch signaling has been shown to act activate R-Ras signaling pathway for the maintenance of apico-basal polarity, in a CSL independent fashion(176). Similarly, it has been shown that Notch activates the phosphatidylinositol-3-kinase (PI3K) pathway without apparent involvement of CSL in cervical cancer(177). Third, non-canonical Notch signaling can happen via CSL but the formation of DNA binding CSL-coactivator complex to regulate target gene expression is independent of NICD. Therefore, CSL can operate independently to the upstream conventional Notch signaling pathway. For example, viral proteins such as EBNA2 (Epstein-Barr-Virus) and 13SE1A (adenovirus) can act as co-activators that bind with CSL in a Notch-independent manner and then, “switch-on” the CSL complex to regulate target gene expressions(178, 179).

I.8 The importance of Notch signaling in epithelialization of neural progenitors.

During Notch signaling, endocytosis of ligands in the signal-sending cell is necessary for the receptor activation in juxtaposed signal-receiving cells. In *Drosophila*, Delta ligand is localized at the basolateral membrane of signal-sending SOP cell, segregated from Notch receptors that are accumulated apically in the juxtaposed signal-receiving cell. It has been shown that internalized Delta ligands are transcytosed to the apical membrane to bind to the Notch receptors accumulated apically(180). Previous PhD student in the lab, Priyanka Sharma, was interested in understanding the importance of apico-basal trafficking of Delta ligands for Notch signaling in zebrafish. She perturbed Mib1 to inhibiting endocytosis of Delta ligands. Interestingly, she observed that Mib1 mediated loss of Notch activation resulted in the loss of apico-basal polarity and cellular organization of neural progenitor cells in the zebrafish spinal cord. While the neural plate of tetrapod embryos is already composed of pseudostratified single layer of neuroepithelial cells that have a well-defined apico-basal polarity(60), apico-basal polarity in the zebrafish neural tube is established only during neurulation. This raised the question whether and how Notch signaling and establishment of polarized neural progenitor cells are connected during zebrafish neurulation? Therefore, she decided to study the role of Notch signaling in the establishment of polarized neural progenitor cells.

Results

I.1 Studying the role of Notch signaling during zebrafish spinal cord morphogenesis.

During the first part of my PhD, I continued the project of Priyanka realizing the fact that perturbation of Notch signaling not only affects apico-basal polarity but also another morphogenetic event during zebrafish neurulation, called C-divisions. C-divisions and epithelialization of neural progenitors are important events during zebrafish neural tube morphogenesis(27). However, it's still unclear what is regulating these two morphogenetic events. The first appearance of apical polarity markers in neural progenitor cells occurs during the process of c-divisions(34, 46). Mutations affecting cell division and polarization of progenitor cells gave similar defects in the neural tube lumen formation(46, 56-58). This suggest that both these events are synergistically providing morphological advantage for the neural tube lumen formation and probably both are regulated by a common signaling pathway.

In zebrafish, Delta/Notch signaling regulates early neurogenesis via lateral inhibition(67, 75, 181). Surprisingly, c-divisions and appearance of major hallmarks of apico-basal polarity such as apical accumulation of Pard3 protein, adherens junction and tight junction components occur only after the beginning of neuronal differentiation (34, 37, 38, 182). This raises the question whether Notch signaling mediated inhibition of neurogenesis and the morphogenetic events such as epithelialization and c-divisions are linked to regulate zebrafish neural tube morphogenesis?

Therefore, in this project, we inhibited Notch signaling in zebrafish embryos to understand the following questions,

- Does Notch signaling promote establishment of apico-basal polarity in the zebrafish neural tube? Does it act as a general regulator of apico-basal polarity in the zebrafish nervous system? Or is Notch signaling only required in specific regions of the neural tube?
- Is Notch signaling important for regulating C-divisions? If yes, how does Notch signaling affect the overall morphogenesis of the neural tube?

Results in this project are presented in the format of an article which is published in the journal Scientific Reports.

I.2 Article published in the journal Scientific Reports

Title: Notch-mediated inhibition of neurogenesis is required for zebrafish spinal cord morphogenesis

Authors/Affiliations:

Priyanka Sharma¹, **Vishnu Muraleedharan Saraswathy**¹, Li Xiang¹, and Maximilian Fürthauer^{1*}

¹ Université Côte d'Azur, CNRS, Inserm, iBV, France.

* Corresponding author: Maximilian Fürthauer (furthauer@unice.fr)

SCIENTIFIC REPORTS

OPEN

Notch-mediated inhibition of neurogenesis is required for zebrafish spinal cord morphogenesis

Priyanka Sharma, Vishnu Muraleedharan Saraswathy, Li Xiang & Maximilian Fürthauer 

The morphogenesis of the nervous system requires coordinating the specification and differentiation of neural precursor cells, the establishment of neuroepithelial tissue architecture and the execution of specific cellular movements. How these aspects of neural development are linked is incompletely understood. Here we inactivate a major regulator of embryonic neurogenesis - the Delta/Notch pathway - and analyze the effect on zebrafish central nervous system morphogenesis. While some parts of the nervous system can establish neuroepithelial tissue architecture independently of Notch, Notch signaling is essential for spinal cord morphogenesis. In this tissue, Notch signaling is required to repress neuronal differentiation and allow thereby the emergence of neuroepithelial apico-basal polarity. Notch-mediated suppression of neurogenesis is also essential for the execution of specific morphogenetic movements of zebrafish spinal cord precursor cells. In the wild-type neural tube, cells divide at the organ midline to contribute one daughter cell to each organ half. Notch signaling deficient animals fail to display this behavior and therefore form a misproportioned spinal cord. Taken together, our findings show that Notch-mediated suppression of neurogenesis is required to allow the execution of morphogenetic programs that shape the zebrafish spinal cord.

The building of functional organs requires controlling the identity, shape and spatial arrangement of their constituent cells. Understanding how these aspects of embryogenesis are linked remains a major challenge. The Delta/Notch pathway governs the specification, proliferation, and differentiation of neuronal precursors in embryonic and adult tissues¹⁻⁵. Notch receptors and Delta ligands are transmembrane proteins that elicit signaling between adjacent cells. In this context, the E3-Ubiquitin ligases Mindbomb and Neuralized promote an endocytic internalization of Delta ligand molecules that is required for Notch receptor activation⁶⁻⁸. Delta/Notch interactions then trigger a metalloprotease-mediated cleavage in the Notch extracellular domain, followed by a γ -Secretase-dependent intramembrane proteolysis that releases the Notch IntraCellular Domain (NICD) into the cytoplasm. NICD enters the nucleus to interact with CSL (for CBF1, Suppressor of Hairless, Lag1) family transcription factors and promote target gene transcription^{1,4}.

Several observations suggest that Notch signaling and neuroepithelial morphogenesis are functionally interdependent. Notch has notably been linked to the formation of radial glia⁹⁻¹², neural progenitor cells that present hallmarks of apico-basal polarity¹³. At the onset of neurogenesis, the neural plate of tetrapod embryos consists of a pseudostratified monolayer of apico-basally polarized cells which act as neural stem cells^{13,14}. Following an expansion of this stem cell pool through symmetric divisions, some neural plate cells divide asymmetrically to generate the first neurons. Concomitant with this onset of neurogenesis, neural plate cells transform into radial glia¹³. During further development, radial glia cells undergo either symmetric, self-renewing divisions or divide asymmetrically to ultimately generate the majority of neurons that are present in the nervous system¹³. As radial glia cells retain most features of epithelial polarity, their presence is essential to maintain the epithelial architecture of the developing neural tube^{10,13,15}. In addition to radial glia cells, studies in the mammalian and zebrafish Central Nervous System (CNS) have revealed the existence of Notch-responsive non-apical progenitor cells^{13,16,17}, identifying thereby an additional level of complexity in the relationships between the cellular organization of the neural primordium, Notch signaling and embryonic neurogenesis.

Université Côte d'Azur, CNRS, Inserm, iBV, Nice, France. Correspondence and requests for materials should be addressed to M.F. (email: furthauer@unice.fr)

In the forebrain of mice and zebrafish, cells undergoing neuronal differentiation present Delta ligands to neighboring progenitors to activate Notch signaling, induce radial glia identity, and thereby maintain neuroepithelial tissue organization^{10,11}. Conversely, the apico-basal organization of the developing neural tube is itself required for Notch signaling as apical adherens junctions between nascent neurons and undifferentiating progenitors are required for Notch receptor activation^{15,18}.

In contrast to tetrapods, the initial stages of zebrafish spinal cord morphogenesis take place in a neural primordium that lacks a polarized epithelial architecture^{19–23}. While the cellular organization of the zebrafish neural plate displays similarities to the pseudostratified epithelium of higher vertebrates^{14,20,23,24}, major hallmarks of apico-basal polarity such as apical Par protein localization, adherens junctions and tight junctions appear only after the beginning of neuronal differentiation, by mid-segmentation stages^{19–23,25}. This raises the question whether and how Notch signaling and neuroepithelial morphogenesis are linked during zebrafish neural development?

A second particularity of the development of the zebrafish is the occurrence of a particular type of morphogenetic cell division^{19,20,22,26}. In these so-called C-divisions, a cell originating from one side of the neural primordium divides at the embryonic midline so that one of its daughters integrates the contralateral half^{19,22,26}. The apical polarity protein Partitioning defective 3 (Pard3) accumulates at the cytokinetic bridge which prefigures the future apical neural tube midline²². Neural primordia in which cell divisions have been blocked establish apico-basal polarity, but fail to form a straight, regular apical neural tube midline²⁷. It has therefore been suggested that C-divisions, while not being absolutely required for the establishment of neural tube apico-basal polarity, confer a morphogenetic advantage to the embryo by relocating cells that would otherwise span the neural tube midline^{20,23,27}. Despite the fact that C-divisions confer robustness to neural tube development, their regulation remains poorly understood. While Pard3 and Planar Cell Polarity (PCP) proteins are known to control C-divisions^{22,26}, the relationship between neurogenic Notch signaling and C-divisions has not been investigated.

In the present study, we inhibit Notch pathway activity and study the impact on zebrafish CNS morphogenesis. Our work reveals that the relationship between Notch signaling and neuroepithelial morphogenesis depends on the biological context. While some regions of the nervous system can acquire apico-basal polarity and neuroepithelial organization independently of Notch, Notch signaling is required for the morphogenesis of the dorso-medial spinal cord. In this tissue, Notch signaling is essential to inhibit neuronal differentiation and thereby allow the emergence of neuroepithelial identity and progressive epithelialization of the developing neural tube. Loss of Notch signaling also impairs the morphogenetic behavior of the cells of the neural primordium, thereby causing the formation of a misproportioned spinal cord. Our findings therefore show that beyond the control of the cellular composition of the nervous system, the ability of the Delta/Notch pathway to restrain neurogenesis is essential for the execution of morphogenetic programs that govern the shaping of the zebrafish spinal cord.

Results

Mindbomb1 is essential for zebrafish spinal cord morphogenesis. Genetic studies in zebrafish have identified the E3-ubiquitin ligase Mindbomb1 (Mib1) as a central regulator of Delta ligand internalization and Notch activation^{6,28}. To study the role of Notch signaling in zebrafish CNS morphogenesis, we inactivated *mib1* using a validated Morpholino²⁹ and *mib1*^{ta52b} mutants⁶. In accordance with published observations²⁹, *mib1* morphants presented an upregulation of DeltaD (DID) due to a failure in Notch-dependent lateral inhibition, and a relocalization of DID from endocytic compartments to the plasma membrane (Fig. 1a,b').

Antibody staining against the apical Par complex component atypical Protein Kinase C (aPKC³⁰) was used to visualize apico-basal polarity. To analyze tissue morphology, fluorescent Phalloidin was used to visualize cortical F-actin. *mib1* morphants display a loss of apical aPKC signal (Fig. 1b') and an overall disorganization of neuroepithelial tissue architecture in the anterior spinal cord (Fig. 1b). A similar loss of neuroepithelial polarity was observed in *mib1*^{ta52b} mutants (Fig. 1c,c'). Wild-type *mib1* RNA injection rescued the polarity defects of *mib1*^{ta52b} mutants, warranting the specificity of our observations (Supplementary Fig. S1).

Our experiments show that loss of Mib1 impairs apico-basal polarity and epithelial organization in the zebrafish spinal cord. Accordingly, no polarized enrichment of the apical polarity proteins Pard3³¹ (Fig. 1d,e), Crumbs³² (Fig. 1f,g) and the tight junction component Zonula Occludens 1 (ZO-1¹⁹, Fig. 1h,i) is detectable in *mib1*^{ta52b} mutants. In accordance with a failure to establish Par complex-dependent polarity, *mib1*^{ta52b} mutants fail to display the Pard3-dependent alignment of γ -Tubulin-positive centrosomes that is observed at the neural tube midline of wild-type siblings (Fig. 1j,k)³³.

The canonical Notch pathway is required for the morphogenesis of the zebrafish spinal cord.

In addition to its role in Delta ligand internalization, Mib1 also regulates the ubiquitination and endocytic trafficking of other substrate proteins^{34,35}. This raises the question whether the neuroepithelial defects of Mib1-depleted embryos are due to the loss of Notch signaling or to a Notch-independent function of Mib1? To address this issue, we interfered with different Notch pathway components and analyzed the effect on spinal cord morphogenesis.

Mib1 loss-of-function impairs the endocytosis of DID, one of the two zebrafish homologues of mammalian Delta-like-1 (Dll1)^{6,29}. Apico-basal polarity is however intact in *dld*^{tr33} mutants (Supplementary Fig. S2a,b). Mib1 also interacts with DeltaA (DIA), the second Dll1 homologue³⁶. Accordingly, *mib1*^{ta52b} mutants display excessive cell surface accumulation of DIA (Fig. 2a,b). Injection of a validated *dla* morpholino³⁷ abolishes DIA immunoreactivity but fails to elicit polarity defects in a wild-type background (Supplementary Fig. S2c,d). In contrast, polarity defects are observed upon *dla* knock-down in *dld*^{tr33} mutants (Fig. 2c,d).

Notch receptor activation results in the γ -Secretase-mediated release of NICD into the cytoplasm, allowing NICD nuclear entry and transcriptional activation of target genes^{1,4}. Blocking Notch signaling using two different

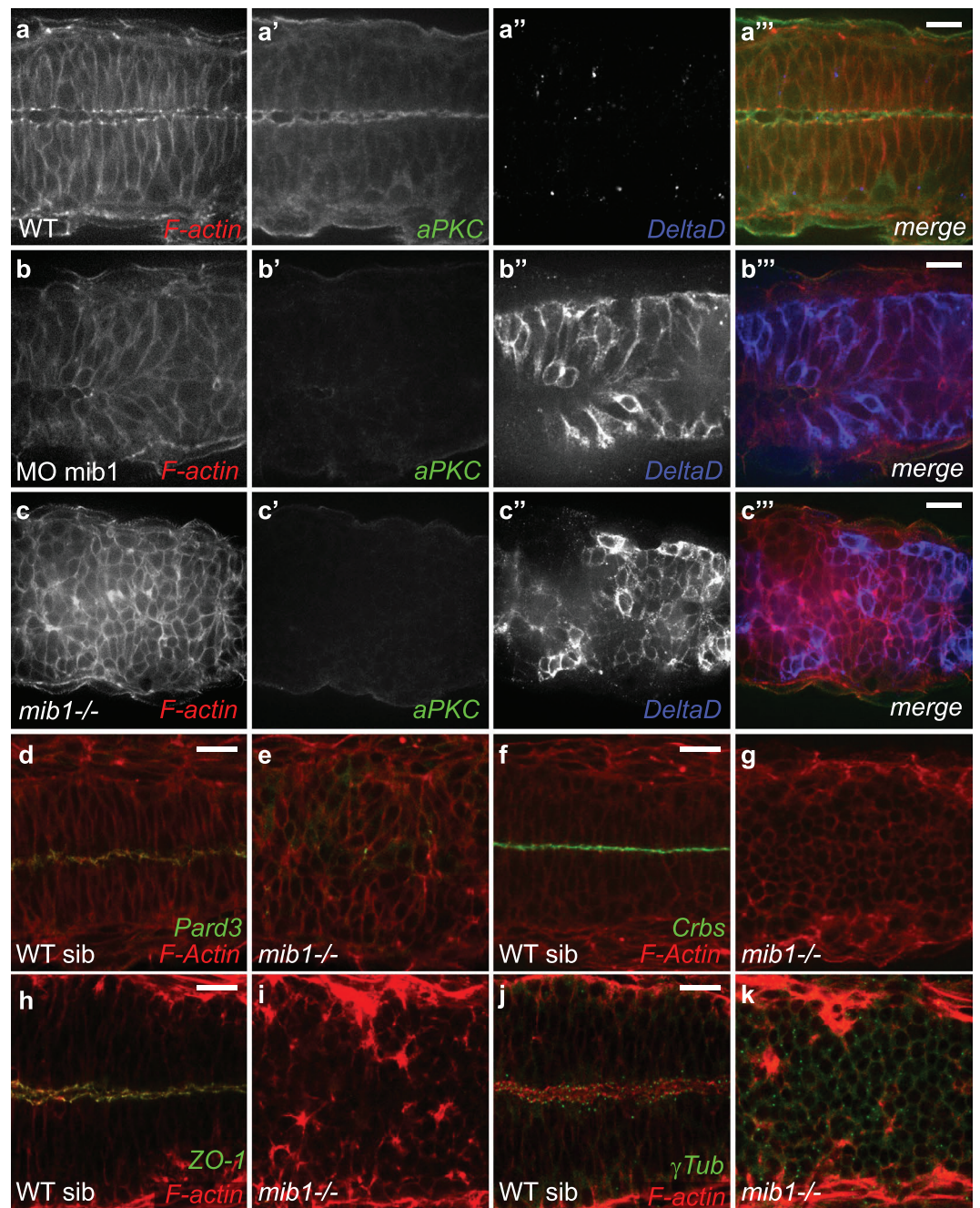


Figure 1. Mindbomb1 is required for zebrafish spinal cord morphogenesis. (a,b) Morpholino knock-down of *mib1* disrupts apical aPKC enrichment and neuro-epithelial morphology (outlined by F-actin staining) in 15/19 embryos. (c) A similar disruption of apico-basal polarity is observed in *mib1* mutants (n = 14). (d,e) *mib1* mutants fail to establish polarized Pard3 localization (e, n = 12). (f,g) No polarized Crumbs enrichment is observed in *mib1* mutants (g, n = 17). (h,i) The apical localization of the tight junction component ZO-1 is disrupted in *mib1* mutants (i, n = 16). (j,k) Centrosomes fail to move towards the neural tube midline in *mib1* mutants (k, n = 16). (a–c,f,g) 30 somites stage. d,e, 18 somites stage, (h–k) 22 somites stage. All images are dorsal views of the anterior spinal cord, anterior left. Scalebars: 20 μ m.

pharmacological γ -Secretase inhibitors, DAPT³⁸ and LY411575³⁹, impaired the apico-basal polarization of the neural tube (Fig. 2e–h).

If the polarity phenotype of Mib1-depleted embryos is a consequence of the loss of Notch signaling, restoring Notch activity should rescue neuroepithelial morphogenesis. Accordingly RNA injection of NICD, which acts as a constitutively activated form of Notch⁴⁰, restores neural tube apico-basal polarity in *mib1*^{ta52b} mutant (Fig. 2i–l) or *mib1* morphant (Supplementary Fig. S2e–h) embryos.

Upon nuclear entry NICD associates with RBPJ/Su(H)/CBF transcription factors to trigger target gene activation^{1,4}. Misexpression of a dominant-negative Su(H) variant⁴¹ impaired neuroepithelial morphogenesis and

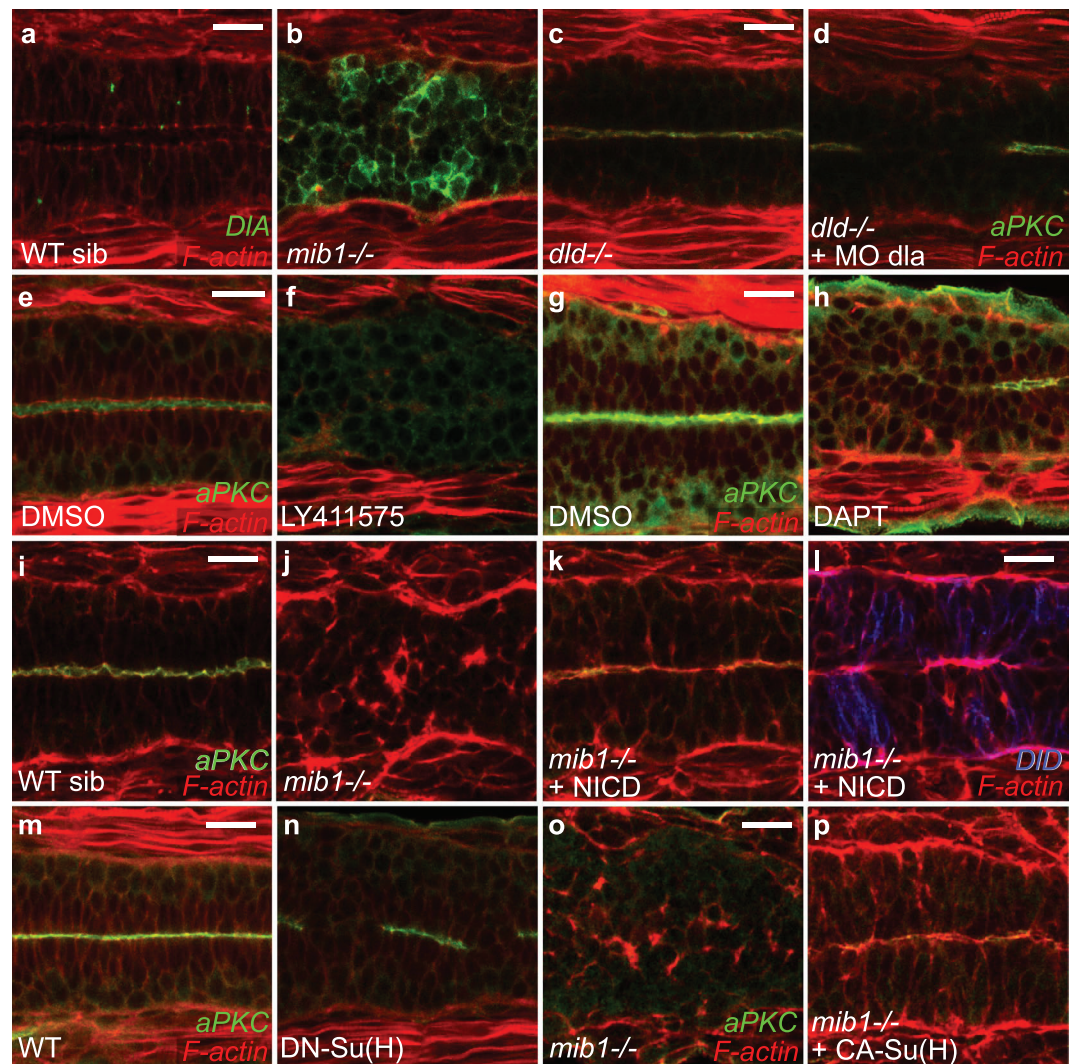


Figure 2. Notch pathway activity is required for spinal cord morphogenesis. (a,b) *mib1* loss of function prevents DIA internalization (n = 9). (c,d) Combined inactivation of *dld* and *dla* disrupts apico-basal polarity in 9/10 embryos. (e,f) The γ -Secretase inhibitor LY411575 disrupts apico-basal polarity (n = 18). (g,h) Similarly the γ -Secretase inhibitor DAPT perturbs polarity in 4/5 embryos. (i-l) RNA injection of a constitutively activated form of Notch (NICD) restores neuro-epithelial morphology and apical aPKC localisation (k) but not DeltaD endocytosis (l) in 22/22 *mib1* mutant embryos. (m,n) Polarity defects are observed in 20/46 embryos injected with RNA encoding dominant-negative Su(H) (DN-Su(H)). (o,p) RNA injection of constitutively activated Su(H) (CA-Su(H)) restores apico-basal polarity in 17/17 *mib1* mutants. All images are dorsal views of the anterior spinal cord, anterior left. (a–f) 22 somites stage, (g,h,m,n) 30 somites stage, (i–l,o,p) 16 somites stage. Scalebars: 20 μ m.

polarized aPKC localization (Fig. 2m,n), consistent with the phenotype of CBF1 knock-out mice⁴². This result was confirmed through simultaneous morpholino knock-down of the two zebrafish Su(H)-homologues RBPJa&b (Supplementary Fig. S2i–l)⁴³. Conversely, RNA microinjection of Constitutively Activated Su(H) (CA-Su(H))⁴¹ restores neuroepithelial tissue organization in *mib1*^{ta52b} mutants (Fig. 2o,p).

Therefore our observations show that not only Mib1 itself, but the activity of the entire canonical Notch pathway is required for zebrafish spinal cord morphogenesis.

Notch signaling is dispensable for the early establishment of floor plate apico-basal polarity. Previous studies have suggested that canonical Notch signaling is dispensable for the initial establishment, but required for the subsequent maintenance of neuroepithelial apico-basal polarity in fish and mice^{42,44}. To address whether the defects of Mib1-depleted embryos similarly arise from a failure to maintain neuroepithelial polarity, we monitored the establishment of neural tube apico-basal polarity in wild-type sibling and *mib1*^{ta52b} mutant embryos.

The emergence of polarity has been studied mostly in the dorsal and medial regions of the zebrafish spinal cord^{19,22}. In accordance with these studies, we find that the dorso-medial spinal cord does not show overt signs of

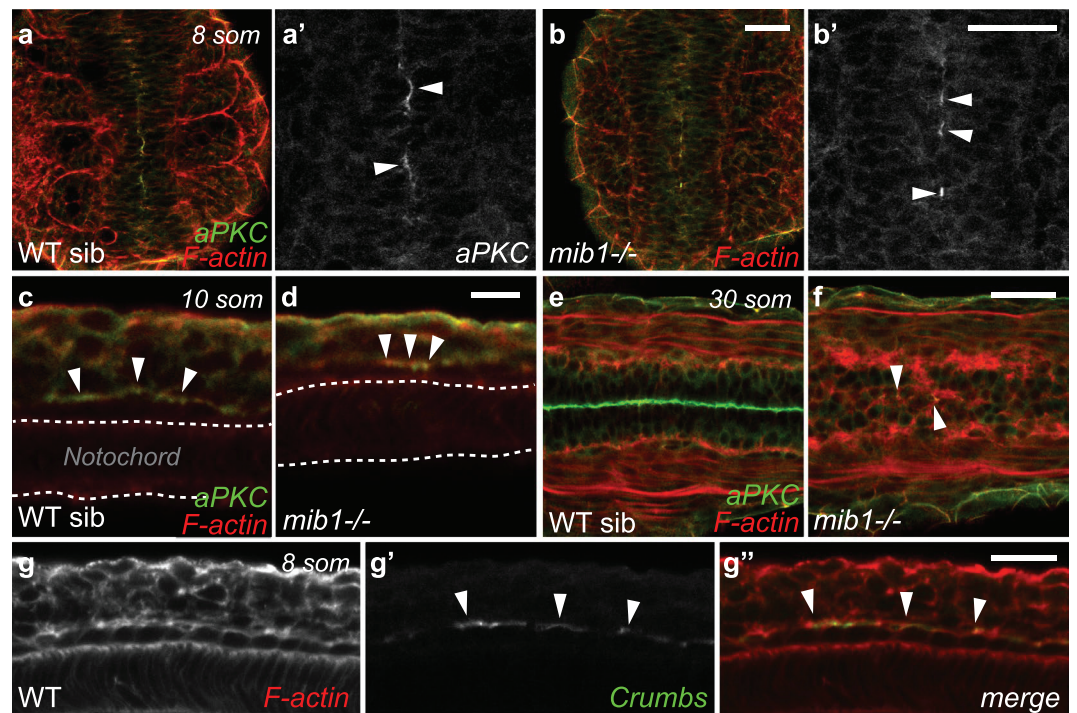


Figure 3. Notch signaling is dispensable for the emergence of floor plate apico-basal polarity. (a,b) At the 8 somites stage, similar discontinuous patches of polarized aPKC are detected in the ventral-most neural tube of WT siblings (a, n = 31) and *mib1* mutants (b, n = 14). Dorsal views, anterior up. (a',b') are high magnification views of the polarized aPKC signal. (c,d) aPKC is enriched at the apical surface of floor plate cells in 10 somites stage WT siblings (c, n = 8) and *mib1* mutants (d, n = 4). Lateral views, anterior left. (e,f) By the 30 somites stage polarized aPKC staining is reduced to few isolated cells in the ventral-most neural tube of *mib1* mutants (arrowheads in f, n = 5). Dorsal view, anterior left. (g) Crumbs protein accumulates at the apical surface of 8 somites stage floor plate cells (arrowheads). Lateral view, anterior left. Scalebars: (a,b) 40 μ m, (c,d) 10 μ m, (e-g) 20 μ m.

apico-basal polarity prior to the 12 somites stage. However, we noticed that apico-basal polarity emerges much earlier in the ventral-most part of neural tube. From the 6 somites stage onwards, embryos display foci of polarized aPKC expression (Fig. 3a,c) that coalesce subsequently into a line (Fig. 3g', Supplementary Fig. S3). Lateral views of the neural tube show that this enrichment of aPKC (Fig. 3c) and Crumbs (Fig. 3g-g', Supplementary Fig. S3) corresponds to the apical surface of the cuboidal cells of the floor plate.

Notch signaling has been implicated in the differentiation of floor plate cells⁴⁵. Mutations in *dla* or *mib1* have been reported to cause a severe reduction in the number of detectable floor plate cells by the end of the segmentation period⁴⁵. Our observations confirm the occurrence of late floor plate defects (Fig. 3e,f), but also reveal that the initial establishment of floor plate cells and their apico-basal polarization do not require *mib1* function (Fig. 3a-d), and may therefore occur independently of Notch signaling. To test this hypothesis, we took advantage of the transgenic *tp1:bglob-GFP* Notch reporter line⁴⁶. Until the 14 somites stage, i.e. mid-way through the embryonic segmentation period, reporter activity was absent from the floor plate, while adjacent tissues displayed fluorescence indicative of Notch signaling (Supplementary Fig. S3). This observation confirms that Notch signaling is dispensable for the initial formation and apico-basal polarization of the ventral-most cells of the neural tube.

Notch signaling restricts neurogenesis to allow the emergence of neuroepithelial tissue organization in the dorso-medial spinal cord. In contrast to the situation in the floor plate, Notch pathway activity is required for the morphogenesis of the more dorsal regions of the spinal cord (Fig. 4). To analyze the emergence of neuroepithelial tissue architecture and apico-basal polarity in the anterior spinal cord, we performed a time course analysis of polarized aPKC localization. In wild-type controls, aPKC becomes progressively enriched at the neural tube midline in the medial and dorsal aspects of the spinal cord from the 12 somites stage onwards (Fig. 4b,f,j,m,n), in accordance with the previously reported ventral to dorsal progression of neural tube maturation^{19,47,48}. In contrast, *mib1^{ta52b}* mutants fail to display neuroepithelial tissue architecture and apico-basal polarity in the dorso-medial spinal cord at all stages examined (Fig. 4d,h,l,m,o). While previous studies have highlighted functions of Notch signaling in the late maintenance of neuroectodermal apico-basal polarity^{42,44}, our findings show that zebrafish *mib1* is required already for the initial establishment of neuroepithelial tissue architecture.

Towards the end of neural development, most neural progenitors downregulate the expression of apical polarity proteins and differentiate into neurons⁴⁹. As inactivation of *mib1* causes premature neuronal differentiation⁶, we wondered whether the loss of neuroepithelial tissue organization in *mib1^{ta52b}* mutants might be correlated

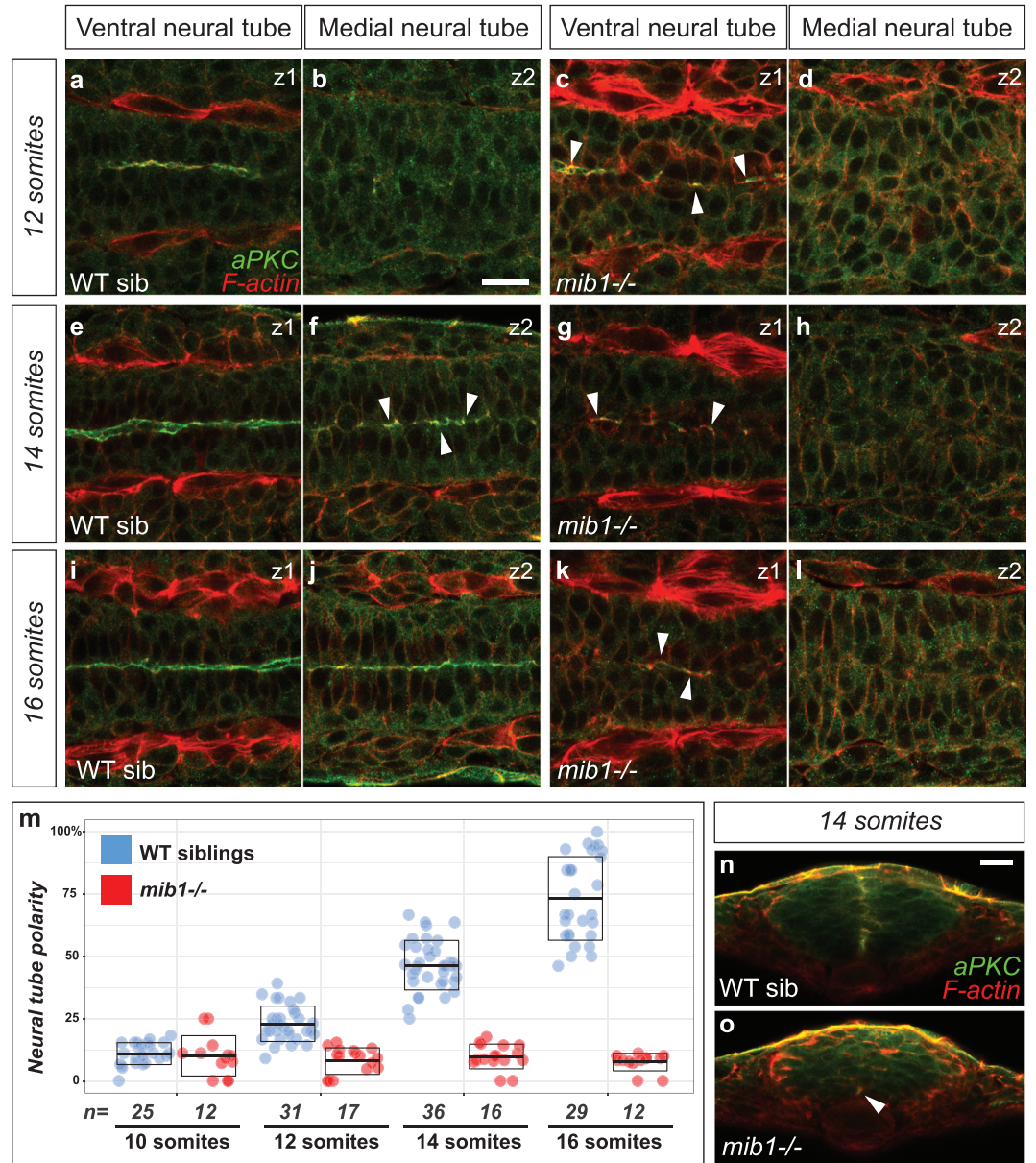


Figure 4. Notch signaling is required for the establishment of apico-basal polarity in the dorso-medial spinal cord. (a–l) Confocal sections taken at different dorso-ventral levels of the anterior spinal cord of WT sibling and *mib1* mutant embryos. Dorsal views, anterior left. z1 corresponds to the ventral-most extent of apico-basally polarized neuro-epithelial tissue (identified by aPKC staining), z2 is localized 12 μm more dorsally in the same embryo. Arrowheads indicate local foci of polarized aPKC in partially polarized tissue. (a–d) At the 12 somites stage polarized aPKC signal is detected in the ventral-most neural tube in WT sibling and *mib1* mutants. (e–l) At later stages polarity is progressively established in more dorsal regions of the neural tube in WT siblings (f,j), but remains limited to the ventral neural tube in *mib1* mutants (g,h,k,l). (m) Quantification of the progressive emergence of apico-basally polarity in the anterior spinal cord (see Methods). Boxes represent mean values ± SD. (n,o) Transversal sections (dorsal up) through the neural tube of 14 somites stage embryos. (n) Polarized aPKC staining starts to spread through the dorso-ventral extent of the neural tube in WT siblings. (o) In *mib1* mutants polarized aPKC enrichment remains limited to the ventral floor plate region (arrowhead). Scalebars: 20 μm.

with a failure to express genes governing neuroepithelial identity and apico-basal polarity. Zebrafish *sox19a* is expressed in undifferentiated neural precursor cells throughout the nervous system, similar to the expression of amniote *sox2*⁵⁰. In accordance with a loss of neural precursors due to excessive neuronal differentiation, *mib1*^{ta52b} mutants display a premature loss of *sox19a* expression in the anterior spinal cord (arrow in Fig. 5d). Accordingly, all cells of the dorso-medial spinal cord start to express the marker of neuronal differentiation *elavl3* (Supplementary Fig. S4c).

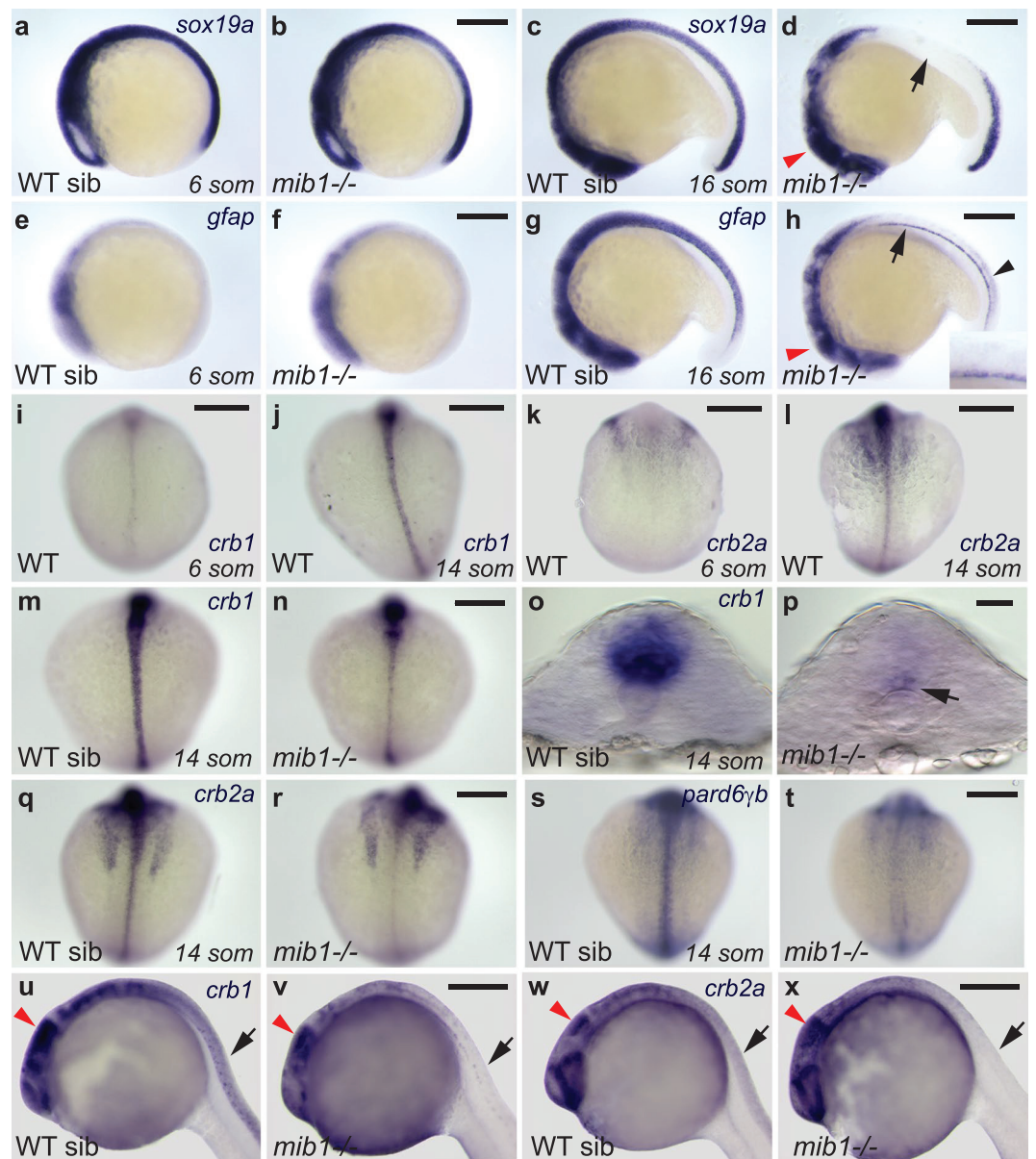


Figure 5. Notch signaling is required to allow the emergence of neuroepithelial identity. (**a,b**) The expression of the neuronal progenitor marker *sox19a* is similarly initiated in WT sibling (**a**) and *mib1* mutant embryos (**b**, $n = 4$). (**c**) By the 16 somites stage, *sox19a* expression is still present in the brain and anterior spinal cord of WT siblings. (**d**) In *mib1* mutants ($n = 17$) *sox19a* is lost in the anterior spinal cord (arrow) but partially retained in the brain (red arrowhead). (**e,f**) At the 6 somites stage, low levels of the radial glia marker *gfap* are detected in the brain region of WT siblings (**e**) or *mib1* mutants (**f**, $n = 10$). (**g**) By the 16 somites stage, WT siblings display *gfap* expression in the brain and spinal cord. (**h**) *mib1* mutants ($n = 17$) fail to upregulate *gfap* expression in the dorso-medial anterior spinal cord (inset). Reduced *gfap* expression levels are observed in the brain (red arrowhead) and caudal spinal cord (black arrowhead). Continuous *gfap* expression is retained in the floor plate (arrow). (**i-l**) The establishment of apico-basal polarity coincides with an upregulation of *crb1* (**i,j**) and *crb2a* (**k,l**) in the spinal cord. (**m,n**) Upregulation of *crb1* expression is impaired in *mib1* mutants (**n**, $n = 11$). (**o,p**) Residual *crb1* expression persists in the ventral-most spinal cord (arrow in **p**) of 14 somites stage *mib1* mutants. (**q,r**) *mib1* mutants display reduced *crb2a* expression in the spinal cord (**r**, $n = 13$). (**s,t**) *pard6γb* expression is lost in the neural tube of *mib1* mutants (**t**, $n = 13$). (**u-w**) In 30 somites stage *mib1* mutants *crb1* (**u**, $n = 10$) and *crb2a* (**w**, $n = 10$) expression are lost in the anterior spinal cord (black arrows) but partially retained in the brain (red arrowheads indicate the midbrain). (**a-h**, **u-x**) lateral views, anterior to the left, dorsal up. (**i-n**, **q-t**) dorsal views of the spinal cord, anterior up. (**o,p**) transversal sections of the neural tube, dorsal up. Scalebars: (**a-n,q-t**) 200 μm , (**o,p**) 20 μm , (**u-x**) 250 μm .

Radial glia cells are neural precursors that display apico-basal polarity and are crucial for the maintenance of neuroepithelial tissue architecture in the brain of zebrafish and higher vertebrates^{10,11}. One of the hallmarks of radial glia is the expression of *glial fibrillary acidic protein* (*gfap*)^{12,13}. In accordance with a lack of apico-basally

polarized neural precursor cells, *gfap* expression levels are very low in the presumptive spinal cord of 6 somites stage embryos (Fig. 5e). While wild-type sibling embryos upregulate *gfap* expression concomitantly with the establishment of apico-basal polarity (Fig. 5g), *mib1^{ta52b}* mutants fail to express *gfap* in the dorso-medial aspect of the anterior spinal cord (Fig. 5h).

Loss of Notch signaling impairs not only *gfap*, but also the expression of core components of the apico-basal polarity machinery belonging to the Par and Crumbs protein complexes⁵¹. While only low levels of *crumbs1* (*crb1*) and *crumbs2a* (*crb2a*) are detectable in the neural tube of wild-type 6 somites stage embryos (Fig. 5i,k), both genes display increased expression by the 14 somites stage (Fig. 5j,l). *mib1^{ta52b}* mutants fail to display this upregulation (Fig. 5m-r). Similarly, reduced expression levels of the Par complex component *pard6γb*⁵² are observed in the spinal cord of *mib1^{ta52b}* mutants (Fig. 5s,t).

Region-specific control of neuroepithelial morphogenesis in the zebrafish spinal cord. Our observations uncover an essential role for the Notch-mediated suppression of neurogenesis in the regulation of neuroepithelial identity in the dorso-medial spinal cord. In addition, the analysis of neuroepithelial gene expressions confirms the existence of a different, Notch-independent regulation of apico-basal polarity in the ventral-most part of the neural tube. In this tissue, *crb1* transcripts are detectable already by the 6 somites stage (Fig. 5i), when first signs of polarized aPKC enrichment become detectable. While *mib1^{ta52b}* mutants fail to upregulate *crb1* expression in the dorso-medial neural tube where polarity is lost, *crb1* expression persists in the ventral-most cells where apico-basal polarity is retained (arrow in Fig. 5p). Similarly, *mib1^{ta52b}* mutant floor plate cells retain the expression of the neuroepithelial/radial glia marker *gfap* (arrow in Fig. 5h). Accordingly, the analysis of the neuronal differentiation marker *elavl3* reveals that, in contrast to more dorsal and lateral spinal cord derivatives, *mib1^{ta52b}* mutant floor plate cells do not undergo neuronal differentiation (Supplementary Fig. S4d).

In contrast to the spinal cord, *mib1^{ta52b}* mutant brains do still express *gfap* and the neuronal precursor marker *sox19a*, albeit at reduced levels (red arrowheads in Fig. 5d,h). Similarly, *crb1* and *crb2a* are still expressed in the brain but no more detectable in the dorso-medial spinal cord of 30 somites stage *mib1^{ta52b}* mutants (Fig. 5u-x).

The occurrence of *mib1^{ta52b}* mutant polarity phenotypes correlates with the differential regulation of neuroepithelial gene expression and neuronal differentiation. In the dorso-medial spinal cord of *mib1^{ta52b}* mutant embryos, all cells undergo neuronal differentiation (Fig. 6l, Supplementary Fig. S4c), polarity gene expression is lost (arrows in Fig. 5v,x), and so is apico-basal polarity (Fig. 6d,h,l). *mib1^{ta52b}* mutant hindbrains present only a partial neurogenic transformation (Fig. 6j') and a partial loss of neuroepithelial polarity (Fig. 6f,j). Finally, polarity gene expression is retained in *mib1^{ta52b}* mutant midbrains (red arrowheads in Fig. 5v,x). Accordingly, *mib1^{ta52b}* mutants display only a very minor increase in neurogenesis (Fig. 6j') and retain the neuroepithelial tissue architecture of the midbrain and MHB (Fig. 6b,j).

To determine whether the retention of apico-basal polarity in the MHB region of *mib1* mutants could be due to residual Notch signaling, we introduced the *tp1bGloB:GFP* reporter⁴⁶ into *mib1* mutants. Notch reporter activity is essentially undetectable at the MHB in both wild-type sibling and homozygous mutant animals (Fig. 6i',j'). These observations suggest that Notch signaling is largely dispensable for MHB development at the stages considered here.

Similar to *mib1* single mutants, *mib1; mib2* double mutant animals present a loss of apico-basal polarity at the level of the spinal cord, but retain neuroepithelial tissue organization in the MHB region (Supplementary Fig. S5, Supplementary Table S1). These findings show that Mindbomb protein function is not required for early MHB morphogenesis and extend previous studies suggesting that *mib2* is dispensable for early embryonic development²⁸.

Apico-basal polarity does not require Notch signaling between midline-crossing mitotic sister cells. A characteristic feature of the morphogenesis of the zebrafish neural tube is the occurrence of midline-crossing C-divisions. As Notch signaling between mitotic sister cells is important for cell fate assignment during later stages of zebrafish neurogenesis^{11,53} we wondered whether Delta/Notch signaling between C-dividing sister cells might be important for apico-basal polarity?

To explore this possibility, *mib1^{ta52b}* mutant cells were transplanted into wild-type hosts. As Mib1 is essential for Delta ligand activity, no Delta/Notch signaling occurs between *mib1^{ta52b}* mutant mitotic sister cells. Despite this fact, mutant cells display a polarized localization of Pard3-GFP at the apical cell surface (Fig. 7a). Conversely, wild-type cells implanted into the dorso-medial spinal cord of *mib1^{ta52b}* mutants hosts fail to display polarized Pard3 localization (Fig. 7b). Spinal cord apico-basal polarity does therefore not require Delta/Notch signaling between midline-crossing mitotic sister cells.

Notch signaling provides a local permissive environment for neuroepithelial morphogenesis. In the mouse and zebrafish forebrain, cells undergoing neuronal differentiation present Delta ligands to activate Notch in neighboring cells and thereby maintain their radial glia identity^{10,11,18}. If a similar mechanism is at work in the zebrafish spinal cord, Notch activity should be required cell autonomously to allow the emergence of neuroepithelial characteristics. To address this issue, we generated mosaic embryos in which Notch signaling is activated only in one half of the neural primordium (Fig. 7c-j, see Methods for details).

In a first set of experiments, RNAs encoding NICD and a red fluorescent membrane label (GAP43-RFP) were co-injected into one blastomere of two cell stage embryos. A second injection was performed to introduce green GAP43-GFP in the other blastomere (Fig. 7c,e). By the end of gastrulation embryos in which the progeny of the two injected blastomeres had populated the left and right sides of the animal were selected and grown further to analyze the morphology and behavior of cells in the neural primordium. In wild-type siblings, NICD-positive and

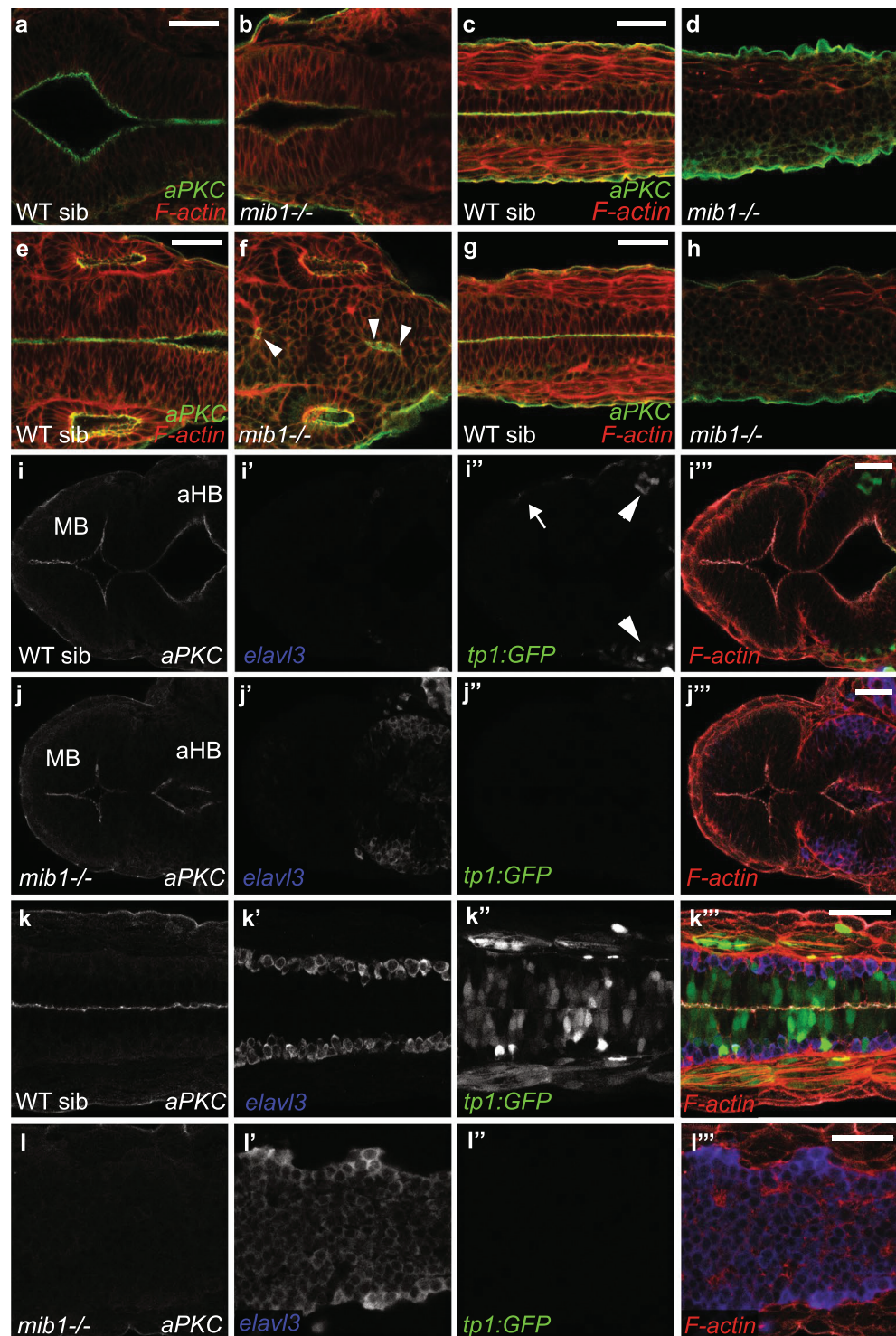


Figure 6. Notch loss of function differentially affects neuroepithelial polarity in the brain and spinal cord. (a–h) In *mib1* mutants neuroepithelial apico-basal polarity is maintained at the level of the midbrain-hindbrain boundary (b, n = 7), partially disrupted at the level of the hindbrain (f, arrowheads indicate residual polarized aPKC signal, n = 7) but completely lost in the dorso-medial spinal cord (d,h). (g,h) represent the most anterior and (c,d) the trunk spinal cord. (i–l) In WT siblings, the tp1bGlob:GFP (tp1:GFP) Notch reporter transgene indicates active signaling in a small number of cells in the anterior hindbrain (aHB, arrowheads in i''). More anteriorly, Notch activity is detected only in epidermal cells (arrow in i''') but not in the midbrain (MB) itself. *mib1* mutants present enhanced levels of neurogenesis (j') and a partial disruption of apical aPKC localisation (j) at the level of the anterior hindbrain (n = 9). Only few *elavl3*-positive neurons are detected in the midbrain, which maintains neuroepithelial organization (j,j'). (k,l) At the level of the anterior spinal cord, WT sibling embryos display widespread Notch reporter activity (k''), basally localized *elavl3*-positive neurons (k') and polarized aPKC enrichment at the apical neural tube midline (k, n = 6). *mib1* mutants present a loss of Notch

reporter expression (P⁺) and a lack of polarized aPKC localization (I, n = 8). Quantification of the area of the neural tube occupied by *elavl3* positive cells reveals an increase in neurogenesis in *mib1* mutants (P, $95.4 \pm 2.6\%$) compared to WT siblings (K, $31.7 \pm 5.8\%$, $p = 1.36E-07$). Pictures (a,c), (b,d), (e,g), (f,h), (i,k) and (j,l) each represent the same embryo imaged at different antero-posterior locations. All images are dorsal views of 30 somites stage embryos, anterior left. Scalebars: 40 μ m.

NICD-negative cells originating from the two neural tube halves both adopted an elongated morphology with cell bodies spanning the apico-basal extent of the neuroepithelium (Fig. 7d,d').

A different result was observed when the same manipulation was carried out in *mib1^{ta52b}* mutants (Fig. 7e,f). In this case, only NICD-positive cells adopted a characteristic epithelial morphology, while NICD-negative cells failed to contact the neural tube midline and populated the basolateral aspect of the neural tube, a behavior suggestive of neuronal differentiation. To confirm that NICD enables the emergence of apico-basal polarity, we performed a second set of experiments where NICD was co-injected with *Pard3-GFP* (Fig. 7g-j). These experiments confirmed that NICD restores an apico-basal polarization of *Pard3* in *mib1^{ta52b}* mutant cells (Fig. 7j).

Our observations suggest that Notch signaling is required cell autonomously to allow the acquisition of neuroepithelial characteristics. However, these experiments also provide evidence that, even in conditions where Notch signaling is active only in one half of the cells of the neural primordium (Fig. 7e,i), *mib1^{ta52b}* mutant neural tubes can present a continuous apical neural tube midline, as indicated by cell morphology (Fig. 7f), *Pard3-GFP* accumulation (Fig. 7j) and aPKC localization (Fig. 7j'). While Notch signaling enables the emergence of neuroepithelial characteristics only in the cells where it is active, the presence of a fraction of Notch-activating cells is therefore sufficient to convey an overall neuroepithelial organization to the spinal cord.

Notch-mediated inhibition of neurogenesis is required for the morphogenetic movements of zebrafish spinal cord precursor cells. In wild type zebrafish, midline-crossing C-divisions cause the intermingling of cells originating from the two halves of the neural tube (Fig. 7d,d')^{19,22}. Our experiments in which Notch signaling was restored in one half of the *mib1^{ta52b}* mutant neural primordium suggested that only NICD-positive but not NICD-negative cells may be able to cross the neural tube midline (Fig. 7f-f';j-j'). The midline-crossing of spinal cord cells has been proposed to confer a morphogenetic advantage for zebrafish spinal cord development^{20,23,27}, but the regulation of this behavior is poorly understood. In particular, it is not clear how this behavior is linked to neurogenic Notch signaling and neuronal differentiation. We decided to address this issue in *mib1^{ta52b}* mutants.

To visualize the midline-crossing of neural tube cells, one blastomere of two cell stage embryos was injected with *GAP43-GFP RNA* (Fig. 8a-j, Supplementary Fig. S6a-h). By the end of gastrulation, embryos in which the progeny of the injected blastomere occupied only the left or the right half of the embryo were selected for further analysis. Midline-crossing of neural tube cells is most prevalent from 14 to 18 hpf^{19,22}. Accordingly, extensive crossing of *GAP43-GFP* positive cells to the contralateral side of the neural tube is observed by the 14 somites stage (i.e. 16 hpf) in wild-type siblings (Supplementary Fig. S6b,j). In contrast, midline crossing is reduced in *mib1^{ta52b}* mutants (Supplementary Fig. S6d,j). Additional experiments confirmed that midline crossing is still reduced at later developmental stages (Fig. 8d,k,l, Supplementary Fig. S6f,h,k, Supplementary Table S2), establishing that this phenotype is not simply due to developmental delay of mutant embryos.

NICD injection restored midline crossing in *mib1^{ta52b}* mutants (Fig. 8f,k, Supplementary Table S2), thereby establishing that this morphogenetic defect is due to a loss of Notch signaling and not to additional Notch-independent functions of *Mib1* in the regulation of cell migration³⁵. Accordingly, midline crossing is also reduced in *dld; dla* deficient embryos (Fig. 8j,m).

When Notch signaling activity is restored in *mib1^{ta52b}* mutant neural tubes through unilateral NICD injection, NICD-negative cells remain confined to one side of the neural tube and adopt a morphology and basolateral localization that is indicative of neuronal differentiation (Fig. 7f'). Staining with the neuronal differentiation marker *elavl3* confirmed the neuronal identity of NICD-negative, non-crossing cells (Supplementary Fig. S7a,b). This observation raises the question whether the inability of *mib1^{ta52b}* mutant cells to cross the neural tube midline may be due to their premature neuronal differentiation? In accordance with this hypothesis, the midline-crossing of NICD-injected *mib1^{ta52b}* mutant cells correlates with a local inhibition of neuronal differentiation (Supplementary Fig. S7c-f).

While loss of Notch signaling and the resulting premature neuronal differentiation impair both the apico-basal polarization and the midline-crossing of neural tube cells, our experiments suggest that these two phenotypes are not strictly interdependent. Indeed, the injection of a dose of NICD that does not restore neural tube apico-basal polarity is already sufficient to rescue midline crossing (Fig. 8g,h,k, Supplementary Fig. S7k,l, Supplementary Tables S2 and S3).

The midline crossing of neural tube cells results in the intercalation of cells originating from the two sides of the neural tube, a behavior reminiscent of convergent extension movements^{22,26}. We therefore wondered whether the shape of the spinal cord primordium is altered in *mib1^{ta52b}* mutants? In accordance with this hypothesis, transversal sections of the anterior spinal cord reveal an increased width-to-height ratio in *mib1^{ta52b}* mutants (Fig. 8n,o,q, Supplementary Table S4).

Loss of Notch signaling activity causes the premature loss of neuroepithelial progenitor cells in the anterior spinal cord (Fig. 5d). As a consequence of this depletion of dividing progenitor cells, *mib1^{ta52b}* mutants present a reduction in neural tube cell number (Supplementary Fig. S8a-d). This raises the question whether the observed alteration in *mib1^{ta52b}* mutant neural tube proportions may be a secondary consequence of this reduction in cell number? Our observations argue against this hypothesis: First, the injection of NICD promotes a partial

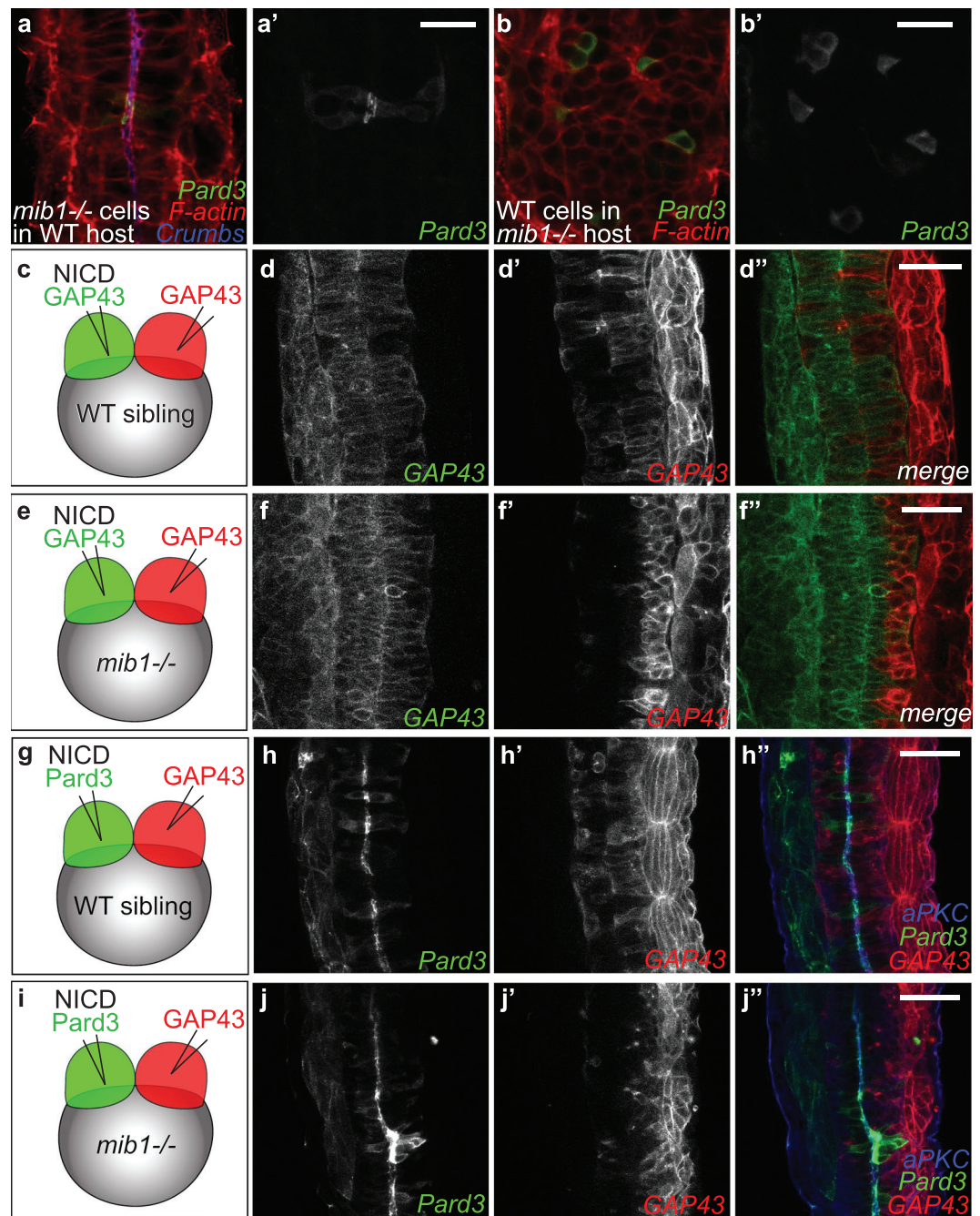


Figure 7. Dissection of the spatial requirement for Notch signaling in neural tube morphogenesis. (a,a') Pard3-GFP expressing *mib1* mutant cells undergo correct polarization when transplanted into WT hosts (n = 30 cells in 6 embryos). (b,b') In contrast, Pard3-GFP expressing WT cells fail to polarize when transplanted into *mib1* mutant hosts (n = 96 cells in 13 embryos). (a,b) are single confocal sections, (a',b') maximum projections of 5 slices separated by 2 μm intervals to visualize GFP-positive clones. (c-f) The two halves of the neural tube were labelled by injecting RNAs encoding red or green fluorescent membrane labels (GAP43) into the 2 blastomeres of 2-cell stage embryos (see Methods). (c,d) In WT sibling embryos half-injected with RNA encoding constitutively activated Notch (NICD), cells originating from both sides of the neural tube cross the neural tube midline to integrate the contra-lateral organ half (n = 7/7). (e,f) If NICD is half-injected into *mib1* mutants, NICD-containing cells display extensive midline crossing (f,f''), while the crossing of NICD-negative cells is reduced in 6/8 embryos (f,f''). (g-j) One half of the embryo was injected with RNA encoding NICD Pard3-GFP, the other half with GAP43-RFP. (g,h) 6/6 WT sibling embryos display apical Pard3 accumulation (h) and bilateral midline crossing (h,h'). (i,j) In *mib1* mutants, NICD causes apico-basal polarization and midline crossing of Pard3-GFP positive cells in 6/6 embryos (j). NICD-negative GAP43-RFP positive cells fail however to cross the neural tube midline in 5/6 embryos (j'). Pictures represent dorsal views of the spinal cord (anterior up) at 30 somites (a,b), 18 somites (d,f) and 21 somites (h,j) stages. Scalebars: a,b 20 μm , (d,f,h,j) 40 μm .

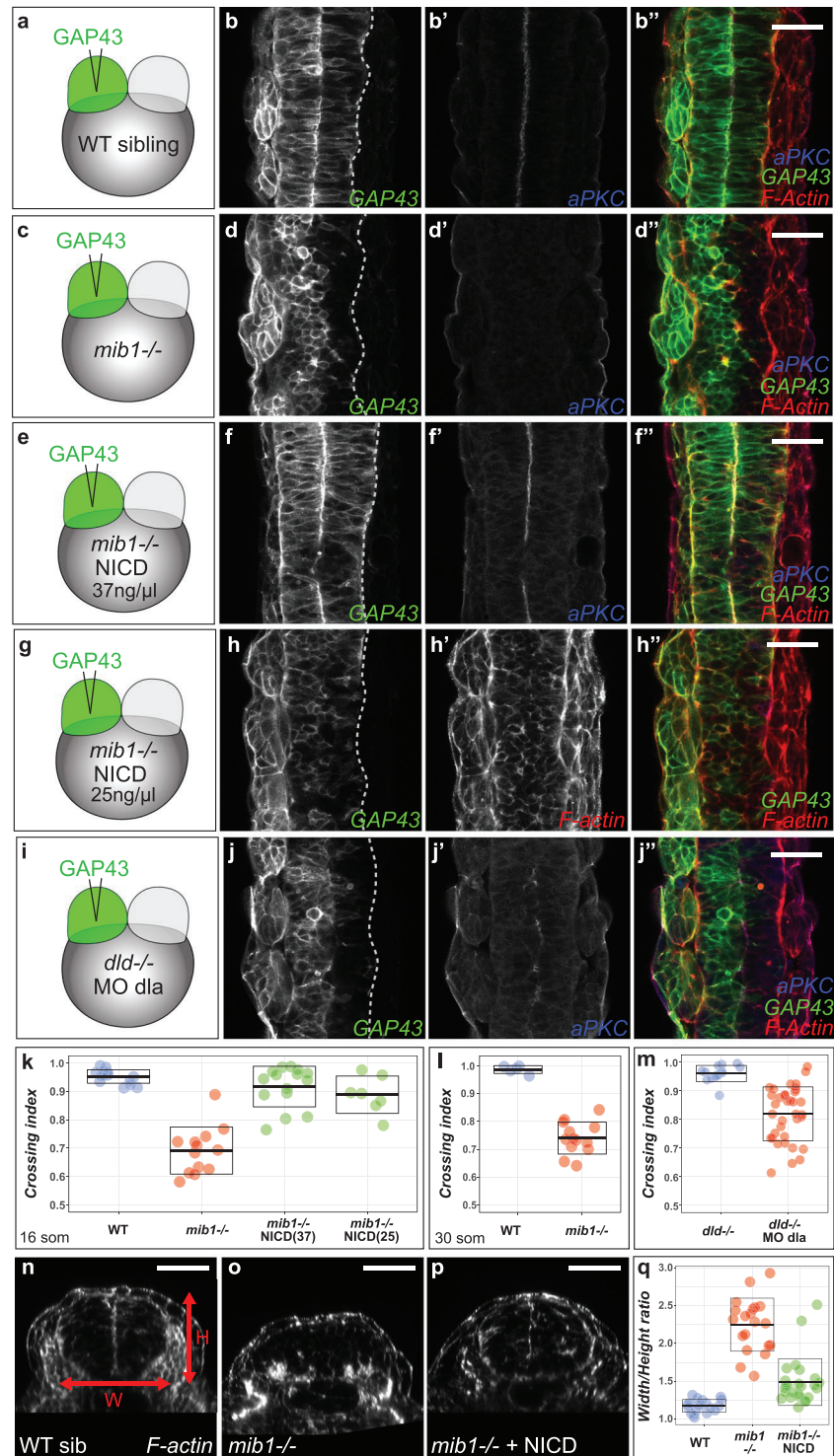


Figure 8. Notch loss of function impairs morphogenetic cell movements in the zebrafish spinal cord. (a–i) To label one half of the neural tube RNA encoding a fluorescent membrane label (GAP43-GFP) was injected into one blastomere of two cell stage embryos (see Methods). (a,b) In 16 somites stage WT siblings, cells from one half of the neural tube cross the organ midline to integrate the contra-lateral half. (c,d) In *mib1* mutants, neural tube cells fail to display this behavior. (e,f) RNA injection of constitutively activated Notch (NICD) at a concentration of 37.5 ng/μl restores apico-basal polarity (apical aPKC enrichment at the neural tube midline in f' compared to d') and midline-crossing cell movements (f) in *mib1* mutants. (g,h) Injection of a lower dose of NICD (25 ng/μl) fails to restore neuroepithelial morphology (note the lack of apical F-actin accumulation at the neural tube midline in h') but is sufficient to promote midline crossing (h). (i,j) Neural tube cells display reduced midline crossing in *dld*; *dla* compound mutant/morphants. (k) Quantification of neural tube midline crossing in WT, *mib1* mutants and NICD-injected *mib1* mutants (for details and statistical analysis see Methods, Supplementary Fig. S6i and Supplementary Table S2). (l) Reduced midline crossing is also observed

if WT sibling (crossing index 0.98 ± 0.01 , $n = 5$) and *mib1* mutants (0.74 ± 0.06 , $n = 13$) are compared at the 30 somites stage ($p = 3.9E-10$, see also Supplementary Fig. S6g,h). **(m)** Midline crossing is reduced in *dld*; *dla* mutants/morphants (0.82 ± 0.09 , $n = 36$) compared to *dld* single mutants (0.96 ± 0.03 , $n = 14$) ($p = 2.1E-10$). **(n–q)** Transversal sections of the anterior spinal cord used to measure neural tube width (W) and Height (H). *mib1* mutants **(o)** present an increased W/H ratio compared to WT siblings **(n)**. NICD RNA injection restores neural tube proportions **(p)**. **(q)** Quantification of W/H ratios, see Supplementary Table S4 for statistical analysis. **(b,d,f,h,j)** dorsal views of the anterior spinal cord at the 16 somites stage, anterior up. **(n–p)** transversal sections of the anterior spinal cord at 30 somites, after the completion of midline crossing. Scalebars: 40 μm . Boxes in **(k,l,m,q)** represent mean values \pm SD.

but clearly significant ($p = 1.14E-08$) restoration of neural tube proportions (Fig. 8p,q) while triggering only a minor and non-significant ($p = 0.129$) increase in neural tube cell number (Supplementary Fig. S8a–d, see Supplementary Tables S4 and S5 for statistical analysis).

The effect of the loss of neuroepithelial progenitors on the number of neural tube cells is expected to become more pronounced as development proceeds. We performed therefore a second additional analysis of neural tube cell number and proportions at an earlier developmental time point. Despite having a number of neural tube cells similar to WT siblings ($p = 0.23$, Supplementary Fig. S8e,f,h), 24 somites stage *mib1*^{ta52b} mutants present already a significantly increased width-to-height ratio ($p = 4.71E-06$, Supplementary Fig. S8e–g), confirming thereby that the altered proportions of *mib1*^{ta52b} neural tubes are not a secondary consequence of changes in the number of cells that compose the neural primordium.

Taken together, our findings suggest that Notch-mediated suppression of neurogenesis is essential to allow neural tube cells to execute specific morphogenetic behaviors that direct the proper shaping of the spinal cord.

Discussion

The aim of the present study was to investigate how cell fate specification and morphogenesis are linked during the development of the zebrafish nervous system. In higher vertebrates, a dual relationship exists between the polarized epithelial organization of the neural plate and neurogenic Notch signaling. Notch activation promotes the maintenance of polarized radial glia cells¹⁰ while the epithelial architecture of the neural primordium is itself required for Notch signaling¹⁸. In contrast, the early zebrafish neural plate does not display hallmarks of apico-basal polarity and the neural tube acquires a neuroepithelial tissue organization only several hours after the beginning of neurogenesis^{19,20}. Our work shows that in spite of these differences, Notch signaling is required for zebrafish spinal cord morphogenesis.

Previous studies have implicated noncanonical, transcription-independent Notch signaling in the late maintenance of apico-basal polarity in the ventral neural tube⁴⁴. In contrast, we show here that the E3-Ubiquitin ligase Mib1, a critical regulator of Delta internalization and Notch activation⁶, is required to initiate the epithelialization of the neural primordium (Figs. 1 & 4), allowing thereby the formation of a neural tube whose tissue organization is similar to the one of tetrapods.

Beyond the control of Delta ligand endocytosis, Mib1 has been shown to inhibit Epb41l5, a protein that facilitates the disassembly of apical junctional complexes³⁴. Likewise Neuralized, which promotes Delta internalization in *Drosophila*, exerts a Notch-independent activity in epithelial morphogenesis⁵⁴. However, our observations show that in the zebrafish spinal cord not only Mib1 itself, but the complete canonical Notch pathway including its transcriptional mediators RBPJ/Su(H) are required for neuroepithelial morphogenesis (Fig. 2).

Already before the onset of neurogenesis, the neural plate of higher vertebrates displays hallmarks of epithelial organization¹³. Our findings show that in zebrafish, the primordium of the developing spinal cord does initially not express markers of polarized neural precursor cells (*gfap*) and components of the apico-basal polarity machinery (*crb1*, *crb2a*, *pard6 γ B*) (Fig. 5). In this context, Notch signaling is required to restrain neuronal differentiation and allow thereby the upregulation of the neuroepithelial gene expression program. Accordingly, Notch signaling deficient animals fail to display the progressive epithelialization observed in the neural tube of wild-type controls (Fig. 4).

Various mechanisms have been shown to govern the establishment of apico-basal polarity in different systems⁵¹. Notch inactivation in the dorso-medial spinal cord of the early zebrafish embryo causes excessive neuronal differentiation and the loss of neuroepithelial gene expression and apico-basal polarity (Fig. 5, Supplementary Fig. S4). It remains to be established whether Notch actively induces neuroepithelial properties or if, alternatively, these characteristics emerge by default as soon as Notch inhibits neuronal differentiation. As available tools do not allow manipulating Notch signaling and neurogenic differentiation independently of each other, it is currently not possible to address this question directly. Our experiments show that the establishment of apico-basal polarity in the floor plate (Fig. 3, Supplementary Fig. S3) and the MHB region (Fig. 6) do not require Mib1 function. In these developmental contexts, Notch signaling appears therefore not to be required to actively promote neuroepithelial tissue organization.

The differences in the mechanisms that control the morphogenesis of various parts of the nervous system are likely due to the fact that the importance of Notch signaling for developmental cell fate decisions varies according to the biological context. In contrast to more dorsal spinal cord cells, floor plate cells give rise essentially to glial derivatives⁵⁵. Accordingly, *mib1* mutant floor plate cells do not undergo neuronal differentiation and retain their apico-basal polarity and expression of the radial glia marker *gfap*. At the level of the MHB, neurogenic differentiation is inhibited by the hairy-related transcription factor *her5*, which acts independently of Notch signaling⁵⁶. This situation is different from the spinal cord where neurogenesis is regulated by the Notch-responsive *her4* gene⁵⁷.

Spinal cord development requires not only neurogenesis but also the execution of specific morphogenetic movements^{20,21,23}. In the zebrafish, cells from one side of the neural tube invade the contra-lateral organ half by undergoing midline-crossing C-divisions^{19,26,27}. We show that Notch-mediated suppression of neurogenesis is required to allow neural tube cells to execute their midline-crossing behavior (Fig. 8, Supplementary Figs S6 and S7).

Manipulations of PCP pathway activity have been shown to impair the midline-crossing behavior of neural tube cells^{22,26}. Due to the general requirement of PCP signaling for embryonic convergent extension movements, these experiments have however not allowed to evaluate the actual impact of this morphogenetic behavior on the shaping of the neural tube. We show that in *mib1^{ta52b}* mutants, which do not display general convergent extension phenotypes, the cells of the neural primordium fail to display midline crossing and give rise to a misproportioned spinal cord (Fig. 8, Supplementary Fig. S8). Our findings suggest that through its ability to restrain neuronal differentiation, the Notch pathway provides a temporal window for neural tube cells to execute specific morphogenetic movements that determine the proportions of the spinal cord primordium prior to neuronal differentiation.

In conclusion, our findings show that, in addition to regulating the timing and identity of neuronal cell fate specification, Notch-mediated suppression of neurogenesis is essential to allow the acquisition of neuroepithelial tissue organization and the execution of specific morphogenetic movements that are required for the proper shaping of the zebrafish spinal cord.

Methods

Zebrafish strains and genotyping. Zebrafish strains were maintained under standard conditions and staged as previously described⁵⁸. Zebrafish embryos were grown in 0.3x Danieau medium.

Depending on the experiment, *mib1* homozygous animals were identified using DeltaD immunostaining (mutant embryos can be identified by upregulated D/D signal at the cell membrane, Fig. 1c^{''}) or molecular genotyping (see below). From the 14 somites stage onwards, somitic segmentation defects allow a pre-selection of *mib1* homozygous mutant embryos prior to confirmation of the mutant genotype by one of the two above-mentioned approaches.

With the exception of the analysis of *mib1*; *mib2* double mutants (Supplementary Fig. S5) genetic inactivation of *mindbomb1* was performed using the *mib1^{ta52b}* allele⁶. A 4-primer-PCR was established to identify *mib1^{ta52b}* and WT alleles in a single PCR reaction. The following primers were used: 5'-ACAGTAACTAAGGAGGGC-3' (generic forward primer), 5'-AGATCGGGCACTCGCTCA-3' (specific reverse primer for the WT allele), 5'-TCAGCTGTGTGGAGACCGCAG-3' (specific forward primer for the *mib1^{ta52b}* allele), and 5'-CTTACCATGCTCTACAC-3' (generic reverse primer). WT and *mib1^{ta52b}* mutant alleles respectively yield 303 bp and 402 bp amplification fragments. As some zebrafish strains present polymorphic *mib1* WT alleles, it is important to validate the applicability of this protocol before using it in a given genetic background.

Analysis of *mib1*; *mib2* double mutants was performed using the *mib1^{tf91}* and *mib2^{chi3}* null mutant alleles²⁸. The presence of the *mib1^{tf91}* allele was detected using the primers 5'-ATGACCACCGGCAGGAATAACC-3' (forward), and 5'-ACATCATAAGCCCCGGAGCAGCGC-3' (reverse, 203 bp amplicon). The corresponding WT allele was detected using the primers: 5'-TAACGGCACCCGCCAATTAC-3' (forward), 5'-GCGACCCAGATTAATAAAGGG-3' (reverse, 307 bp amplicon).

mib2^{chi3} mutant animals were identified by PCR amplification and sequencing of the mutation-carrying genomic region with the primers 5'-GCTCATCAGGGTCATGTAGAG-3' (forward) and 5'-CTCCTATTGTTTGTGAGTGCAAAC-3' (reverse, 254 bp amplicon).

PCR amplifications were carried out using GoTaq polymerase (Promega) at 1.5 mM MgCl₂ using the following cycling parameters: 2 min 95 °C - 10 cycles [30 sec. 95 °C - 30 sec. 65 to 55 °C - 60 sec. 72 °C] - 25 cycles [30 sec. 95 °C - 30 sec. 55 °C - 60 sec. 72 °C] - 5 min 72 °C.

To inactivate *deltad* we used *dld/aei^{AR33}* mutant embryos obtained through incrossing of homozygous mutant adult fish. To visualize Notch signaling activity, we used the *tp1bglob:eGFP* transgenic line⁴⁶.

mRNA and morpholino injections. Microinjections into dechorionated embryos were carried out using a pressure microinjector (Eppendorf FemtoJet). Capped mRNAs were synthesized using the SP6 mMessage mMachine kit (Ambion) and poly-adenylated using a polyA tailing kit (Ambion). RNA and morpholinos were injected together with 0.2% Phenol Red.

RNA microinjection was performed using the following constructs and concentrations: Mindbomb1-pCS2 + (125 ng/μl)³⁶; Pard3-GFP-pCS2 + (50 ng/μl)³¹; DN-Su(H)-pCS2 + (600 ng/μl)⁴¹; CA-Su(H)-pCS2 + (40 ng/μl)⁴¹; Myc-Notch-Intra-pCS2 + (25–37.5 ng/μl)⁴⁰; Gap43-GFP-pCS2 + (20 ng/μl) and GAP43-RFP-pCS2 + (30 ng/μl).

Morpholino oligonucleotides were injected at the indicated concentrations to knock down the following genes: *mindbomb1*: 5'-GCAGCCTCACCTGTAGGCGCACTGT-3' (1000 μM)⁶; *deltaA*: 5'-CTTCTCTTTTCGCCGACTGATTCAT-3' (250 μM)³⁷; *RBPJa*: 5'-GCGCCATCTTACCAACTCTCTCTA-3' (50 μM) and *RBPJb*: 5'-GCGCCATCTTCCACAAACTCTCACC-3' (50 μM). To ensure that the phenotypes of *dld/dld^{AR33}* morphant/mutants and *RBPJa&b* double morphants were not due to non-specific p53-mediated responses, we performed these experiments in the presence of a validated p53 Morpholino (5'-GCGCCATGCTTTGCAAGAATTG-5', 333 μM)⁶⁰.

Gamma-secretase inhibitor treatment. At mid-gastrulation zebrafish embryos were transferred to 0.3x Danieau medium containing 50 μM LY411575³⁹ (Sigma) or 100 μM DAPT³⁸ (Sigma) dissolved in DMSO. Embryos were raised till the 30 somites stage before being processed for antibody staining. Control embryos were mock-treated with DMSO alone.

Whole mount *in situ* hybridization. *In situ* hybridization was performed according to Thisse *et al.*⁶¹. DIG-labeled antisense RNA probes were transcribed from PCR products carrying the T7-promoter sequence (5'-TAATACGACTCACTATAGGG-3') on the reverse primer. PCR amplicons for the different genes were flanked by the following sequences: *sox19a*: forward: 5'-CGATGTCGGGTGAAGATG-3', reverse: 5'-CTGTCAAGGTTGTCAAGTCAC-3' *gfap*: forward: 5'-TAAAGAGTCCACTACGGAGAGG-3', reverse: 5'-GGCACCACAATGAAGTAATGTCC-3', *crumbs1*: forward: 5'-TGTACCACCAGCCCATGTCATA-3', reverse: 5'-cctcatcacagtttgaccac-3'; *crumbs2a*: forward: 5'-TGAGAGTGGCCCCCTGCCTTAAT-3', reverse: 5'-acagtcacagcggtagc-3'; *pard6γb*: forward: 5'-GACTACAGCAACTTTGGCACCAGCACTCT-3', reverse: 5'-gtgatgactgtccatcctc-3'.

Immunocytochemistry. Embryos were fixed in 4% paraformaldehyde in PEM (PIPES 80 mM, EGTA 5 mM, MgCl₂ 1 mM) for 1.5 hours at room temperature or overnight at 4 °C, before being permeabilized with 0.2% TritonX-100 in PEM-PFA for 30 minutes at room temperature. Subsequent washes and antibody incubations were performed in PEM + 0,2% TritonX-100. Primary antibodies used were: Mouse@DeltaD⁶ (1:500, Abcam ab73331); Mouse@DeltaA⁶² (1:250, ZIRC 18D2); Rabbit@aPKC³⁰ (1:250, Santa Cruz sc-216); Mouse@ZO1⁶³ (1:500, Invitrogen 1A12); Mouse@HuC/D⁶⁴ (1:500, Invitrogen 16A11); Rabbit@γ-Tubulin (1:250, Sigma T5192).

Cell transplantations. For cell transplantation embryos were maintained in 1x Danieau medium +5% penicillin-streptomycin. Donor embryos were labelled by injection of RNA encoding *Pard3*-GFP at the one-cell stage. Cell transplantations were carried out at late blastula/early gastrula stages. In each experiment, 20–30 cells were aspirated from the donor embryo using a manual microinjector (Sutter Instruments) and transplanted into the host embryo. Transplanted embryos were grown till the 30 somites stage in agarose-coated petri dishes with 0.3x Danieau and 5% penicillin-streptomycin before being fixed and processed for antibody staining.

Analysis of neural tube cell midline-crossing behaviour. To label one half of the neural tube, GAP43-GFP RNA was injected into one blastomere of 2-cell stage zebrafish embryos. The embryos were then grown till the bud stage, at which time point the localisation of the fluorescent cells was analysed using a fluorescence stereomicroscope (Leica M205 FA). In a typical experiment, about 50% of the embryos displayed a unilateral localisation of GFP-positive cells and were kept to be grown till the desired stage before being fixed and processed for antibody staining. In contrast to the cells of the neural tube, somitic precursors do not cross the embryonic midline in the course of development. Consequently, successful half-injection results in a unilateral labelling of the somites that becomes visible at confocal analysis.

To quantify the extent of neural tube cell midline crossing, a crossing index was determined for each individual embryo as the fraction of the neural tube populated by GFP-positive cells (Supplementary Fig. S6i). Measurements were performed at the level of the medial neural tube. The total neural tube area and the GFP-positive area were outlined manually in Fiji using the F-actin and GFP channels.

To separately label the two opposite sides of the neural tube, 50 2-cell stage embryos were initially injected into one blastomere with RNA encoding the first fluorescent membrane label (e.g. GAP43-GFP). The presence of Phenol red in the injection mix allows identifying the injected blastomere for several minutes after injection. A second injection needle was then used to inject the second RNA (e.g. GAP43-RFP) into the other blastomere. Embryos were grown till the bud stage and screened for efficient double half injection as described above.

Microscopy and image analysis. For confocal imaging, embryos were mounted in 0.75% low melting point agarose (Sigma) in glass bottom dishes (MatTek corporation). Embryos were imaged on Spinning disk (Andor) or Laser scanning confocal microscopes (Zeiss LSM510, 710, 780 and 880) using 40x Water or 60x Oil immersion objectives. *In situ* gene expression patterns were documented on a Leica M205FA-Fluocombi stereomicroscope. Image analysis was performed using ImageJ (<http://rbs.info.nih.gov/ij/>) or Zeiss ZEN software.

For the quantification of the temporal progression of apico-basal polarity in the neural tube (Fig. 4m), we acquired confocal stacks spanning the entire dorso-ventral extent of the neural tube. The percentage of neural tube polarity was then calculated for each embryo as the number of confocal slices displaying polarized aPKC enrichment, divided by the total number of slices of the neural tube stack. Examples of individual confocal slices at different dorso-ventral locations are shown in Fig. 4a–l.

For the quantification of neurogenesis, we measured the fraction of the neural tube area that was positive for the neuronal marker *elav3* using Fiji. The total area of the neural tube was outlined manually using the F-actin signal. The area occupied by neuronal cells was estimated by applying a constant intensity threshold to the *elav3* channel.

For the analysis of cell number and width-to-height (W/H) ratio in the spinal cord, embryos were stained with fluorescent Phalloidin and DAPI and mounted in glass bottom dishes with the dorsal surface of the embryo facing the coverslip. Embryos were imaged using a Zeiss LSM880 confocal microscope. A line scan was performed at the border between the 2nd somite and the 3rd somite to obtain a transversal section of the spinal cord. Zeiss ZEN imaging software was used to measure the width and the height of the spinal cord.

The number of Dapi-positive nuclei by transversal neural tube section was quantified in Fiji using the manual multi-point selection tool. Due to the thickness of the neural tube, nuclei in the ventral part of the neural tube (i.e. farthest from the objective) appear dimmer than more dorsal ones. Contrast adjustments during the quantification procedure were therefore used to reliably quantify both dorsal and ventral nuclei.

Statistical analysis. Statistical analysis was carried out using the R/RStudio packages for statistical computing. Analysis of experiments involving more than two conditions was performed using Welch's Anova (one-way.test function), followed by a Games-Howell post-hoc test (posthocTGH function) for pairwise comparisons

between different experimental groups. For experiments involving only two experimental conditions, p-values were calculated using Welch's two-sample t-Test (t.test function). Mean values are indicated \pm SD. Data normality and variance were analyzed using the stat.desc and leveneTest functions.

Use of research animals. Animal experiments were performed in the iBV Zebrafish facility (experimentation authorization #B-06-088-17) in accordance with the guidelines of the ethics committee Ciepal Azur and the iBV animal welfare committee.

Data Availability

The datasets generated and analysed during the current study are available from the corresponding author on reasonable request.

References

- Hori, K., Sen, A. & Artavanis-Tsakonas, S. Notch signaling at a glance. *J Cell Sci* **126**, 2135–2140, <https://doi.org/10.1242/jcs.127308> (2013).
- Shin, J., Poling, J., Park, H. C. & Appel, B. Notch signaling regulates neural precursor allocation and binary neuronal fate decisions in zebrafish. *Development* **134**, 1911–1920 (2007).
- Haddon, C. *et al.* Multiple delta genes and lateral inhibition in zebrafish primary neurogenesis. *Development* **125**, 359–370 (1998).
- Bray, S. J. Notch signalling: a simple pathway becomes complex. *Nat Rev Mol Cell Biol* **7**, 678–689 (2006).
- Chapouton, P. *et al.* Notch activity levels control the balance between quiescence and recruitment of adult neural stem cells. *J Neurosci* **30**, 7961–7974, <https://doi.org/10.1523/JNEUROSCI.6170-09.2010> (2010).
- Itoh, M. *et al.* Mind bomb is a ubiquitin ligase that is essential for efficient activation of Notch signaling by Delta. *Dev Cell* **4**, 67–82 (2003).
- Le Borgne, R. & Schweisguth, F. Unequal segregation of Neuralized biases Notch activation during asymmetric cell division. *Dev Cell* **5**, 139–148 (2003).
- Fürthauer, M. & González-Gaitán, M. Endocytic regulation of notch signalling during development. *Traffic* **10**, 792–802 (2009).
- Gaiano, N., Nye, J. S. & Fishell, G. Radial glial identity is promoted by Notch1 signaling in the murine forebrain. *Neuron* **26**, 395–404 (2000).
- Yoon, K. J. *et al.* Mind bomb 1-expressing intermediate progenitors generate notch signaling to maintain radial glial cells. *Neuron* **58**, 519–531, <https://doi.org/10.1016/j.neuron.2008.03.018> (2008).
- Dong, Z., Yang, N., Yeo, S. Y., Chitnis, A. & Guo, S. Intralineaage directional Notch signaling regulates self-renewal and differentiation of asymmetrically dividing radial glia. *Neuron* **74**, 65–78, <https://doi.org/10.1016/j.neuron.2012.01.031> (2012).
- Kim, H. *et al.* Notch-regulated oligodendrocyte specification from radial glia in the spinal cord of zebrafish embryos. *Dev Dyn* **237**, 2081–2089, <https://doi.org/10.1002/dvdy.21620> (2008).
- Götz, M. & Huttner, W. B. The cell biology of neurogenesis. *Nat Rev Mol Cell Biol* **6**, 777–788, <https://doi.org/10.1038/nrm1739> (2005).
- Norden, C. Pseudostratified epithelia - cell biology, diversity and roles in organ formation at a glance. *J Cell Sci* **130**, 1859–1863, <https://doi.org/10.1242/jcs.192997> (2017).
- Miyamoto, Y., Sakane, F. & Hashimoto, K. N-cadherin-based adherens junction regulates the maintenance, proliferation, and differentiation of neural progenitor cells during development. *Cell Adh Migr* **9**, 183–192, <https://doi.org/10.1080/19336918.2015.1005466> (2015).
- McIntosh, R., Norris, J., Clarke, J. D. & Alexandre, P. Spatial distribution and characterization of non-apical progenitors in the zebrafish embryo central nervous system. *Open Biol* **7**, <https://doi.org/10.1098/rsob.160312> (2017).
- Kimura, Y., Satou, C. & Higashijima, S. V2a and V2b neurons are generated by the final divisions of pair-producing progenitors in the zebrafish spinal cord. *Development* **135**, 3001–3005 (2008).
- Hatakeyama, J. *et al.* Cadherin-based adhesions in the apical endfoot are required for active Notch signaling to control neurogenesis in vertebrates. *Development* **141**, 1671–1682, <https://doi.org/10.1242/dev.102988> (2014).
- Geldmacher-Voss, B., Reugels, A. M., Pauls, S. & Campos-Ortega, J. A. A 90-degree rotation of the mitotic spindle changes the orientation of mitoses of zebrafish neuroepithelial cells. *Development* **130**, 3767–3780 (2003).
- Araya, C., Ward, L. C., Girdler, G. C. & Miranda, M. Coordinating cell and tissue behavior during zebrafish neural tube morphogenesis. *Dev Dyn* **245**, 197–208, <https://doi.org/10.1002/dvdy.24304> (2016).
- Korzh, V. Stretching cell morphogenesis during late neurulation and mild neural tube defects. *Dev Growth Differ* **56**, 425–433, <https://doi.org/10.1111/dgd.12143> (2014).
- Tawk, M. *et al.* A mirror-symmetric cell division that orchestrates neuroepithelial morphogenesis. *Nature* **446**, 797–800 (2007).
- Cearns, M. D., Escuin, S., Alexandre, P., Greene, N. D. & Copp, A. J. Microtubules, polarity and vertebrate neural tube morphogenesis. *J Anat* **229**, 63–74, <https://doi.org/10.1111/joa.12468> (2016).
- Hong, E. & Brewster, R. N-cadherin is required for the polarized cell behaviors that drive neurulation in the zebrafish. *Development* **133**, 3895–3905, <https://doi.org/10.1242/dev.02560> (2006).
- Alexandre, P., Reugels, A. M., Barker, D., Blanc, E. & Clarke, J. D. Neurons derive from the more apical daughter in asymmetric divisions in the zebrafish neural tube. *Nat Neurosci* **13**, 673–679 (2010).
- Ciruna, B., Jenny, A., Lee, D., Mlodzik, M. & Schier, A. F. Planar cell polarity signalling couples cell division and morphogenesis during neurulation. *Nature* **439**, 220–224 (2006).
- Buckley, C. E. *et al.* Mirror-symmetric microtubule assembly and cell interactions drive lumen formation in the zebrafish neural rod. *EMBO J* **32**, 30–44 (2013).
- Mikami, S., Nakaura, M., Kawahara, A., Mizoguchi, T. & Itoh, M. Mindbomb 2 is dispensable for embryonic development and Notch signalling in zebrafish. *Biol Open* **4**, 1576–1582, <https://doi.org/10.1242/bio.014225> (2015).
- Matsuda, M. & Chitnis, A. B. Interaction with Notch determines endocytosis of specific Delta ligands in zebrafish neural tissue. *Development* **136**, 197–206 (2009).
- Horne-Badovinac, S. *et al.* Positional cloning of heart and soul reveals multiple roles for PKC lambda in zebrafish organogenesis. *Curr Biol* **11**, 1492–1502 (2001).
- von Trotha, J. W., Campos-Ortega, J. A. & Reugels, A. M. Apical localization of ASIP/PAR-3:EGFP in zebrafish neuroepithelial cells involves the oligomerization domain CR1, the PDZ domains, and the C-terminal portion of the protein. *Dev Dyn* **235**, 967–977, <https://doi.org/10.1002/dvdy.20715> (2006).
- Omori, Y. & Malicki, J. oko meduzy and related crumbs genes are determinants of apical cell features in the vertebrate embryo. *Curr Biol* **16**, 945–957, <https://doi.org/10.1016/j.cub.2006.03.058> (2006).
- Hong, E., Jayachandran, P. & Brewster, R. The polarity protein Pard3 is required for centrosome positioning during neurulation. *Dev Biol* **341**, 335–345, <https://doi.org/10.1016/j.ydbio.2010.01.034> (2010).
- Matsuda, M. *et al.* Epb4115 competes with Delta as a substrate for Mib1 to coordinate specification and differentiation of neurons. *Development*. <https://doi.org/10.1242/dev.138743> (2016).

35. Mizoguchi, T., Ikeda, S., Watanabe, S., Sugawara, M. & Itoh, M. Mib1 contributes to persistent directional cell migration by regulating the Ctnnd1-Rac1 pathway. *Proc Natl Acad Sci USA* **114**, E9280–E9289, <https://doi.org/10.1073/pnas.1712560114> (2017).
36. Zhang, C., Li, Q. & Jiang, Y. J. Zebrafish Mib and Mib2 are mutual E3 ubiquitin ligases with common and specific delta substrates. *J Mol Biol* **366**, 1115–1128, <https://doi.org/10.1016/j.jmb.2006.11.096> (2007).
37. Latimer, A. J., Dong, X., Markov, Y. & Appel, B. Delta-Notch signaling induces hypochord development in zebrafish. *Development* **129**, 2555–2563 (2002).
38. Geling, A., Steiner, H., Willem, M., Bally-Cuif, L. & Haass, C. A gamma-secretase inhibitor blocks Notch signaling *in vivo* and causes a severe neurogenic phenotype in zebrafish. *EMBO Rep* **3**, 688–694, <https://doi.org/10.1093/embo-reports/kvf124> (2002).
39. Rothenaigier, I. *et al.* Clonal analysis by distinct viral vectors identifies bona fide neural stem cells in the adult zebrafish telencephalon and characterizes their division properties and fate. *Development* **138**, 1459–1469, <https://doi.org/10.1242/dev.058156> (2011).
40. Takke, C. & Campos-Ortega, J. A. her1, a zebrafish pair-rule like gene, acts downstream of notch signalling to control somite development. *Development* **126**, 3005–3014 (1999).
41. Wettstein, D. A., Turner, D. L. & Kintner, C. The Xenopus homolog of Drosophila Suppressor of Hairless mediates Notch signaling during primary neurogenesis. *Development* **124**, 693–702 (1997).
42. Main, H., Radenkovic, J., Jin, S. B., Lendahl, U. & Andersson, E. R. Notch signaling maintains neural rosette polarity. *PLoS One* **8**, e62959 (2013).
43. Echeverri, K. & Oates, A. C. Coordination of symmetric cyclic gene expression during somitogenesis by Suppressor of Hairless involves regulation of retinoic acid catabolism. *Dev Biol* **301**, 388–403, <https://doi.org/10.1016/j.ydbio.2006.10.003> (2007).
44. Ohata, S. *et al.* Dual roles of Notch in regulation of apically restricted mitosis and apicobasal polarity of neuroepithelial cells. *Neuron* **69**, 215–230 (2011).
45. Appel, B. *et al.* Delta-mediated specification of midline cell fates in zebrafish embryos. *Curr Biol* **9**, 247–256, doi:S0960-9822(99)80113-4 [pii] (1999).
46. Parsons, M. J. *et al.* Notch-responsive cells initiate the secondary transition in larval zebrafish pancreas. *Mech Dev* **126**, 898–912 (2009).
47. Zou, J., Wen, Y., Yang, X. & Wei, X. Spatial-temporal expressions of Crumbs and Nagie oko and their interdependence in zebrafish central nervous system during early development. *Int J Dev Neurosci* **31**, 770–782, <https://doi.org/10.1016/j.ijdevneu.2013.09.005> (2013).
48. Yang, X., Zou, J., Hyde, D. R., Davidson, L. A. & Wei, X. Stepwise maturation of apicobasal polarity of the neuroepithelium is essential for vertebrate neurulation. *J Neurosci* **29**, 11426–11440, <https://doi.org/10.1523/JNEUROSCI.1880-09.2009> (2009).
49. Hudish, L. I., Blasky, A. J. & Appel, B. miR-219 regulates neural precursor differentiation by direct inhibition of apical par polarity proteins. *Dev Cell* **27**, 387–398, <https://doi.org/10.1016/j.devcel.2013.10.015> (2013).
50. Okuda, Y. *et al.* Comparative genomic and expression analysis of group B1 sox genes in zebrafish indicates their diversification during vertebrate evolution. *Dev Dyn* **235**, 811–825, <https://doi.org/10.1002/dvdy.20678> (2006).
51. Rodriguez-Boulan, E. & Macara, I. G. Organization and execution of the epithelial polarity programme. *Nat Rev Mol Cell Biol* **15**, 225–242, <https://doi.org/10.1038/nrm3775> (2014).
52. Munson, C. *et al.* Regulation of neurocoel morphogenesis by Pard6 gamma b. *Dev Biol* **324**, 41–54, <https://doi.org/10.1016/j.ydbio.2008.08.033> (2008).
53. Kressmann, S., Campos, C., Castanon, I., Fürthauer, M. & González-Gaitán, M. Directional Notch trafficking in Sara endosomes during asymmetric cell division in the spinal cord. *Nat Cell Biol* **17**, 333–339, <https://doi.org/10.1038/ncb3119> (2015).
54. Chanet, S. & Schweisguth, F. Regulation of epithelial polarity by the E3 ubiquitin ligase Neuralized and the Bearded inhibitors in Drosophila. *Nat Cell Biol* **14**, 467–476 (2012).
55. Bonilla, S. *et al.* Identification of midbrain floor plate radial glia-like cells as dopaminergic progenitors. *Glia* **56**, 809–820, <https://doi.org/10.1002/glia.20654> (2008).
56. Geling, A., Plessy, C., Rastegar, S., Strähle, U. & Bally-Cuif, L. Her5 acts as a prepattern factor that blocks neurogenin1 and coe2 expression upstream of Notch to inhibit neurogenesis at the midbrain-hindbrain boundary. *Development* **131**, 1993–2006, <https://doi.org/10.1242/dev.01093> (2004).
57. Takke, C., Dornseifer, P., v Weizsäcker, E. & Campos-Ortega, J. A. her4, a zebrafish homologue of the Drosophila neurogenic gene E(spl), is a target of NOTCH signalling. *Development* **126**, 1811–1821 (1999).
58. Kimmel, C. B., Ballard, W. W., Kimmel, S. R., Ullmann, B. & Schilling, T. F. Stages of embryonic development of the zebrafish. *Dev Dyn* **203**, 253–310, <https://doi.org/10.1002/aja.1002030302> (1995).
59. Holley, S. A., Geisler, R. & Nüsslein-Volhard, C. Control of her1 expression during zebrafish somitogenesis by a delta-dependent oscillator and an independent wave-front activity. *Genes Dev* **14**, 1678–1690 (2000).
60. Robu, M. E. *et al.* p53 activation by knockdown technologies. *PLoS Genet* **3**, e78, <https://doi.org/10.1371/journal.pgen.0030078> (2007).
61. Thisse, C. & Thisse, B. High-resolution *in situ* hybridization to whole-mount zebrafish embryos. *Nat Protoc* **3**, 59–69, <https://doi.org/10.1038/nprot.2007.514> (2008).
62. Tallafuss, A., Trepman, A. & Eisen, J. S. Delta mRNA and protein distribution in the zebrafish nervous system. *Dev Dyn* **238**, 3226–3236, <https://doi.org/10.1002/dvdy.22136> (2009).
63. Itoh, M., Nagafuchi, A., Yonemura, S., Kitani-Yasuda, T. & Tsukita, S. The 220-kD protein colocalizing with cadherins in non-epithelial cells is identical to ZO-1, a tight junction-associated protein in epithelial cells: cDNA cloning and immunoelectron microscopy. *J Cell Biol* **121**, 491–502 (1993).
64. Marusich, M. F. & Weston, J. A. Identification of early neurogenic cells in the neural crest lineage. *Dev Biol* **149**, 295–306 (1992).

Acknowledgements

This study was supported by a CNRS/INSERM ATIP/Avenir 2010 grant and an HFSP Career Development Award (00036/2010) to M.F. P.S. benefited from an FRM 4th year PhD fellowship (FDT20140930987). L.X. was supported by an ARC postdoctoral fellowship (PDF20121206203). V.M.S. is supported by the LABEX SIGNALIFE PhD program (ANR-11-LABX-0028-01). Confocal microscopy was performed with the help of the iBV PRISM imaging platform. *mib2^{chl3}* was obtained from the Japanese National Bioresource Project. We thank L. Bally-Cuif, Y.J. Jiang, M. Itoh, C. Kinter, J. Malicki, A. Oates, E. Ober, S. Sokol, and D. Stainier for the sharing of fish lines and reagents. We are grateful to S. Polès, M.A. Derieppe, R. Rebillard and F. Paput for excellent technical assistance.

Author Contributions

P.S. performed the experiments reported in Figures 1a–g, 2a–f,m,n, 4, 5i–x, 6a–h, 7a,b and S2a–h. V.M.S. performed the experiments of Figures 1h–k, 2i–l,o,p, 7c–j, 8, S2i–l, S5, S6, S7 and S8. L.X. performed the experiment displayed in Figure 2g,h. M.F. provided the data for Figures 3, 5a–h, 6i–l, S1, S3 and S4. M.F. designed and supervised the study and wrote the manuscript. All authors analyzed the data and contributed to the final version of the manuscript.

Additional Information

Supplementary information accompanies this paper at <https://doi.org/10.1038/s41598-019-46067-1>.

Competing Interests: The authors declare no competing interests.

Publisher's note: Springer Nature remains neutral with regard to jurisdictional claims in published maps and institutional affiliations.



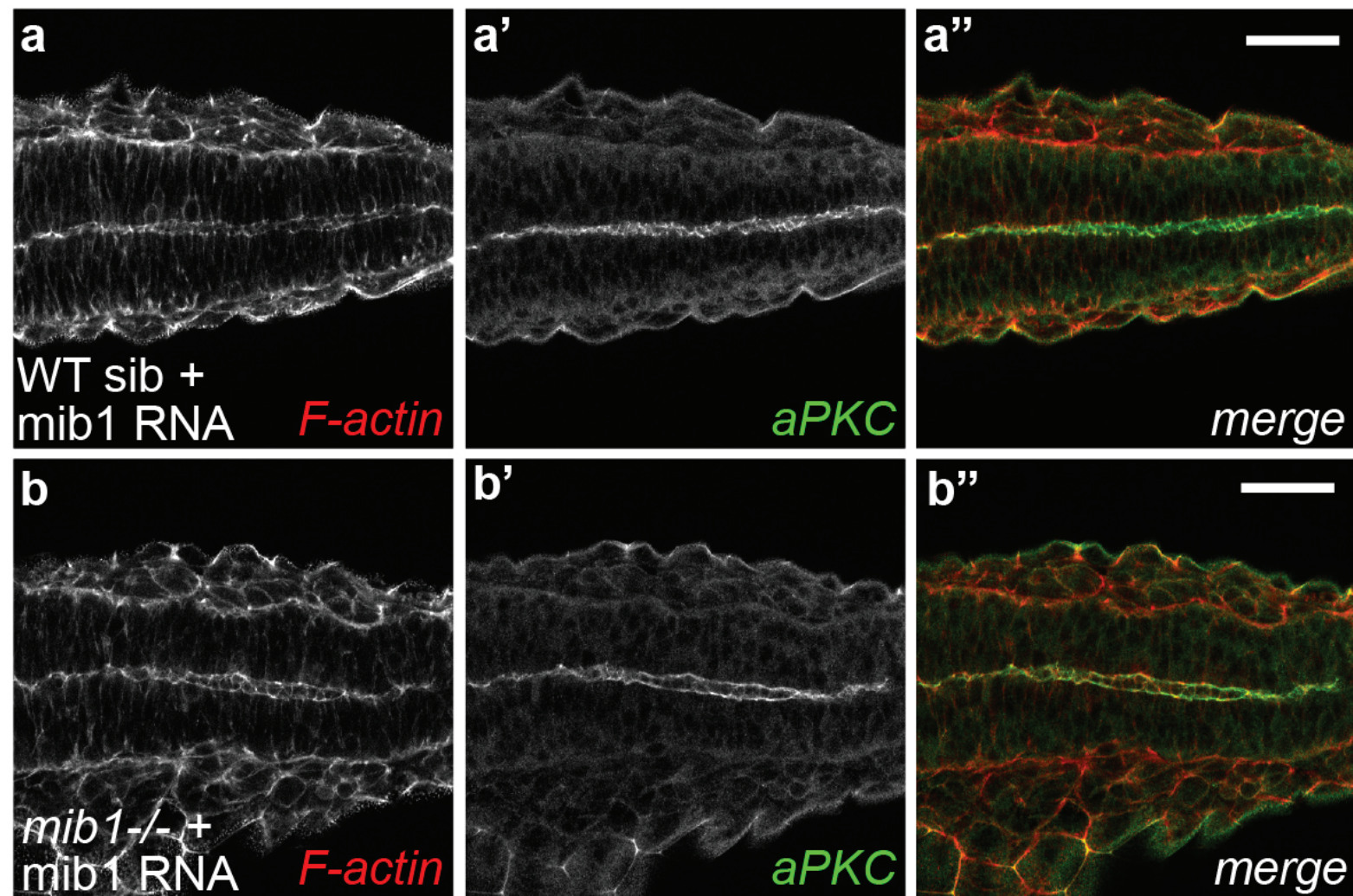
Open Access This article is licensed under a Creative Commons Attribution 4.0 International License, which permits use, sharing, adaptation, distribution and reproduction in any medium or format, as long as you give appropriate credit to the original author(s) and the source, provide a link to the Creative Commons license, and indicate if changes were made. The images or other third party material in this article are included in the article's Creative Commons license, unless indicated otherwise in a credit line to the material. If material is not included in the article's Creative Commons license and your intended use is not permitted by statutory regulation or exceeds the permitted use, you will need to obtain permission directly from the copyright holder. To view a copy of this license, visit <http://creativecommons.org/licenses/by/4.0/>.

© The Author(s) 2019

Supplementary Information

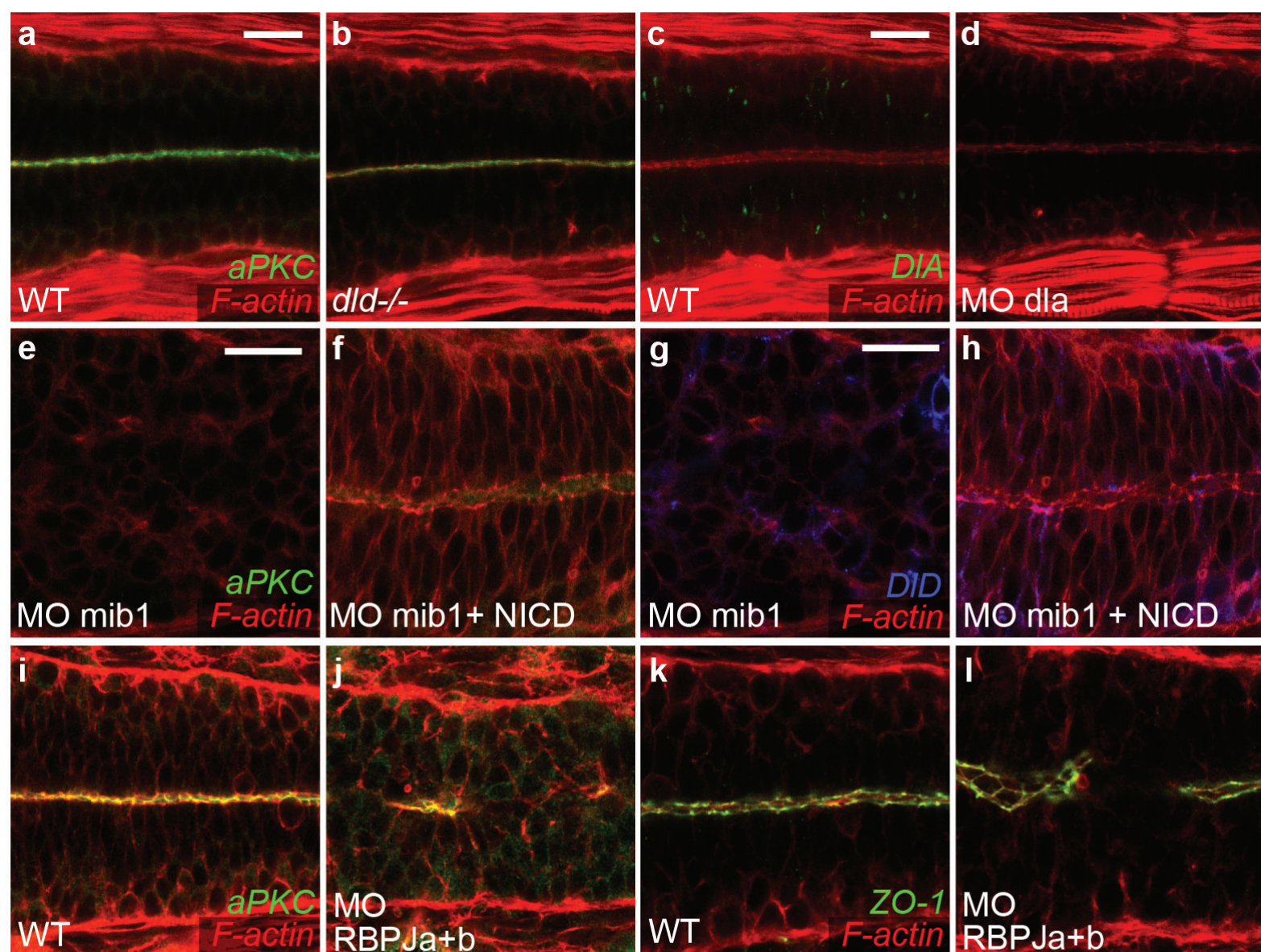
**Notch-mediated inhibition of neurogenesis is required for
zebrafish spinal cord morphogenesis**

***Priyanka Sharma, Vishnu Muraleedharan Saraswathy, Li Xiang
and Maximilian Fürthauer***



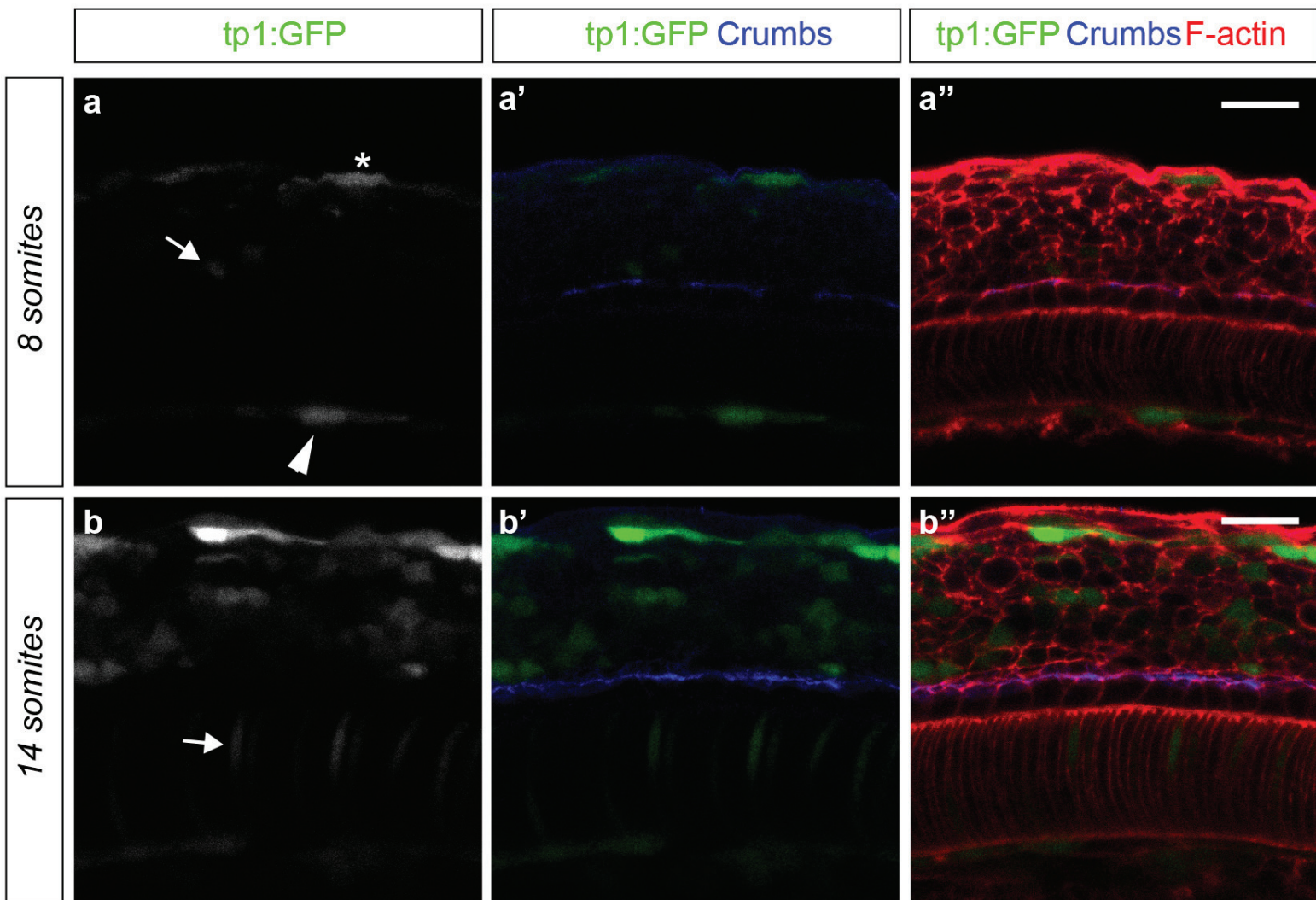
Mindbomb1 is important for zebrafish spinal cord morphogenesis
(a,b) Injection of RNA encoding wild-type Mib1 protein restores neuroepithelial morphology (visualized using F-actin staining) and polarized accumulation of the apical marker aPKC in *mib1* mutants (5/7 embryos full rescue, 2/7 partial rescue). Dorsal views of the anterior spinal cord at the 18 somites stage, anterior left. Scalebars: 50 μ m.

Supplementary Figure S1



Notch pathway components are required for the apico-basal polarity of the zebrafish spinal cord (a,b) Apical aPKC staining and cortical F-Actin indicate normal apico-basal polarity and neuroepithelial morphology in *dld*^{AR33} mutants (n=8/8). (c,d) *dla* morpholino injection does not alter neuroepithelial morphology but abolishes *DIA* immuno-reactivity (n=4/4). (e-h) RNA injection of a constitutively activated form of Notch (NICD) restores neuroepithelial morphology and apical aPKC localisation (f) but not DeltaD endocytosis (h) in 14/17 embryos. (i-l) Embryos injected with morpholinos against *RBPJa* & *b* display a partial loss of apico-basal polarity as visualized by a partial disruption of apical aPKC (j, n=23/29) and ZO-1 (l, n=16/16). (a-d) 26 somites stage, (e-l) 30 somites stage. Phalloidin staining of F-actin is used to highlight cell outlines. Scalebars: 20 μm.

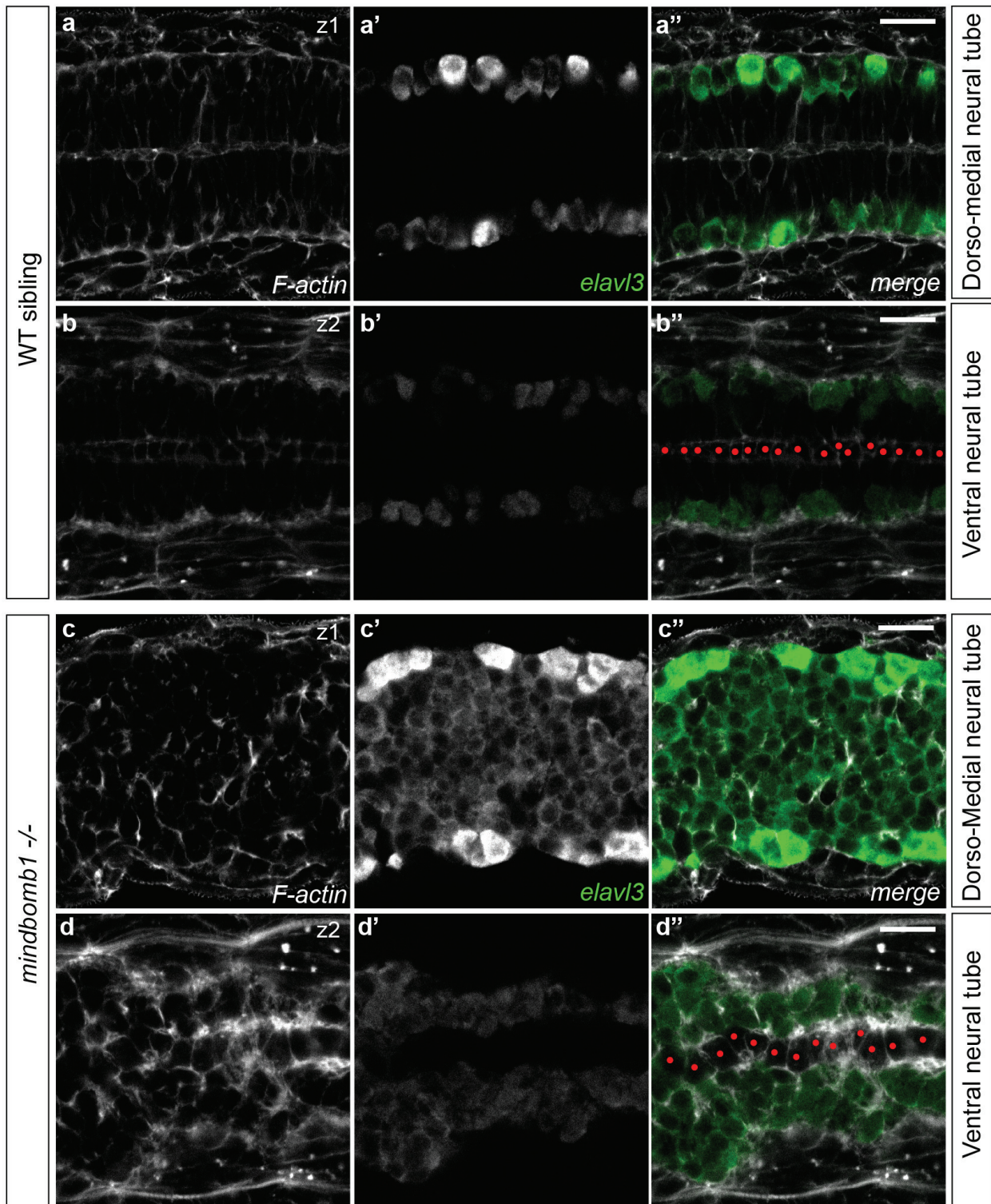
Supplementary Figure S2



Early floor plate morphogenesis occurs in the absence of detectable Notch reporter activity

(a,b) Lateral views of floor plate cells at the level of the anterior spinal cord, anterior to the left, dorsal up. (a) At the 8 somites stage, the activity of the transgenic Notch reporter line *tp1:bglob-GFP* (*tp1:GFP*) is detected in isolated neural tube cells (arrow), hypocord cells (arrowhead) and epidermal cells (star) (n=13). (b) At 14 somites, numerous GFP-positive cells are found in the neural tube and additional reporter expression is detected in notocord cells (arrow) (n=13). Floor plate cells, which can be identified through their cuboidal morphology (F-Actin in a'',b'') do not display Notch reporter activity. 8 and 14 somites stage embryos were imaged using the same confocal settings. For display purposes, contrast enhancement was then used to improve the visibility of the weak 8 somites stage *tp1:GFP* and Crumbs signals in a-a''. Scalebars: 20 μ m.

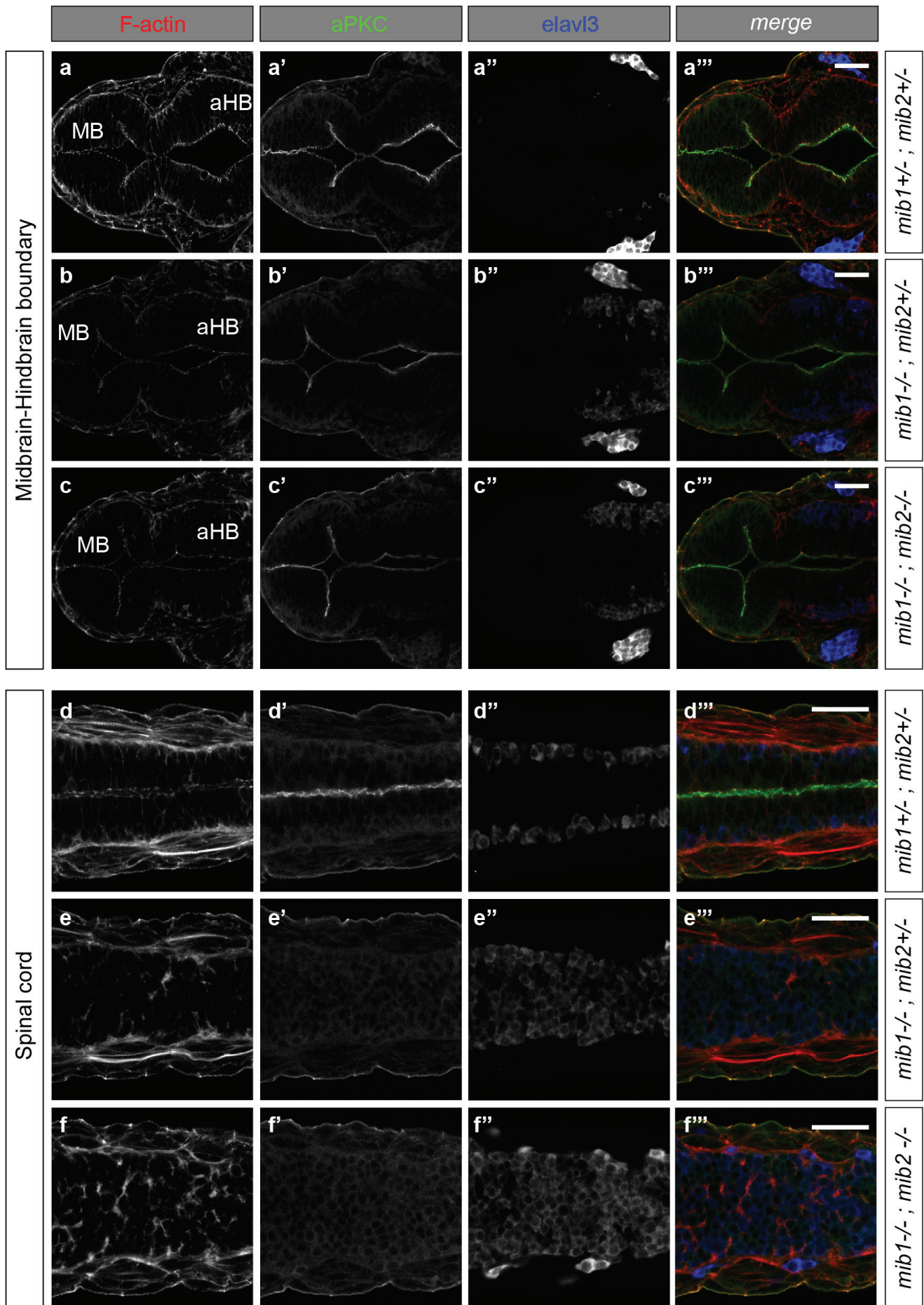
Supplementary Figure S3



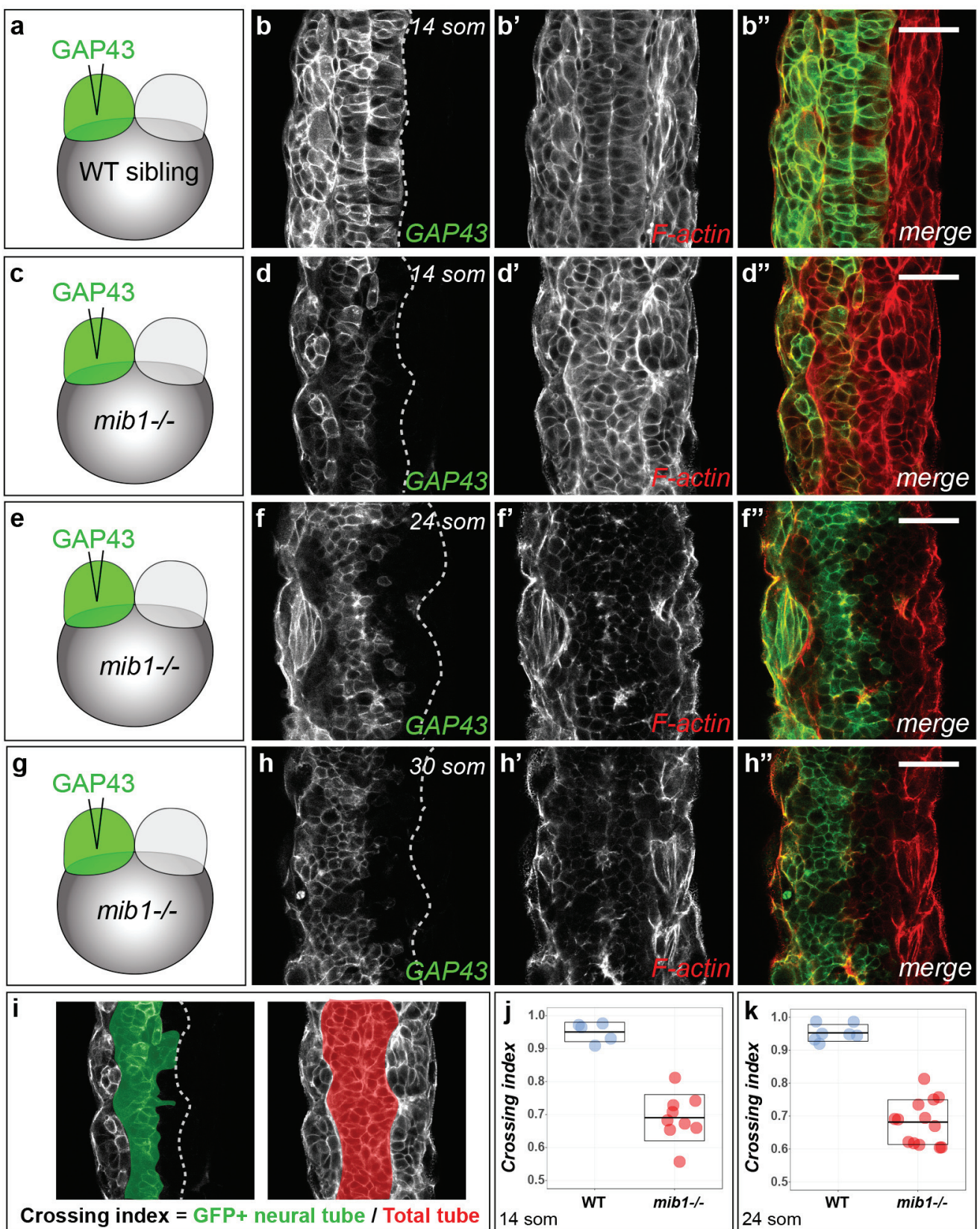
Excessive neuronal differentiation causes neural tube morphogenesis defects in *mindbomb1* mutants

(a-d) In 22 somites stage WT siblings, the neuronal differentiation marker *elavl3a* is expressed in some cells of the dorso-medial (a',a'') or ventral (b,b'') spinal cord. In *mib1* mutants, all dorso-medial neural tube cells differentiate as neurons (c',c''), causing a loss apico-basally polarized precursor cells and a disruption of neuroepithelial morphology (n=4/4). In the medial spinal cord of *mib1* mutants the *elavl3* signal occupies 76.5±10.2% of the neural tube surface compared to 14.6±2.5%, in WT siblings (p=7.61E-04). In the ventral neural tube, floor plate cells can be identified by their cuboidal morphology (red dots in b'',d''). In *mib1* mutants, floor plate cells are the only ones not undergoing neuronal differentiation (d',d'', n=4/4). In this region, *elavl3* occupies 60.5±0.69% of the neural tube compared to 14.2±2.5%, in WT siblings (p=1.52E-05). a,b and c,d are views of the same embryo at different z levels. All images are dorsal views of the anterior spinal cord, anterior left. Scalebars: 20 μm.

Supplementary Figure S4

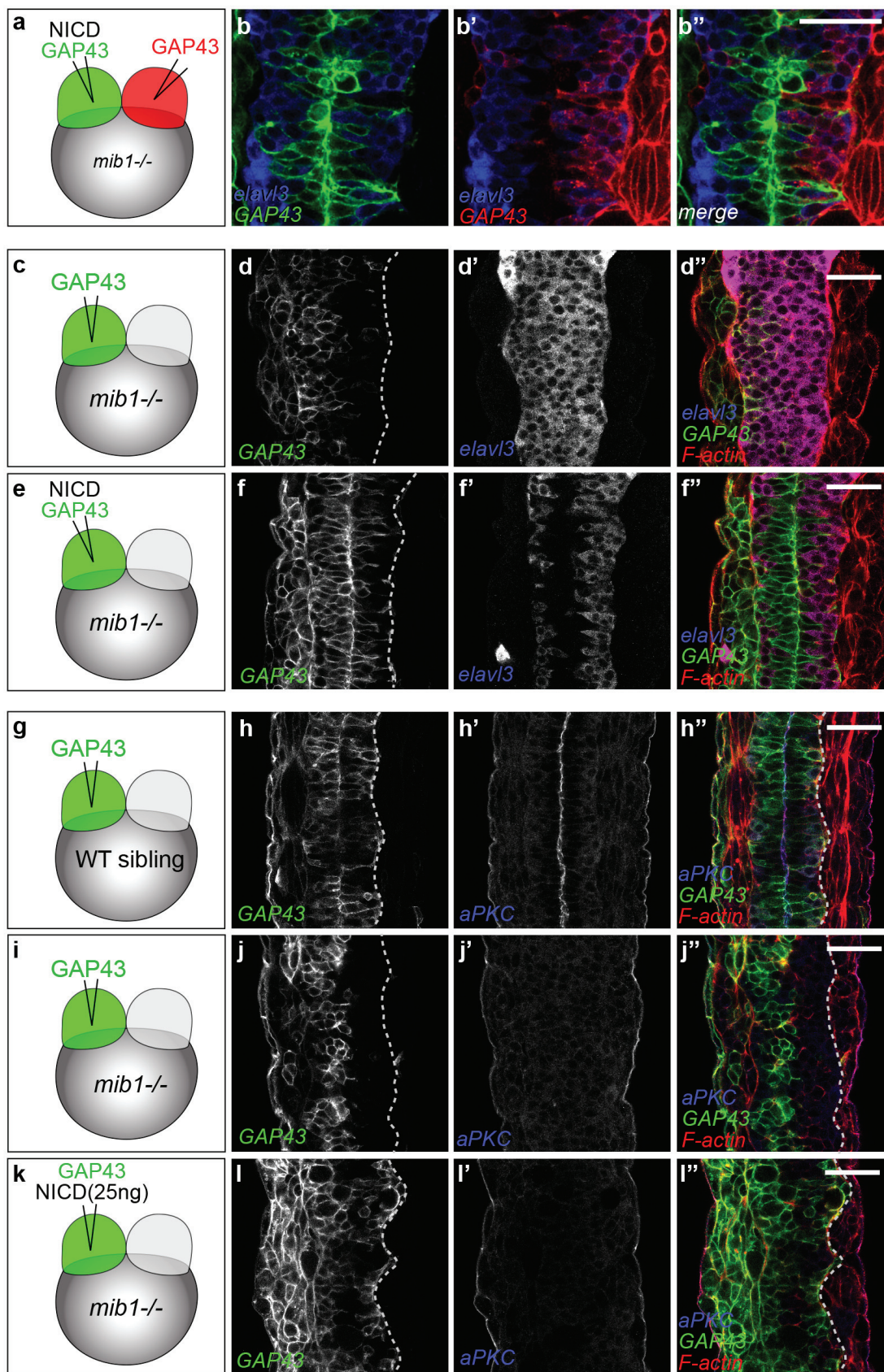


***mindbomb1* ; *mindbomb2* double mutants retain neuroepithelial polarity in the midbrain-hindbrain boundary region**
(a-f) Dorsal views of the midbrain-hindbrain boundary region **(a-c)** and anterior spinal cord **(d-f)** at the 30 somites stage, anterior left. **(a,d)** Neuronal differentiation (visualized using *elavl3*) and neuroepithelial polarity (highlighted by apical aPKC accumulation) occur normally in *mib1*^{tf91/+}; *mib2*^{chi3/+} transheterozygotes (n=3, compare to WT siblings in **Fig. 6i**). **(b,c,e,f)** *mib1*^{tf91/ff91}; *mib2*^{chi3/+} (n=10) and *mib1*^{tf91/ff91}; *mib2*^{chi3/chi3} double mutant (n=6) animals present a similar increase in neurogenesis the level of the anterior hindbrain (aHB, **b''**, **c''**) and the anterior spinal cord (**e''**, **f''**). See Supplementary Table S1 for a quantification of spinal cord neurogenesis. Neuroepithelial polarity is disrupted in the spinal cord (**e'**, **f'**) but maintained in the midbrain (MB, **b'**, **c'**). **(a,d)**, **(b,e)**, **(c,f)** represent different regions of the same embryos. Scalebars: 40 μ m.



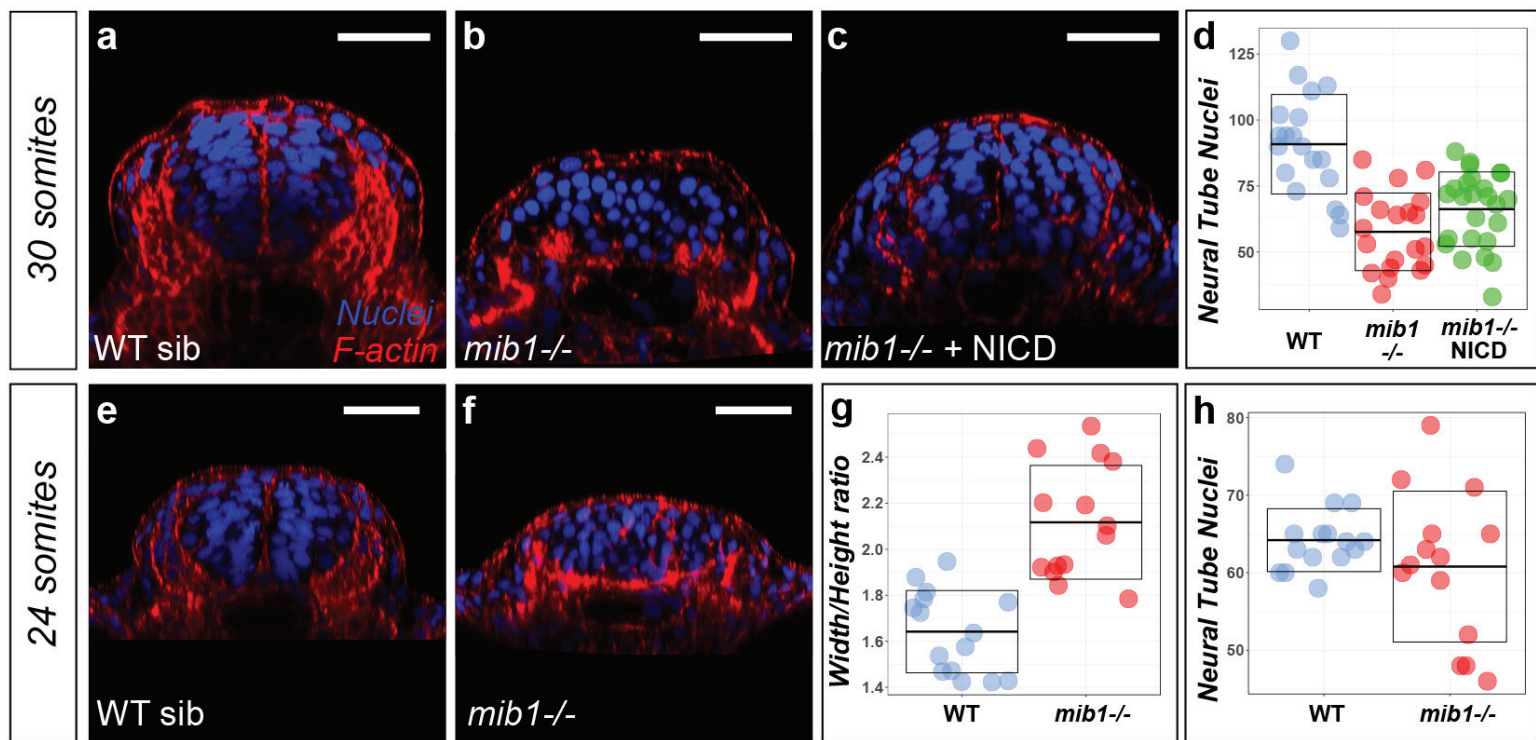
***Mindbomb1* loss of function impairs the midline-crossing behavior of neural tube cells**

(a-j) One half of the neural tube was labelled by injecting RNA encoding a green membrane label (GAP43-GFP) into one blastomere of 2-cell stage embryos (see Methods). (a,b) In 14 somites stage WT sibling embryos, cells originating from one side of the neural tube have crossed the neural tube midline to integrate the contra-lateral organ half. (c,d) In *mib1* mutants cells fail to cross to the contra-lateral side. (e-h) This inhibition of midline-crossing persists if *mib1* mutants are analysed a 24 somites (e,f) or 30 somites (g,h, see Fig. 6I for quantification). (i) For the quantification of neural tube cell midline crossing, the total area of the neural tube (red) and the area of the neural tube populated by GFP-positive cells (green) were outlined (see Methods for details). The neural tube cell midline crossing index represents the fraction of the neural tube that is occupied by GFP-positive cells. (j) Neural tube cell midline crossing is reduced in 14 somites stage *mib1* mutants (0.69 ± 0.07 , $n=9$) compared to WT siblings (0.95 ± 0.03 , $n=5$) ($p=7.0E-07$). (k) Neural tube cell midline crossing is reduced in 24 somites stage *mib1* mutants (0.68 ± 0.07 , $n=13$) compared to WT siblings (0.95 ± 0.03 , $n=7$) ($p=4.2E-10$). (b,d,f,h,i) dorsal views of the anterior spinal cord, anterior up. Scalebars: 40 μ m.



Notch-mediated suppression of neurogenesis is required for midline-crossing cell divisions in the zebrafish neural tube

(a,b) Activated Notch (NICD) was expressed in one half of *mib1* mutant neural tubes. NICD suppresses neurogenesis (visualized by the neuronal marker *elav13*) and promotes midline-crossing in NICD-injected cells identified by green membrane label (b). Contralateral NICD-negative cells (red membrane label) do not cross the midline and undergo neuronal differentiation (b', n=7). (c-f) In *mib1* mutant embryos all cells of the dorso-medial spinal cord differentiate as neurons and the exchange of cells between the two halves of the neural tube is reduced (d, n=10). Unilateral NICD injection results in a local suppression of neurogenesis and restores the midline crossing of *elav13*-negative cells (f, n=10). Accordingly, the neuronal *elav13* signal occupies a lower percentage of the neural tube in NICD-injected *mib1* mutants (f', 52.2±12.4%) than in *mib1* mutant controls (d', 83.2±9.3%, p=8.40E-06). Conversely NICD-injected *mib1* mutants present a higher midline crossing index (f, 0.86±0.05%) than *mib1* mutant controls (d, 0.63±0.05%, p=3.45E-09). (g-l) Unilateral injection of a low dose of NICD into *mib1* mutants fails to rescue neepithelial polarity (visualized by aPKC in h', j', l') but restores the exchange of neural tube cells between the two sides of the neural tube (h, j, l, see Supplementary Table S3 for statistics). (b,d,f,h,j,l) dorsal views of the anterior spinal cord at the 18 somites (b,h,j,l) and 16 somites (d,f) stage, anterior up. Scalebars: 40 μm.



Loss of Notch signaling affects the cell number and proportions of the neural tube

(a-d) Nuclear Dapi staining was used to estimate the number of cells present on transversal sections of the anterior spinal cord (dorsal up, see Methods for details). The number of nuclei present in 30 somites stage *mib1* mutants (b,d) is reduced compared to WT siblings (a,d). The injection of RNA encoding constitutively activated Notch (NICD) causes a weak but not statistically significant increase in the number of *mib1* mutant neural tube cells (see Supplementary Table S5 for statistical analysis). The data set used for this analysis is the same used for the analysis of neural tube Width-to-Height ratio in Fig. 8q. (a,b,c) correspond to the display items of Fig. 8n-p. (e,f,g) At the 24 somites stage, *mib1* mutants present a significant increase in the neural tube Width-to-Height ratio (2.12 ± 0.25 , $n=14$) compared to WT siblings (1.64 ± 0.18 , $n=15$) ($p=4.71E-06$). (e,f,h) In contrast, the number of *mib1* mutant neural tube cells shows only a minor and not statistically significant decrease (60.8 ± 9.7) when compared to WT siblings (64.2 ± 4.1) ($p=0.23$). Boxes in d,g,h represent mean values \pm SD. Scalebars: 40 μ m.

Supplementary Figure S8

Supplementary Table S1:**Percentage of the neural tube area occupied by *elavl3*-positive neurons**

	<i>Mean value</i>	<i>Standard deviation</i>	<i>Number of embryos</i>
<i>mib1</i> ^{+/-} ; <i>mib2</i> ^{+/-}	25.584	3.919	3
<i>mib1</i> ^{-/-} ; <i>mib2</i> ^{+/-}	74.473	11.574	10
<i>mib1</i> ^{-/-} ; <i>mib2</i> ^{-/-}	73.304	11.675	6
<i>Test statistics for Welch's Anova</i>			
F= 80.946	p= 1.194E-06		
<i>p-values for pairwise comparisons (Games-Howell post-hoc test)</i>			
	<i>mib1</i> ^{-/-} ; <i>mib2</i> ^{+/-}	<i>mib1</i> ^{-/-} ; <i>mib2</i> ^{-/-}	
<i>mib1</i> ^{+/-} ; <i>mib2</i> ^{+/-}	9.573E-07	1.401E-04	
<i>mib1</i> ^{-/-} ; <i>mib2</i> ^{+/-}		0.979	

Supplementary Table S2:**Midline crossing index of zebrafish neural tube cells at the 16 somites stage**

	<i>Mean value</i>	<i>Standard deviation</i>	<i>Number of embryos</i>
Wild-type	0.952	0.024	15
<i>mib1</i> ^{-/-}	0.691	0.083	13
<i>mib1</i> ^{-/-} + NICD(37)	0.917	0.071	15
<i>mib1</i> ^{-/-} + NICD(25)	0.888	0.066	7
<i>Test statistics for Welch's Anova</i>			
F= 38.526	p= 6.622E-08		
<i>p-values for pairwise comparisons (Games-Howell post-hoc test)</i>			
	<i>mib1</i> ^{-/-}	<i>mib1</i> ^{-/-} + NICD(37)	<i>mib1</i> ^{-/-} + NICD(25)
Wild-type	1.949E-07	0.296	0.147
<i>mib1</i> ^{-/-}		4.031E-07	1.749E-04
<i>mib1</i> ^{-/-} + NICD(37)			0.792

Supplementary Table S3:**Midline crossing index of zebrafish neural tube cells at the 18 somites stage**

	<i>Mean value</i>	<i>Standard deviation</i>	<i>Number of embryos</i>
Wild-type	0.915	0.047	8
<i>mib1</i> ^{-/-}	0.579	0.055	11
<i>mib1</i> ^{-/-} + NICD (25, half-injected)	0.818	0.083	9
<i>Test statistics for Welch's Anova</i>			
F= 99.889	p= 1.220E-09		
<i>p-values for pairwise comparisons (Games-Howell post-hoc test)</i>			
	<i>mib1</i> ^{-/-}	<i>mib1</i> ^{-/-} + NICD (25, half-injected)	
Wild-type	3.281E-10	0.0253	
<i>mib1</i> ^{-/-}		1.177E-05	

Supplementary Table S4:**Neural tube Width-to-Height ratio at the 30 somites stage**

	<i>Mean value</i>	<i>Standard deviation</i>	<i>Number of embryos</i>
Wild-type	1.173	0.085	19
<i>mib1</i> ^{-/-}	2.248	0.351	20
<i>mib1</i> ^{-/-} + NICD(37)	1.489	0.310	25
<i>Test statistics for Welch's Anova</i>			
F= 93.993	p= 3.885E-14		
<i>p-values for pairwise comparisons (Games-Howell post-hoc test)</i>			
	<i>mib1</i> ^{-/-}	<i>mib1</i> ^{-/-} + NICD(37)	
Wild-type	2.565E-11	1.119E-04	
<i>mib1</i> ^{-/-}		1.137E-08	

Supplementary Table S5:**Neural tube cell number at the 30 somites stage**

	<i>Mean nuclei number</i>	<i>Standard deviation</i>	<i>Number of embryos</i>
Wild-type	90.842	18.848	19
<i>mib1</i> ^{-/-}	57.650	14.705	20
<i>mib1</i> ^{-/-} + NICD(37)	66.240	14.090	25
<i>Test statistics for Welch's Anova</i>			
F= 18.766	p= 2.211E-06		
<i>p-values for pairwise comparisons (Games-Howell post-hoc test)</i>			
	<i>mib1</i> ^{-/-}	<i>mib1</i> ^{-/-} + NICD(37)	
Wild-type	1.819E-06	1.120E-04	
<i>mib1</i> ^{-/-}		0.129	

I.3 Author contributions

I have made major contributions to this story which was a continuation of work from a previous PhD student, Priyanka Sharma. We have shown that Notch signaling is crucial for regulating morphogenetic events such as establishment of apico-basal polarity and c-divisions during zebrafish neurulation. Priyanka mainly did experiments to show the importance of Notch signaling in epithelialization of neural progenitors, which are shown in Fig. 1a-g, Fig. 2a-f, m, n, Fig.4, Fig. 6a-h, Fig.7a,b and Fig.S2a-h. However, I have also made significant contribution to her part of the project by doing the following experiments,

Fig. 1h,i: Showing that the apical localization of the tight junction component ZO-1 is disrupted in *mib1* mutants

Fig. 1j,k: Showing that the centrosomes fail to move towards the neural tube midline in *mib1* mutants.

Fig. 2i-l: Proving that the RNA injection of a constitutively activated form of Notch (NICD) can rescue neuro-epithelial morphology and apical localization of aPKC in *mib1* mutants.

Fig. 2o,p: Showing that RNA injection of constitutively activated form of Su(H) restores apico-basal polarity in *mib1* mutants.

Fig. S2i-l: Showing that embryos injected with morpholinos against RBPJa and b disrupts apico-basal polarity

Fig. S5: Demonstrating *mib1*; *mib2* mutants retain neuroepithelial polarity in the midbrain-hindbrain boundary region.

Fig. 7c-j'': Showing that cell autonomous Notch signaling is required for neuroepithelial morphogenesis.

My major contribution comes in the second axis of the project where I demonstrated that Notch signaling is required for regulating midline crossing c-divisions and thereby, Notch signaling is able to define the shape of the neural tube by regulating the width-to-height ratio. Results from my experiments are depicted in following figures,

Fig. 8: Notch loss of function impairs morphogenetic cell movements in the zebrafish spinal cord.

Fig. S6: Mindbomb1 loss of function impairs the midline-crossing behavior of neural tube cells throughout the neurulation.

Fig. S7: Notch mediated suppression of neurogenesis is required for midline crossing c-divisions in the neural tube.

Fig. S8: Loss of Notch signaling affects the cell number and proportions of the neural tube.

Conclusion

The aim of this project was to study the role of Delta/Notch signaling in regulating zebrafish spinal cord morphogenesis. The establishment of apico-basal polarity and midline crossing C-divisions are important for proper morphogenesis of the zebrafish neural tube. Our study revealed that depletion of Notch signaling results in the loss of apico-basal polarity in the anterior dorso-medial spinal cord. Notch signaling is regulating apico-basal polarity in the spinal cord via the canonical Notch signaling pathway. Our data also demonstrate that loss of Notch signaling causes precocious neurogenesis and therefore, mutant embryos failed to promote the establishment of polarized radial glial cells. This indicates that Notch signaling is directly or indirectly promoting polarized cell types in the anterior dorso-medial spinal cord. However, Notch signaling is not a general regulator of apico-basal polarity since apico-basal polarity emerged normally in the floor plate cells of *mibl* mutant embryos. Similarly, Mib1 regulated Notch signaling is also dispensable for the establishment polarity in the midbrains/midbrain-hindbrain boundary regions. These results show that the role of Notch signaling in establishing apico-basal polarity is region specific.

Interestingly, our data also show that C-divisions are also perturbed in *mibl* mutant embryos and the regulation of C-divisions is via the conventional Notch signaling pathway. Perturbation of C-divisions in *mibl* mutants is due to premature neuronal differentiation since all the cells that were unable to cross the midline were adopting neuronal fate. Interestingly, embryos that show defective C-divisions exhibit misproportioned spinal cords that have increased width to height ratio. Therefore, our data show that Notch signaling is important for zebrafish spinal cord morphogenesis.

Chapter - II

Analyzing the role of Mindbomb1 in the Planar Cell

Polarity pathway

Introduction

During the first part of my PhD, Mindbomb1 (Mib1) morphants were used to inhibit Notch signaling to study the role of Delta/Notch signaling in neurulation. Interestingly, Mib1 morphant embryos showed defects in convergent extension (CE), i.e. convergence along the medio-lateral axis that results in extension along the anterior-posterior axis, during gastrulation. CE movements during vertebrate gastrulation are regulated via the Planar Cell Polarity (PCP) pathway. This raised the question whether Mib1 is playing a role in PCP, which led to the second part of my PhD. Therefore, in the introduction section of chapter two, first, I will outline different functions regulated by the PCP pathway and then, summarize different components that regulate PCP in both invertebrates and vertebrates. Finally, I will describe different Mib1 functions independent of Notch signaling.

II.1 Functions regulated by the PCP pathway

PCP is the collective alignment of cell polarity across the plane of the tissue orthogonal to the apico-basal axis. Functions of PCP during development can be broadly divided into three categories: orientation of cellular structures (such as hairs and cilia), orientation of cell division axis and regulation of different types of directed cell migrations.

II.1.a PCP and Orientation of hairs and cilia.

PCP was initially described in the insect *Oncopeltus fasciatus*(223). It was shown that structures including hair cells that cover the insect body and ommatidia of the retina are polarized as well as oriented in the same fashion(224). Later, genetic analysis in *Drosophila* identified several mutants responsible for orientation of cuticular processes in several regions of the insect body(225). For example, genetic mutants of *prickle*, *spiny legs*, *frizzled* and *inturned* showed defects in orientation of actin-based hairs on the adult wing(225). Further studies have identified several other genes that are responsible for orientation of cuticular hairs, bristles and ommatidia in *Drosophila* and they have been classified as PCP genes(Fig.11A,C)(226).

In mammals, the cochlear region of the ear contains sensory hair cells that function in mechanotransduction of sound waves into electrical impulses by which hearing is made possible. These sensory hair cells possess oriented ciliary structures that are important for

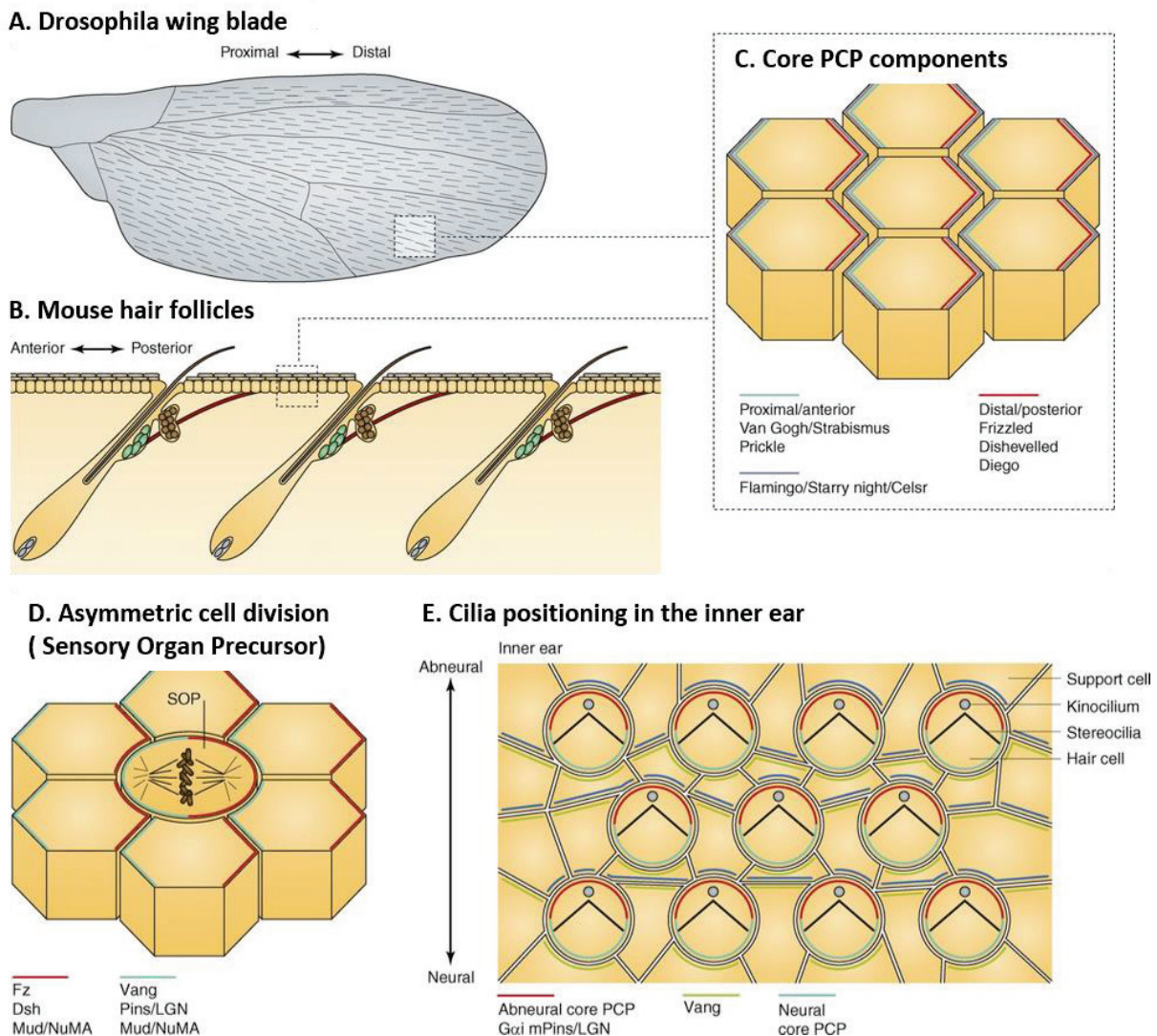


Figure 11. Orientation function regulated by Planar Cell Polarity. A,B) In the *Drosophila* wing blade and mouse hair follicles, PCP signaling orients direction of wing hairs in the proximal distal axis and mouse hair follicles in the anterior-posterior axis. C) This orientation is achieved by asymmetric distribution of core PCP components in individual cells along their respective axis and thereby, creates a global polarity in the whole tissue. D) In *Drosophila* SOP cells, spindle orientation along the A-P axis is dependent on the PCP pathway. Dishevelled interacts with Mud/NuMA and the dynein complex posteriorly while Vang links Pins/LGN-Mud/NuMA-dynein on the anterior to orient the spindle axis. E) In the inner ear, orientation of ciliary structures is achieved by asymmetric localization of components along the abneural-neural axis. (Devenport, 2014)

mechanotransduction. PCP proteins such as Vangl2 and Frizzled are shown to be asymmetrically localized in these sensory hair cells and perturbation of PCP genes cause defects in orientation of ciliary structures in the inner ear (Fig.11E)(227-229). Similarly, mammalian body hairs also show a special orientation along the anterior-posterior (A-P) axis(230). The null mutant of the PCP component *frizzled6* shows a whorled hair pattern in mice indicating the role of the PCP pathway in regulating alignment of body hairs(231). Studies have confirmed that PCP genes are required for polarized gene expression and cytoskeletal changes in individual hair follicles regulate global alignment of body hairs (Fig. 11D)(230).

Unlike non-motile cilia that mainly function in perception and integration of environmental cues, motile cilia beat to regulate directional flow of fluids/particles. Motile cilia are present in several structures including the mouse ventral node or zebrafish Kupffer's vesicle that determine left-right asymmetry of the organism, floorplate cells at the ventral surface of the neurocoel that regulate cerebrospinal fluid distribution and the airway epithelium that clears mucus/contaminants from the lungs(232-234). These motile cilia in vertebrates also present an A-P orientation, and there is an asymmetric distribution of PCP components in these different cell types regulating directionality and orientation of motile cilia(235-237).

II.1.b PCP and Oriented cell divisions.

Oriented cell division plays a crucial role during embryogenesis by determining different factors including axis determination, cell fate diversity generation and morphogenesis of tissues and organs(238). The PCP pathway has been identified as an essential regulator of spindle orientation(239). In *C. elegans*, the PCP pathway acts along with SRC-1 kinase on mitotic spindle rotation by triggering cortical enrichment of Dynactin during first zygotic divisions(240). PCP mutations in *C. elegans* randomizes spindle orientation during this early division, and removal of both SRC-1 and PCP components aggravated the phenotype(240, 241). A similar function of the PCP pathway is observed during asymmetric cell division of sensory organ precursor (SOP) cells in *Drosophila*. During SOP cell division, cell fate determinants are asymmetrically localized to the opposite poles of a cell and this asymmetric localization is planar polarized among several SOP cells along the anterior-posterior (A-P) axis of the pupae (Fig. 11D) (239, 242). In PCP mutant pupae, cell fate determinants localize asymmetrically but with a random position relative to the A-P axis which will result in random distribution of cuticular sensory bristles(242-244).

In vertebrates, oriented cell division plays a crucial role during gastrulation resulting in tissue elongation(238, 245). This has been best exemplified during zebrafish gastrulation where oriented cell division of epiblast cells are biased along the A-P axis resulting in axis extension along the same axis(246). This A-P orientation of cell division is dependent on PCP components such as Wnt-11, Disheveled and Strabismus (246). Overexpression of a mutant form of *disheveled* causes defects in axis elongation due to randomized division orientation(246). Later during the mid-segmentation period of zebrafish development, the PCP pathway is important for the medio-lateral cell divisions called C-divisions, which are important for neurulation(44, 45).

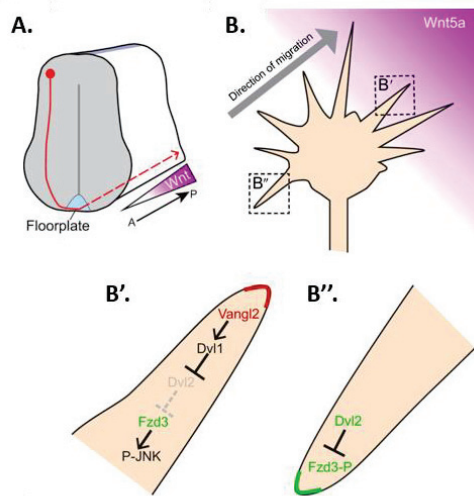
II.1.c PCP and cell migration

- Axon guidance

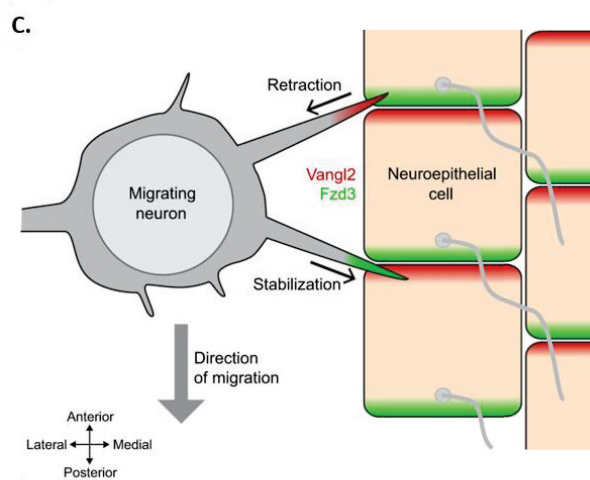
In vivo, cells migrate from one location to another by interacting with other cell types, ECM components and following different gradient cues. For example, during nervous system development, neurons and axon growth cones travel through a complex neuroepithelial environment to reach their target destination. The PCP pathway has been implicated in such directional migration of individual cells. PCP has been shown to play an important role in axon guidance in both vertebrates and invertebrates(247). For example, commissural neurons in the dorsal spinal cord project anteriorly after midline crossing in a PCP-dependent manner (248)(Fig. 12A) . In mutants of PCP components in mouse, such as *frizzled3*, *vangl2*, and *celsr3*, commissural neurons either stall or project randomly after midline crossing(249, 250). This axon guidance is achieved through directional cues provided by gradients of several Wnt ligands (such as Wnt4a, Wnt5a, Wnt7b) that act in the PCP pathway(249-251). It has been shown that in the presence of Wnt5a and Vangl2, Dvl2 promote Arf6-mediated Fzd3 endocytosis at filopodial tips, which further activates growth cone turning via JNK activation (Fig. 12B)(250, 252, 253).

Similarly, longitudinal migration of facial branchiomotor neurons (FBMNs) in both zebrafish and mice is dependent on the PCP pathway (Fig. 12C) (253). Chimeric studies have shown that Vangl2 and Frizzled3a (Fzd3a) play an important role in the directional migration of FBMNs by stabilizing and destabilizing filopodial protrusions(254). Inside the FBMN, Fzd3a is required to stabilize

Axon guidance of commissural neurons



Directional migration of a FBMN neuron



Neural crest cells migration

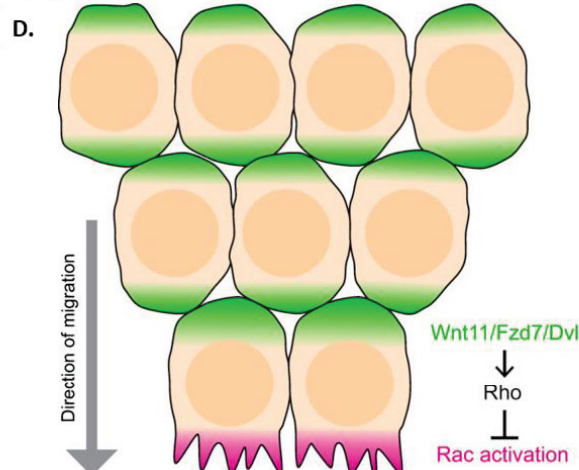


Figure 12. Directional migration regulated by Planar Cell Polarity. A) Schematic cross-section of the spinal cord where at first commissural neurons (red) project axons ventrally and then, after crossing the midline floor plate, turn and project anteriorly. B) Axon guidance is initiated by cues provided by Wnt gradient, B') where filopodia pointing towards Wnt will initiate Fzd3 internalization which will in turn activate JNK that further regulates axon guidance. B'') In the filopodia pointing away from the Wnt source, Fzd3 will be hyperphosphorylated in a Dvl2-dependent fashion that will inhibit Fzd3 internalization and further downstream signaling. C) During directional migration of facial branchiomotor neuron (FBMN), Fzd3 in neurons and Vangl2 in neuroepithelial environment will stabilize FBMN filopodia, whereas Vangl2 in FBMN and Fzd3 in the environment destabilizes them. D) During Neural Crest cells migration, Fzd-Dvl (green) are localized at the cell surface where protrusions are supposed to be inhibited. Fzd-Dvl activates Rho to promote actomyosin contractility and which in turn inhibits Rac1. Therefore, Rho activation is restricted only at the migratory front to initiate filopodial protrusions. (Davey and Moens, 2017)

filopodia whereas Vangl2 has an antagonistic destabilizing role (Fig. 12C). Conversely, in the neuroepithelial cells of the migratory environment, Fzd3a destabilizes FBMN filopodia whereas Vangl2 has a stabilizing role (Fig. 12C) (254).

- Neural crest cell migration

The neural crest (NC) is a multipotent cell population derived from the junction of the neural and non-neural ectoderm. NC cells migrate in response to chemotropic cues and give rise to several neural and non-neural tissues(255). NC cells migrate in a cohort with cells at the front having highest directional persistence and maximum protrusive activity(255). PCP signaling is responsible for this outward directionality by regulating contact-mediated inhibition of protrusive activity at all other membranes except the migratory front (Fig. 12D) (256). This is achieved by asymmetric distribution of PCP components such as Fzd7 and Dvl at non-protrusive cell surfaces of NC cells. Then, PCP signaling via Fzd-Dvl complex at homotypic NC contacts leads to local activation of RhoA, which promotes retraction at the rear end of the cell via Rock2-mediated actomyosin contractility. Also, RhoA/Rock2 activation inhibits Rac1, a related small GTPase protein, so that Rac1 activity gets polarized only towards the leading edge of the cell, where it drives protrusive activity (Fig. 12D) (256-258). NC cells with disrupted PCP signaling were unable to maintain contact-mediated inhibition of protrusive activity and thus, crawl on top of one another with both leading and trailing cells extending protrusions in all directions(256).

- Cancer cell migration

Recent studies show that, upregulation of PCP components is observed in many cancers and this overexpression is mostly associated with a poor prognosis of patients(259, 260). One of the most prominent roles of PCP deregulation is in cancer cell invasion and metastasis. Triple Negative Breast Cancer (TNBC), one of the most aggressive cancers with no available targeted therapy so far, shows the overexpression of PCP components Prickle1 and Vangl2(261, 262). Prickle1 is interacting with Vangl2 to regulate focal adhesion dynamics in TNBCs (263) and downregulation of Prickle1 strongly impairs cell motility and metastasis (264). A similar mechanism is present in skin cancers such as melanoma, where overexpression of the PCP ligand Wnt-5a is correlated with enhanced cell invasion, metastasis and poor patient outcome(265). During cancer cell migration, there is a polarized localization of PCP components. The Fzd-Dvl complex is localised at protrusive structures and the Vangl-Prickle complex is localised along the non-protrusive cell

cortex(264, 266). Asymmetric localisation of PCP components along with its downstream signalling components activate RhoA, which in turn modulates acto-myosin networks and focal adhesion dynamics to allow cancer cells to efficiently migrate and undergo metastasis(264).

II.1.d Convergent Extension

Convergent extension (CE) is a fundamental and conserved collective cell movement that forms elongated tissue during embryogenesis. During CE, cells sense global and tissue level planar polarity and they intercalate in their medio-lateral (M-L) axis to narrow the tissue width and consequently increase the tissue length along the A-P axis (Fig. 13A). CE was initially observed during notochord formation in *Xenopus* embryos(267, 268). Later, CE has shown to be important for morphogenesis of several other tissues in different organisms including elongation of the neural plate in *Xenopus*(269), zebrafish(270), chick(25), and mouse embryos(271); formation of the kidney tubules in *Xenopus*(272); and the formation of cochlea in mouse embryos(273). Initially, two models have been proposed for the process of convergent extension: The crawling model and The contraction model(274).

- The crawling mode of cellular intercalation.

The crawling mode of cell intercalation was first proposed during *Xenopus* notochord formation(275). The cells in the notochord form actin-rich protrusions called lamellipodia at both tips to crawl through spaces between neighboring cells and undergo cellular intercalation (Fig. 13B) (267, 276). These crawling cells can move bidirectionally along the mediolateral axis following bipolar membrane protrusions. Formation of lamellipodia is achieved via active turnover of the actin cytoskeleton, through continuous polymerization and depolymerization(277, 278). Rho and Rac, members of the Ras superfamily of guanosine triphosphatases (GTPases)(279), regulate actin polymerization and branching by controlling actin-binding proteins such as Arp2/3, disheveled-associated activator of morphogenesis 1 (DAAM1, a Formin family protein), Diaphanous and Cofilin(280-283). Overexpression of dominant negative forms of Rho and Rac in *Xenopus* causes perturbation in membrane protrusions, and consequently defects in CE(284). These cellular protrusions act in tandem with actomyosin mediated contractions at the cell cortex to provide directionality to cell intercalations(285, 286). PCP proteins have been shown to play a crucial role in crawling mode of cell intercalations. Inhibition of the PCP component Disheveled

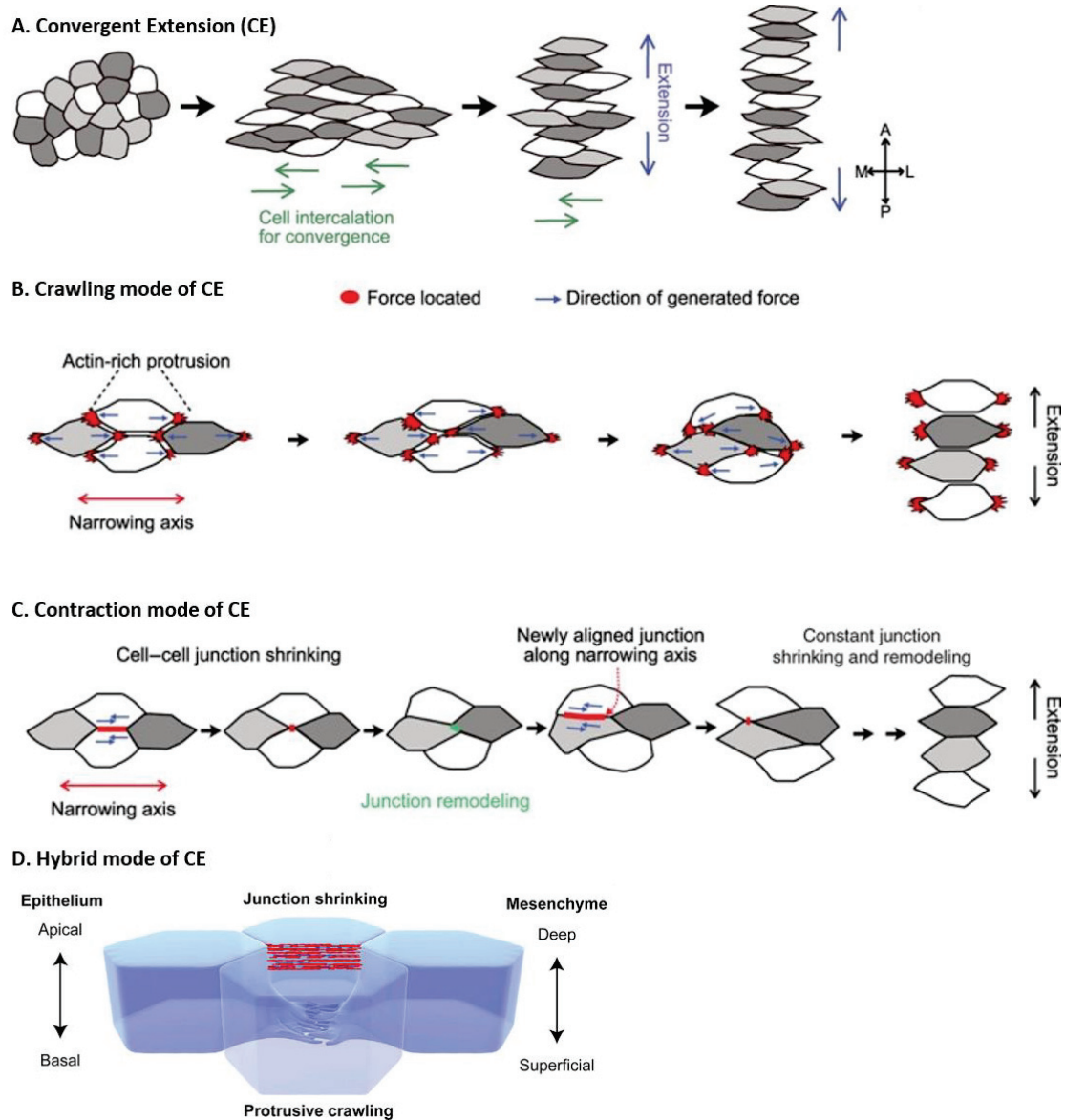


Figure 13. Convergent Extension (CE) is regulated by Planar Cell Polarity. A) CE is a process by which cells intercalate medio-laterally to narrow the width of the tissue and consequently elongate the length of the tissue. B) This process can happen via crawling, where bipolar protrusions are formed in cells that intercalate C) or by shrinkage of junctions that are aligned medio-laterally. D) Recent evidences suggest that, both mechanisms are functional in the same cells that intercalate leading to a hybrid mode of CE. (picture adapted from *Shindo, 2018* ; *Huebner and Wallingford, 2018*)

(Dvl) causes defective bipolar protrusions because of disrupted actin polymerization, by blocking the functions of Daam1 and Arp3 via Rho and Rac respectively(280, 287).

Regulation of cell-adhesion properties are crucial during the crawling mode of intercalation, where cells loosen their adhesive forces to squeeze between neighboring cells. C-cadherin, a transmembrane cell-cell adhesion molecule, has been shown to get internalized during early gastrulation in *Xenopus*(288). Paraxial protocadherin, a member of the cadherin super family, is another adhesion molecule that is responsible for the regulation of membrane protrusions during early CE in *Xenopus* notochord formation(289).

- The contraction mode of cell intercalation

The contraction mode of cell intercalation was discovered in *Drosophila* during germband extension, a process of epithelial tissue elongation(290, 291). During the contraction mode, there is an accumulation of actomyosin complex at cell-cell junctions aligned medio-laterally(292). Upon activation of these actomyosin complexes, contractile forces are generated to shrink junctions and thereby, pull neighboring cells inward to undergo cellular intercalation along with junctional remodeling, and results in A-P axis extension (Fig. 13C) (292). Coupled with the contraction of junctional actomyosin, there is a population of medial actomyosin that oscillates and flows toward the shrinking cell junctions in a synchronous fashion with cell junction shortening(293, 294). The PCP pathway is also important for the contraction mode of intercalation in vertebrates. The PCP protein CELSR is required for activation of actomyosin at cell-cell junctions during neural plate formation in chick embryos(25). Moreover, Dvl is required for the localization of actomyosin during both kidney tubule elongation and notochord formation in *Xenopus*(272). In zebrafish, the PCP pathway has been shown to regulate morphogenesis of the early myocardium by restricting local actomyosin contractility to allow epithelial cell remodeling(295). However, PCP signaling is not required for cell intercalations during *Drosophila* germband extension(291). In *Drosophila*, Toll receptors regulate the contraction mode of cell intercalation during germband extension(296).

In the contraction mode of cellular intercalation, dynamic regulations of cell adhesion molecules are important. Cadherins play significant role in cell-cell adhesions during CE mediated by the contraction mode. E-cadherins are required for medial actomyosin flow and they exhibit an

oscillation pattern synchronized to actomyosin pulses at the shrinking cell-cell junction during germband extension(293, 297).

- A unified model for cell intercalation

Recent studies indicate that the crawling and contraction modes are not necessarily exclusive but act together in regulating CE movements (Fig. 13D) (298). This was evident from junction shrinking observed during intercalation of mesenchymal cells in *Xenopus*(299). Earlier studies have indicated only cell crawling during CE of the *Xenopus* dorsal marginal zone, whereas now it's clear that polarized shrinkage of junctions also contributes to tissue elongation at a depth of 4-5 μm in the same tissue(299). Moreover, in the mouse neural plate, neural epithelial cells undergo two modes of cell intercalation in a spatially distinct manner within the same tissue, where cellular protrusions occur at the basal surface of cells and junction shrinkage happens apically(26). These results suggest that the cell crawling and junction shrinking mechanisms act in concert.

II.2 The molecular basis of PCP signaling.

Two conserved signaling pathways control PCP from *Drosophila* to mammals. They are the core PCP pathway and the Fat, Dachous and Four-jointed (Ft-Ds-Fj) pathway(300-302).

II.2.a Classification of Wnt signaling pathways.

Wnt proteins are secreted glycoproteins that activate different signal transduction pathways. They regulate crucial aspects of cell fate determination, cell migration, cell polarity, neural patterning and organogenesis during embryonic development(303). Wnt signaling can be divided to two main branches: the canonical Wnt/ β -Catenin pathway and the non-canonical pathways. Non-canonical Wnt pathways are further subdivided into the Wnt/ Ca^{2+} and PCP pathways (Fig. 14).

Canonical Wnt signaling regulates the concentration of the transcriptional co-activator β -Catenin. β -Catenin can translocate into the nucleus to regulate target gene expressions along with transcription factors of the T-cell factor (TCF)/lymphocyte enhancer factor (LEF) family(304). In the absence of Wnt, β -Catenin is kept low in the cytoplasm by a destruction complex that consists of proteins including the scaffolding protein Axin1, Casein kinase 1 (Ck1) and Glycogen synthase kinase 3 (Gsk3)(305). Ck1 and Gsk3 sequentially phosphorylate the N-terminus region of β -

Catenin which will lead to β -Catenin degradation. In the presence of Wnt, Fzd receptor and its co-receptor Lrp5/6 (Low density lipoprotein receptor-related protein 5/6) along with Dsh recruits the destruction complex to the membrane, thus, liberating β -Catenin from degradation so that it can translocate into the nucleus to regulate target gene expressions (Fig. 14)(304, 306, 307).

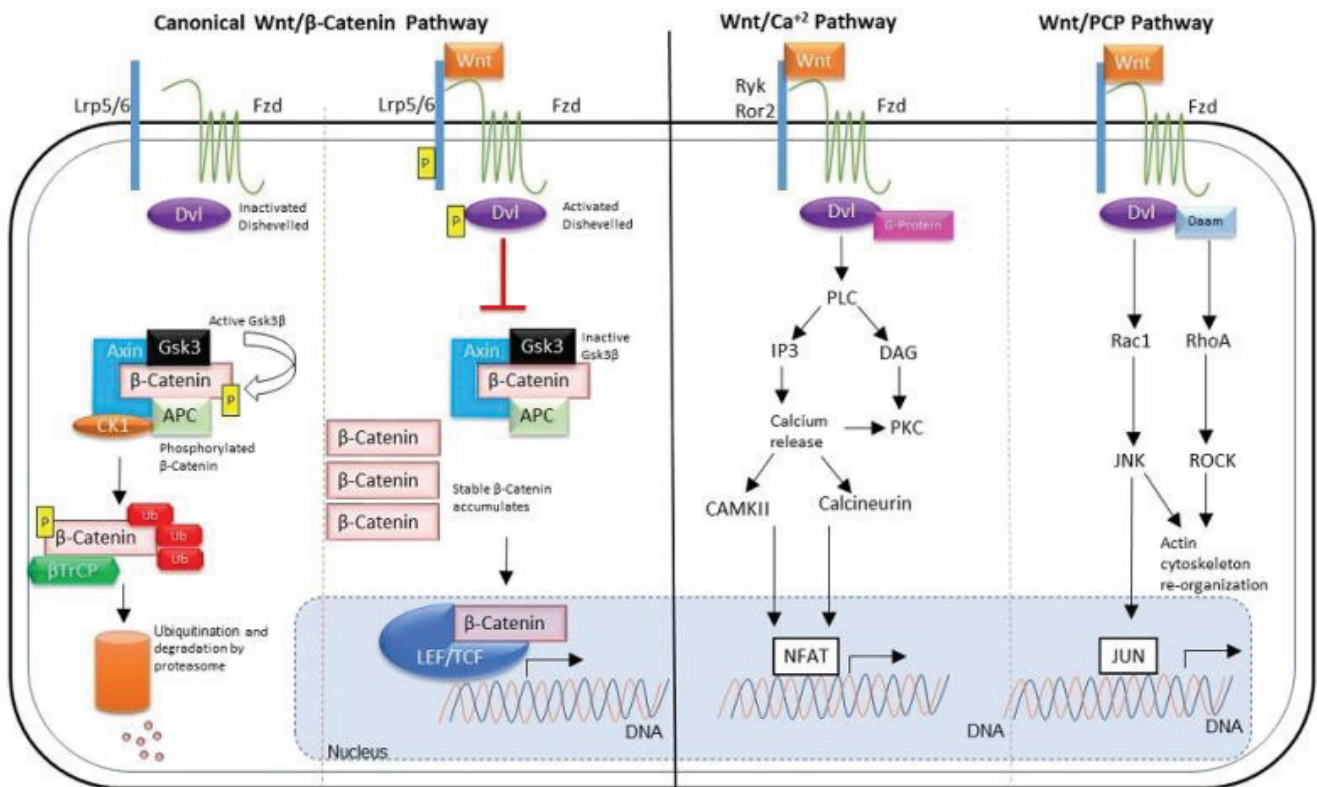


Figure 14. Classification of Wnt signaling pathways. The three branches of Wnt signaling are β -Catenin pathway, Ca^{2+} pathway and PCP pathway. Canonical Wnt signaling regulates the concentration of transcriptional co-activator β -Catenin and further downstream target gene expression. Activation of the Wnt/ Ca^{2+} pathway has been demonstrated to affect gene transcription through NFAT. The PCP pathway has been shown to regulate cytoskeletal remodeling via RhoA. In addition, Rac and subsequent c-JNK activation can regulate gene transcription. (Garcia et al., 2018)

The non-canonical Wnt signaling pathways are independent of β -Catenin function. Out of the two non-canonical pathways, the Wnt/ Ca^{2+} pathway regulates intracellular Ca^{2+} release from the endoplasmic reticulum through trimeric G-proteins(308). The calcium release and intracellular

accumulation activates several Ca^{2+} sensitive proteins, such as protein kinase C (PKC) and calcium/calmodulin-dependent kinase II (CamKII). CamKII has been shown to activate the transcription factor NFAT to promote ventral cell fates in *Xenopus* embryos. The Wnt/ Ca^{2+} pathway has been shown to antagonize the Wnt/ β -Catenin pathway. CamKII can activate TGF β activated kinase (TAK1) and Nemo-like kinase (NLK) to inhibit β -Catenin/TCF signaling (Fig. 14).

The PCP pathway, the second branch of non-canonical Wnt signaling, is the most relevant Wnt signaling pathway for the second part of my thesis. Therefore, PCP signaling is explained in detail below.

II.2.b The core PCP /non-canonical Wnt signaling pathway.

The core PCP pathway starts with secreted Wnt glycoproteins such as Wingless (Wg) and dWnt4 in *Drosophila* (309, 310), and Wnt5a and Wnt11 in vertebrates(311-314). The core PCP pathway in *Drosophila* consists of six core components. Three of the six core components are transmembrane proteins such as Frizzled, Vang (also known as Strabismus (Stbm); Vangl-like (Vangl) in vertebrates) and the atypical cadherin Flamingo (Fmi; also known as Starrynight (Stan); Celsr in vertebrates)(315-317). The next three core components are cytoplasmic proteins such as Dishevelled (Dsh; Dishevelled-like (Dvl) in vertebrates, Prickle (Pk) and Diego (Dgo; Inversin and Diversin in vertebrates)(315-319). There are several number of core PCP components in vertebrates due to multiple members per core component (Table 1).

The downstream signaling of the PCP pathway involves small GTPases of the Rho subfamily (Rho, Rac and cdc42), the Rho-associated kinase (ROK), the STE20-like kinase Mishapen (Msn in flies) and the JNK-type mitogen-activated protein kinase (MAPK) cascade(320, 321). The importance of these different downstream signaling components varies since the downstream readout of PCP signaling varies according to the developmental context. For example, ROK is involved in the cytoskeletal regulation of PCP by regulating acto-myosin remodeling(322, 323). In *Xenopus*, the formin homology domain protein Daam1 has been proposed to act as a bridging factor between Dsh and Rho GTPase/ROK for PCP dependent cytoskeletal reorganization(281). JNK signaling has been reported to get activated downstream of the PCP pathway during vertebrate CE and orientation of the ommatidial preclusters in the *Drosophila* eye(324-326).

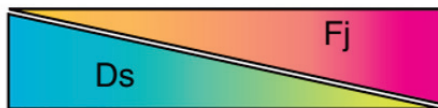
Table 1: PCP signaling components in both vertebrates and invertebrates (323, 340)

<i>Drosophila</i> genes	Vertebrate genes	Molecular features
Core PCP pathway components/co-factors/ligands		
<i>Frizzled (Fz)</i>	<i>Fzd1</i> <i>Fzd2</i> <i>Fzd3</i> <i>Fzd6</i> <i>Fzd7 and others</i> <i>(best analyzed in mice)</i>	<i>Seven-pass transmembrane receptors, bind Wnt ligands; intracellular binding to Dsh; recruit Dsh and Dgo to membrane; co-IP with Fmi/Celsr</i>
<i>Dishevelled (Dsh)</i>	<i>Dvl1</i> <i>Dvl2</i> <i>Dvl3</i> <i>XDsh (Xenopus)</i>	<i>Cytoplasmic protein containing DIX, PDZ, DEP domains; recruited to membrane by Fz; binds Fz, Pk, Vang, and Dgo; undergoes extensive phosphorylation</i>
<i>Van Gogh [Vang; also known as Strabismus (Dtbm)]</i>	<i>Vangl2</i> <i>Vangl1</i> <i>Trilobite (tri/Vangl, zebrafish)</i> <i>xStbm (Xenopus)</i>	<i>four-pass transmembrane protein; binds Pk, Dsh, and Dgo; recruits Pk to membrane; co-IPs with Fmi/Celsr</i>
<i>Flamingo [Fmi; also known as starry night (Stan)]</i>	<i>Celsr1</i> <i>Celsr2</i> <i>Celsr3</i>	<i>Atypical cadherin with seven-pass transmembrane receptor features; homophilic cell adhesion; co-IPs with Fzs and Vang(l)s</i>
<i>Prickle (Pk; also known as prickle-spiny legs)</i>	<i>Pk1</i> <i>Pk2</i> <i>xPk (Xenopus)</i>	<i>Cytoplasmic protein with three LIM domains and PET domain; recruited to membrane by Vang; physically interacts with Vang, Dsh, and Dgo; competes with Dgo for Dsh binding</i>

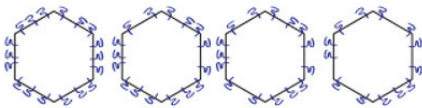
<i>Diego (Dgo)</i>	<i>Diversin (ankyrin repeat domain 6) Inversin (invs)</i>	<i>Cytoplasmic ankyrin repeat proteins; recruited to membrane by Fz; bind Dsh, Vang, and Pk; compete with Pk for Dsh binding</i>
<i>Wnt4, Wingless (Wg)</i>		<i>Secreted glycoprotein ligand</i>
	<i>Wnt5, Wnt11</i>	<i>Secreted glycoprotein ligand</i>
	<i>mRor2 (mouse), XRor2 (Xenopus)</i>	<i>Receptor tyrosine kinase; contains extracellular Frizzled-like CRDs and Krigle domain; acts as a coreceptor for Wnt5a to mediate noncanonical Wnt signaling</i>
<i>Derailed</i>	<i>Ryk (mouse)</i>	<i>Receptor tyrosine kinase; contains extracellular Wnt-binding WIP domain; acts as coreceptor for Wnt5a</i>
<i>Furrowed (fw)</i>		<i>Selectin family cell adhesion molecule; promotes homophilic adhesion; co-IPs with Fz</i>
<i>VhaPRR</i>		<i>Subunit of proton pump V- ATPase; colocalizes and co-IPs with Fmi</i>
	<i>Rspo3</i>	<i>Roof plate specific spondin, secreted protein</i>
	<i>Syndecan4</i>	<i>Cell surface heparin sulfate proteoglycan, cell adhesion receptors</i>
	<i>Knypek/glypican4 (kny/gpc4)</i>	<i>Membrane-associated Heparan sulfate proteoglycan</i>
	<i>Protein tyrosine kinase 7 (PTK7)</i>	<i>Transmembrane protein, tyrosine kinase homology domain</i>
	<i>Receptor for activated protein kinase C1 (rack1)</i>	<i>Adaptor/scaffolding protein, WD40 repeats</i>
Fat-Daschous-Four-jointed pathway components		
<i>Fat (Ft)</i>	<i>Fat1, Fat2, Fat3, Fat4</i>	<i>Transmembrane protein, atypical cadherin, extracellular cadherin repeats, EGF domain, Laminin domain</i>

<i>Dachsous (Ds)</i>	<i>Dachsous 1 (Ds1/Dsch1), Dachsous 2 (Ds2/Dsch2)</i>	<i>Transmembrane protein, atypical cadherin, extracellular cadherin repeats</i>
<i>Four-jointed (Fj)</i>	<i>Four-jointed (Fjx)</i>	<i>Type II transmembrane protein potentially secreted after cleavage</i>
<i>Atrophin (Atro)</i>	<i>Atrophin1 (Atn1), Atrophin2 (Atn2)</i>	<i>A transcriptional co-repressor</i>

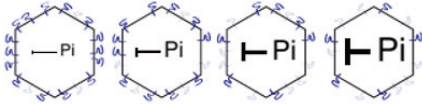
A. Proximal \longrightarrow Distal



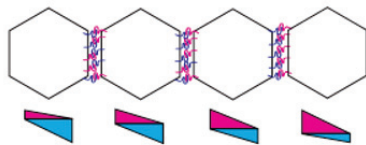
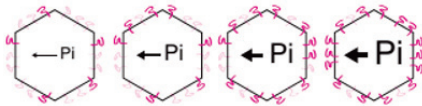
Ds expression





Ds activity




Ft activity



 Dachsous (high affinity for Ft)

 p-Fat (high affinity for Ds)

 p-Dachsous (low affinity for Ft)


 Fat (low affinity for Ds)

Figure 15. Mechanism of Fat, Dachsous and Four-jointed pathway. Ft and Fj are expressed in opposing gradients. Fj phosphorylates both Ft and Ds to create different binding affinities for each other along the P-D axis. Phosphorylated Ft has an increased affinity for Ds whereas Ds phosphorylation decreases its affinity for Ft. This opposing gradient is converted into subcellular asymmetries of Ft and Ds heterodimers which in turn regulates PCP. (Aw and Devenport, 2017)

II.2.c The Fat, Dachshous and Four-jointed (Ft-Ds-Fj) pathway.

The orientation of cuticular hairs in *Drosophila* depends on both the core PCP pathway and the Ft-Ds-Fj systems(327, 328). Ft and Ds are large protocadherins that localize to opposite sides of the cell where they form intercellular heterodimers(329-331). Their interaction is modulated by the Golgi-associated kinase Fj which phosphorylates extracellular domains of Ft and Ds(332-334). Ds and Fj are expressed in opposing gradients in several *Drosophila* tissues and these opposing gradients act as global cues that are converted into Ft-Ds subcellular asymmetries(335, 336). The subcellular Ft-Ds asymmetry is generated by phosphorylation activity of Fj on both Ft and Ds (Fig. 14). The phosphorylated Ft has an increased affinity for Ds whereas Ds phosphorylation decreases its affinity for Ft. Thereby, the Fj gradient generates complementary affinity gradients of Ft and Ds (Fig. 15)(332, 333).

In *Drosophila*, Ft physically interacts with Atrophin (Atro), a transcriptional co-repressor, to mediate downstream PCP signaling(337). Both Ft and Atro are also required to control Fj expression. Loss of Atro leads to PCP defects in eyes and wings that phenocopy the loss of Ft(337). Moreover, *atro* mutant flies exhibit a strong genetic interaction with Ft in regulating planar polarity(337). The Ft-Ds system is well studied in *Drosophila* but less well analyzed in vertebrates, nonetheless it is conserved in vertebrates as well(301). In mammals, four Ft homologs have been identified (Ft1-4). Ft4 mutant mice show PCP defects including misorientation of hair cells, shorter anterior-posterior body axis and a broadened spinal cord(338). Later, it has been shown that Ft1 and Ft4 cooperate during mouse development to control renal tubular elongation, cochlear extension, cranial neural tube formation and patterning of outer hair cells in the cochlea(301). Moreover, the mammalian orthologue of Atro, Atn1 and Atn21, are shown to modulate Ft4 activity during vertebral arch fusion and renal tubular elongation, indicating a conserved interaction of Ft-Atro in PCP(301).

The core PCP pathway and the Ft-Ds-Fj pathway are considered to act in parallel to regulate PCP. However, in some tissues in *Drosophila*, it has been shown that these two pathways crosstalk to establish PCP(339).

II.3 Mechanism of establishing PCP

Planar polarity is achieved by asymmetric distribution of proteins or structures along the plane of the tissue. In order to polarize a group of cells in a tissue, polarity information from an individual cell must be communicated between neighboring cells. Such cell-cell communication is achieved through physical interaction of PCP signaling complexes at cellular junctions. Therefore, there is an intracellular segregation of two polarity complexes to opposing sides (anterior/proximal and posterior/distal) of each cell, leading to the formation of a Fz-Fmi-Dsh-Dgo complex on one side and a Vang-Fmi-Pk complex on the other side (Fig.16) (300, 340, 341). Different mechanisms play a crucial role in creating this asymmetry.

II.3.a Inhibitory and stabilizing interactions

One of the mechanisms by which asymmetric distribution of PCP components is achieved is through intracellular mutual inhibitory interactions between the two complexes. At the anterior/proximal side of the cell, Vang positively regulates the function of Pk by recruiting Pk to the membrane and binding to it(342, 343). Vang and Pk have been shown to inhibit the formation of Fz-Dsh complex by directly binding to Dsh and affecting Dsh levels and stability(343-346). Specifically, Pk can bind to Dsh and thereby prevent Fz-mediated membrane recruitment of Dsh(346). At the posterior/distal side of the cell, Dgo antagonizes the effect of Pk on Dsh and thereby protects and stabilizes the Fz-Dsh complex. Dgo binding to Dsh competes with Pk binding to Dsh and thus, antagonizes the inhibitory effect of Pk(346). Therefore, a series of mutual inhibitory interactions enable the two complexes, Fz-Dsh-Dgo-Fmi and Vang-Pk-Fmi, to resolve into mutually exclusive regions of each cell. Similar observations of mutually exclusive localization of these two complexes are observed in vertebrate PCP models such as the inner ear, skin and the limb of mouse, and presomitic-mesoderm of the zebrafish(229-231, 347-349).

Apart from this intracellular antagonism, Fz-Dsh-Dgo-Fmi and Vang-Pk-Fmi complexes stabilize each other intercellularly to provide a positive feedback function to asymmetric distribution. Fmi, a seven-pass atypical cadherin, is an essential component for this positive feedback function(350-353). Fmi acts as a homophilic adhesion component and it has been shown to colocalize and coimmunoprecipitate with both Fz and Vang(350, 352, 354). Homophilic Fmi bridges span the cell membrane and facilitate intercellular Fz-Vang interactions by recruiting and stabilizing their complexes across membranes and thereby, providing an essential platform to propagate PCP from

cell to cell(342, 350, 353, 355). The recruitment of junctional PCP complexes by Fmi is necessary for intercellular communication of polarity, however it is not sufficient for the establishment of a robust PCP pattern within planar polarized cells. Therefore, there are additional feedback interactions that can amplify asymmetric PCP patterns. One such amplification process occurs through activities of cytoplasmic components Dsh, Dgo and Pk. These cytoplasmic components act by clustering transmembrane signaling complexes into stable PCP enrichments(343, 345, 356-359). For example, FRAP analysis of Fz-containing puncta that are associated to cytoplasmic PCP components showed higher stability compared to the diffused Fz-GFP and it had limited lateral mobility in the membrane(356). And in the absence of Dsh, Pk or Dgo, the size, intensity and stability of Fz-containing puncta diminishes(356).

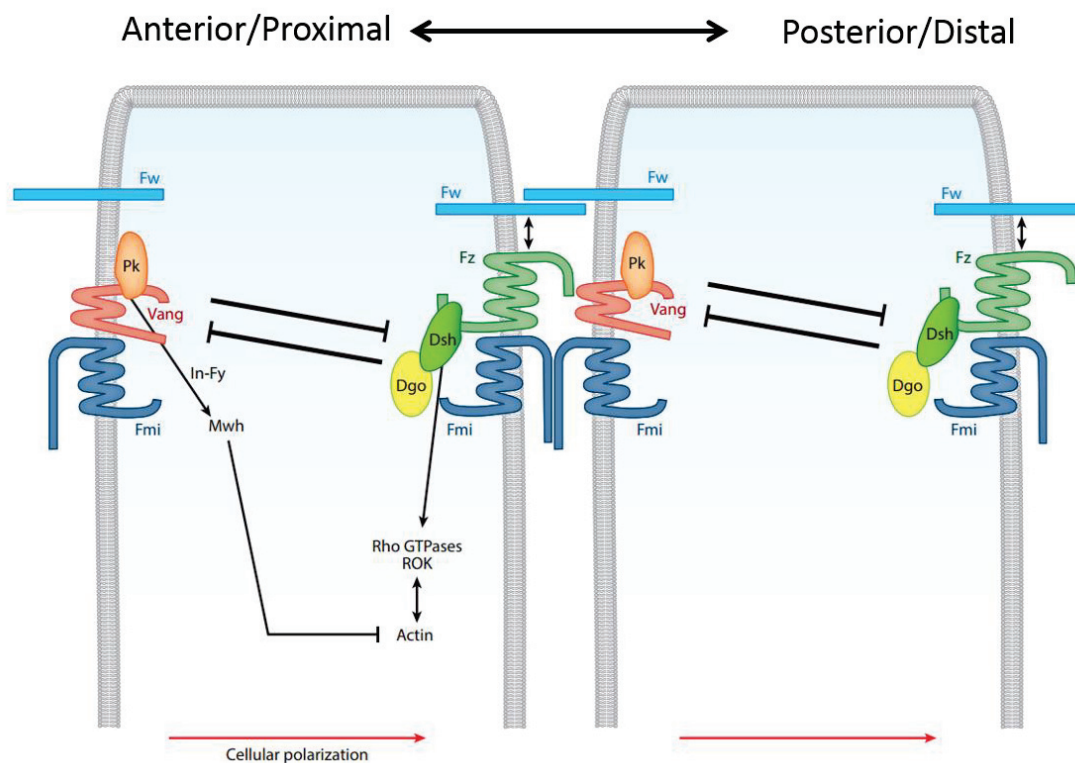


Figure 16. PCP core component interactions across a cell border. Core PCP components are asymmetrically distributed across the anterior/proximal -posterior/distal axis of the tissue. Mutual inhibitory and stabilizing interactions help the cells to resolve the PCP complexes Fz-Fmi-Dsh-Dgo and Vang-Fmi-Pk into two opposite sides of the cell. This asymmetric distribution further regulates polarized cytoskeletal remodeling and thereby, regulates PCP patterning. (picture adapted from *Yang and Mlodzik, 2015*)

II.3.b Polarized microtubule trafficking of PCP components.

Another mechanism contributing to PCP asymmetry is microtubule based polarized trafficking (Fig. 17). Live imaging of fluorescently tagged PCP proteins in *Drosophila* pupal wings showed that Fz and Dsh containing particles travel across the cell in a proximal to distal direction(327, 360, 361). This directed transport could amplify asymmetry or even provide the initial asymmetry by removing proximal Fz-Dsh-Fmi complexes and relocating them to the distal side. Directed PCP transport is mediated by an array of subapical, noncentrosomal microtubules (MTs) that align along the proximal-distal axis, with plus ends biased towards the distal side(339, 360-362). The Ft-Ds-Fj module is required for proximal to distal MT alignment, which indicates a cross-talk between the core PCP pathway and the Ft-Ds-Fj pathway in orienting cytoskeletal structures(339).

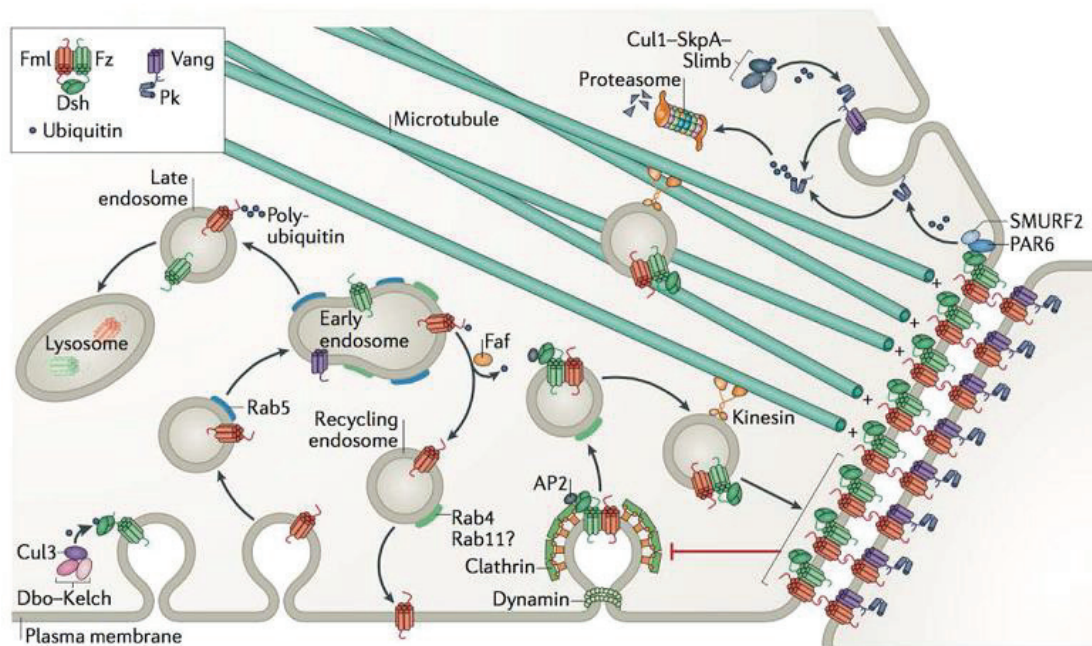


Figure 17. Endocytosis, trafficking and degradation events during PCP patterning. Core PCP components are asymmetrically distributed across the anterior/proximal -posterior/distal axis of the tissue. Microtubules show a slight bias towards the P-D direction by which directional transport of Fz-Dsh-Fmi complex is achieved. Dynamin and Clathrin-mediated endocytosis along with post-translational modifications including ubiquitination regulate asymmetric distribution of PCP components. (Butler and Wallingford, 2017)

Microtubule orientation also correlates with PCP asymmetry in mouse tracheal epithelial cells, where PCP coordinates the alignment of motile cilia(236). MTs are polarized with their plus ends oriented towards the Fz-Dvl domain and disruption of MTs with nocodazole impairs core PCP component's localization. Similarly, MTs are required for establishing Pk asymmetry during zebrafish gastrulation(363). Initially, it was thought that polarized microtubules are essential only for establishing PCP asymmetries but dispensable for maintaining these patterns(363, 364). However, a recent study showed that polarized trafficking of PCP components by microtubules is required for both establishment and maintenance of PCP in monociliated floorplate cells of the zebrafish neural tube(365).

II.3.c Endocytosis and endosomal trafficking facilitates asymmetric sorting.

To generate and maintain PCP patterns, different components need to be trafficked to specific membrane domains and mislocalized components need to be removed from the membrane (Fig. 17) . In mammalian cells, exit of Vangl2 from the trans-Golgi network (TGN) requires Arfrp1 (an Arf-like GTPase) and the clathrin adaptor complex AP-1 (366). This indicates that differential sorting of PCP components to opposite sides of the cell could initiate from the TGN itself. For removing mislocalized components, both the Rab GTPase Rab5 and Dynamin have been shown to play an important role in the internalization of mislocalized PCP components(352, 367). Inhibition of endocytosis leads to overaccumulation of Fmi at the plasma membrane(352). Along with Fmi, both Fz and Vang are also known to undergo active membrane turnover by endocytosis (Fig. 16) (352, 356). In addition, Fz facilitates feedback amplification of asymmetry by promoting removal of Fmi-Van-Pk complexes from domains where Fz is accumulated(368). This function of Fz is proposed to be mediated via Pk. Ubiquitination of Pk by an E3 ubiquitin ligase complex consisting of Cullin-1, SkpA and the Supernumerary limbs complex can promote internalization of Fmi-Vang-Pk complexes, and this Pk-dependent internalization of Fmi is significantly reduced in Fz mutants(368).

Endocytosis is essential not only for establishing PCP patterns, but also for adjusting patterns during cell rearrangements and mitotic events(369). In the developing mammalian epidermis, PCP components are internalized and redistributed during mitosis and this is essential for proper patterning of the skin and planar polarization of hair follicles(370). These events of internalization and redistribution are synchronized during cell division through Celsr phosphorylation. The

phosphorylation of Celsr1 by Polo-like kinase-1 promotes its internalization along with the associated Fzd proteins(371). Endocytosis has also been shown to regulate PCP mediated cell adhesion and migration. E-cadherin internalization and subsequent recycling back to surface is important for the regulation of PCP mediated zebrafish gastrulation movements(372). Inhibition of endocytosis by blocking Rab5c activity caused abnormal tissue movements, which phenocopied the gastrulation phenotypes of *wnt11* mutant and enhancing Rab5c activity in *wnt11* mutants rescued the phenotypes of *wnt11* mutant(373).

II.3.d Post-translational modifications fine-tune PCP protein function.

Post-translational modifications such as phosphorylation and ubiquitination are reported to alter the level, localization and function of PCP components. For example, Dvl and Vangl proteins have multiple phosphorylation sites that can be modified to regulate protein localization and function(341, 374). Mouse Dvl2 is phosphorylated in response to Wnt5a stimulation which promotes Dvl2 association with the ubiquitin ligase Smurf2 and the apical polarity protein Par6(375). This complex further regulates Pk1 protein stability by promoting Pk1 ubiquitination and consequent proteasomal degradation(375). Wnt5a can also promote Vangl2 phosphorylation through the tyrosine-protein kinase receptor Ror2, and this phosphorylation increases the activity of Vangl2(347). Thus, during mouse limb bud P-D elongation, the Wnt5a gradient is able to generate a Vangl2 activity gradient and thereby, planar polarize chondrocytes along the P-D axis which in turn mediates limb elongation(347). In addition, the serine/threonine kinase misshapen-like 1 (Mink1) phosphorylates a conserved residue of Pk1, which promotes its membrane localization with Vangl2 and thereby, apical enrichment of Vangl2-Pk1 complexes(376).

On the other hand, ubiquitination of PCP components is shown to affect their protein levels. The ubiquitin ligase Smurf1 regulates the level of Pk1 via ubiquitin mediated degradation in response to Wnt5a stimulation(375). Similarly, Skp1, a subunit of the SCF E3 ligase, regulates Pk levels by promoting its degradation in a Vang-dependent manner in *Drosophila*(377). Transmembrane PCP proteins are often sorted into lysosomes after ubiquitination since blocking of lysosomal maturation causes accumulation of Fmi and Fz intracellularly(352). In order to regulate lysosomal turnover of proteins, there are deubiquitinating enzymes like Fat facets (Faf) that regulates recycling of Fmi back to the plasma membrane from early endosomes (Fig. 17) (378). The modulation of PCP protein levels by ubiquitin-mediated degradation/recycling can generate

asymmetric protein distributions by restricting the amount of PCP proteins to only one side. For example, in flies, regulation of Dsh by a Cullin-3-BTB ubiquitin ligase complex limits its level at cell junctions, and reduction of Cullin-3 leads to an increase in the overall level of core PCP protein and thus, a reduction of asymmetry(378). Therefore, Cullin-3 reduction caused defects in *Drosophila* wing hair polarity, which phenocopies Dsh overexpression defects(378).

II.4 Additional regulators of the core PCP pathway.

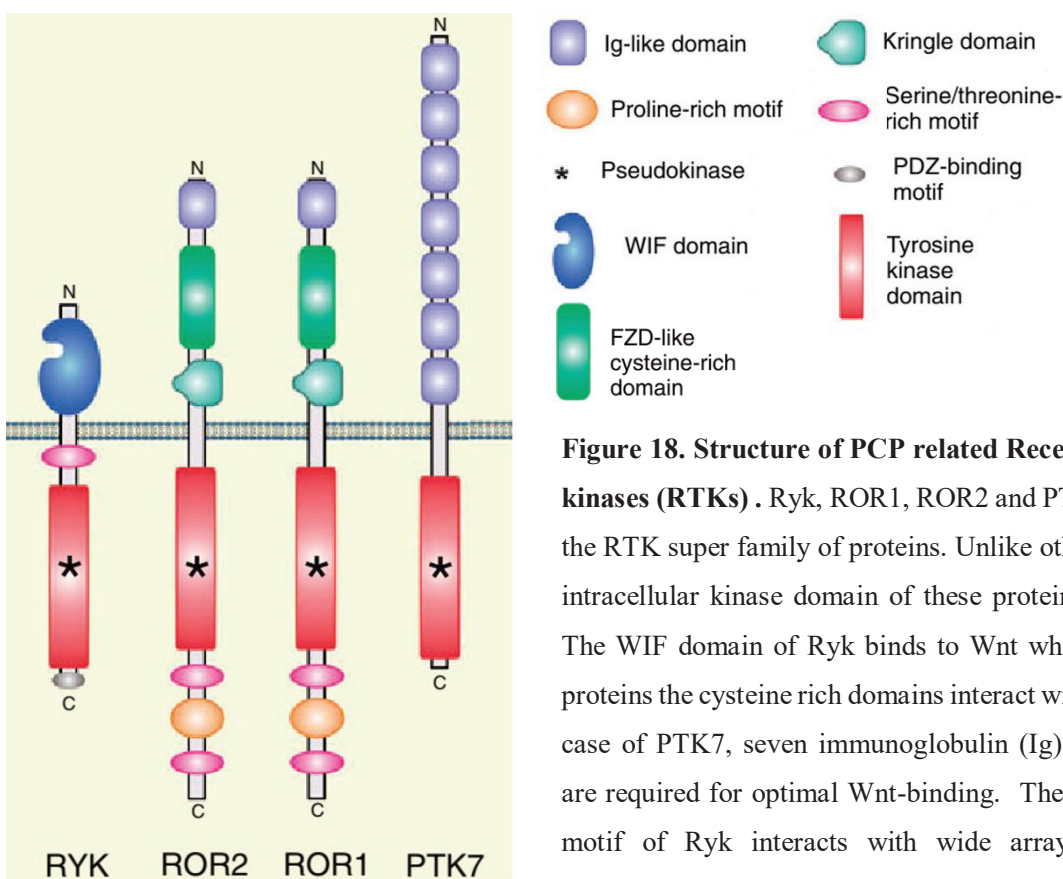
Apart from the core components, there are additional players that are important for core PCP pathway activity, but they are not only dedicated to the PCP pathway. Furrowed (Fw), a selectin family member and the VhaPRR accessory subunit of the proton pump V-ATPase are two such components in *Drosophila*(379, 380). The function of Fw is partially overlapping with Fmi, as it is required to stabilize Fz in plasma membrane complexes and promote homophilic cell adhesions(350, 379). Functional studies on the role of VhaPRR suggest that it affects trafficking or membrane stability of Fmi and possibly Fz(381).

In vertebrates, there are several additional regulators of the core PCP pathway because there are often multiple members per core component as well as transmembrane co-factor proteins that assist core PCP components to relay PCP signaling (Table 1). Wnt9b and Wnt7a are Wnt ligands that are known to have functions in canonical β -Catenin signaling but also take part in PCP signaling(382, 383). Rspo3 (roof plate specific spondin 3), a secreted protein, is known to bind Syndecan4 (Sdc4) to regulate PCP regulated gastrulation movements(384). Rspo3 mediated PCP signaling requires Wnt5a to induce Sdc4-dependent, clathrin-mediated endocytosis and further relay of signaling via downstream components such as Fz7, Dvl and JNK. Zebrafish *knypek* mutants display CE defects due to the inactivation of the gene *glypican4*, which also appears to promote PCP signaling(385).

In addition, non-canonical Wnts are known to bind co-receptors belonging to the receptor tyrosine kinase family (RTKs) of proteins including PTK7 (Protein tyrosine kinase 7), Ror1, Ror2 (RTK like orphan receptor-1 or 2) and Ryk (Receptor related to tyrosine kinase)(386). RTKs are central regulators of crucial developmental, physiological and pathological signaling pathways(387). Molecularly, RTKs are single pass transmembrane proteins that contain an intracellular protein

tyrosine kinase (PTK) domain. The catalytic activity of the PTK domain is a key signaling element for most RTKs, however Ryk, ROR1/2 and PTK7 have an inactive PTK domain and are called pseudo kinases (386)(Fig. 18). PTK7 regulates membrane recruitment of Dvl through two different mechanisms: one which is dependent on Receptor of activated protein kinase C1 (Rack1) and another dependent on the interaction with Fz7(388). Ror2 is Wnt5a co-factor that enhances the asymmetric localization of Vangl2 via Wnt5a-dependent phosphorylation of Vangl2(347). Similarly, Wnt5a also induces Dvl phosphorylation through Ror1 and Ror2(389). Ryk (Derailed in *Drosophila*) is a transmembrane protein that mediates the function of Wnt5 in axon guidance in *Drosophila* (390)and modulates degradation of Vangl2 in mice(391).

Ryk is one of the potential candidates that could be regulated by Mib1 during zebrafish PCP. Therefore, the role of Ryk in PCP is addressed in detail below.



II.4.a Ryk is an important regulator of the core PCP pathway.

Ryk protein is conserved across a wide range of metazoan genomes. Initial studies have revealed that Ryk and its homologues are playing crucial roles in axon-path finding and formation of facio-cranial bones in *Drosophila* and mice respectively(392, 393). Later, sequence analysis of the Ryk extracellular domain showed that Ryk can bind to Wnt family proteins(390, 394). Structurally, Ryk has a N-terminal WIF1 (Wnt inhibitory factor) domain that can bind to Wnt ligands and a catalytically inactive PTK domain at the C-terminus. The PDZ binding motif at the C-terminus of Ryk interacts with a wide array of proteins including Src family kinases(393, 395-397), that regulate fundamental process including cell growth, differentiation, migration and survival(398).(Fig. 18). Mechanistically, Ryk can act as a scaffolding protein that promotes binding of intracellular proteins and other receptors. This can bring activating proteins in proximity to substrates or promote membrane localization of intracellular signaling proteins. For example, Ryk has been shown to recruit Dvl family proteins, that are important for both canonical and non-canonical Wnt signaling, to the plasma membrane(395). Ryk has also been shown to undergo sequential proteolytic cleavages releasing the extracellular domain into the extracellular space and the intracellular region into the cytoplasm. This proteolytic cleavage reactions are shown to be important for the function of Ryk in neuronal differentiation and axon guidance(399-401).

Ryk has been implicated in both canonical and non-canonical Wnt signaling pathways. In the canonical Wnt/ β -Catenin signaling pathway, studies have reported that Ryk is required for activation of a β -Catenin/TCF-responsive reporter gene(159, 395, 402). Wnt1 and Wnt3A, Wnt ligands responsible for canonical signaling, require Ryk to stimulate TCF-dependent transcription(395). Moreover, Wnt1 has been shown to relay signaling via a Ryk/Fzd8 receptor complex(395). Ryk has also been shown to form complex with Mindbomb1 (Mib1) to activate Wnt/ β -Catenin signaling(159). The N-terminus of Mib1 binds to the intracellular domain of Ryk to ubiquitinate Ryk. Mib1 mediated ubiquitination of Ryk is necessary for mediating β -Catenin signaling even though ubiquitinated Ryk protein will be degraded. In *C. elegans*, Ryk genetically interacts with Mib1 during vulva cell fate determination by regulating oriented division of vulval precursor cells(159).However, Ryk was also reported to mediate suppression of canonical Wnt-signaling in the promotion of osteoclast differentiation(403).

Studies in vertebrates suggest that Ryk is predominantly signaling through non-canonical Wnt signaling pathways including the Wnt/PCP pathway. Ryk is important for PCP regulated functions including CE during gastrulation, orientation of cilia and axon guidance. Ryk has been proposed to regulate CE movements during gastrulation through two different mechanisms in two different organisms. In *Xenopus*, Ryk regulates CE via inducing hyperphosphorylation of Dvl and its subsequent accumulation at the membrane(404). As a result, Ryk along with Wnt11 and Fz7 promotes endocytosis of Dvl and thereby regulate CE movements. Ryk has also shown to be required for activation of the downstream PCP component RhoA(404). In zebrafish, Ryk is provided both maternally and zygotically, and during gastrulation it is expressed throughout the embryo(405). During this time, Wnt5b and Ryk act synergistically to regulate CE movements. Wnt5b overexpression promotes endocytosis of Ryk from the membrane and thus increases filopodial and lamellipodial protrusions(405). Therefore, Ryk expressing cells have the capability to migrate away from Wnt5b expressing cells whereas Ryk morphant cells remain immobile(405). These experiments indicate that Ryk is necessary for polarized cellular projections and directional migration in response to Wnt/PCP signaling(405).

In mouse, Ryk deficient embryos present a disrupted polarity of stereociliary hair cells in the cochlea(391, 396). Moreover, the trans-heterozygotes of both Vangl2 and Ryk gave severe neural tube closure defects in contrast to either of the single heterozygotes, which indicates a genetic interaction between Ryk and Vangl2 (391, 396). Additionally, Wnt5a helps the formation of Ryk-Vangl2 complex by which it increases the stability of Vangl2 in the membrane(391). The interaction of Ryk with Vangl2 also plays an important role in axon guidance. Mouse corticospinal tract (CST) axons are repelled by a high Wnt5a expression in the rostral spinal cord relative to a low expression in the caudal spinal cord(406). Accordingly, an increased endosomal distribution of Vangl2 occurs in the presence of higher Wnt5a concentrations whereas more Vangl2 is retained at the cell membrane when the Wnt5a concentration is low(407). This asymmetric distribution of Vangl2 is necessary for the axon growth cone to turn away from high Wnt5a concentrations(407). Asymmetric distribution of Vangl2 in the axon growth cone is mediated by Ryk-Vangl2 interaction(407).

It is important to note that, *in vitro*, Mib1 has been shown to form a complex with Ryk and ubiquitinate Ryk . Also, in *C. elegans*, Mib1 genetically interacts with Ryk during vulva cell fate

determination by regulating oriented division of vulval precursor cells(159). These evidences suggest that Ryk could be one of the potential targets of Mib1 in regulating PCP in zebrafish.

II.5 Mindbomb1 functions independent of Notch signaling.

During the first part of my Phd, morphants of Mib1 have shown defects in PCP regulated CE movements during zebrafish gastrulation. Since post-translational modifications such as ubiquitination is one of the mechanisms by which PCP is regulated, we suspect that Mib1 might be regulating one or several PCP components via ubiquitination. Interestingly, Mib1 has been shown to regulate Ryk, that has functions in both canonical and non-canonical Wnt signaling, via ubiquitination. This led us to explore functions of Mib1 outside the realm of Notch signaling. Studies indicate that Mib1 has several functions independent of the Notch signaling pathway including the regulation of Wnt/ β -Catenin signaling, cell migration, apoptosis, NF- κ B signaling and ciliogenesis.

II.5.a Mib1 regulates Ryk mediated Wnt/ β -Catenin signaling.

Mib1 has been shown to form a complex with Ryk to activate Wnt/ β -Catenin signaling(159). Ryk is required for CTNNB1-dependent Wnt signaling because a loss of function of Ryk inhibits the ability of Wnt-3A to activate a CTNNB1-dependent transcriptional reporter in human embryonic kidney cells (HEK293T)(395). Moreover, Ryk is required for Wnt/CTNNB1 signaling *in vivo* as well since Lin-18/Ryk shows a genetic interaction with Wnt/Mom2 and TCF/Pop-1 during vulval cell fate specification in *C. elegans*(408). Mass spectrometric analysis has identified Mib1 as one of the interacting partners of Ryk. Mib1 is responsible for Ryk ubiquitination and internalization and thereby, regulates its turnover at the membrane(159). The loss of function of Ryk or Mib1 downregulates Wnt/CTNNB1 target gene expression which indicates that internalization of Ryk by Mib1 is necessary for Wnt/CTNNB1 signaling even though Ryk might be degraded afterwards. Moreover, ceMib1 shows genetic interaction with lin-18/Ryk during vulval development(159).

II.5.b Mib1 regulates directional cell migration.

In vitro assays have shown that Mib1 is required for persistent directional cell migration(198). Mib1 regulates directional cell migration by controlling Rac1 activation via Catenin delta 1. Rac1, Cdc42 and RhoA belong to small GTPases family of proteins that control the formation of dynamic actin-rich structures such as lamellipodia, filopodia and stress fibers respectively(409). Rac1

activation specifically at the migratory front is required for persistent directional cell migration(410, 411). Catenin delta 1 (Ctnnd1; also known as p120 catenin), a member of Armadillo repeat protein family, that is known to regulate cadherin localization, also controls actin rearrangements by modulating Rac1 activity(412-414). Mib1 has been shown to monoubiquitinate Ctnnd1 to suppress Ctnnd1 mediated Rac1 activations(198). Therefore, Mib1 knockdown increased the number of protrusions and speed of migration, but in a random direction. Similarly, *in vivo*, Mib1 mutant zebrafish embryos display defects in the migration of posterior lateral line primordium (pLLP) cells due to a lack of directional movement(198).

II.5.c Mib1 regulates apoptosis via the extrinsic cell death pathway.

Mib1 was first identified as DAPK (Death-associated protein kinase) interacting protein, therefore called DIP1(415). DAPK is a multidomain Ser/Thr protein kinase that plays an important role in apoptosis regulation. Mib1 overexpression in HeLa cells antagonized the anti-apoptotic function of DAPK and thereby, promoted caspase-dependent apoptosis(415). Later Mib1 was found to bind to cellular Fas-associated death domain (FADD)-like IL-1b converting enzyme (FLICE)-like inhibitory proteins (cFLIP)(158). cFLIP inhibits death receptor-induced apoptosis by preventing the activation of Caspase8(416). The interaction of Mib1 with cFLIP reduces the inhibitory activity of cFLIP on Caspase8 and thus Caspase8 is free to induce cell death(158).

II.5.d Mib1 regulates NF- κ B signaling.

Mib1 has been shown to act as a positive regulator of Nuclear factor (NF)- κ B activation(417). NF- κ B is a family of transcription factors involved in regulating divergent functions such as apoptosis, tumorigenesis and immune response(418). The NF- κ B family consists of five members : p65 (RelA), RelB, c-Rel, p100 (precursor of p52) and p105 (precursor of p50). These five members form homodimers and heterodimers in different combinations (such as p65:p50, cRel:p50, p50:p50 etc.), and the dimerized complex translocates into the nucleus to regulate gene expressions(419). When there is no stimulus for NF- κ B signaling, dimers such as p65:p50 will be bound to I κ B α , an inhibitor that prevents the translocation of NF- κ B dimers into the nucleus(420). Mib1 has been shown to negatively regulate the stability of I κ B α through its E3-ubiquitin ligase activity and thereby, promote NF- κ B signal transduction(417). In contrast, Mib1 deficient cells showed a dramatic upregulation of I κ B α which will in turn downregulate NF- κ B signaling(417).

II.5.e Mib1 is important for the regulation of ciliogenesis.

Recent studies have indicated that Mib1 plays a crucial role in centriole biogenesis and ciliogenesis(421, 422). Centrioles are the core components of the centrosome and they also function as basal bodies for the formation of cilia and flagella(423, 424). A pair of centrioles surrounded by pericentriolar material (PCM) constitutes the centrosome, the main microtubule organizing center of animal cells(425, 426). Mib1 has been shown to interact with several components of the centrosome including Plk4 (Polo-like kinase 4), PCM1, Talpid3, CEP131 and CEP290. Mib1 acts as an E3-ubiquitin ligase to regulate abundance of these components(421, 422, 427, 428). Since Mib1 can degrade many components of the centrosome by ubiquitination, there exist deubiquitinating proteins to counteract Mib1 function such as CYLD (DUB cylindromatosis) and USP9X(427, 429). CYLD functions to remove ubiquitin chains bound to Mib1, whereas USP9X removes ubiquitin chains from PCM1 that is already ubiquitinated by Mib1. In both ways, these deubiquitinating proteins protect PCM1 from getting degraded by Mib1.

II.5.f Role of Mib1 in regulating PCP.

Ubiquitination is one of the mechanisms by which PCP components establish their asymmetric cell distribution to regulate PCP(340). The role of the E3-ubiquitin ligase Mib1 in PCP is unknown. During the first part of my PhD, morphants of Mib1 displayed defects in PCP regulated CE movements during zebrafish gastrulation. This indicates that Mib1 might be playing an important role in PCP and most probably through its ubiquitination activity. Notch independent functions of Mib1 show that Mib1 interacts with Ryk that can function in both canonical and non-canonical Wnt signaling. In *C. elegans*, Mib1 genetically interacts with Ryk during vulva cell fate determination by regulating oriented division of vulval precursor cells(159). In addition, *In vitro* assays have shown that Mib1 is required for persistent directional cell migration(198). Oriented cell division and directed cell migration are often associated as functions of PCP. These experiments suggest that Mib1 might be playing an important role in PCP. Therefore, I decided to study whether and how Mib1 plays a role in regulating PCP during zebrafish development.

Results

II.1 Analyzing the role of Mib1 in the planar cell polarity pathway

Preliminary results from the first part of my PhD led me to analyze the role of Mib1 in PCP. To study the function of Notch signaling in neural tube morphogenesis, we often depleted Mib1 using genetic mutants and morphants. Depletion of Mib1 showed defects in c-division, a unique morphogenetic process that happens during zebrafish neurulation, that are regulated by the PCP pathway. This indicated that either Notch signaling might be cross-talking with the PCP pathway or Mib1 might be playing a role in the PCP pathway independent of Notch signaling. Studying the role of Mib1/Notch signaling in PCP during neurulation was difficult since neurogenic phenotypes of Notch inhibition could mask other defects. Therefore, I decided to study convergent extension (CE) during gastrulation stage where Notch signaling defects are not visible. The PCP pathway regulates CE movements during gastrulation to elongate the axis of embryos. Surprisingly, *mib1^{ta52b}* mutants, which entirely lack Notch signaling activity(430), didn't show any CE phenotypes but Mib1 morphants showed significant defects in CE. However, the CE defects showed by Mib1 morphants raised the following questions,

- 1) Why did Mib1 morphants show a different phenotype compared to *mib1^{ta52b}* mutants ? Is this just an artifact of our Mib1 morpholino ?
- 2) If the phenotypes of Mib1 morphants are not an artifact, what are the differences between *mib1^{ta52b}* mutant and Mib1 morphant proteins ? Do other *mib1* mutant alleles show CE defects?
- 3) Does Mib1 plays an important role in PCP independent of Notch signaling?
- 4) If Mib1 plays a Notch independent role in PCP, what are the interacting partners of Mib1 in the PCP pathway? What is the mechanism by which Mib1 regulates PCP?

Results in this project are presented in the format of an article which is currently under review in the journal PNAS Brief Reports.

II.2 Article under review in the journal PNAS Brief reports.

Title: The E3 Ubiquitin Ligase Mindbomb1 controls zebrafish Planar Cell Polarity

Authors/Affiliations:

Vishnu Muraleedharan Saraswathy¹, Priyanka Sharma¹ and Maximilian Fürthauer^{1*}

¹ Université Côte d'Azur, CNRS, Inserm, iBV, F-06108 Nice, France.

* Corresponding author: Maximilian Fürthauer (furthauer@unice.fr)

Tel : 0033489150835

ORCID: 0000-0001-6344-6585

Keywords: PCP, Convergent extension, Mindbomb, Ryk

ABSTRACT

The trafficking of Planar Cell Polarity (PCP) pathway proteins is essential for cell migration and embryonic morphogenesis. The E3 Ubiquitin-ligase Mindbomb1 (Mib1) has been extensively studied for its role in Delta/Notch signaling where it promotes an endocytosis of Delta ligands that is essential for Notch activation. We report that independently of its role in Notch signaling, zebrafish Mib1 regulates gastrulation stage Convergent Extension (CE) movements by controlling the endocytic internalization of the PCP pathway component Ryk.

Results and Discussion

Vertebrate Notch signaling involves multiple ligands, receptors and downstream transcription factors. In contrast the internalization of Delta ligands - an endocytic event required for Notch receptor activation – depends essentially on Mib1 (75). Due to this position at a molecular bottleneck of the pathway, Mib1 inactivation is often used to disrupt Notch signaling. We report that in addition to previously reported Notch loss of function phenotypes (75, 431), the inhibition of zebrafish Mib1 function causes defects in gastrulation stage CE movements. Injection of a validated *mib1* exon1/intron1 splice morpholino (75, 431) impaired axial extension at the end of gastrulation (Fig. 1A) and caused a subsequent widening of notochord, somites and neural plate (Fig. 1B). An RNA encoding wild type (WT) Mib1 that cannot be targeted by the *mib1* morpholino rescues axis extension (Fig. 1A), warranting the specificity of the observed defects.

Zebrafish Mib1 interacts with Catenin delta1 to control cell migration (198). This activity is disrupted by the *mib1^{ta52b}* point mutation in the C-terminal RING finger domain (RF3, Fig. 1C) (198). The *mib1^{ta52b}* mutation does however not impair axial extension (Fig. 1D), suggesting thereby that morphant CE phenotypes are indicative of a novel Mib1 function. Sequencing of *mib1* cDNA in *mib1* morphants revealed a retention of intron1 that causes the appearance of an early stop codon which could disrupt Mib1 functions that are not affected by the C-terminal *mib1^{ta52b}* mutation (Fig. 1C). Accordingly, *mib1^{ta52b}* RNA injection rescues *mib1* morphant CE defects (Fig. 1E).

The observation that *mib1^{ta52b}* mutants present defective Notch signaling (75, 431) but intact CE (Fig. 1D) suggests that Mib1 regulates CE independently of Notch. Accordingly, constitutively activated Notch (NICD) rescues Notch-dependent defects in the nervous system (431) but not CE (Fig. 1F). Vertebrate CE requires non-canonical Wnt/PCP signaling (270, 317). To test if Mib1 is required for PCP, we overexpressed the PCP downstream effector RhoA in *mib1* morphants. RhoA restores axis extension (Fig. 1G), suggesting thereby that Mib1 is required for the PCP-dependent control of embryonic CE movements.

All known Mib1 functions require its E3 ubiquitin ligase activity (75, 156, 198). To address if this activity of Mib1 is also required for CE, we attempted to rescue the *mib1* morphant CE defects using a Mib1 variant that lacks the three RING finger domains that are essential for ubiquitination activity (Mib1^{ΔRF123}, Fig. 1C). Rather than rescuing the defects of *mib1* morphants, Mib1^{ΔRF123}

injection enhanced their CE phenotypes and impaired axis extension in WT animals (Fig. 1H). As RING finger deficient Mib1 variants can act as dominant negatives (156, 160), the enhanced CE defects of Mib1^{ARF123}-injected *mib1* morphants are likely due to its capacity to interfere with maternally provided Mib1 that is not targeted by the *mib1* splice morpholino. A Mib1 variant lacking only the last RING finger (Mib1 Δ RF3, Fig. 1C) yielded similar results (Fig. 1I). Our results suggest that the ability of Mib1 to regulate CE is dependent on its E3 ligase activity, and raise the question whether Mib1 may control CE movements by regulating the Ubiquitin-dependent trafficking of a PCP pathway component?

Mib ubiquitinates the Wnt coreceptor Receptor like tyrosine kinase (Ryk) to promote canonical Wnt/ β -Catenin signaling in *C.elegans* (159). Studies in mice, frogs and zebrafish have implicated Ryk in non-canonical Wnt/PCP signaling (396, 404, 405). Ryk localizes to the cell surface and intracellular endocytic compartments (Fig. 2A) (159, 404, 405). To determine whether Mib1 may affect CE by controlling Ryk internalization, we analyzed the effect of Mib1 on Ryk localization during zebrafish gastrulation. Mib1 overexpression depleted Ryk from the cell cortex and triggered its accumulation in intracellular compartments (Fig. 2B). Conversely, morpholino knock-down of Mib1 causes a reduction in the number of Ryk-GFP positive endosomes (Fig. 2E).

The fact that the CE defects of *mib1* morphants can be enhanced by the coinjection of Mib1^{ARF123} or Mib1^{ARF3} (Fig. 1H and I) suggests that Mib1 function is only partially depleted in *mib1* morphants. Accordingly, the injection of a higher dose of Ryk-GFP RNA restores the number of Ryk positive endosomes and rescues the CE defects of *mib1* morphants (Fig. 2E and H). However, even a high dose of Ryk-GFP fails to rescue endosome number and CE in *mib1* morphants coinjected with dominant-negative Mib1^{ARF123} (Fig. 2E-H), suggesting thereby that CE requires Mib1-mediated Ryk endocytosis. The axis extension phenotypes of *mib1* morphants are further enhanced by the coinjection of a validated *ryk* morpholino (405), strengthening the hypothesis that Mib1 and Ryk interact to control CE movements (Fig. 2I). Ryk has been shown to interact with Vangl2, another transmembrane protein whose endocytic trafficking is crucial for PCP (391). Mib1 overexpression has however no effect on Vangl2 localization (Fig. 2C,D) and Vangl2 overexpression does not rescue the CE defects of *mib1* morphants (Fig. 2J).

To provide genetic evidence for a function of Mib1 in PCP we studied CE in *mib1* null mutants. A previously reported null mutant (*mib1*^{tfi91} (75), Fig. 1C) presents CE defects that are statistically

significant but weaker than in *mib1* morphants (Fig. 2L). Similar phenotypes are observed for a newly generated null allele (*mib1^{nce2a}*, Fig.1C) in homozygous mutant or *mib1^{tfi91/nce2a}* transheterozygous animals (Fig. 2L). *mib1^{tfi91}* and *mib1^{nce2a}* introduce stop codons in the beginning of the *mib1* open reading frame, a mutation pattern that can cause nonsense mediated decay of mutant mRNAs and trigger transcriptional compensation (432). Accordingly, *mib1* transcripts are reduced in *mib1^{tfi91}* (Fig. 2K) and *mib1^{nce2a}* mutants but not in *mib1^{ta52b}*. Genetic compensation could occur through a mechanism that promotes Ryk internalization independently of Mib1. *mib1^{tfi91}* mutants present however a reduction in Ryk endosomes that is similar to the one of *mib1* morphants (Fig. 2M-O). Our findings reveal thereby a resilience of the PCP pathway that allows to partially correct defects that arise from a failure in Ryk endocytosis.

Mib1 is best known for its crucial role in Notch signaling (75), but a number of studies have started to identify Notch-independent function of this E3 ubiquitin ligase (156, 198). Our work identifies Mib1 as a novel regulator of the PCP pathway that directs CE by controlling Ryk endocytosis. As processes such as the morphogenesis of the vertebrate nervous system involve both Notch and PCP signaling, it appears therefore important to take great care when interpreting Mib1 loss of function phenotypes.

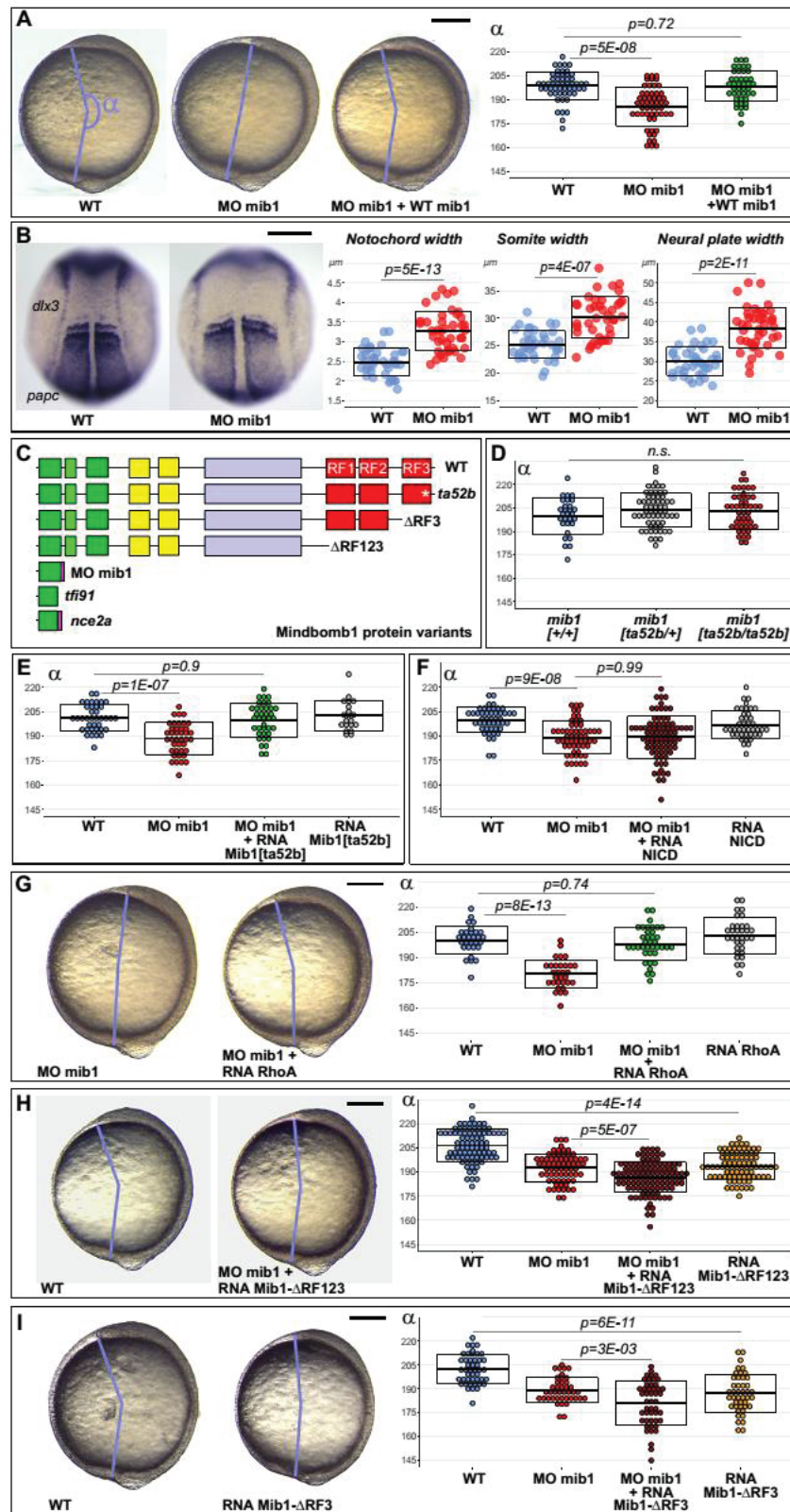


Figure 1: Mib1 regulates PCP-dependent convergent extension movements. (Legend continued in the next page)

(A) CE was quantified at bud stage by measuring the axis extension angle α . CE is reduced in *mib1* morphants but rescued by WT *mib1* RNA (Kruskal-Wallis test, $\chi^2=39$). (B) *mib1* morphants present a widening of notochord, somites and neural plate. Dorsal views, anterior up, 2 somites stage. *dlx3 in situ* hybridization outlines the neural plate, papc the somites and the adaxial cells lining the notochord. (C) Mib1 variants used in the study. (D) CE is intact in *mib1^{ta52b}* mutants (One way Anova, F=1.1). (E) *mib1^{ta52b}* RNA restores *mib1* morphant CE (One way Anova, F=17). (F) Activated Notch (NICD) fails to rescue *mib1* morphant CE defects (Welch Anova, F=18). (G) RhoA rescues *mib1* morphant CE (One way Anova, F=37). (H,I) Mib1 variants lacking all (Mib1 Δ RF123, H) or the last (Mib1 Δ RF3, I) RING finger impair CE in *mib1* morphant or WT embryos (Welch Anova, F=66 (H), F=33 (I)). (A,G,H,I) lateral views, anterior up, dorsal to the right. Boxes in (A,B, D-I) represent mean values \pm SD. Scalebars: 20 μ m.

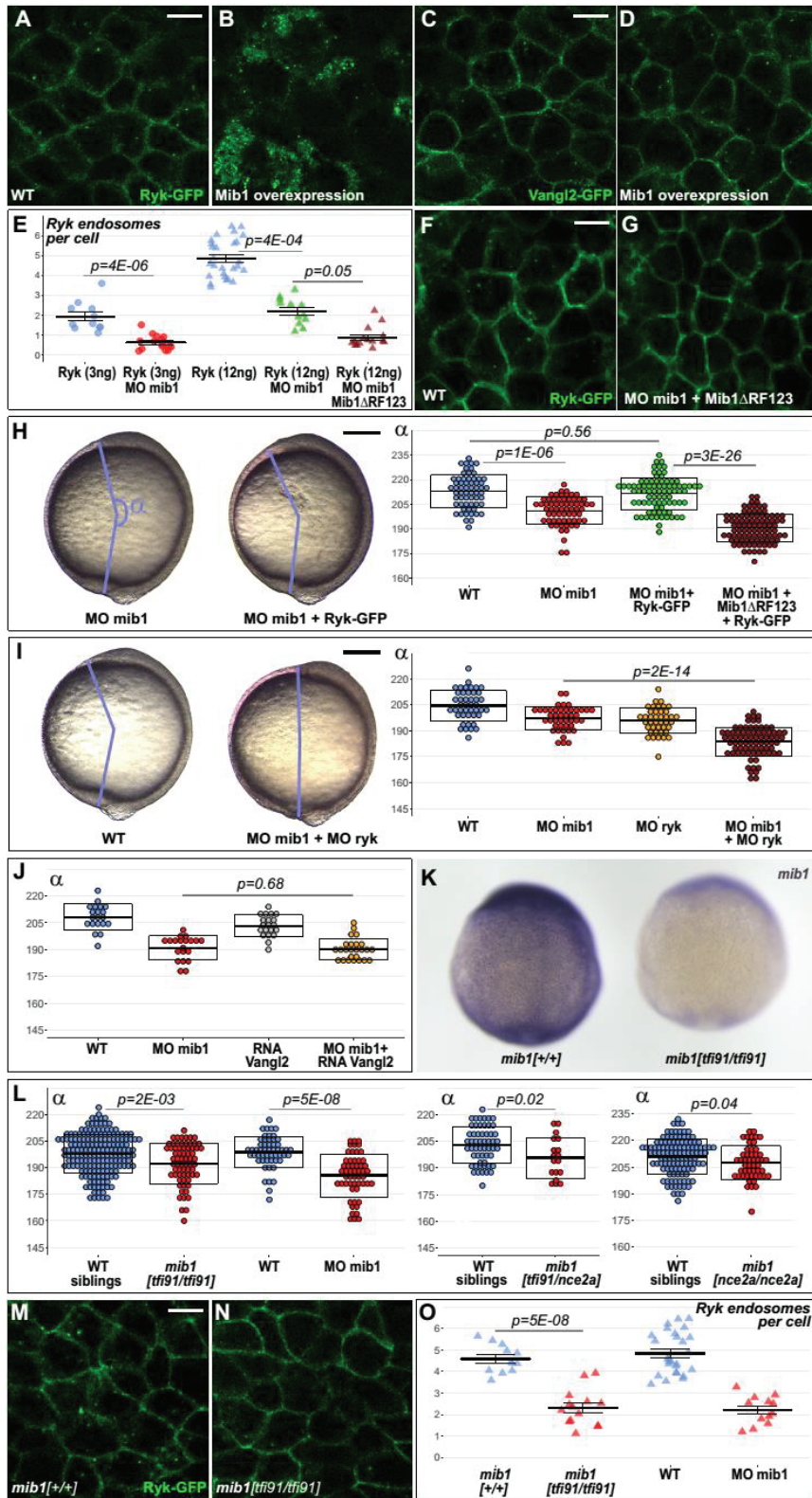


Figure 2: Mib1 controls PCP by regulating Ryk endocytosis. (Legend continued in the next page)

(A-D) *mib1* overexpression triggers Ryk internalization in 20/21 embryos (B) but has no effect on Vangl2 (D, n=23). (E-G) The number of Ryk-GFP endosomes (3 ng/ μ l Ryk-GFP RNA) is reduced in *mib1* morphants. A higher Ryk-GFP RNA dose (12ng/ μ l) restores endosome number in *mib1* morphants but not in embryos coinjected with *Mib1* Δ RF123 (Kruskal-Wallis test, $\chi^2=43$). (H) 12ng/ μ l Ryk-GFP RNA rescues CE in *mib1* morphants but not in embryos coinjected with *Mib1* Δ RF123 (Kruskal-Wallis test, $\chi^2=160$). (I) Ryk morpholino injection aggravates *mib1* morphant CE defects (Welch Anova, F=64). (J) Vangl2 RNA does not rescue *mib1* morphant CE (Kruskal-Wallis test, $\chi^2=52$). (K) *In situ* hybridization reveals reduced *mib1* transcript levels in *mib1*^{tr91} mutants (n=27). (L) CE defects in *mib1* null mutants. *Mib1* morphant data from Fig. 1A are included for comparison. (M-O) Ryk endosomes (12ng/ μ l Ryk-GFP RNA) are reduced in *mib1* null mutants. (O) includes *Mib1* morphant data from Fig. 2E for comparison. In (E,O) each point represents the mean number of endosomes for 20 cells from a single embryo; bars represent mean values \pm SEM. Boxes in (H-J,L) represent mean values \pm SD. (A-D,F,G,M,N) 90% epiboly stage, dorsal views, anterior up. (H,I,K) Lateral (H,I) and dorsal (K) views at bud stage, anterior up. Scalebars: (A-D,F,G,M,N) 10 μ m, (H,I) 20 μ m.

Materials and Methods

Use of research animals

Experiments were performed in the iBV Zebrafish facility (authorization #B-06-088-17) in accordance with the guidelines of the ethics committee Ciepal Azur and the iBV animal welfare committee.

Generation of a *mib1* null mutant

Crispr/Cas mutagenesis was used to generate *mib1^{nce2a}* which introduces a frame shift after amino acid 57 yielding a 69 amino acid protein.

RNA and morpholino injections

RNAs encoding Mib1 variants (*l60*) were injected at 250 ng/μl (Fig. 2A-D) or 125 ng/μl (all other experiments). Morpholinos were injected at 500 μM (*mib1* 5'-GCAGCCTCACCTGTAGGCGCACTGT-3',(75)) or 250 μM (*ryk* 5'-GGCAGAAACATCACAGCCCACCGTC-3'.)

Image analysis and statistics

Image quantification was performed using ImageJ. Statistical analysis was performed using R. Normality and variance were analyzed using Shapiro-Wilk and Levene's tests and the procedures for further analysis chosen accordingly. Welch's t-test was used for two condition experiments. Post hoc analysis for multiple comparisons was performed using Tukey's (after one way Anova), Games Howell (for Welch's Anova) or Dunn's test (after Kruskal-Wallis test).

ACKNOWLEDGEMENTS

This study was supported by a CNRS/INSERM ATIP/Avenir 2010 grant and an HFSP Career Development Award (00036/2010) to MF and the project grants ARC PJA20181208167 and ANR DroZeMyo (ANR-17-CE13-0024-02). VMS is supported by the LABEX SIGNALIFE PhD program (ANR-11-LABX-0028-01). PS benefited from an FRM 4th year PhD fellowship (FDT20140930987). Confocal microscopy was performed at the iBV PRISM imaging platform. We thank L.Bally-Cuif, CP.Heisenberg, M.Itoh, YJ.Jiang, D.Slusarski and C.Vesque for sharing fish lines and reagents. We are grateful to S.Polès and R.Rebillard for excellent technical assistance.

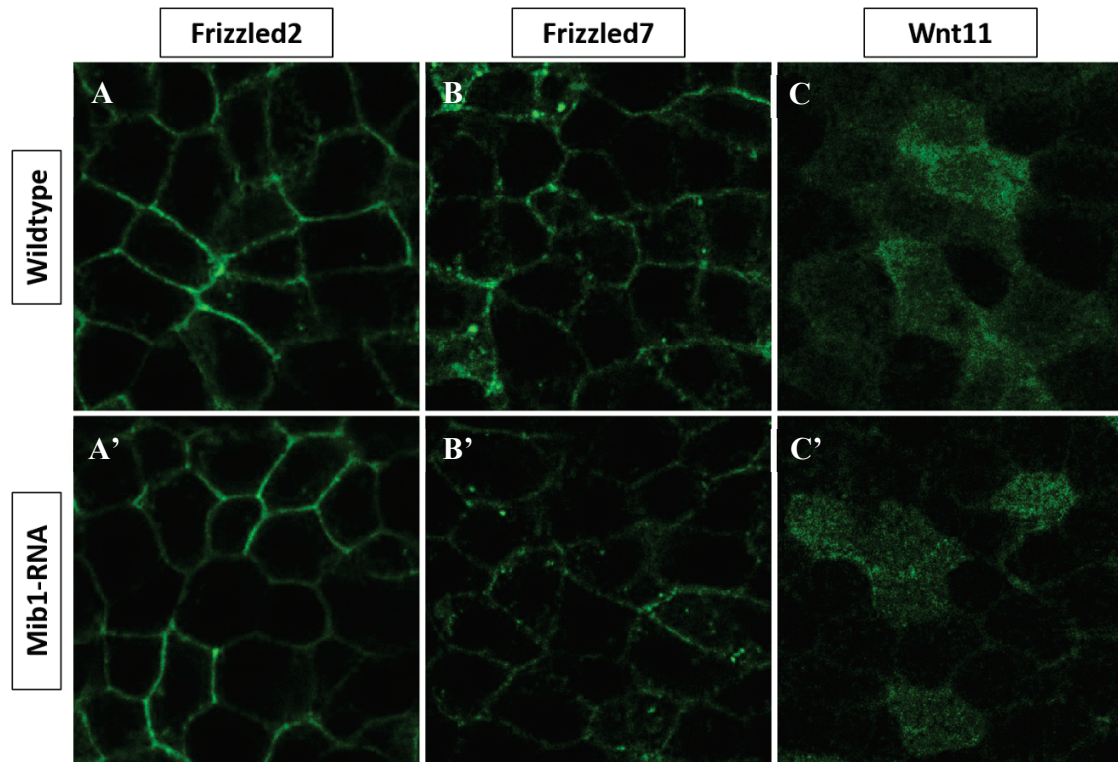
AUTHOR CONTRIBUTIONS

VMS, PS and MF performed experiments and analyzed the data. MF designed the study and wrote the manuscript.

The authors declare no competing interests.

II.3 Supplementary Information

III.3.a Overexpression of Mib1 doesn't change localization of PCP components other than Ryk.



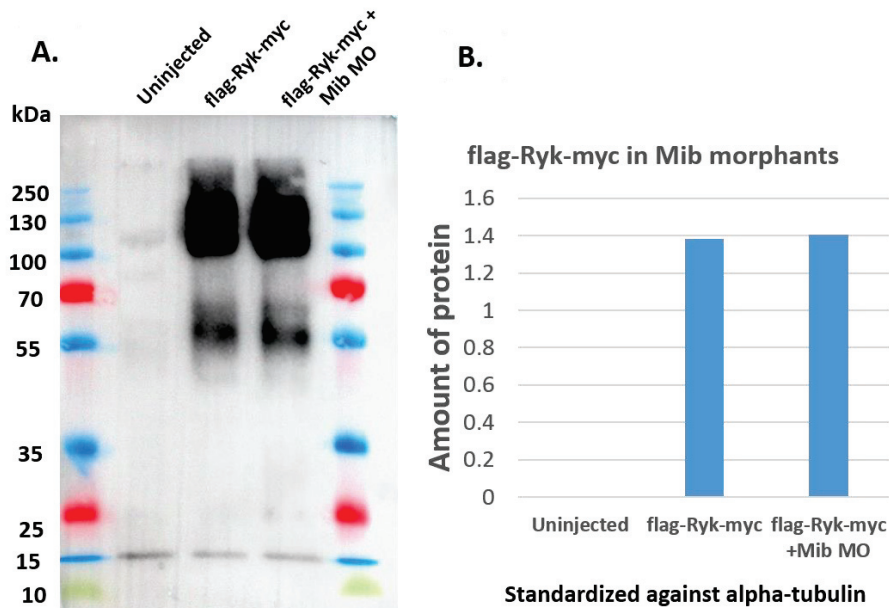
Supplementary Figure 1. Localization of Fz2, Fz7 and Wnt11 under Mib1 overexpression.

Localization of Frizzled2, Frizzled7 and Wnt11 is not changing under Mib1 overexpression condition compared to the wildtype. A, A') 50ng of Fz2 mRNA was injected into wildtype embryos. Fz2 was localized at both the plasma membrane and endocytic vesicles. Localization of Fz2 was not changed when 250ng of Mib1 mRNA was injected together. B, B') 75ng of Fz7 was injected into wildtype embryos. Fz7 localized at the plasma membrane as well as endocytic vesicles. However, the localization of Fz7 was unchanged in the presence of 250ng of Mib1 mRNA. C, C') 100ng of Wnt11 was injected into wildtype embryos. Wnt11 displayed diffused cytoplasmic signal, which was unchanged even in the presence of 250 ng of Mib1 RNA.

We have shown that the PCP component Ryk is dragged in from the membrane when Mib1 is overexpressed. This raised the question whether Mib1 can drag in any other PCP component either along with Ryk or independently of Ryk. Therefore, I studied the localization of PCP components

Fz2, Fz7 and Wnt11 under Mib1 overexpression. However, there was no obvious change in the localization of these PCP components under Mib1 overexpression (Fig. S1). Similar analysis for Ror2, Dvl and Knypek is yet to be done.

III.3.b The total amount of Ryk protein is not changed in Mib1 morphants.



Supplementary Figure 2. Ryk protein level is not affected in Mib1 morphants. (Preliminary result) A) 125 ng flag-Ryk-myc was injected into wildtype embryos and Mib1 morphants (500uM). Then total protein was extracted (under non-reducing condition) and probed against mouse anti-myc (1:1000) after western blotting. The band for Ryk intra-cellular domain was obtained at 55 kDa. Other bands obtained at higher molecular weights are probably dimerized proteins. 5% skimmed milk is used as blocking solution. Anti-mouse-HRP (1:10000) was used as secondary antibody. 30ug of protein was loaded into each lane of a 12% gel. B) The amount of Ryk protein remains unchanged in Mib1 morphants compared to the wildtype.

We have shown that the number of Ryk containing endocytic vesicles are reduced in both Mib1 morphants and *mibl* mutants. This raised the question whether the overall level of Ryk protein is reduced in Mib1 morphant or mutant embryos. To address this question, I have injected flag-Ryk-myc into both wildtype embryos and Mib1 morphants. Western blotting was performed using

protein extracts from these two conditions and probed against the flag-tag to show the amount of Ryk proteins present. Quantification of the bands representing intra-cellular domain of Ryk (~55 kDa) showed that the amount of protein is not different in *Mib1* morphants compared to wildtype embryos.

II.3.c Supplementary materials and methods

Quantification of gastrulation stage convergent extension movements

Bud stage embryos were imaged laterally on a Leica M205FA stereomicroscope and the angle between the anterior extremity of the hatching gland and the posterior extremity of the tail bud was quantified using the ImageJ angle tool. The reference point for the angle measurement was defined by manually fitting an oval ROI to the embryo and using the ImageJ Measure function to determine the coordinates of the centroid.

RNA *in situ* hybridizations

Whole mount RNA *in situ* hybridizations were performed according to standard protocols(219). The following probes for *dlx3* and *papc* are used in this study(385). DIG-labeled antisense RNA probes were transcribed from PCR products carrying the T7-promoter sequence (5'-TAATACGACTCACTATAGGG-3') on the reverse primer. To generate *mib1* probe, we used the following primers: forward: 5'- CCGAGTGCCATGCGTGTGCTGC - 3', reverse 5'-GCGTAATACGACTCACTATAGGGAGATCCTCGCCCTTGCTCACCAT - 3', to amplify *mib1* sequence from the plasmid *mib1*-GFP-pCS2+(67).

Imaging and Quantification of endocytic vesicles

RNAs of Ryk-eGFP along with Histone-RFP was injected into embryos at one cell stage. Then, embryos were fixed at 90% epiboly stage at room temperature in PEM (80 mM Sodium-Pipes, 5 mM EGTA, 1 mM MgCl₂) -4% PFA -0.2% Triton X-100 for 1 hour. After washing 2 × 5 min in PEMT (PEM -0.2% TritonX100), 10 min in PEM -50 mM NH₄Cl, 2 × 5 min in PEMT and blocking in PEMT -2% BSA, embryos were incubated 1 h at room temperature with Phalloidin. Following incubation, embryos were washed during 5, 10, 15, and 20 min in PEMT. Embryos were mounted in PEM -0.75% LMP-Agarose and analyzed on a Spinning disk confocal microscope.

The embryos that have got equal amount of RNAs are selected for the quantification of endocytic vesicles, based on the intensity of Histone-RFP signal. Endocytic vesicles (visually distinct punctae labelled by Ryk-eGFP) are counted manually for around 20 cells per embryo. All the z-stacks representing a single cell were analyzed for counting endocytic vesicles. The starting and ending stack for each cell is judged based on the nucleus and cell membrane of that particular cell.

Molecular genotyping

The wildtype and mutant alleles of Mib1 were identified through allele-specific PCRs. For *mib1^{ft91}*, forward: 5'- TAACGGCACCCGCCCAATTAC – 3' and reverse: 5'- GCGACCCCAGATTAATAAAGGG – 3' primers were used to detect wildtype allele; forward: 5'- ATGACCACCGGCAGGAATAACC – 3' and reverse: 5'- ACATCATAAGCCCCGGAGCAGCGC – 3' primers were used to detect mutant allele.

For *mib1^{ncc2a}*, genotyping was done either through sequencing the mutation carrying DNA sequence by using the flanking primers: forward: 5' – TGACTGGAAGTGGGGGAAGC – 3' and reverse: 5'- TGTAGGCGCACTGTCCAATATC – 3', or by phenotypically identifying the embryos after growing them to 24hpf.

Western Blotting

The following protocol was used for western blotting (433). The following antibodies were used: c-Myc (Santa Cruz -sc-42), alpha-Tubulin (Sigma- T6199), mouse-IgG-HRP (Amersham-NA9310).

II.4 Author contributions

I have done all the experiments in this project except Fig. 1B. Previous PhD student Priyanka had done some preliminary experiments which helped me to develop this project. However, none of those data is included in this manuscript.

Conclusion

The aim of this project was to understand the role of Mib1 in the PCP pathway. PCP controls convergent extension (CE) movements during zebrafish gastrulation to elongate the embryonic axis. The efficiency of CE movements during gastrulation can be quantified by measuring the angle of extension (CE angle) between the head and bud of a bud stage embryo. Our study shows that depletion of Mib1 causes defects in CE movements during gastrulation and therefore, results in a shorter CE angle. CE defects of Mib1 morphants can be rescued by mRNAs of both wild type Mib1 (that is not targeted by the Mib1 morpholino) and Mib1^{ta52b}. These experiments indicate two important points: 1) The CE defects of Mib1 morpholino is not an artifact; 2) The ta52b mutation of Mib1 is dispensable for the PCP pathway. We also showed that Mib1 mediated PCP signaling regulates the morphogenesis of notochord, somites and neural plate. Interestingly, the role of Mib1 in CE movements is independent of its conventional role in the Notch signaling pathway. Moreover, the CE defects of Mib1 depleted embryos can be rescued by the PCP effector protein RhoA indicating that Mib1 is indeed acting via the PCP pathway. Our data also demonstrate that Mib1 is acting as an E3-ubiquitin ligase to regulate CE movements, and that the third ring finger domain is important for its function.

Interestingly, we found that Mib1 is important for the endocytic regulation of the PCP component Ryk. Overexpression of Mib1 drags in all the Ryk from the membrane whereas, the depletion of Mib1 impairs Ryk internalization. Like Mib morphants, Mib1 null mutants also impair internalization of Ryk as well as CE movements during gastrulation. Our data demonstrate that Mib1 regulated Ryk internalization is important for its role in PCP, since CE defects of Mib1 morphants during gastrulation are rescued by overexpression of Ryk-eGFP.

In conclusion, our study discovered that independent of its function in Notch signaling, Mib1 is important for regulating the PCP pathway during zebrafish embryogenesis.

Chapter - III

Discussion and Perspectives

Discussion & Perspectives – 1

III.1 Analyzing the role of Notch signaling in zebrafish neural tube morphogenesis.

The aim of the first part of my PhD was to understand the relationship between the Notch signaling pathway and the morphogenesis of the zebrafish neural tube. In tetrapods, neural tube morphogenesis starts with a neural plate structure that has a layer of pseudo-stratified epithelial cells with a clear apical and basal polarity(17, 60). These polarized epithelial cells provide structural architecture for the developing neural tube(65). Notch signaling has been shown to play an important role in maintenance of polarized epithelial cells and thereby, morphogenesis of the tetrapod neural tube(65). Interestingly, the epithelial architecture of the neural primordium itself is required for Notch signaling(68), indicating a dual relationship between polarized epithelial organization and Notch signaling. In contrast, the early zebrafish neural plate does not show any hallmarks of apico-basal polarity and polarization of the neural progenitor cells occur during Notch regulated neurogenesis(14). Additionally, early zebrafish neurulation shows unique midline crossing c-divisions that provide morphogenetic advantage for the developing neural tube(36, 45, 46). Both c-divisions and epithelialization of neural progenitor cells act in tandem to regulate morphogenesis of the zebrafish neural tube. Our work shows that despite of the differences between neurulation of tetrapods and teleost fish, Notch signaling is required for zebrafish spinal cord morphogenesis.

III.1.a Notch signaling and apico-basal polarity.

- Promoting apico-basal polarity

Our data show that canonical Notch signaling is important for the establishment of a polarized neural tube during early zebrafish neurulation. Perturbing canonical Notch pathway components, such as Mib1, Delta ligands, γ -secretase and the transcription factor component Suppressor of Hairless Su(H)/RBPJ, resulted in a spinal cord with disorganized cells that lack apico-basal polarity components. Moreover, an activated form of the Notch intra-cellular domain (NICD) and a constitutively active form of Su(H) rescued apico-basal polarity in the *mib1^{ta52b}* mutant spinal cord. Interestingly, a previous study has shown that non-canonical Notch signaling regulates the late maintenance of apico-basal polarity in the zebrafish neural tube(176). They have also shown that the apical polarity component Crumbs negatively regulates Notch signaling. These data along

with our results indicate a possible feedback mechanism between Notch signaling and polarity complexes for maintenance of polarity at later stages.

However, our data did not allow to determine whether Notch plays an instructive role in establishing apico-basal polarity. Inactivation of Notch signaling caused precocious neurogenesis in the spinal cord. This was evident from the upregulation of the early neuronal marker *elavl3* in *mib1^{ta52b}* mutant embryos. Therefore, *mib1* mutant embryos failed to upregulate polarized neural precursor cells that express the marker *gfap* and other components of the apico-basal polarity machinery (*crb1*, *crb2a* and *pard6γB*). Demonstrating an active role of Notch signaling in promoting apico-basal polarity would require suppressing neurogenesis without manipulating Notch signaling in neural progenitor cells. Unfortunately, current tools did not allow us to achieve this, therefore it has not been possible to address this question.

- Region specific regulation of apico-basal polarity.

Even though loss of Notch signaling affected the establishment of apico-basal polarity in the medio-lateral spinal cord, apico-basal polarity was unaffected in the floor plate and midbrain-hindbrain boundary (MHB) region. This could arise because of two possibilities: 1) We mainly used *mib1^{ta52b}* mutant to inhibit Notch signaling. *mib2*, a paralogue of *mib1*, could redundantly function in establishing apico-basal polarity in these tissues; 2) The importance of Notch signaling varies depending on the tissue context. *Mib2* has been shown to be dispensable for embryonic development and Notch signaling in zebrafish(77). Moreover, we analyzed apico-basal polarity defects in double mutant embryos of *mib1* and *mib2*. In accordance with the literature, double mutants didn't show any difference in phenotypes compared to the *mib1^{ta52b}* single mutants. Therefore, the second possibility might be the reason for region specific regulation of apico-basal polarity by Notch signaling. The floor plate is the signaling center in the ventral neural tube of vertebrates that is required for neural patterning and axonal guidance(434, 435). Previous studies suggested that Notch signaling is required for the maintenance of floor plate cells but not for their initial development(206, 436). Also, in contrast to more dorsal spinal cord cells, floor plate cells essentially give rise to glial derivatives(214). Therefore, in *mib1^{ta52b}* mutant embryos, floor plate cells do not undergo neuronal differentiation and retain their apico-basal polarity and expression of the radial glial marker *gfap*. Similarly, there is a difference in the regulation of neurogenesis at the MHB compared to the dorsal spinal cord. *Her/Hes* genes, members of the Hairy-E(Spl) family,

are responsible for the inhibition of neurogenesis(437). Ectopic expression of Her/Hes genes downregulates the proneural factor *neurog1* whereas loss-of-function experiments show an increase in *neurog1* expression(438). These hairy genes can be divided into two groups based on their dependency on active Notch signaling. In the MHB region, neurogenic differentiation is inhibited by *her5* that acts independently of Notch signaling whereas in the spinal cord, neurogenesis is regulated by the Notch-responsive *her4* gene(215, 216).

III.1.b Notch signaling and c-divisions.

Zebrafish spinal cord development shows a unique morphogenetic process called midline crossing c-divisions. Neural progenitor cells from one half of the developing neural tube come to the midline and undergo mirror symmetric cell divisions to deposit one of the daughter cells in the contralateral side of the developing neural tube(38, 44, 46). Our data show that Notch signaling is important for c-divisions, because neural progenitor cells in the spinal cord of *mib1^{ta52b}* mutant embryos failed to cross the midline, and an activated form of the NICD could rescue the phenotype. Moreover, cells that failed to cross the midline were showing neuronal marker expression. These experiments indicate that Notch mediated suppression of neurogenesis is essential for neural progenitor cells to execute their midline crossing c-divisions.

The midline crossing behavior of neural progenitor cells is associated with PCP pathway activity. This raised the possibility that Notch signaling might be cross-talking with the PCP pathway. However, *mib1^{ta52b}* mutant embryos didn't show any convergent extension phenotypes but failed to perform c-divisions. This indicates that c-division defects caused by Notch activity inhibition are mainly due to precocious neurogenesis.

III.1.c Notch signaling and neural tube morphogenesis.

Establishment of apico-basal polarity in neural progenitor cells (epithelialization) and c-divisions are important events during morphogenesis of the zebrafish neural tube(27). We have shown that the inhibition of Notch signaling failed to establish polarized radial glial cells that are necessary for providing structural architecture for the developing neural tube. Moreover, lack of polarized neural progenitor cells affected the formation of an apical midline of the neural tube that develops into the future neural tube lumen.

The first appearance of polarity markers at the neural tube midline occurs during c-divisions(46). Studies have shown that mutations affecting apico-basal polarity and c-divisions display similar neural tube midline defects, which indicate that these two processes are inter-connected(27). We demonstrate that Notch mediated suppression of neurogenesis is necessary for both epithelialization and c-divisions during zebrafish neural tube morphogenesis, and inhibition of Notch signaling gave rise to a spinal cord that has defective shape. Therefore, our findings suggest that through its ability to restrain neuronal differentiation, the Notch pathway provides a temporal window for neural progenitor cells to perform specific morphogenetic movements that determine the shape of the spinal cord.

Discussion & Perspectives – 2

III.2 Analyzing the role of Mindbomb1 in the planar cell polarity pathway.

The aim of the second part of my PhD was to investigate the role of Mib1 in PCP. Mib1 is well studied for its role in the Notch signaling pathway, nonetheless, Mib1 plays several functions independent of Notch signaling. My study found that Mib1, independent of its function in the Delta/Notch pathway, regulates PCP signaling via Ryk endocytosis during zebrafish gastrulation.

III.2.a Mib1 regulates axis extension during gastrulation.

During vertebrate gastrulation, PCP controls convergent and extension (CE) movements that elongate embryonic tissue along the anterior-posterior (A-P) axis and narrow them medio-laterally (M-L). Mutants of PCP components display phenotypes including a short body axis and broadened tissues (such as somites and neural plate). I have shown that both Mib1 morphant and *mib1* null mutant embryos show defects in CE movements. And CE defects of Mib1 morphant embryos could be rescued by the PCP effector protein RhoA, indicating that Mib1 is acting via the PCP pathway to regulate CE. This is the first time in literature that Mib1 has been shown to regulate PCP regulated CE movements. Therefore, it will be interesting to understand the mechanisms by which Mib1 regulate CE.

Studies have indicated that axis extension during vertebrate gastrulation requires directional cell migration and oriented cell division(246, 267). Evidences from the literature suggest that Mib1 is associated with both directional cell migration and oriented cell division. For example, *in vitro* studies have shown that Mib1 is required for persistent directional cell migration by controlling Rac1 activation, a member of small GTPases family of proteins that regulate cell protrusions , important for directed cell migration(198). In addition, *mib1* mutant zebrafish embryos show defects in the migration of posterior lateral line primordium (pLLP) cells due to the lack of directional cell movement(198). Mib1 has also been shown to regulate cell division orientation in *C. elegans*. Mutants of *lin-18/ryk* disrupt oriented divisions of p7.p vulval precursor cells(408) and ceMib has been shown to genetically interact with *lin-18/Ryk* to regulate oriented cell divisions (159). These evidences suggest that Mib1 might be regulating both oriented divisions and directed cell migration during vertebrate gastrulation. Therefore, it will be interesting to look at these two

processes during zebrafish gastrulation to understand the mechanisms by which Mib1 regulates CE movements.

Cell division orientation during gastrulation can be studied by injecting fluorescent markers that label components of DNA (eg. Histone)(439). Therefore, it is interesting to understand cell division orientation in both *mib1* mutants and Mib1 morphants during gastrulation. To assess directed cell migration during M-L intercalation, we can study the shape of cells during gastrulation in both Mib1 morphant and *mib1* mutant embryos by labelling them with a membrane marker. During zebrafish gastrulation, cells that undergo CE show a transition from round to mediolaterally elongated morphology, indicative of directional migration towards the midline(440). Vangl2 mutant cells that fail undergo elongation show defective M-L intercalation (440). It will be interesting to understand if the cell shape changes in both *mib1* mutants and morphants during zebrafish gastrulation.

III.2.b Mib1 controls axis extension independently of Notch signaling.

Mib1 is well studied for its role in the activation of Notch signaling by ubiquitination mediated endocytosis of Notch ligands. However, several studies have shown that Mib1 also does functions independent of Notch signaling(158, 198, 415, 417, 421, 441). I have shown that the role of Mib1 in the PCP pathway is independent of Notch signaling. *mib1^{ta52b}* mutant embryos that completely lacks Notch activity(430) didn't show any axis extension defects during gastrulation, indicating that Notch signaling is dispensable for PCP regulated axis extension. In addition, I showed that CE defects of Mib1 morphant embryos were rescued by Mib1 mRNA carrying the ta52b mutation whereas the activated form of Notch intracellular domain (NICD) failed to rescue CE defects.

However, Notch mediated suppression of neurogenesis was required for midline crossing c-divisions during zebrafish neurulation (Chapter I), which have been shown to be regulated by PCP components(34, 44, 45). Therefore, during neurulation, Notch signaling might be facilitating PCP regulated c-divisions. If we independently suppress neurogenesis during neurulation, it would be interesting to see if Notch signaling acts upstream of the PCP pathway to regulate c-divisions. This could be done by rescuing neurogenic phenotypes of both *mib1^{tfi91}* mutants and morphants by NICD injection and then, observing the effects on c-divisions.

III.2.c Mib1 acts as an E3-ubiquitin ligase in axis extension.

Mib1 is an E3-ubiquitin ligase that has an N-terminus domain which binds to target substrates and a C-terminus domain that contains three RING finger (RF) domains necessary for binding to E2-ubiquitin enzymes. Thus, Mib1 acts as a platform where an E2-ubiquitin enzyme can transfer activated ubiquitin molecules to the target substrate(155). My data demonstrate that the E3-ubiquitin ligase activity of Mib1 is necessary for its function in the PCP pathway. Mib1 mRNA that lacks all three RF domains (Mib1 Δ RF) failed to rescue CE defects of Mib1 morphants. Moreover, injection of Mib1 Δ RF mRNA itself caused CE defects, indicating a dominant negative activity. In addition, my data show that the third RF domain is important for the function of Mib1 in PCP since a Mib1 mRNA construct that lacks just the third RF domain (Mib1 Δ RF3) phenocopied Mib1 Δ RF.

Mib1 has always been reported to function as an E3-ubiquitin ligase in the existing literature. Interestingly, the RF3 domain of Mib1 is important for both Notch signaling and Notch independent functions(156). Whether all the three RF domains of Mib1 are necessary for E3-ubiquitin ligase activity is not clear. In the case of Mib1, RF domains bind to the E2 ubiquitin enzyme loaded with ubiquitin moieties, and then ubiquitin molecules are transferred from the E2-enzyme directly to the target substrate bound at the N-terminus of Mib1(156). One possible function of three RF domains is to finetune the binding specificity of different E2 ubiquitin enzymes that are required for different substrates. Unfortunately, E2 ubiquitin enzymes are poorly studied and we don't yet have identified any substrate specific E2 ubiquitin enzyme that binds to RF domains in a function specific manner(152). However, it is possible to address the question whether the RF3 domain of Mib1 is necessary and sufficient for its function in the PCP pathway. We have to create an mRNA construct of Mib1 RNA that lacks/inactivates both the RF1 and RF2 domains but retains the RF3 domain. Then, a rescue experiment of CE defects of Mib1 morphants will tell whether the RF3 domain of Mib1 is necessary and sufficient for PCP pathway activity.

Interestingly, Mib1 Δ RF3 mRNA didn't rescue CE defects of Mib1 morphant embryos, indicating that only ta52b mutation is dispensable for the role of Mib1 in PCP, but the RF3 domain is still necessary for PCP signaling. This observation agrees with the existing functions of Mib1, where RF3 domain is important. RF3 domain of Mib1 is essential for functions of Mib1 such as neurogenesis, apoptosis and ubiquitination of Ryk (75, 158, 442). This raises the question, why

ta52b mutation doesn't affect the role of Mib1 in the PCP pathway? One possible hypothesis is that the ta52b mutation only affects binding/stability of a substrate-specific E2 ubiquitin enzyme necessary for Delta ubiquitination and consequent Notch signaling. And the substrate-specific E2 ubiquitin enzyme required for PCP signaling binds to the C-terminus of Mib1 irrespective of the ta52b mutation. The substrate specificity of E2 ubiquitin enzymes are poorly studied. There are around 40 different E2 ubiquitin enzymes identified in the human genome(443). A yeast two-hybrid screen has identified seven different E2-enzymes interacting with Mib1(153). Out of these seven, it will be interesting to see if there are any E2 enzymes dedicated only for Notch signaling or PCP signaling. Analyzing CE defects after knocking down each of these seven E2 enzymes in *mib1^{ta52b}* mutant background will identify the PCP pathway specific E2 enzyme of Mib1.

III.2.d Differences between Mib1 morphants and Mib1 mutants in axis extension.

- *mib1^{ta52b}* mutant vs. other null mutant and morphant embryos

Results from the first part of my PhD, which showed *mib1^{ta52b}* mutant embryos have defective c-divisions, gave us a hint that Mib1 is important for the PCP pathway either via Notch signaling or through a Notch independent function. Therefore, we decided to analyze CE defects of *mib1^{ta52b}* mutant embryos(430). Surprisingly, *mib1^{ta52b}* homozygous mutant embryos didn't show any CE defects compared to wildtype siblings, indicating that the ta52b mutation in the RF3 domain is dispensable for the PCP pathway. However, Mib1 morphant embryos showed a significant decrease in axis extension angle. Several studies have shown such kind of inconsistencies between morphant and mutant phenotype(444). This raised the question, what is the difference between Mib1 morphant and *mib1^{ta52b}* mutant?

We used a splice-blocking antisense morpholino targeting the intron1-exon1(e/i-1) boundary of the Mib1 pre-mRNA sequence. When a morpholino is blocking the first or last intron/exon boundary of a pre-mRNA, it will result in a final mRNA with the first intron or last intron inserted, respectively(445). I showed that Mib1 e/i-1 morpholino will give rise to a truncated protein of 91AA. On the other hand, *mib1^{ta52b}* mutation is only a point mutation (Met to Arg) at the 1013th amino acid present in the RF3 domain, which otherwise gives a stable full-length protein. Thus, the difference in phenotype between *mib1^{ta52b}* mutant and Mib1 e/i-1 morphant could be due to the difference in the translated Mib1 protein, implicating that the Mib1^{ta52b} mutant protein itself is functional in the case of Mib1 mediated PCP signaling. This was evident from an experiment

which showed that *mib1^{ta52b}* mutant mRNA is capable of rescuing CE defects of Mib1 e/i-1 morpholino. Additionally, the null mutants of *mib1* (*mib1^{tfi91}* and *mib1^{nce2a}*) that generate truncated mutant proteins that are comparable to the protein of Mib1 e/i-1 morpholino (61 and 68 amino acids respectively) also showed defects in CE.

- Genetic compensation between *mib1* null mutant and morphant embryos

I have observed that CE defects in Mib1 morphants are stronger than *mib1* null mutants. This raised the question what could partially compensate for the phenotypes of *mib1* null mutants? It has been shown that Mib1 mRNA is deposited maternally(75). However, maternal Mib1 mRNA deposition cannot explain weaker phenotypes of *mib1* null mutants since the Mib1 e/i-1 morpholino can target only the zygotic Mib1 pre-mRNA sequences. Therefore, phenotypes observed in Mib1 e/i-1 morpholino are solely due the depletion of zygotic Mib1 mRNA. Another possible reason, for weaker phenotypes in *mib1* null mutants, could be due to the skipping of the mutation containing exon via a cryptic splice sites during pre-mRNA maturation(446). However, I didn't find any exon skipping during cDNA sequencing of both *mib1* null mutant embryos (*mib1^{tfi91}* and *mib1^{nce2a}*).

Next, I have checked for evidences of genetic compensation triggered by mutant mRNA degradation through non-sense mediated decay (NMD). NMD occurs to mRNAs that carry pre-termination codons due to a non-sense mutation, which will flag the mRNA to undergo degradation. This non-sense mediated degradation will trigger upregulation of one or several 'similar genes' to compensate the function of the degraded mRNA(447-449) and thus, genetic mutants show weaker or no phenotypes compared to other methods of gene knockdown. *In situ* hybridization for Mib1 RNA in *mib1^{ta52b}*, *mib1^{tfi91}* and *mib1^{nce2a}* embryos revealed that Mib1 mRNA is degraded in both *mib1^{tfi91}* and *mib1^{nce2a}* but not in *mib1^{ta52b}*, indicating the activation of NMD pathway in both *mib1* null mutants. Attempts to block NMD by targeting NMD pathway components didn't succeed since the knockdown of NMD pathway components itself gave CE defects. It would be interesting to see at which level and what component(s) is/are partially compensating PCP defects of *mib1* null mutants. A comparison between RNA sequencing data of *mib1^{tfi91}* or *mib1^{nce2a}* with *mib1^{ta52b}* mutant embryos might allow to identify the genes upregulated in *mib1* null mutants that partially compensate for functions of the PCP pathway.

III.2.e Mib1 mediated Ryk endocytosis is necessary for axis extension.

Mib1 mediated endocytosis of full-length Ryk is important for Wnt/ β -Catenin signaling(159). Similarly, I have shown that Mib1 regulates Ryk endocytosis to mediate PCP regulated CE movements during zebrafish gastrulation. Overexpression of Mib1 drags in Ryk from the cell membrane whereas depletion of Mib1 reduces the amount of Ryk in endocytic vesicles. Both Mib1 morphant and mutant embryos show a similar reduction in the number of Ryk carrying endocytic vesicles, indicating that partial genetic compensation of *mib1* null mutants via NMD is not occurring at the level of Ryk endocytosis. My data further demonstrate that Mib1 mediated endocytosis of Ryk is necessary for axis extension because overexpression of Ryk-eGFP rescues CE defects in Mib morphants by increasing the number of Ryk containing endocytic vesicles. This raises the question, what is responsible for endocytosis of Ryk in Mib1 morphant embryos? Is this residual Mib1 proteins or another redundant factor? Overexpression of the same amount of Ryk-eGFP didn't rescue CE defects of embryos injected with both Mib1 morpholino and Mib- Δ RF RNA. This indicates that residual Mib1 proteins are responsible for Ryk endocytosis in Mib1 morphants. Interestingly, rescue of CE defects in Mib1 morphants using a concentration gradient of Ryk-eGFP revealed that a threshold number of Ryk carrying endocytic vesicles are necessary for regulating the PCP pathway. Embryos injected with a sub-optimal concentration of both Ryk and Mib1 morpholino show aggravated axis extension defects compared single morphants, confirming the interaction between Ryk and Mib1 during axis extension. I am currently in the process of generating double mutants of *ryk* and *mib1* to study their genetic interaction in the PCP pathway. It is important note that Mib1 and Ryk play a crucial role in canonical Wnt/ β -Catenin signaling in invertebrates and non-canonical Wnt/PCP pathway in vertebrates.

III.2.f Significance of Mib1 mediated Ryk endocytosis.

My study identified a novel role of Mib1 in the PCP pathway, where it regulates endocytosis of the PCP component Ryk. This interaction between Mib1 and Ryk raises the question, what is the functional significance of Mib1 mediated Ryk endocytosis in PCP signaling? An obvious function of Mib1 mediated Ryk endocytosis could be ubiquitination mediated degradation of Ryk. But the rescue of CE defects in Mib1 morphants by Ryk-eGFP overexpression implies that the function of Mib1 mediated Ryk endocytosis is more than just degradation. This observation is similar to the role of Mib1 and Ryk in Wnt/ β -Catenin signaling. During Wnt/ β -Catenin signaling, it has been

shown that Mib1 regulates Ryk protein turnover by reducing its steady-state levels at the plasma membrane(442). Nonetheless, both Ryk and Mib1 functions are necessary for Wnt/ β -Catenin signaling(442). Previous studies have suggested that Mib1 mediated Ryk endocytosis could function at different levels in PCP regulated CE movements including the formation of an endosomal signaling complex, the regulation of cell division orientation, the regulation of cell migration and stabilization of PCP components or to create asymmetric distribution of PCP components.

- formation of an endosomal signaling complex

In Wnt/ β -Catenin signaling, several studies indicated that endocytosis of the ligand-receptor complex facilitates downstream signaling(450). During Wnt/ β -Catenin signaling, endocytosis could regulate signal activation by endosomal acidification, stabilizing and sequestering pathway components and ubiquitin mediated degradation(307). Similar mechanisms could function in the case of Mib1 regulated Ryk endocytosis in the PCP pathway. In *Xenopus*, CE movements are regulated via Clathrin mediated endocytosis of Dishevelled (Dvl) along with Frizzled7 (Fz7)(404). Endocytosis of Dvl is required for further downstream signaling. Ryk interacts with β arr2, an essential adaptor in Clathrin-mediated endocytosis, and Fz7 to promote endocytosis of Dvl in response to Wnt-11. Thus, endocytosis of Ryk could facilitate the formation of an endosomal signaling complex to promote downstream signaling. Therefore, it is possible that Mib1 is promoting endocytosis of other PCP components along with Ryk to form an endosomal signaling complex.

My experiments show that other PCP components such as Vangl2, Fz2 and Fz7 are not internalized along with Ryk during Mib1 overexpression. But one caveat of these experiments is that they are performed without external stimulation of Wnt/PCP ligands such as Wnt11 and Wnt5a. It will be interesting to see whether Mib1 can internalize these PCP components along with Ryk only in the presence of Wnt ligands. Analysis of the localization of Knypek, Dvl and Ror2 during Mib1 overexpression is yet to be done.

- Regulation of cell division orientation

Mib1 has been shown to regulate cell division orientation along with Ryk in *C. elegans*. Mutants of *lin-18/ryk* disrupt oriented divisions of p7.p vulval precursor cells(408) and ceMib genetically

interacts with Ryk in regulating oriented cell divisions(159). In addition, Mib1 is important for centriole biogenesis(421). A pair of centrioles surrounded by pericentriolar material (PCM) constitutes the centrosome, the main microtubule organizing center that controls cell division in animal cells. Therefore, it is possible that Mib1 mediated Ryk endocytosis is required for regulating cell division orientation during zebrafish gastrulation. Mib1 has been shown to colocalize with peri centriolar components for regulating their function(422). It would be interesting to see if Mib1 co-localizes with Ryk at the centrosome during zebrafish gastrulation.

- Regulation of cell migration.

Ryk has been implicated in directional cell migration during gastrulation and axon guidance(405, 407). Wnt5b and Ryk act synergistically to regulate CE movements during zebrafish gastrulation(405). Wnt5b overexpression promotes endocytosis of Ryk from the membrane and thus increases filopodial and lamellipodial protrusions(405). Thereby, Ryk expressing cells achieve the capability to migrate away from the Wnt5b source. It would be interesting to see if Mib1 is necessary for Ryk internalization that is stimulated by Wnt5b overexpression during zebrafish gastrulation. My data show that the overexpression of Mib1 internalizes Ryk from the plasma membrane. If Ryk internalization under Wnt5b overexpression is perturbed in *mib1^{tfi91}* mutant and morphant embryos, we can confirm that Mib1 is necessary for Ryk internalization during directed cell migration.

During axon guidance, Ryk-Vangl2 interactions enable increased endosomal distribution of Vangl2 in the presence of high Wnt5a concentrations and conversely increase membrane localization of Vangl2 at low Wnt5a concentrations(407). This asymmetric distribution of Vangl2 enables axon growth cone to turn away from high Wnt5a concentrations. During axon guidance, it would be interesting to see if Ryk-Vangl2 interaction in response to Wnt5a gradient is disrupted in a Mib1 mutant and morphant background.

- Stabilization of PCP components.

Post-translational modifications such as phosphorylation and ubiquitination are reported to alter the level, localization and function of PCP components(374, 375). Mindbomb1, an E3-ubiquitin ligase, could determine the localization and stability of other PCP components via Ryk endocytosis. Ryk has been shown to transduce Wnt5a signaling by forming a complex

Vangl2(391). It has been shown that Ryk promotes the stability of Vangl2 at the plasma membrane by forming a complex. Thus, Ryk regulates PCP by modulating the degradation of the core PCP component Vangl2(391). My data demonstrate that Mib1 regulates endocytosis of Ryk from the plasma membrane. This essential means that Mib1 can indirectly affect the stability of other PCP components such as Vangl2 by regulating Ryk endocytosis. However, I have shown that Mib1 overexpression doesn't affect the endocytosis Vangl2-GFP, but this was in the absence of any Wnt stimulation. It would be interesting to look at the levels of transgenic Vangl2-GFP in Mib1 morphant and mutant backgrounds, to understand the role of Mib1 in regulating stability of the PCP component Vangl2.

All the above-mentioned studies indicate that there could be different possible mechanisms by which Mib1 mediated Ryk endocytosis regulates the PCP pathway. Therefore, further research must be done to decipher the interaction between Mib1 and Ryk in PCP signaling.

Chapter - IV

General Conclusion

General Conclusion

During my PhD, I studied two different cell signaling pathways that regulate morphogenesis during zebrafish development. I found that the Notch signaling pathway and Mib1 mediated Planar Cell Polarity (PCP) pathway regulate neural tube morphogenesis and embryonic axis extension respectively.

During the first part of my PhD, I addressed the role of Notch signaling in zebrafish neural tube morphogenesis. Notch signaling has been well studied for its role in regulating neurogenesis during zebrafish development. However, whether and how it regulates morphogenesis of the zebrafish neural tube is unknown. Epithelialization and c-division are important events during zebrafish neural tube morphogenesis. Our findings show that, in addition to regulating the timing and identity of neuronal cell fate specification, Notch mediated suppression of neurogenesis is essential for the acquisition of polarized neuroepithelial tissue architecture and the execution specific morphogenetic movements called c-divisions, in order to properly shape the zebrafish spinal cord.

Observations from the first part of my PhD led to the identification of the role of Mindbomb1(Mib1) in PCP signaling. Mib1, an E3-ubiquitin ligase required for Notch activation, regulates convergent extension (CE) movements during zebrafish gastrulation, that are required for the axis elongation of the embryo. Interestingly, I found that Mib1, independent of its function in Notch signaling, act in the PCP pathway to regulate axis extension. In the PCP pathway, Mib1 acts as an E3-ubiquitin ligase and regulates endocytosis of the PCP component Ryk to mediate CE during gastrulation. Thus, my study discovered that independent of its role in Delta/Notch signaling, Mib1 is important for the PCP pathway during zebrafish gastrulation.

References

1. L. A. Lowery, H. Sive, Totally tubular: the mystery behind function and origin of the brain ventricular system. *Bioessays* **31**, 446-458 (2009).
2. D. J. Andrew, A. J. Ewald, Morphogenesis of epithelial tubes: Insights into tube formation, elongation, and elaboration. *Dev Biol* **341**, 34-55 (2010).
3. B. Lubarsky, M. A. Krasnow, Tube morphogenesis: making and shaping biological tubes. *Cell* **112**, 19-28 (2003).
4. A. I. Baumholtz, I. R. Gupta, A. K. Ryan, Claudins in morphogenesis: Forming an epithelial tube. *Tissue Barriers* **5**, e1361899 (2017).
5. M. L. Iruela-Arispe, G. J. Beitel, Tubulogenesis. *Development* **140**, 2851-2855 (2013).
6. S. Sigurbjornsdottir, R. Mathew, M. Leptin, Molecular mechanisms of de novo lumen formation. *Nat Rev Mol Cell Biol* **15**, 665-676 (2014).
7. G. C. Schoenwolf, J. L. Smith, Mechanisms of neurulation: traditional viewpoint and recent advances. *Development* **109**, 243-270 (1990).
8. M. L. Iruela-Arispe, G. E. Davis, Cellular and molecular mechanisms of vascular lumen formation. *Dev Cell* **16**, 222-231 (2009).
9. M. Bagnat, I. D. Cheung, K. E. Mostov, D. Y. Stainier, Genetic control of single lumen formation in the zebrafish gut. *Nat Cell Biol* **9**, 954-960 (2007).
10. A. Rugendorff, A. Younossi-Hartenstein, V. Hartenstein, Embryonic origin and differentiation of the Drosophila heart. *Roux Arch Dev Biol* **203**, 266-280 (1994).
11. Y. Blum *et al.*, Complex cell rearrangements during intersegmental vessel sprouting and vessel fusion in the zebrafish embryo. *Dev Biol* **316**, 312-322 (2008).
12. G. E. Davis, C. W. Camarillo, An alpha 2 beta 1 integrin-dependent pinocytic mechanism involving intracellular vacuole formation and coalescence regulates capillary lumen and tube formation in three-dimensional collagen matrix. *Exp Cell Res* **224**, 39-51 (1996).
13. J. L. Walker *et al.*, Diverse roles of E-cadherin in the morphogenesis of the submandibular gland: insights into the formation of acinar and ductal structures. *Dev Dyn* **237**, 3128-3141 (2008).
14. L. A. Lowery, H. Sive, Strategies of vertebrate neurulation and a re-evaluation of teleost neural tube formation. *Mech Dev* **121**, 1189-1197 (2004).
15. B. G. Freeman, Surface modifications of neural epithelial cells during formation of the neural tube in the rat embryo. *J Embryol Exp Morphol* **28**, 437-448 (1972).
16. J. Wakely, R. A. Badley, Organization of actin filaments in early chick embryo ectoderm: an ultrastructural and immunocytochemical study. *J Embryol Exp Morphol* **69**, 169-182 (1982).
17. J. F. Colas, G. C. Schoenwolf, Towards a cellular and molecular understanding of neurulation. *Dev Dyn* **221**, 117-145 (2001).
18. C. D. Stern. (Cold Spring Harbor Laboratory Press., Cold Spring Harbor, New York, 2019), vol. 2004.
19. G. C. Schoenwolf, M. L. Powers, Shaping of the chick neuroepithelium during primary and secondary neurulation: role of cell elongation. *Anat Rec* **218**, 182-195 (1987).
20. R. N. Gunawardane, S. B. Lizarraga, C. Wiese, A. Wilde, Y. Zheng, gamma-Tubulin complexes and their role in microtubule nucleation. *Curr Top Dev Biol* **49**, 55-73 (2000).

21. C. Lee, H. M. Scherr, J. B. Wallingford, Shroom family proteins regulate gamma-tubulin distribution and microtubule architecture during epithelial cell shape change. *Development* **134**, 1431-1441 (2007).
22. C. Lee, M. P. Le, J. B. Wallingford, The shroom family proteins play broad roles in the morphogenesis of thickened epithelial sheets. *Dev Dyn* **238**, 1480-1491 (2009).
23. J. D. Hildebrand, Shroom regulates epithelial cell shape via the apical positioning of an actomyosin network. *J Cell Sci* **118**, 5191-5203 (2005).
24. J. D. Hildebrand, P. Soriano, Shroom, a PDZ domain-containing actin-binding protein, is required for neural tube morphogenesis in mice. *Cell* **99**, 485-497 (1999).
25. T. Nishimura, H. Honda, M. Takeichi, Planar cell polarity links axes of spatial dynamics in neural-tube closure. *Cell* **149**, 1084-1097 (2012).
26. M. Williams, W. Yen, X. Lu, A. Sutherland, Distinct apical and basolateral mechanisms drive planar cell polarity-dependent convergent extension of the mouse neural plate. *Dev Cell* **29**, 34-46 (2014).
27. C. Araya, L. C. Ward, G. C. Girdler, M. Miranda, Coordinating cell and tissue behavior during zebrafish neural tube morphogenesis. *Dev Dyn* **245**, 197-208 (2016).
28. C. M. Griffith, M. J. Wiley, E. J. Sanders, The vertebrate tail bud: three germ layers from one tissue. *Anat Embryol (Berl)* **185**, 101-113 (1992).
29. G. C. Schoenwolf, Histological and ultrastructural studies of secondary neurulation in mouse embryos. *Am J Anat* **169**, 361-376 (1984).
30. M. Catala, M. A. Teillet, N. M. Le Douarin, Organization and development of the tail bud analyzed with the quail-chick chimaera system. *Mech Dev* **51**, 51-65 (1995).
31. R. B. Brun, J. A. Garson, Neurulation in the Mexican salamander (*Ambystoma mexicanum*): a drug study and cell shape analysis of the epidermis and the neural plate. *J Embryol Exp Morphol* **74**, 275-295 (1983).
32. T. E. Schroeder, Neurulation in *Xenopus laevis*. An analysis and model based upon light and electron microscopy. *J Embryol Exp Morphol* **23**, 427-462 (1970).
33. L. A. Davidson, R. E. Keller, Neural tube closure in *Xenopus laevis* involves medial migration, directed protrusive activity, cell intercalation and convergent extension. *Development* **126**, 4547-4556 (1999).
34. M. Tawk *et al.*, A mirror-symmetric cell division that orchestrates neuroepithelial morphogenesis. *Nature* **446**, 797-800 (2007).
35. E. Hong, R. Brewster, N-cadherin is required for the polarized cell behaviors that drive neurulation in the zebrafish. *Development* **133**, 3895-3905 (2006).
36. C. Papan, J. A. Campos-Ortega, On the formation of the neural keel and neural tube in the zebrafish *Danio (Brachydanio) rerio*. *Roux Arch Dev Biol* **203**, 178-186 (1994).
37. X. Yang, J. Zou, D. R. Hyde, L. A. Davidson, X. Wei, Stepwise maturation of apicobasal polarity of the neuroepithelium is essential for vertebrate neurulation. *J Neurosci* **29**, 11426-11440 (2009).
38. B. Geldmacher-Voss, A. M. Reugels, S. Pauls, J. A. Campos-Ortega, A 90-degree rotation of the mitotic spindle changes the orientation of mitoses of zebrafish neuroepithelial cells. *Development* **130**, 3767-3780 (2003).
39. B. Schmitz, C. Papan, J. A. Campos-Ortega, Neurulation in the anterior trunk region of the zebrafish *Brachydanio rerio*. *Roux Arch Dev Biol* **202**, 250-259 (1993).
40. C. B. Kimmel, R. M. Warga, T. F. Schilling, Origin and organization of the zebrafish fate map. *Development* **108**, 581-594 (1990).

41. C. B. Kimmel, W. W. Ballard, S. R. Kimmel, B. Ullmann, T. F. Schilling, Stages of embryonic development of the zebrafish. *Dev Dyn* **203**, 253-310 (1995).
42. C. B. Kimmel, R. M. Warga, D. A. Kane, Cell cycles and clonal strings during formation of the zebrafish central nervous system. *Development* **120**, 265-276 (1994).
43. C. Papan, J. A. Campos-Ortega, A clonal analysis of spinal cord development in the zebrafish. *Dev Genes Evol* **207**, 71-81 (1997).
44. B. Ciruna, A. Jenny, D. Lee, M. Mlodzik, A. F. Schier, Planar cell polarity signalling couples cell division and morphogenesis during neurulation. *Nature* **439**, 220-224 (2006).
45. E. Quesada-Hernandez *et al.*, Stereotypical cell division orientation controls neural rod midline formation in zebrafish. *Curr Biol* **20**, 1966-1972 (2010).
46. C. E. Buckley *et al.*, Mirror-symmetric microtubule assembly and cell interactions drive lumen formation in the zebrafish neural rod. *EMBO J* **32**, 30-44 (2013).
47. M. Zigman, A. Trinh le, S. E. Fraser, C. B. Moens, Zebrafish neural tube morphogenesis requires Scribble-dependent oriented cell divisions. *Curr Biol* **21**, 79-86 (2011).
48. L. A. Lowery, H. Sive, Initial formation of zebrafish brain ventricles occurs independently of circulation and requires the *nagie oko* and *snakehead/atplala.1* gene products. *Development* **132**, 2057-2067 (2005).
49. M. Khursheed, M. D. Bashyam, Apico-basal polarity complex and cancer. *J Biosci* **39**, 145-155 (2014).
50. D. M. Bryant, K. E. Mostov, From cells to organs: building polarized tissue. *Nat Rev Mol Cell Biol* **9**, 887-901 (2008).
51. A. Hutterer, J. Betschinger, M. Petronczki, J. A. Knoblich, Sequential roles of Cdc42, Par-6, aPKC, and Lgl in the establishment of epithelial polarity during *Drosophila* embryogenesis. *Dev Cell* **6**, 845-854 (2004).
52. T. Yamanaka *et al.*, Lgl mediates apical domain disassembly by suppressing the PAR-3-aPKC-PAR-6 complex to orient apical membrane polarity. *J Cell Sci* **119**, 2107-2118 (2006).
53. P. J. Plant *et al.*, A polarity complex of mPar-6 and atypical PKC binds, phosphorylates and regulates mammalian Lgl. *Nat Cell Biol* **5**, 301-308 (2003).
54. S. Sotillos, M. T. Diaz-Meco, E. Caminero, J. Moscat, S. Campuzano, DaPKC-dependent phosphorylation of Crumbs is required for epithelial cell polarity in *Drosophila*. *J Cell Biol* **166**, 549-557 (2004).
55. K. Ebnet *et al.*, Regulation of cell polarity by cell adhesion receptors. *Semin Cell Dev Biol* **81**, 2-12 (2018).
56. S. Horne-Badovinac *et al.*, Positional cloning of heart and soul reveals multiple roles for PKC lambda in zebrafish organogenesis. *Curr Biol* **11**, 1492-1502 (2001).
57. C. Munson *et al.*, Regulation of neurocoel morphogenesis by Pard6 gamma b. *Dev Biol* **324**, 41-54 (2008).
58. N. Bit-Avragim *et al.*, Divergent polarization mechanisms during vertebrate epithelial development mediated by the Crumbs complex protein *Nagie oko*. *J Cell Sci* **121**, 2503-2510 (2008).
59. N. Akhtar, C. H. Streuli, An integrin-ILK-microtubule network orients cell polarity and lumen formation in glandular epithelium. *Nat Cell Biol* **15**, 17-27 (2013).
60. C. Norden, Pseudostratified epithelia - cell biology, diversity and roles in organ formation at a glance. *J Cell Sci* **130**, 1859-1863 (2017).

61. M. Gotz, W. B. Huttner, The cell biology of neurogenesis. *Nat Rev Mol Cell Biol* **6**, 777-788 (2005).
62. C. Siebel, U. Lendahl, Notch Signaling in Development, Tissue Homeostasis, and Disease. *Physiol Rev* **97**, 1235-1294 (2017).
63. H. Shimojo, T. Ohtsuka, R. Kageyama, Oscillations in notch signaling regulate maintenance of neural progenitors. *Neuron* **58**, 52-64 (2008).
64. N. Gaiano, J. S. Nye, G. Fishell, Radial glial identity is promoted by Notch1 signaling in the murine forebrain. *Neuron* **26**, 395-404 (2000).
65. J. Hatakeyama *et al.*, Hes genes regulate size, shape and histogenesis of the nervous system by control of the timing of neural stem cell differentiation. *Development* **131**, 5539-5550 (2004).
66. H. Kim *et al.*, Notch-regulated oligodendrocyte specification from radial glia in the spinal cord of zebrafish embryos. *Dev Dyn* **237**, 2081-2089 (2008).
67. Z. Dong, N. Yang, S. Y. Yeo, A. Chitnis, S. Guo, Intralinear directional Notch signaling regulates self-renewal and differentiation of asymmetrically dividing radial glia. *Neuron* **74**, 65-78 (2012).
68. J. Hatakeyama *et al.*, Cadherin-based adhesions in the apical endfoot are required for active Notch signaling to control neurogenesis in vertebrates. *Development* **141**, 1671-1682 (2014).
69. P. Alexandre, A. M. Reugels, D. Barker, E. Blanc, J. D. Clarke, Neurons derive from the more apical daughter in asymmetric divisions in the zebrafish neural tube. *Nat Neurosci* **13**, 673-679 (2010).
70. R. Schmidt, U. Strähle, S. Scholpp, in *Neural Dev.* (2013), vol. 8, pp. 3.
71. K. G. Guruharsha, M. W. Kankel, S. Artavanis-Tsakonas, The Notch signalling system: recent insights into the complexity of a conserved pathway. *Nat Rev Genet* **13**, 654-666 (2012).
72. S. J. Bray, Notch signalling in context. *Nat Rev Mol Cell Biol* **17**, 722-735 (2016).
73. R. Le Borgne, A. Bardin, F. Schweisguth, The roles of receptor and ligand endocytosis in regulating Notch signaling. *Development* **132**, 1751-1762 (2005).
74. U. M. Fiuza, A. M. Arias, Cell and molecular biology of Notch. *J Endocrinol* **194**, 459-474 (2007).
75. M. Itoh *et al.*, Mind bomb is a ubiquitin ligase that is essential for efficient activation of Notch signaling by Delta. *Dev Cell* **4**, 67-82 (2003).
76. W. Wang, G. Struhl, Distinct roles for Mind bomb, Neuralized and Epsin in mediating DSL endocytosis and signaling in *Drosophila*. *Development* **132**, 2883-2894 (2005).
77. S. Mikami, M. Nakaura, A. Kawahara, T. Mizoguchi, M. Itoh, Mindbomb 2 is dispensable for embryonic development and Notch signalling in zebrafish. *Biol Open* **4**, 1576-1582 (2015).
78. B. K. Koo *et al.*, Mind bomb 1 is essential for generating functional Notch ligands to activate Notch. *Development* **132**, 3459-3470 (2005).
79. S. Bray, Notch signalling in *Drosophila*: three ways to use a pathway. *Semin Cell Dev Biol* **9**, 591-597 (1998).
80. M. D. Martin-Bermudo, A. Carmena, F. Jimenez, Neurogenic genes control gene expression at the transcriptional level in early neurogenesis and in mesectoderm specification. *Development* **121**, 219-224 (1995).

81. A. L. Parks, S. S. Huppert, M. A. Muskavitch, The dynamics of neurogenic signalling underlying bristle development in *Drosophila melanogaster*. *Mech Dev* **63**, 61-74 (1997).
82. M. L. Allende, E. S. Weinberg, The expression pattern of two zebrafish achaete-scute homolog (ash) genes is altered in the embryonic brain of the cyclops mutant. *Dev Biol* **166**, 509-530 (1994).
83. B. Appel, J. S. Eisen, Regulation of neuronal specification in the zebrafish spinal cord by Delta function. *Development* **125**, 371-380 (1998).
84. C. Haddon *et al.*, Multiple delta genes and lateral inhibition in zebrafish primary neurogenesis. *Development* **125**, 359-370 (1998).
85. B. Appel, L. A. Givan, J. S. Eisen, Delta-Notch signaling and lateral inhibition in zebrafish spinal cord development. *BMC Dev Biol* **1**, 13 (2001).
86. M. S. Rhyu, L. Y. Jan, Y. N. Jan, Asymmetric distribution of numb protein during division of the sensory organ precursor cell confers distinct fates to daughter cells. *Cell* **76**, 477-491 (1994).
87. R. Le Borgne, F. Schweisguth, Unequal segregation of Neuralized biases Notch activation during asymmetric cell division. *Dev Cell* **5**, 139-148 (2003).
88. A. Hutterer, J. A. Knoblich, Numb and alpha-Adaptin regulate Sanpodo endocytosis to specify cell fate in *Drosophila* external sensory organs. *EMBO Rep* **6**, 836-842 (2005).
89. J. F. de Celis, S. Bray, Feed-back mechanisms affecting Notch activation at the dorsoventral boundary in the *Drosophila* wing. *Development* **124**, 3241-3251 (1997).
90. C. A. Micchelli, E. J. Rulifson, S. S. Blair, The function and regulation of cut expression on the wing margin of *Drosophila*: Notch, Wingless and a dominant negative role for Delta and Serrate. *Development* **124**, 1485-1495 (1997).
91. K. Wahi, M. S. Bochter, S. E. Cole, The many roles of Notch signaling during vertebrate somitogenesis. *Semin Cell Dev Biol* **49**, 68-75 (2016).
92. J. Lewis, Autoinhibition with transcriptional delay: a simple mechanism for the zebrafish somitogenesis oscillator. *Curr Biol* **13**, 1398-1408 (2003).
93. B. K. Liao, D. J. Jorg, A. C. Oates, Faster embryonic segmentation through elevated Delta-Notch signalling. *Nat Commun* **7**, 11861 (2016).
94. Y.-J. Jiang *et al.*, Notch signalling and the synchronization of the somite segmentation clock. *Nature* **408**, 475 (2019).
95. V. C. Luca *et al.*, Structural biology. Structural basis for Notch1 engagement of Delta-like 4. *Science* **347**, 847-853 (2015).
96. J. Cordle *et al.*, A conserved face of the Jagged/Serrate DSL domain is involved in Notch trans-activation and cis-inhibition. *Nat Struct Mol Biol* **15**, 849-857 (2008).
97. C. R. Chillakuri *et al.*, Structural analysis uncovers lipid-binding properties of Notch ligands. *Cell Rep* **5**, 861-867 (2013).
98. E. M. Maine, J. L. Lissemore, W. T. Starmer, A phylogenetic analysis of vertebrate and invertebrate Notch-related genes. *Mol Phylogenet Evol* **4**, 139-149 (1995).
99. J. L. Lissemore, W. T. Starmer, Phylogenetic analysis of vertebrate and invertebrate Delta/Serrate/LAG-2 (DSL) proteins. *Mol Phylogenet Evol* **11**, 308-319 (1999).
100. I. Rebay *et al.*, Specific EGF repeats of Notch mediate interactions with Delta and Serrate: implications for Notch as a multifunctional receptor. *Cell* **67**, 687-699 (1991).
101. N. A. Rana *et al.*, in *J Biol Chem.* (2011), vol. 286, pp. 31623-31637.
102. F. Logeat *et al.*, The Notch1 receptor is cleaved constitutively by a furin-like convertase. (1998).

103. W. R. Gordon *et al.*, Structural basis for autoinhibition of Notch. *Nat Struct Mol Biol* **14**, 295-300 (2007).
104. G. van Tetering *et al.*, Metalloprotease ADAM10 is required for Notch1 site 2 cleavage. *J Biol Chem* **284**, 31018-31027 (2009).
105. J. S. Mumm *et al.*, A ligand-induced extracellular cleavage regulates gamma-secretase-like proteolytic activation of Notch1. *Mol Cell* **5**, 197-206 (2000).
106. J. J. Wilson, R. A. Kovall, Crystal structure of the CSL-Notch-Mastermind ternary complex bound to DNA. *Cell* **124**, 985-996 (2006).
107. Y. Nam, P. Sliz, L. Song, J. C. Aster, S. C. Blacklow, Structural basis for cooperativity in recruitment of MAML coactivators to Notch transcription complexes. *Cell* **124**, 973-983 (2006).
108. S. J. Bray, M. Gomez-Lamarca, Notch after cleavage. *Curr Opin Cell Biol* **51**, 103-109 (2018).
109. V. C. Luca *et al.*, Notch-Jagged complex structure implicates a catch bond in tuning ligand sensitivity. *Science* **355**, 1320-1324 (2017).
110. M. B. Andrawes *et al.*, Intrinsic selectivity of Notch 1 for Delta-like 4 over Delta-like 1. *J Biol Chem* **288**, 25477-25489 (2013).
111. R. A. Kovall, B. Gebelein, D. Sprinzak, R. Kopan, The Canonical Notch Signaling Pathway: Structural And Biochemical Insights Into Shape, Sugar, And Force. *Dev Cell* **41**, 228-241 (2017).
112. V. M. Panin, V. Papayannopoulos, R. Wilson, K. D. Irvine, Fringe modulates Notch-ligand interactions. *Nature* **387**, 908-912 (1997).
113. L. Seugnet, P. Simpson, M. Haenlin, Requirement for dynamin during Notch signaling in *Drosophila* neurogenesis. *Dev Biol* **192**, 585-598 (1997).
114. P. J. Kooch, R. G. Fehon, M. A. Muskavitch, Implications of dynamic patterns of Delta and Notch expression for cellular interactions during *Drosophila* development. *Development* **117**, 493-507 (1993).
115. K. M. Klueg, M. A. Muskavitch, Ligand-receptor interactions and trans-endocytosis of Delta, Serrate and Notch: members of the Notch signalling pathway in *Drosophila*. *J Cell Sci* **112 (Pt 19)**, 3289-3297 (1999).
116. A. L. Parks, K. M. Klueg, J. R. Stout, M. A. Muskavitch, Ligand endocytosis drives receptor dissociation and activation in the Notch pathway. *Development* **127**, 1373-1385 (2000).
117. A. Chitnis, WHY IS DELTA ENDOCYTOSIS REQUIRED FOR EFFECTIVE ACTIVATION OF NOTCH? *Dev Dyn* **235**, 886-894 (2006).
118. R. Le Borgne, Regulation of Notch signalling by endocytosis and endosomal sorting. *Curr Opin Cell Biol* **18**, 213-222 (2006).
119. W. Wang, G. Struhl, *Drosophila* Epsin mediates a select endocytic pathway that DSL ligands must enter to activate Notch. *Development* **131**, 5367-5380 (2004).
120. S. F. Heuss, D. Ndiaye-Lobry, E. M. Six, A. Israel, F. Logeat, The intracellular region of Notch ligands Dll1 and Dll3 regulates their trafficking and signaling activity. *Proc Natl Acad Sci U S A* **105**, 11212-11217 (2008).
121. K. N. Lovendahl, S. C. Blacklow, W. R. Gordon, The Molecular Mechanism of Notch Activation. *Adv Exp Med Biol* **1066**, 47-58 (2018).
122. F. Chowdhury *et al.*, Defining Single Molecular Forces Required for Notch Activation Using Nano Yoyo. *Nano Lett* **16**, 3892-3897 (2016).

123. W. R. Gordon *et al.*, Mechanical Allostery: Evidence for a Force Requirement in the Proteolytic Activation of Notch. *Dev Cell* **33**, 729-736 (2015).
124. D. Seo *et al.*, A Mechanogenetic Toolkit for Interrogating Cell Signaling in Space and Time. *Cell* **165**, 1507-1518 (2016).
125. B. Shergill, L. Meloty-Kapella, A. A. Musse, G. Weinmaster, E. Botvinick, Optical tweezers studies on Notch: single-molecule interaction strength is independent of ligand endocytosis. *Dev Cell* **22**, 1313-1320 (2012).
126. L. Meloty-Kapella, B. Shergill, J. Kuon, E. Botvinick, G. Weinmaster, Notch ligand endocytosis generates mechanical pulling force dependent on dynamin, epsins, and actin. *Dev Cell* **22**, 1299-1312 (2012).
127. T. Klein, K. Brennan, A. M. Arias, An intrinsic dominant negative activity of serrate that is modulated during wing development in *Drosophila*. *Dev Biol* **189**, 123-134 (1997).
128. A. C. Miller, E. L. Lyons, T. G. Herman, cis-Inhibition of Notch by endogenous Delta biases the outcome of lateral inhibition. *Curr Biol* **19**, 1378-1383 (2009).
129. C. Baek *et al.*, Mib1 prevents Notch Cis-inhibition to defer differentiation and preserve neuroepithelial integrity during neural delamination. *PLoS Biol* **16**, e2004162 (2018).
130. M. Boareto *et al.*, Jagged-Delta asymmetry in Notch signaling can give rise to a Sender/Receiver hybrid phenotype. (2015).
131. E. Ladi *et al.*, The divergent DSL ligand Dll3 does not activate Notch signaling but cell autonomously attenuates signaling induced by other DSL ligands. *J Cell Biol* **170**, 983-992 (2005).
132. G. F. Hoyne, G. Chapman, Y. Sontani, S. E. Pursglove, S. L. Dunwoodie, A cell autonomous role for the Notch ligand Delta-like 3 in alphabeta T-cell development. *Immunol Cell Biol* **89**, 696-705 (2011).
133. N. Nandagopal, L. A. Santat, M. B. Elowitz, Cis-activation in the Notch signaling pathway. *Elife* **8**, (2019).
134. R. Kopan, M. X. Ilagan, The canonical Notch signaling pathway: unfolding the activation mechanism. *Cell* **137**, 216-233 (2009).
135. R. A. Kovall, S. C. Blacklow, Mechanistic insights into Notch receptor signaling from structural and biochemical studies. *Curr Top Dev Biol* **92**, 31-71 (2010).
136. H. Wang *et al.*, NOTCH1-RBPJ complexes drive target gene expression through dynamic interactions with superenhancers. *Proc Natl Acad Sci U S A* **111**, 705-710 (2014).
137. C. J. Fryer, E. Lamar, I. Turbachova, C. Kintner, K. A. Jones, Mastermind mediates chromatin-specific transcription and turnover of the Notch enhancer complex. *Genes Dev* **16**, 1397-1411 (2002).
138. B. D. VanderWielen, Z. Yuan, D. R. Friedmann, R. A. Kovall, Transcriptional repression in the Notch pathway: thermodynamic characterization of CSL-MINT (Msx2-interacting nuclear target protein) complexes. *J Biol Chem* **286**, 14892-14902 (2011).
139. K. J. Collins, Z. Yuan, R. A. Kovall, Structure and function of the CSL-KyoT2 corepressor complex: a negative regulator of Notch signaling. *Structure* **22**, 70-81 (2014).
140. P. Kurth, A. Preiss, R. A. Kovall, D. Maier, Molecular analysis of the notch repressor-complex in *Drosophila*: characterization of potential hairless binding sites on suppressor of hairless. *PLoS One* **6**, e27986 (2011).
141. P. Mulligan *et al.*, A SIRT1-LSD1 corepressor complex regulates Notch target gene expression and development. *Mol Cell* **42**, 689-699 (2011).

142. R. Liefke *et al.*, Histone demethylase KDM5A is an integral part of the core Notch-RBP-J repressor complex. *Genes Dev* **24**, 590-601 (2010).
143. A. Yatim *et al.*, NOTCH1 nuclear interactome reveals key regulators of its transcriptional activity and oncogenic function. *Mol Cell* **48**, 445-458 (2012).
144. O. Y. Lubman, M. X. G. Ilagan, R. Kopan, D. Barrick, Quantitative Dissection of the Notch:CSL Interaction: Insights into the Notch Transcriptional Switch. *J Mol Biol* **365**, 577-589 (2007).
145. J. E. Johnson, R. J. Macdonald, Notch-independent functions of CSL. *Curr Top Dev Biol* **97**, 55-74 (2011).
146. Z. Yuan *et al.*, Structure and Function of the Su(H)-Hairless Repressor Complex, the Major Antagonist of Notch Signaling in *Drosophila melanogaster*. *PLoS Biol* **14**, e1002509 (2016).
147. A. Krejčí, S. Bray, Notch activation stimulates transient and selective binding of Su(H)/CSL to target enhancers. *Genes Dev* **21**, 1322-1327 (2007).
148. D. Castel *et al.*, Dynamic binding of RBPJ is determined by Notch signaling status. *Genes Dev* **27**, 1059-1071 (2013).
149. B. E. Housden *et al.*, Transcriptional dynamics elicited by a short pulse of notch activation involves feed-forward regulation by E(spl)/Hes genes. *PLoS Genet* **9**, e1003162 (2013).
150. O. Staub, D. Rotin, Role of ubiquitylation in cellular membrane transport. *Physiol Rev* **86**, 669-707 (2006).
151. L. Sun, Z. J. Chen, The novel functions of ubiquitination in signaling. *Curr Opin Cell Biol* **16**, 119-126 (2004).
152. R. Budhidarmo, Y. Nakatani, C. L. Day, RINGs hold the key to ubiquitin transfer. *Trends Biochem Sci* **37**, 58-65 (2012).
153. S. J. van Wijk *et al.*, A comprehensive framework of E2-RING E3 interactions of the human ubiquitin-proteasome system. *Mol Syst Biol* **5**, 295 (2009).
154. C. M. Pickart, M. J. Eddins, Ubiquitin: structures, functions, mechanisms. *Biochim Biophys Acta* **1695**, 55-72 (2004).
155. B. J. McMillan *et al.*, A Tail of Two Sites: A Bipartite Mechanism for Recognition of Notch Ligands by Mind Bomb E3 Ligases. *Mol Cell* **57**, 912-924 (2015).
156. B. Guo, B. J. McMillan, S. C. Blacklow, Structure and Function of the Mind bomb E3 ligase in the context of Notch Signal Transduction. *Curr Opin Struct Biol* **41**, 38-45 (2016).
157. N. Kurochkina, U. Guha, in *Biophys Rev.* (2013), vol. 5, pp. 29-39.
158. L. Zhang, P. J. Gallagher, in *Am J Physiol Cell Physiol.* (2009), vol. 297, pp. C1275-1283.
159. J. D. Berndt *et al.*, Mindbomb 1, an E3 ubiquitin ligase, forms a complex with RYK to activate Wnt/beta-catenin signaling. *J Cell Biol* **194**, 737-750 (2011).
160. C. Zhang, Q. Li, Y. J. Jiang, Zebrafish Mib and Mib2 are mutual E3 ubiquitin ligases with common and specific delta substrates. *J Mol Biol* **366**, 1115-1128 (2007).
161. C. Haddon, Y. J. Jiang, L. Smithers, J. Lewis, Delta-Notch signalling and the patterning of sensory cell differentiation in the zebrafish ear: evidence from the mind bomb mutant. *Development* **125**, 4637-4644 (1998).
162. Y. J. Jiang *et al.*, Mutations affecting neurogenesis and brain morphology in the zebrafish, *Danio rerio*. *Development* **123**, 205-216 (1996).
163. N. D. Lawson *et al.*, Notch signaling is required for arterial-venous differentiation during embryonic vascular development. *Development* **128**, 3675-3683 (2001).

164. A. F. Schier *et al.*, Mutations affecting the development of the embryonic zebrafish brain. *Development* **123**, 165-178 (1996).
165. F. J. van Eeden *et al.*, Mutations affecting somite formation and patterning in the zebrafish, *Danio rerio*. *Development* **123**, 153-164 (1996).
166. G. A. Deblandre, E. C. Lai, C. Kintner, *Xenopus* neuralized is a ubiquitin ligase that interacts with XDelta1 and regulates Notch signaling. *Dev Cell* **1**, 795-806 (2001).
167. E. C. Lai, G. A. Deblandre, C. Kintner, G. M. Rubin, *Drosophila* neuralized is a ubiquitin ligase that promotes the internalization and degradation of delta. *Dev Cell* **1**, 783-794 (2001).
168. E. Pavlopoulos *et al.*, neuralized Encodes a peripheral membrane protein involved in delta signaling and endocytosis. *Dev Cell* **1**, 807-816 (2001).
169. D. Henrique *et al.*, Maintenance of neuroepithelial progenitor cells by Delta-Notch signalling in the embryonic chick retina. *Curr Biol* **7**, 661-670 (1997).
170. H. C. Park, B. Appel, Delta-Notch signaling regulates oligodendrocyte specification. *Development* **130**, 3747-3755 (2003).
171. S. Bingham *et al.*, Neurogenic Phenotype of mind bomb Mutants Leads to Severe Patterning Defects in the Zebrafish Hindbrain. *Dev Dyn* **228**, 451-463 (2003).
172. E. C. Lai, F. Roegiers, X. Qin, Y. N. Jan, G. M. Rubin, The ubiquitin ligase *Drosophila* Mind bomb promotes Notch signaling by regulating the localization and activity of Serrate and Delta. *Development* **132**, 2319-2332 (2005).
173. R. Le Borgne, S. Remaud, S. Hamel, F. Schweisguth, Two distinct E3 ubiquitin ligases have complementary functions in the regulation of delta and serrate signaling in *Drosophila*. *PLoS Biol* **3**, e96 (2005).
174. A. Miyamoto, R. Lau, P. W. Hein, J. M. Shipley, G. Weinmaster, Microfibrillar proteins MAGP-1 and MAGP-2 induce Notch1 extracellular domain dissociation and receptor activation. *J Biol Chem* **281**, 10089-10097 (2006).
175. T. Rauen *et al.*, YB-1 acts as a ligand for Notch-3 receptors and modulates receptor activation. *J Biol Chem* **284**, 26928-26940 (2009).
176. S. Ohata *et al.*, Dual roles of Notch in regulation of apically restricted mitosis and apicobasal polarity of neuroepithelial cells. *Neuron* **69**, 215-230 (2011).
177. K. Veeraghavalu *et al.*, Complementations of human papillomavirus type 16 E6 and E7 by Jagged1-specific Notch1-phosphatidylinositol 3-kinase signaling involves pleiotropic oncogenic functions independent of CBF1;Su(H);Lag-1 activation. *J Virol* **79**, 7889-7898 (2005).
178. S. Ansieau, L. J. Strobl, A. Leutz, Activation of the Notch-regulated transcription factor CBF1/RBP-Jkappa through the 13SE1A oncoprotein. *Genes Dev* **15**, 380-385 (2001).
179. T. Henkel, P. D. Ling, S. D. Hayward, M. G. Peterson, Mediation of Epstein-Barr virus EBNA2 transactivation by recombination signal-binding protein J kappa. *Science* **265**, 92-95 (1994).
180. N. Benhra, F. Vignaux, A. Dussert, F. Schweisguth, R. Le Borgne, Neuralized promotes basal to apical transcytosis of delta in epithelial cells. *Mol Biol Cell* **21**, 2078-2086 (2010).
181. K. J. Yoon *et al.*, Mind bomb 1-expressing intermediate progenitors generate notch signaling to maintain radial glial cells. *Neuron* **58**, 519-531 (2008).
182. M. D. Cearns, S. Escuin, P. Alexandre, N. D. Greene, A. J. Copp, Microtubules, polarity and vertebrate neural tube morphogenesis. *J Anat* **229**, 63-74 (2016).

183. K. Hori, A. Sen, S. Artavanis-Tsakonas, Notch signaling at a glance. *J Cell Sci* **126**, 2135-2140 (2013).
184. J. Shin, J. Poling, H. C. Park, B. Appel, Notch signaling regulates neural precursor allocation and binary neuronal fate decisions in zebrafish. *Development* **134**, 1911-1920 (2007).
185. S. J. Bray, Notch signalling: a simple pathway becomes complex. *Nat Rev Mol Cell Biol* **7**, 678-689 (2006).
186. P. Chapouton *et al.*, Notch activity levels control the balance between quiescence and recruitment of adult neural stem cells. *J Neurosci* **30**, 7961-7974 (2010).
187. M. Fürthauer, M. González-Gaitán, Endocytic regulation of notch signalling during development. *Traffic* **10**, 792-802 (2009).
188. M. Götz, W. B. Huttner, The cell biology of neurogenesis. *Nat Rev Mol Cell Biol* **6**, 777-788 (2005).
189. Y. Miyamoto, F. Sakane, K. Hashimoto, N-cadherin-based adherens junction regulates the maintenance, proliferation, and differentiation of neural progenitor cells during development. *Cell Adh Migr* **9**, 183-192 (2015).
190. R. McIntosh, J. Norris, J. D. Clarke, P. Alexandre, Spatial distribution and characterization of non-apical progenitors in the zebrafish embryo central nervous system. *Open Biol* **7**, (2017).
191. Y. Kimura, C. Satou, S. Higashijima, V2a and V2b neurons are generated by the final divisions of pair-producing progenitors in the zebrafish spinal cord. *Development* **135**, 3001-3005 (2008).
192. V. Korzh, Stretching cell morphogenesis during late neurulation and mild neural tube defects. *Dev Growth Differ* **56**, 425-433 (2014).
193. M. Matsuda, A. B. Chitnis, Interaction with Notch determines endocytosis of specific Delta ligands in zebrafish neural tissue. *Development* **136**, 197-206 (2009).
194. J. W. von Trotha, J. A. Campos-Ortega, A. M. Reugels, Apical localization of ASIP/PAR-3:EGFP in zebrafish neuroepithelial cells involves the oligomerization domain CR1, the PDZ domains, and the C-terminal portion of the protein. *Dev Dyn* **235**, 967-977 (2006).
195. Y. Omori, J. Malicki, oko meduzy and related crumbs genes are determinants of apical cell features in the vertebrate embryo. *Curr Biol* **16**, 945-957 (2006).
196. E. Hong, P. Jayachandran, R. Brewster, The polarity protein Pard3 is required for centrosome positioning during neurulation. *Dev Biol* **341**, 335-345 (2010).
197. M. Matsuda *et al.*, Epb4115 competes with Delta as a substrate for Mib1 to coordinate specification and differentiation of neurons. *Development*, (2016).
198. T. Mizoguchi, S. Ikeda, S. Watanabe, M. Sugawara, M. Itoh, Mib1 contributes to persistent directional cell migration by regulating the Ctnnd1-Rac1 pathway. *Proc Natl Acad Sci U S A* **114**, E9280-E9289 (2017).
199. A. J. Latimer, X. Dong, Y. Markov, B. Appel, Delta-Notch signaling induces hypochord development in zebrafish. *Development* **129**, 2555-2563 (2002).
200. A. Geling, H. Steiner, M. Willem, L. Bally-Cuif, C. Haass, A gamma-secretase inhibitor blocks Notch signaling in vivo and causes a severe neurogenic phenotype in zebrafish. *EMBO Rep* **3**, 688-694 (2002).
201. I. Rothnagler *et al.*, Clonal analysis by distinct viral vectors identifies bona fide neural stem cells in the adult zebrafish telencephalon and characterizes their division properties and fate. *Development* **138**, 1459-1469 (2011).

202. C. Takke, J. A. Campos-Ortega, *her1*, a zebrafish pair-rule like gene, acts downstream of notch signalling to control somite development. *Development* **126**, 3005-3014 (1999).
203. D. A. Wettstein, D. L. Turner, C. Kintner, The *Xenopus* homolog of *Drosophila* Suppressor of Hairless mediates Notch signaling during primary neurogenesis. *Development* **124**, 693-702 (1997).
204. H. Main, J. Radenkovic, S. B. Jin, U. Lendahl, E. R. Andersson, Notch signaling maintains neural rosette polarity. *PLoS One* **8**, e62959 (2013).
205. K. Echeverri, A. C. Oates, Coordination of symmetric cyclic gene expression during somitogenesis by Suppressor of Hairless involves regulation of retinoic acid catabolism. *Dev Biol* **301**, 388-403 (2007).
206. B. Appel *et al.*, Delta-mediated specification of midline cell fates in zebrafish embryos. *Curr Biol* **9**, 247-256 (1999).
207. M. J. Parsons *et al.*, Notch-responsive cells initiate the secondary transition in larval zebrafish pancreas. *Mech Dev* **126**, 898-912 (2009).
208. J. Zou, Y. Wen, X. Yang, X. Wei, Spatial-temporal expressions of *Crumbs* and *Nagie oko* and their interdependence in zebrafish central nervous system during early development. *Int J Dev Neurosci* **31**, 770-782 (2013).
209. L. I. Hudish, A. J. Blasky, B. Appel, miR-219 regulates neural precursor differentiation by direct inhibition of apical par polarity proteins. *Dev Cell* **27**, 387-398 (2013).
210. Y. Okuda *et al.*, Comparative genomic and expression analysis of group B1 *sox* genes in zebrafish indicates their diversification during vertebrate evolution. *Dev Dyn* **235**, 811-825 (2006).
211. E. Rodriguez-Boulan, I. G. Macara, Organization and execution of the epithelial polarity programme. *Nat Rev Mol Cell Biol* **15**, 225-242 (2014).
212. S. Kressmann, C. Campos, I. Castanon, M. Fürthauer, M. González-Gaitán, Directional Notch trafficking in Sara endosomes during asymmetric cell division in the spinal cord. *Nat Cell Biol* **17**, 333-339 (2015).
213. S. Chanut, F. Schweisguth, Regulation of epithelial polarity by the E3 ubiquitin ligase Neuralized and the Bearded inhibitors in *Drosophila*. *Nat Cell Biol* **14**, 467-476 (2012).
214. S. Bonilla *et al.*, Identification of midbrain floor plate radial glia-like cells as dopaminergic progenitors. *Glia* **56**, 809-820 (2008).
215. A. Geling, C. Plessy, S. Rastegar, U. Strähle, L. Bally-Cuif, *Her5* acts as a prepattern factor that blocks *neurogenin1* and *coe2* expression upstream of Notch to inhibit neurogenesis at the midbrain-hindbrain boundary. *Development* **131**, 1993-2006 (2004).
216. C. Takke, P. Dornseifer, E. v Weizsäcker, J. A. Campos-Ortega, *her4*, a zebrafish homologue of the *Drosophila* neurogenic gene *E(spl)*, is a target of NOTCH signalling. *Development* **126**, 1811-1821 (1999).
217. S. A. Holley, R. Geisler, C. Nüsslein-Volhard, Control of *her1* expression during zebrafish somitogenesis by a delta-dependent oscillator and an independent wave-front activity. *Genes Dev* **14**, 1678-1690 (2000).
218. M. E. Robu *et al.*, p53 activation by knockdown technologies. *PLoS Genet* **3**, e78 (2007).
219. C. Thisse, B. Thisse, High-resolution in situ hybridization to whole-mount zebrafish embryos. *Nat Protoc* **3**, 59-69 (2008).
220. A. Tallafuss, A. Trepman, J. S. Eisen, DeltaA mRNA and protein distribution in the zebrafish nervous system. *Dev Dyn* **238**, 3226-3236 (2009).

221. M. Itoh, A. Nagafuchi, S. Yonemura, T. Kitani-Yasuda, S. Tsukita, The 220-kD protein colocalizing with cadherins in non-epithelial cells is identical to ZO-1, a tight junction-associated protein in epithelial cells: cDNA cloning and immunoelectron microscopy. *J Cell Biol* **121**, 491-502 (1993).
222. M. F. Marusich, J. A. Weston, Identification of early neurogenic cells in the neural crest lineage. *Dev Biol* **149**, 295-306 (1992).
223. P. A. Lawrence, P. Hayward, The development of a simple pattern: spaced hairs in *Oncopeltus fasciatus*. *J Cell Sci* **8**, 513-524 (1971).
224. P. A. Lawrence, P. M. Shelton, The determination of polarity in the developing insect retina. *J Embryol Exp Morphol* **33**, 471-486 (1975).
225. D. Gubb, A. Garcia-Bellido, A genetic analysis of the determination of cuticular polarity during development in *Drosophila melanogaster*. *J Embryol Exp Morphol* **68**, 37-57 (1982).
226. P. N. Adler, Planar signaling and morphogenesis in *Drosophila*. *Dev Cell* **2**, 525-535 (2002).
227. J. A. Curtin *et al.*, Mutation of *Celsr1* disrupts planar polarity of inner ear hair cells and causes severe neural tube defects in the mouse. *Curr Biol* **13**, 1129-1133 (2003).
228. M. Montcouquiol *et al.*, Asymmetric localization of *Vangl2* and *Fz3* indicate novel mechanisms for planar cell polarity in mammals. *J Neurosci* **26**, 5265-5275 (2006).
229. Y. Wang, N. Guo, J. Nathans, The role of *Frizzled3* and *Frizzled6* in neural tube closure and in the planar polarity of inner-ear sensory hair cells. *J Neurosci* **26**, 2147-2156 (2006).
230. D. Devenport, E. Fuchs, Planar polarization in embryonic epidermis orchestrates global asymmetric morphogenesis of hair follicles. *Nat Cell Biol* **10**, 1257-1268 (2008).
231. N. Guo, C. Hawkins, J. Nathans, *Frizzled6* controls hair patterning in mice. *Proc Natl Acad Sci U S A* **101**, 9277-9281 (2004).
232. N. Hirokawa, Y. Tanaka, Y. Okada, S. Takeda, Nodal flow and the generation of left-right asymmetry. *Cell* **125**, 33-45 (2006).
233. A. G. Kramer-Zucker *et al.*, Cilia-driven fluid flow in the zebrafish pronephros, brain and Kupffer's vesicle is required for normal organogenesis. *Development* **132**, 1907-1921 (2005).
234. R. J. Francis *et al.*, Initiation and maturation of cilia-generated flow in newborn and postnatal mouse airway. *Am J Physiol Lung Cell Mol Physiol* **296**, L1067-1075 (2009).
235. A. Borovina, S. Superina, D. Voskas, B. Ciruna, *Vangl2* directs the posterior tilting and asymmetric localization of motile primary cilia. *Nat Cell Biol* **12**, 407-412 (2010).
236. E. K. Vladar, R. D. Bayly, A. M. Sangoram, M. P. Scott, J. D. Axelrod, Microtubules enable the planar cell polarity of airway cilia. *Curr Biol* **22**, 2203-2212 (2012).
237. C. Boutin *et al.*, A dual role for planar cell polarity genes in ciliated cells. *Proc Natl Acad Sci U S A* **111**, E3129-3138 (2014).
238. T. E. Gillies, C. Cabernard, Cell division orientation in animals. *Curr Biol* **21**, R599-609 (2011).
239. M. Segalen, Y. Bellaiche, Cell division orientation and planar cell polarity pathways. *Semin Cell Dev Biol* **20**, 972-977 (2009).
240. Y. Bei *et al.*, SRC-1 and Wnt signaling act together to specify endoderm and to control cleavage orientation in early *C. elegans* embryos. *Dev Cell* **3**, 113-125 (2002).

241. A. Schlesinger, C. A. Shelton, J. N. Maloof, M. Meneghini, B. Bowerman, Wnt pathway components orient a mitotic spindle in the early *Caenorhabditis elegans* embryo without requiring gene transcription in the responding cell. *Genes Dev* **13**, 2028-2038 (1999).
242. M. Gho, F. Schweisguth, Frizzled signalling controls orientation of asymmetric sense organ precursor cell divisions in *Drosophila*. *Nature* **393**, 178-181 (1998).
243. Y. Bellaïche, O. Beaudoin-Massiani, I. Stuttem, F. Schweisguth, The planar cell polarity protein Strabismus promotes Pins anterior localization during asymmetric division of sensory organ precursor cells in *Drosophila*. *Development* **131**, 469-478 (2004).
244. B. Lu, T. Usui, T. Uemura, L. Jan, Y. N. Jan, Flamingo controls the planar polarity of sensory bristles and asymmetric division of sensory organ precursors in *Drosophila*. *Curr Biol* **9**, 1247-1250 (1999).
245. Y. Li, A. Li, J. Junge, M. Bronner, Planar cell polarity signaling coordinates oriented cell division and cell rearrangement in clonally expanding growth plate cartilage. *Elife* **6**, (2017).
246. Y. Gong, C. Mo, S. E. Fraser, Planar cell polarity signalling controls cell division orientation during zebrafish gastrulation. *Nature* **430**, 689 (2004).
247. F. Tissir, A. M. Goffinet, Shaping the nervous system: role of the core planar cell polarity genes. *Nat Rev Neurosci* **14**, 525-535 (2013).
248. G. Chai, A. M. Goffinet, F. Tissir, Celsr3 and Fzd3 in axon guidance. *Int J Biochem Cell Biol* **64**, 11-14 (2015).
249. A. I. Lyuksyutova *et al.*, Anterior-posterior guidance of commissural axons by Wnt-frizzled signaling. *Science* **302**, 1984-1988 (2003).
250. B. Shafer, K. Onishi, C. Lo, G. Colakoglu, Y. Zou, Vangl2 promotes Wnt/planar cell polarity-like signaling by antagonizing Dvl1-mediated feedback inhibition in growth cone guidance. *Dev Cell* **20**, 177-191 (2011).
251. A. G. Fenstermaker *et al.*, Wnt/planar cell polarity signaling controls the anterior-posterior organization of monoaminergic axons in the brainstem. *J Neurosci* **30**, 16053-16064 (2010).
252. K. Onishi *et al.*, Antagonistic functions of Dishevelleds regulate Frizzled3 endocytosis via filopodia tips in Wnt-mediated growth cone guidance. *J Neurosci* **33**, 19071-19085 (2013).
253. C. F. Davey, C. B. Moens, Planar cell polarity in moving cells: think globally, act locally. *Development* **144**, 187-200 (2017).
254. C. F. Davey, A. W. Mathewson, C. B. Moens, PCP Signaling between Migrating Neurons and their Planar-Polarized Neuroepithelial Environment Controls Filopodial Dynamics and Directional Migration. *PLoS Genet* **12**, e1005934 (2016).
255. R. Mayor, E. Theveneau, The neural crest. *Development* **140**, 2247-2251 (2013).
256. C. Carmona-Fontaine *et al.*, Contact Inhibition of Locomotion in vivo controls neural crest directional migration. *Nature* **456**, 957-961 (2008).
257. H. K. Matthews *et al.*, Directional migration of neural crest cells in vivo is regulated by Syndecan-4/Rac1 and non-canonical Wnt signaling/RhoA. *Development* **135**, 1771-1780 (2008).
258. A. J. Ridley, Rho GTPase signalling in cell migration. *Curr Opin Cell Biol* **36**, 103-112 (2015).
259. A. M. Daulat, J. P. Borg, Wnt/Planar Cell Polarity Signaling: New Opportunities for Cancer Treatment. *Trends Cancer* **3**, 113-125 (2017).

260. A. C. Humphries, M. Mlodzik, From instruction to output: Wnt/PCP signaling in development and cancer. *Curr Opin Cell Biol* **51**, 110-116 (2018).
261. T. M. Puvirajesinghe *et al.*, Identification of p62/SQSTM1 as a component of non-canonical Wnt VANGL2-JNK signalling in breast cancer. *Nat Commun* **7**, 10318 (2016).
262. A. M. Daulat *et al.*, PRICKLE1 Contributes to Cancer Cell Dissemination through Its Interaction with mTORC2. *Dev Cell* **37**, 311-325 (2016).
263. B. C. Lim *et al.*, Prickle1 promotes focal adhesion disassembly in cooperation with the CLASP-LL5beta complex in migrating cells. *J Cell Sci* **129**, 3115-3129 (2016).
264. L. Zhang *et al.*, A lateral signalling pathway coordinates shape volatility during cell migration. *Nat Commun* **7**, 11714 (2016).
265. A. T. Weeraratna *et al.*, Wnt5a signaling directly affects cell motility and invasion of metastatic melanoma. *Cancer Cell* **1**, 279-288 (2002).
266. V. Luga *et al.*, Exosomes mediate stromal mobilization of autocrine Wnt-PCP signaling in breast cancer cell migration. *Cell* **151**, 1542-1556 (2012).
267. R. Keller *et al.*, Mechanisms of convergence and extension by cell intercalation. *Philos Trans R Soc Lond B Biol Sci* **355**, 897-922 (2000).
268. R. E. Keller, M. Danilchik, R. Gimlich, J. Shih, The function and mechanism of convergent extension during gastrulation of *Xenopus laevis*. *J Embryol Exp Morphol* **89 Suppl**, 185-209 (1985).
269. J. B. Wallingford, R. M. Harland, Neural tube closure requires Dishevelled-dependent convergent extension of the midline. *Development* **129**, 5815-5825 (2002).
270. M. Tada, C. P. Heisenberg, Convergent extension: using collective cell migration and cell intercalation to shape embryos. *Development* **139**, 3897-3904 (2012).
271. P. Ybot-Gonzalez *et al.*, Convergent extension, planar-cell-polarity signalling and initiation of mouse neural tube closure. *Development* **134**, 789-799 (2007).
272. S. S. Lienkamp *et al.*, Vertebrate kidney tubules elongate using a planar cell polarity-dependent, rosette-based mechanism of convergent extension. *Nat Genet* **44**, 1382-1387 (2012).
273. M. F. Chacon-Heszele, D. Ren, A. B. Reynolds, F. Chi, P. Chen, Regulation of cochlear convergent extension by the vertebrate planar cell polarity pathway is dependent on p120-catenin. *Development* **139**, 968-978 (2012).
274. A. Shindo, Models of convergent extension during morphogenesis. *Wiley Interdiscip Rev Dev Biol* **7**, (2018).
275. R. E. KELLER, The Cellular Basis of Gastrulation in *Xenopus laevis*: Active, Postinvolution Convergence and Extension by Mediolateral Interdigitation. *Integrative and Comparative Biology* **24**, 589-603 (1984).
276. R. Keller, J. Shih, C. Domingo, The patterning and functioning of protrusive activity during convergence and extension of the *Xenopus* organiser. *Dev Suppl*, 81-91 (1992).
277. N. Watanabe, T. J. Mitchison, Single-molecule speckle analysis of actin filament turnover in lamellipodia. *Science* **295**, 1083-1086 (2002).
278. M. Krause, A. Gautreau, Steering cell migration: lamellipodium dynamics and the regulation of directional persistence. *Nat Rev Mol Cell Biol* **15**, 577-590 (2014).
279. L. M. Machesky, A. Hall, Role of actin polymerization and adhesion to extracellular matrix in Rac- and Rho-induced cytoskeletal reorganization. *J Cell Biol* **138**, 913-926 (1997).
280. W. Liu *et al.*, Mechanism of activation of the Formin protein Daam1. *Proc Natl Acad Sci U S A* **105**, 210-215 (2008).

281. R. Habas, Y. Kato, X. He, Wnt/Frizzled activation of Rho regulates vertebrate gastrulation and requires a novel Formin homology protein Daam1. *Cell* **107**, 843-854 (2001).
282. S. L. Lai *et al.*, Diaphanous-related formin 2 and profilin I are required for gastrulation cell movements. *PLoS One* **3**, e3439 (2008).
283. J. P. Mahaffey, J. Grego-Bessa, K. F. Liem, Jr., K. V. Anderson, Cofilin and Vangl2 cooperate in the initiation of planar cell polarity in the mouse embryo. *Development* **140**, 1262-1271 (2013).
284. E. Tahinci, K. Symes, Distinct functions of Rho and Rac are required for convergent extension during *Xenopus* gastrulation. *Dev Biol* **259**, 318-335 (2003).
285. H. Y. Kim, L. A. Davidson, Punctuated actin contractions during convergent extension and their permissive regulation by the non-canonical Wnt-signaling pathway. *J Cell Sci* **124**, 635-646 (2011).
286. R. Keller, D. Shook, P. Skoglund, The forces that shape embryos: physical aspects of convergent extension by cell intercalation. *Phys Biol* **5**, 015007 (2008).
287. N. Kinoshita, H. Iioka, A. Miyakoshi, N. Ueno, in *Genes Dev.* (2003), vol. 17, pp. 1663-1676.
288. S. Ogata *et al.*, TGF-beta signaling-mediated morphogenesis: modulation of cell adhesion via cadherin endocytosis. *Genes Dev* **21**, 1817-1831 (2007).
289. X. Chen, B. M. Gumbiner, Paraxial protocadherin mediates cell sorting and tissue morphogenesis by regulating C-cadherin adhesion activity. *J Cell Biol* **174**, 301-313 (2006).
290. K. D. Irvine, E. Wieschaus, Cell intercalation during *Drosophila* germband extension and its regulation by pair-rule segmentation genes. *Development* **120**, 827-841 (1994).
291. J. A. Zallen, E. Wieschaus, Patterned gene expression directs bipolar planar polarity in *Drosophila*. *Dev Cell* **6**, 343-355 (2004).
292. C. Bertet, L. Sulak, T. Lecuit, Myosin-dependent junction remodelling controls planar cell intercalation and axis elongation. *Nature* **429**, 667-671 (2004).
293. M. Rauzi, P. F. Lenne, T. Lecuit, Planar polarized actomyosin contractile flows control epithelial junction remodelling. *Nature* **468**, 1110-1114 (2010).
294. J. K. Sawyer *et al.*, A contractile actomyosin network linked to adherens junctions by Canoe/afadin helps drive convergent extension. *Mol Biol Cell* **22**, 2491-2508 (2011).
295. A. M. Merks *et al.*, Planar cell polarity signalling coordinates heart tube remodelling through tissue-scale polarisation of actomyosin activity. *Nat Commun* **9**, 2161 (2018).
296. A. C. Pare *et al.*, A positional Toll receptor code directs convergent extension in *Drosophila*. *Nature* **515**, 523-527 (2014).
297. R. Levayer, T. Lecuit, Oscillation and polarity of E-cadherin asymmetries control actomyosin flow patterns during morphogenesis. *Dev Cell* **26**, 162-175 (2013).
298. R. J. Huebner, J. B. Wallingford, Coming to Consensus: A Unifying Model Emerges for Convergent Extension. *Dev Cell* **46**, 389-396 (2018).
299. A. Shindo, J. B. Wallingford, PCP and septins compartmentalize cortical actomyosin to direct collective cell movement. *Science* **343**, 649-652 (2014).
300. M. T. Butler, J. B. Wallingford, Planar cell polarity in development and disease. *Nat Rev Mol Cell Biol* **18**, 375-388 (2017).
301. S. Saburi, I. Hester, L. Goodrich, H. McNeill, Functional interactions between Fat family cadherins in tissue morphogenesis and planar polarity. *Development* **139**, 1806-1820 (2012).

302. P. Sharma, H. McNeill, Fat and Dachshous cadherins. *Prog Mol Biol Transl Sci* **116**, 215-235 (2013).
303. Y. Komiya, R. Habas, Wnt signal transduction pathways. *Organogenesis* **4**, 68-75 (2008).
304. B. T. MacDonald, K. Tamai, X. He, Wnt/ β -catenin signaling: components, mechanisms, and diseases. *Dev Cell* **17**, 9-26 (2009).
305. V. S. Li *et al.*, Wnt signaling through inhibition of beta-catenin degradation in an intact Axin1 complex. *Cell* **149**, 1245-1256 (2012).
306. C. Gao, Y. G. Chen, Dishevelled: The hub of Wnt signaling. *Cell Signal* **22**, 717-727 (2010).
307. L. Brunt, S. Scholpp, The function of endocytosis in Wnt signaling. *Cell Mol Life Sci* **75**, 785-795 (2018).
308. A. D. Kohn, R. T. Moon, Wnt and calcium signaling: beta-catenin-independent pathways. *Cell Calcium* **38**, 439-446 (2005).
309. A. Sagner *et al.*, Establishment of global patterns of planar polarity during growth of the *Drosophila* wing epithelium. *Curr Biol* **22**, 1296-1301 (2012).
310. J. Wu, A. C. Roman, J. M. Carvajal-Gonzalez, M. Mlodzik, Wg and Wnt4 provide long-range directional input to planar cell polarity orientation in *Drosophila*. *Nat Cell Biol* **15**, 1045-1055 (2013).
311. P. Andre, H. Song, W. Kim, A. Kispert, Y. Yang, in *Development*. (2015), vol. 142, pp. 1516-1527.
312. J. Gros, O. Serralbo, C. Marcelle, WNT11 acts as a directional cue to organize the elongation of early muscle fibres. *Nature* **457**, 589-593 (2009).
313. C. P. Heisenberg *et al.*, Silberblick/Wnt11 mediates convergent extension movements during zebrafish gastrulation. *Nature* **405**, 76-81 (2000).
314. A. Kikuchi, H. Yamamoto, A. Sato, S. Matsumoto, New insights into the mechanism of Wnt signaling pathway activation. *Int Rev Cell Mol Biol* **291**, 21-71 (2011).
315. P. N. Adler, The frizzled/stan pathway and planar cell polarity in the *Drosophila* wing. *Curr Top Dev Biol* **101**, 1-31 (2012).
316. L. V. Goodrich, D. Strutt, Principles of planar polarity in animal development. *Development* **138**, 1877-1892 (2011).
317. R. S. Gray, I. Roszko, L. Solnica-Krezel, Planar cell polarity: coordinating morphogenetic cell behaviors with embryonic polarity. *Dev Cell* **21**, 120-133 (2011).
318. J. R. Seifert, M. Mlodzik, Frizzled/PCP signalling: a conserved mechanism regulating cell polarity and directed motility. *Nat Rev Genet* **8**, 126-138 (2007).
319. J. Singh, M. Mlodzik, Planar cell polarity signaling: coordination of cellular orientation across tissues. *Wiley Interdiscip Rev Dev Biol* **1**, 479-499 (2012).
320. M. Mlodzik, Planar cell polarization: do the same mechanisms regulate *Drosophila* tissue polarity and vertebrate gastrulation? *Trends Genet* **18**, 564-571 (2002).
321. M. T. Veeman, J. D. Axelrod, R. T. Moon, A second canon. Functions and mechanisms of beta-catenin-independent Wnt signaling. *Dev Cell* **5**, 367-377 (2003).
322. F. Marlow, J. Topczewski, D. Sepich, L. Solnica-Krezel, Zebrafish Rho kinase 2 acts downstream of Wnt11 to mediate cell polarity and effective convergence and extension movements. *Curr Biol* **12**, 876-884 (2002).
323. C. G. Winter *et al.*, *Drosophila* Rho-associated kinase (Drok) links Frizzled-mediated planar cell polarity signaling to the actin cytoskeleton. *Cell* **105**, 81-91 (2001).

324. H. Yamanaka *et al.*, JNK functions in the non-canonical Wnt pathway to regulate convergent extension movements in vertebrates. *EMBO Rep* **3**, 69-75 (2002).
325. M. Boutros, N. Paricio, D. I. Strutt, M. Mlodzik, Dishevelled activates JNK and discriminates between JNK pathways in planar polarity and wingless signaling. *Cell* **94**, 109-118 (1998).
326. U. Weber, N. Paricio, M. Mlodzik, Jun mediates Frizzled-induced R3/R4 cell fate distinction and planar polarity determination in the *Drosophila* eye. *Development* **127**, 3619-3629 (2000).
327. M. Matis, J. D. Axelrod, Regulation of PCP by the Fat signaling pathway. *Genes Dev* **27**, 2207-2220 (2013).
328. C. Thomas, D. Strutt, The roles of the cadherins Fat and Dachshous in planar polarity specification in *Drosophila*. *Dev Dyn* **241**, 27-39 (2012).
329. A. A. Ambegaonkar, G. Pan, M. Mani, Y. Feng, K. D. Irvine, Propagation of Dachshous-Fat planar cell polarity. *Curr Biol* **22**, 1302-1308 (2012).
330. F. Bosveld *et al.*, Mechanical control of morphogenesis by Fat/Dachshous/Four-jointed planar cell polarity pathway. *Science* **336**, 724-727 (2012).
331. A. Brittle, C. Thomas, D. Strutt, Planar polarity specification through asymmetric subcellular localization of Fat and Dachshous. *Curr Biol* **22**, 907-914 (2012).
332. M. A. Simon, A. Xu, H. O. Ishikawa, K. D. Irvine, Modulation of fat:dachshous binding by the cadherin domain kinase four-jointed. *Curr Biol* **20**, 811-817 (2010).
333. A. L. Brittle, A. Repiso, J. Casal, P. A. Lawrence, D. Strutt, Four-jointed modulates growth and planar polarity by reducing the affinity of dachshous for fat. *Curr Biol* **20**, 803-810 (2010).
334. H. O. Ishikawa, H. Takeuchi, R. S. Haltiwanger, K. D. Irvine, Four-jointed is a Golgi kinase that phosphorylates a subset of cadherin domains. *Science* **321**, 401-404 (2008).
335. M. P. Zeidler, N. Perrimon, D. I. Strutt, The four-jointed gene is required in the *Drosophila* eye for ommatidial polarity specification. *Curr Biol* **9**, 1363-1372 (1999).
336. M. P. Zeidler, N. Perrimon, D. I. Strutt, Multiple roles for four-jointed in planar polarity and limb patterning. *Dev Biol* **228**, 181-196 (2000).
337. M. Fanto *et al.*, The tumor-suppressor and cell adhesion molecule Fat controls planar polarity via physical interactions with Atrophin, a transcriptional co-repressor. *Development* **130**, 763-774 (2003).
338. S. Saburi *et al.*, Loss of Fat4 disrupts PCP signaling and oriented cell division and leads to cystic kidney disease. *Nat Genet* **40**, 1010-1015 (2008).
339. T. Harumoto *et al.*, Atypical cadherins Dachshous and Fat control dynamics of noncentrosomal microtubules in planar cell polarity. *Dev Cell* **19**, 389-401 (2010).
340. D. Devenport, The cell biology of planar cell polarity. *J Cell Biol* **207**, 171-179 (2014).
341. Y. Yang, M. Mlodzik, Wnt-Frizzled/planar cell polarity signaling: cellular orientation by facing the wind (Wnt). *Annu Rev Cell Dev Biol* **31**, 623-646 (2015).
342. R. Bastock, H. Strutt, D. Strutt, Strabismus is asymmetrically localised and binds to Prickle and Dishevelled during *Drosophila* planar polarity patterning. *Development* **130**, 3007-3014 (2003).
343. A. Jenny, R. S. Darken, P. A. Wilson, M. Mlodzik, Prickle and Strabismus form a functional complex to generate a correct axis during planar cell polarity signaling. *Embo j* **22**, 4409-4420 (2003).

344. G. Das, A. Jenny, T. J. Klein, S. Eaton, M. Mlodzik, Diego interacts with Prickle and Strabismus/Van Gogh to localize planar cell polarity complexes. *Development* **131**, 4467-4476 (2004).
345. A. Jenny, J. Reynolds-Kenneally, G. Das, M. Burnett, M. Mlodzik, Diego and Prickle regulate Frizzled planar cell polarity signalling by competing for Dishevelled binding. *Nat Cell Biol* **7**, 691-697 (2005).
346. D. R. Tree *et al.*, Prickle mediates feedback amplification to generate asymmetric planar cell polarity signaling. *Cell* **109**, 371-381 (2002).
347. B. Gao *et al.*, Wnt signaling gradients establish planar cell polarity by inducing Vangl2 phosphorylation through Ror2. *Dev Cell* **20**, 163-176 (2011).
348. M. Montcouquiol *et al.*, Identification of Vangl2 and Scrb1 as planar polarity genes in mammals. *Nature* **423**, 173-177 (2003).
349. C. Yin, M. Kiskowski, P. A. Pouille, E. Farge, L. Solnica-Krezel, Cooperation of polarized cell intercalations drives convergence and extension of presomitic mesoderm during zebrafish gastrulation. *J Cell Biol* **180**, 221-232 (2008).
350. T. Usui *et al.*, Flamingo, a seven-pass transmembrane cadherin, regulates planar cell polarity under the control of Frizzled. *Cell* **98**, 585-595 (1999).
351. P. A. Lawrence, J. Casal, G. Struhl, Cell interactions and planar polarity in the abdominal epidermis of *Drosophila*. *Development* **131**, 4651-4664 (2004).
352. H. Strutt, D. Strutt, Differential stability of flamingo protein complexes underlies the establishment of planar polarity. *Curr Biol* **18**, 1555-1564 (2008).
353. W. S. Chen *et al.*, Asymmetric homotypic interactions of the atypical cadherin flamingo mediate intercellular polarity signaling. *Cell* **133**, 1093-1105 (2008).
354. J. Wu, M. Mlodzik, The frizzled extracellular domain is a ligand for Van Gogh/Stbm during nonautonomous planar cell polarity signaling. *Dev Cell* **15**, 462-469 (2008).
355. D. I. Strutt, Asymmetric localization of frizzled and the establishment of cell polarity in the *Drosophila* wing. *Mol Cell* **7**, 367-375 (2001).
356. H. Strutt, S. J. Warrington, D. Strutt, Dynamics of core planar polarity protein turnover and stable assembly into discrete membrane subdomains. *Dev Cell* **20**, 511-525 (2011).
357. D. Strutt, H. Strutt, Differential activities of the core planar polarity proteins during *Drosophila* wing patterning. *Dev Biol* **302**, 181-194 (2007).
358. J. D. Axelrod, J. R. Miller, J. M. Shulman, R. T. Moon, N. Perrimon, Differential recruitment of Dishevelled provides signaling specificity in the planar cell polarity and Wingless signaling pathways. *Genes Dev* **12**, 2610-2622 (1998).
359. J. D. Axelrod, Unipolar membrane association of Dishevelled mediates Frizzled planar cell polarity signaling. *Genes Dev* **15**, 1182-1187 (2001).
360. Y. Shimada, S. Yonemura, H. Ohkura, D. Strutt, T. Uemura, Polarized transport of Frizzled along the planar microtubule arrays in *Drosophila* wing epithelium. *Dev Cell* **10**, 209-222 (2006).
361. J. Olofsson, K. A. Sharp, M. Matis, B. Cho, J. D. Axelrod, Prickle/spiny-legs isoforms control the polarity of the apical microtubule network in planar cell polarity. *Development* **141**, 2866-2874 (2014).
362. M. Matis, D. A. Russler-Germain, Q. Hu, C. J. Tomlin, J. D. Axelrod, Microtubules provide directional information for core PCP function. *Elife* **3**, e02893 (2014).

363. D. S. Sepich, M. Usmani, S. Pawlicki, L. Solnica-Krezel, Wnt/PCP signaling controls intracellular position of MTOCs during gastrulation convergence and extension movements. *Development* **138**, 543-552 (2011).
364. D. Shi *et al.*, Dynamics of planar cell polarity protein Vangl2 in the mouse oviduct epithelium. *Mech Dev* **141**, 78-89 (2016).
365. A. W. Mathewson, D. G. Berman, C. B. Moens, Microtubules are required for the maintenance of planar cell polarity in monociliated floorplate cells. *Dev Biol*, (2019).
366. Y. Guo, G. Zanetti, R. Schekman, A novel GTP-binding protein-adaptor protein complex responsible for export of Vangl2 from the trans Golgi network. *Elife* **2**, e00160 (2013).
367. G. Mottola, A. K. Classen, M. Gonzalez-Gaitan, S. Eaton, M. Zerial, A novel function for the Rab5 effector Rabenosyn-5 in planar cell polarity. *Development* **137**, 2353-2364 (2010).
368. B. Cho, G. Pierre-Louis, A. Sagner, S. Eaton, J. D. Axelrod, Clustering and negative feedback by endocytosis in planar cell polarity signaling is modulated by ubiquitinylation of prickle. *PLoS Genet* **11**, e1005259 (2015).
369. A. K. Classen, K. I. Anderson, E. Marois, S. Eaton, Hexagonal packing of Drosophila wing epithelial cells by the planar cell polarity pathway. *Dev Cell* **9**, 805-817 (2005).
370. D. Devenport, D. Oristian, E. Heller, E. Fuchs, Mitotic internalization of planar cell polarity proteins preserves tissue polarity. *Nat Cell Biol* **13**, 893-902 (2011).
371. R. Shrestha *et al.*, Mitotic Control of Planar Cell Polarity by Polo-like Kinase 1. *Dev Cell* **33**, 522-534 (2015).
372. F. Ulrich, C. P. Heisenberg, Probing E-cadherin endocytosis by morpholino-mediated Rab5 knockdown in zebrafish. *Methods Mol Biol* **440**, 371-387 (2008).
373. F. Ulrich *et al.*, Wnt11 functions in gastrulation by controlling cell cohesion through Rab5c and E-cadherin. *Dev Cell* **9**, 555-564 (2005).
374. I. Cervenka *et al.*, Dishevelled is a NEK2 kinase substrate controlling dynamics of centrosomal linker proteins. *Proc Natl Acad Sci U S A* **113**, 9304-9309 (2016).
375. M. Narimatsu *et al.*, Regulation of planar cell polarity by Smurf ubiquitin ligases. *Cell* **137**, 295-307 (2009).
376. A. M. Daulat *et al.*, Mink1 regulates beta-catenin-independent Wnt signaling via Prickle phosphorylation. *Mol Cell Biol* **32**, 173-185 (2012).
377. H. Strutt, V. Thomas-MacArthur, D. Strutt, Strabismus promotes recruitment and degradation of farnesylated prickle in Drosophila melanogaster planar polarity specification. *PLoS Genet* **9**, e1003654 (2013).
378. H. Strutt, E. Searle, V. Thomas-MacArthur, R. Brookfield, D. Strutt, A Cul-3-BTB ubiquitylation pathway regulates junctional levels and asymmetry of core planar polarity proteins. *Development* **140**, 1693-1702 (2013).
379. M. L. Chin, M. Mlodzik, The Drosophila selectin furrowed mediates intercellular planar cell polarity interactions via frizzled stabilization. *Dev Cell* **26**, 455-468 (2013).
380. T. Buechling *et al.*, Wnt/Frizzled signaling requires dPRR, the Drosophila homolog of the prorenin receptor. *Curr Biol* **20**, 1263-1268 (2010).
381. T. Hermle, M. C. Guida, S. Beck, S. Helmstadter, M. Simons, Drosophila ATP6AP2/VhaPRR functions both as a novel planar cell polarity core protein and a regulator of endosomal trafficking. *Embo j* **32**, 245-259 (2013).
382. C. M. Karner *et al.*, Wnt9b signaling regulates planar cell polarity and kidney tubule morphogenesis. *Nat Genet* **41**, 793-799 (2009).

383. F. Le Grand, A. E. Jones, V. Seale, A. Scimè, M. A. Rudnicki, Wnt7a Activates the Planar Cell Polarity Pathway to Drive the Symmetric Expansion of Satellite Stem Cells. *Cell Stem Cell* **4**, 535-547 (2009).
384. B. Ohkawara, A. Glinka, C. Niehrs, Rspo3 binds syndecan 4 and induces Wnt/PCP signaling via clathrin-mediated endocytosis to promote morphogenesis. *Dev Cell* **20**, 303-314 (2011).
385. J. Topczewski *et al.*, The zebrafish glypican knypek controls cell polarity during gastrulation movements of convergent extension. *Dev Cell* **1**, 251-264 (2001).
386. J. P. Roy, M. M. Halford, S. A. Stacker, The biochemistry, signalling and disease relevance of RYK and other WNT-binding receptor tyrosine kinases. *Growth Factors* **36**, 15-40 (2018).
387. M. A. Lemmon, J. Schlessinger, in *Cell*. (United States, 2010), vol. 141, pp. 1117-1134.
388. P. Wehner, I. Shnitsar, H. Urlaub, A. Borchers, RACK1 is a novel interaction partner of PTK7 that is required for neural tube closure. *Development* **138**, 1321-1327 (2011).
389. H. Y. Ho *et al.*, Wnt5a-Ror-Dishevelled signaling constitutes a core developmental pathway that controls tissue morphogenesis. *Proc Natl Acad Sci U S A* **109**, 4044-4051 (2012).
390. S. Yoshikawa, R. D. McKinnon, M. Kokel, J. B. Thomas, Wnt-mediated axon guidance via the Drosophila Derailed receptor. *Nature* **422**, 583-588 (2003).
391. P. Andre *et al.*, The Wnt coreceptor Ryk regulates Wnt/planar cell polarity by modulating the degradation of the core planar cell polarity component Vangl2. *J Biol Chem* **287**, 44518-44525 (2012).
392. C. A. Callahan, M. G. Muralidhar, S. E. Lundgren, A. L. Scully, J. B. Thomas, Control of neuronal pathway selection by a Drosophila receptor protein-tyrosine kinase family member. *Nature* **376**, 171-174 (1995).
393. M. M. Halford *et al.*, Ryk-deficient mice exhibit craniofacial defects associated with perturbed Eph receptor crosstalk. *Nat Genet* **25**, 414-418 (2000).
394. L. Patthy, The WIF module. *Trends Biochem Sci* **25**, 12-13 (2000).
395. W. Lu, V. Yamamoto, B. Ortega, D. Baltimore, Mammalian Ryk is a Wnt coreceptor required for stimulation of neurite outgrowth. *Cell* **119**, 97-108 (2004).
396. M. L. Macheda *et al.*, The Wnt receptor Ryk plays a role in mammalian planar cell polarity signaling. *J Biol Chem* **287**, 29312-29323 (2012).
397. I. M. Petrova *et al.*, Homodimerization of the Wnt receptor DERAILED recruits the Src family kinase SRC64B. *Mol Cell Biol* **33**, 4116-4127 (2013).
398. S. J. Parsons, J. T. Parsons, Src family kinases, key regulators of signal transduction. *Oncogene* **23**, 7906-7909 (2004).
399. W. H. Chang *et al.*, Smek1/2 is a nuclear chaperone and cofactor for cleaved Wnt receptor Ryk, regulating cortical neurogenesis. *Proc Natl Acad Sci U S A* **114**, E10717-e10725 (2017).
400. J. Lyu, R. L. Wesselschmidt, W. Lu, Cdc37 regulates Ryk signaling by stabilizing the cleaved Ryk intracellular domain. *J Biol Chem* **284**, 12940-12948 (2009).
401. E. Reynaud *et al.*, Guidance of Drosophila Mushroom Body Axons Depends upon DRL-Wnt Receptor Cleavage in the Brain Dorsomedial Lineage Precursors. *Cell Rep* **11**, 1293-1304 (2015).
402. A. Adamo *et al.*, RYK promotes the stemness of glioblastoma cells via the WNT/ beta-catenin pathway. *Oncotarget* **8**, 13476-13487 (2017).

403. F. Santiago, J. Oguma, A. M. Brown, J. Laurence, Noncanonical Wnt signaling promotes osteoclast differentiation and is facilitated by the human immunodeficiency virus protease inhibitor ritonavir. *Biochem Biophys Res Commun* **417**, 223-230 (2012).
404. G. H. Kim, J. H. Her, J. K. Han, Ryk cooperates with Frizzled 7 to promote Wnt11-mediated endocytosis and is essential for *Xenopus laevis* convergent extension movements. *J Cell Biol* **182**, 1073-1082 (2008).
405. S. Lin, L. M. Baye, T. A. Westfall, D. C. Slusarski, Wnt5b-Ryk pathway provides directional signals to regulate gastrulation movement. *J Cell Biol* **190**, 263-278 (2010).
406. Y. Liu *et al.*, Ryk-mediated Wnt repulsion regulates posterior-directed growth of corticospinal tract. *Nat Neurosci* **8**, 1151-1159 (2005).
407. X. Duan, Y. Gao, Y. Liu, Ryk regulates Wnt5a repulsion of mouse corticospinal tract through modulating planar cell polarity signaling. *Cell Discov* **3**, 17015 (2017).
408. T. Inoue *et al.*, *C. elegans* LIN-18 is a Ryk ortholog and functions in parallel to LIN-17/Frizzled in Wnt signaling. *Cell* **118**, 795-806 (2004).
409. C. D. Nobes, A. Hall, Rho, rac, and cdc42 GTPases regulate the assembly of multimolecular focal complexes associated with actin stress fibers, lamellipodia, and filopodia. *Cell* **81**, 53-62 (1995).
410. R. J. Petrie, A. D. Doyle, K. M. Yamada, Random versus directionally persistent cell migration. *Nat Rev Mol Cell Biol* **10**, 538-549 (2009).
411. G. Reig, E. Pulgar, M. L. Concha, Cell migration: from tissue culture to embryos. *Development* **141**, 1999-2013 (2014).
412. P. D. McCrea, J. I. Park, Developmental functions of the P120-catenin sub-family. *Biochim Biophys Acta* **1773**, 17-33 (2007).
413. I. Grosheva, M. Shtutman, M. Elbaum, A. D. Bershadsky, p120 catenin affects cell motility via modulation of activity of Rho-family GTPases: a link between cell-cell contact formation and regulation of cell locomotion. *J Cell Sci* **114**, 695-707 (2001).
414. N. K. Noren, B. P. Liu, K. Burrige, B. Kreft, p120 catenin regulates the actin cytoskeleton via Rho family GTPases. *J Cell Biol* **150**, 567-580 (2000).
415. Y. Jin, E. K. Blue, S. Dixon, Z. Shao, P. J. Gallagher, A death-associated protein kinase (DAPK)-interacting protein, DIP-1, is an E3 ubiquitin ligase that promotes tumor necrosis factor-induced apoptosis and regulates the cellular levels of DAPK. *J Biol Chem* **277**, 46980-46986 (2002).
416. M. Irmeler *et al.*, Inhibition of death receptor signals by cellular FLIP. *Nature* **388**, 190-195 (1997).
417. L. J. Liu *et al.*, in *Cell Res.* (England, 2012), vol. 22, pp. 603-606.
418. M. S. Hayden, S. Ghosh, Signaling to NF-kappaB. *Genes Dev* **18**, 2195-2224 (2004).
419. M. S. Hayden, S. Ghosh, Shared principles in NF-kappaB signaling. *Cell* **132**, 344-362 (2008).
420. G. Courtois, M. O. Fauvarque, The Many Roles of Ubiquitin in NF-kappaB Signaling. *Biomedicines* **6**, (2018).
421. L. Cajanek, T. Glatter, E. A. Nigg, The E3 ubiquitin ligase Mib1 regulates Plk4 and centriole biogenesis. *J Cell Sci* **128**, 1674-1682 (2015).
422. L. Wang, K. Lee, R. Malonis, I. Sanchez, B. D. Dynlacht, Tethering of an E3 ligase by PCMI regulates the abundance of centrosomal KIAA0586/Talpid3 and promotes ciliogenesis. *Elife* **5**, (2016).

423. H. Ishikawa, W. F. Marshall, Ciliogenesis: building the cell's antenna. *Nat Rev Mol Cell Biol* **12**, 222-234 (2011).
424. N. Santos, J. F. Reiter, Building it up and taking it down: the regulation of vertebrate ciliogenesis. *Dev Dyn* **237**, 1972-1981 (2008).
425. M. Bornens, The centrosome in cells and organisms. *Science* **335**, 422-426 (2012).
426. P. Gonczy, Towards a molecular architecture of centriole assembly. *Nat Rev Mol Cell Biol* **13**, 425-435 (2012).
427. T. Douanne *et al.*, CYLD Regulates Centriolar Satellites Proteostasis by Counteracting the E3 Ligase MIB1. *Cell Rep* **27**, 1657-1665.e1654 (2019).
428. B. H. Villumsen *et al.*, A new cellular stress response that triggers centriolar satellite reorganization and ciliogenesis. *Embo j* **32**, 3029-3040 (2013).
429. K. J. Han *et al.*, Deubiquitylase USP9X maintains centriolar satellite integrity by stabilizing pericentriolar material 1 protein. *J Cell Sci* **132**, (2019).
430. C. Zhang, Q. Li, C. H. Lim, X. Qiu, Y. J. Jiang, The characterization of zebrafish antimorphic mib alleles reveals that Mib and Mind bomb-2 (Mib2) function redundantly. *Dev Biol* **305**, 14-27 (2007).
431. P. Sharma, V. M. Saraswathy, L. Xiang, M. Fürthauer, Notch-mediated inhibition of neurogenesis is required for zebrafish spinal cord morphogenesis. *Sci Rep* **9**, 9958 (2019).
432. M. A. El-Brolosy *et al.*, Genetic compensation triggered by mutant mRNA degradation. *Nature* **568**, 193-197 (2019).
433. V. Link, A. Shevchenko, C. P. Heisenberg, in *BMC Dev Biol.* (2006), vol. 6, pp. 1.
434. S. A. Colamarino, M. Tessier-Lavigne, The role of the floor plate in axon guidance. *Annu Rev Neurosci* **18**, 497-529 (1995).
435. M. Placzek, The role of the notochord and floor plate in inductive interactions. *Curr Opin Genet Dev* **5**, 499-506 (1995).
436. A. J. Latimer, J. Shin, B. Appel, her9 promotes floor plate development in zebrafish. *Dev Dyn* **232**, 1098-1104 (2005).
437. C. Stigloher, P. Chapouton, B. Adolf, L. Bally-Cuif, Identification of neural progenitor pools by E(Spl) factors in the embryonic and adult brain. *Brain Res Bull* **75**, 266-273 (2008).
438. S. Scholpp *et al.*, Her6 regulates the neurogenetic gradient and neuronal identity in the thalamus. *Proc Natl Acad Sci U S A* **106**, 19895-19900 (2009).
439. I. Castanon *et al.*, Anthrax toxin receptor 2a controls mitotic spindle positioning. *Nat Cell Biol* **15**, 28-39 (2013).
440. I. Roszko, S. S. D, J. R. Jessen, A. Chandrasekhar, L. Solnica-Krezel, in *Development.* (2015), vol. 142, pp. 2508-2520.
441. J. Ray *et al.*, in *Oncol Rep.* (2019), vol. 42, pp. 1047-1056.
442. J. D. Berndt *et al.*, in *J Cell Biol.* (2011), vol. 194, pp. 737-750.
443. D. M. Wenzel, K. E. Stoll, R. E. Klevit, E2s: structurally economical and functionally replete. *Biochem J* **433**, 31-42 (2011).
444. F. O. Kok *et al.*, Reverse genetic screening reveals poor correlation between morpholino-induced and mutant phenotypes in zebrafish. *Dev Cell* **32**, 97-108 (2015).
445. P. A. Morcos, Achieving targeted and quantifiable alteration of mRNA splicing with Morpholino oligos. *Biochem Biophys Res Commun* **358**, 521-527 (2007).

446. J. L. Anderson *et al.*, mRNA processing in mutant zebrafish lines generated by chemical and CRISPR-mediated mutagenesis produces unexpected transcripts that escape nonsense-mediated decay. *PLoS Genet* **13**, e1007105 (2017).
447. A. Rossi *et al.*, Genetic compensation induced by deleterious mutations but not gene knockdowns. *Nature* **524**, 230-233 (2015).
448. M. A. El-Brolosy *et al.*, Genetic compensation triggered by mutant mRNA degradation. *Nature* **568**, 193-197 (2019).
449. Z. Ma *et al.*, PTC-bearing mRNA elicits a genetic compensation response via Upf3a and COMPASS components. *Nature* **568**, 259-263 (2019).
450. Q. Feng, N. Gao, Keeping Wnt signalosome in check by vesicular traffic. *J Cell Physiol* **230**, 1170-1180 (2015).